ORNL/TM-1999/290
SNS-108030200TR0001R00

# Migration of Activation Products from the Oak Ridge Spallation Neutron Source Facility Shield Berm on Chestnut Ridge on the Oak Ridge Reservation

L. R. Dole
J. O. Johnson
D. M. Hetrick
D. B. Watson
D. D. Huff
J. R. DeVore
G. S. McNealy
J. M. Barnes

This report has been reproduced from the best available copy.

Reports are available to the public from the following source.

National Technical Information Service
5285 Port Royal Road
Springfield, VA 22161
**Telephone** 703-605-6000 (1-800-553-6847)
**TDD** 703-487-4639
**Fax** 703-605-6900
**E-mail** orders@ntis.fedworld.gov
**Web site** http://www.ntis.gov/ordering.htm

Reports are available to U.S. Department of Energy (DOE) employees, DOE contractors, Energy Technology Data Exchange (ETDE) representatives, and International Nuclear Information System (INIS) representatives from the following source.

Office of Scientific and Technical Information
P.O. Box 62
Oak Ridge, TN 37831
**Telephone** 423-576-8401
**Fax** 423-576-5728
**E-mail** reports@adonis.osti.gov
**Web site** http://www.osti.gov/products/sources.html

Reports produced after January 1, 1996, are generally available via the DOE Information Bridge.
**Web site** http://www.doe.gov/bridge

This report was prepared as an account of work sponsored by an agency of the United States Government. Neither the United States Government nor any agency thereof, nor any of their employees, makes any warranty, express or implied, or assumes any legal liability or responsibility for the accuracy, completeness, or usefulness or any information, apparatus, product, or process disclosed, or represents that its use would not infringe privately owned rights. Reference herein to any specific commercial product, process, or service by trade name, trademark, manufacturer, or otherwise, does not necessarily constitute or imply its endorsement, recommendation, or favoring by the United States Government or any agency thereof. The views and opinions of authors expressed herein do not necessarily state or reflect those of the United States Government or any agency thereof.

ORNL/TM-1999/290
SNS-108030200TR0001R00

# MIGRATION OF ACTIVATION PRODUCTS FROM THE OAK RIDGE SPALLATION NEUTRON SOURCE FACILITY SHIELD BERM ON CHESTNUT RIDGE ON THE OAK RIDGE RESERVATION

L. R. Dole
J. O. Johnson
D. M. Hetrick
D. B. Watson
D. D. Huff
J. R. DeVore
G. S. McNealy
J. M. Barnes

Date Published: November 1999

Prepared by the
OAK RIDGE NATIONAL LABORATORY
Oak Ridge, Tennessee 37831-6363
managed by
Lockheed Martin Energy Research Corp.
for the
U.S. Department of Energy
under contract DE-AC05-96OR22464

## CONTENTS

**Page**


LIST OF FIGURES ..... v
LIST OF TABLES ..... vii
ACRONYMS ..... ix
1. EXECUTIVE SUMMARY ..... 1-1
   1.1 REFERENCES ..... 1-1
2. INTRODUCTION AND BACKGROUND ..... 2-1
   2.1 DESCRIPTION OF THE SNS FACILITY AND ITS INTENDED OPERATIONS ..... 2-1
   2.2 SNS OAK RIDGE RESERVATION SITE DESCRIPTION ..... 2-3
      2.2.1 SNS Site Geology ..... 2-3
      2.2.2 SNS Site Soils ..... 2-5
      2.2.3 SNS Site Hydrology ..... 2-10
   2.3 REFERENCES ..... 2-10
3. ACTIVATION PRODUCTS IN THE SNS SHIELD BERM ..... 3-1
   3.1 ACTIVATION ANALYSES ..... 3-2
      3.1.1 Activation Analysis Calculation Methodology ..... 3-3
      3.1.2 Radiation Transport Calculations ..... 3-3
      3.1.3 Activation Calculations ..... 3-4
   3.2 MODEL FOR ACTIVATION CALCULATIONS ..... 3-5
   3.3 DESCRIPTION OF THE RESULTS REPORTED IN APPENDIX A ..... 3-15
      3.3.1 Uncertainties in the Nuclide Production Rates in the SNS Components ..... 3-16
   3.4 REFERENCES ..... 3-17
4. DIFFUSION-CONTROLLED RELEASES OF NUCLIDES FROM THE SNS SHIELD BERM ..... 4-1
   4.1 TOTAL CONTAMINANT AVAILABILITY FOR TRANSPORT ..... 4-1
   4.2 NO ADVECTIVE FLOW THROUGH THE SHIELD BERM ..... 4-2
   4.3 DIFFUSION FROM SHIELD BERM WITH NO RETARDATION INTO THE SURROUNDING SOIL ..... 4-2
      4.3.1 Estimating the Retardation Factors and the Diffusion Coefficients ..... 4-4
      4.3.2 Diffusion-Controlled Contaminant Releases from the Shield Berm ..... 4-6
   4.4 SITE-SPECIFIC SNS HYDROLOGICAL SETTING AND ASSUMPTIONS FOR THE DIFFUSION-CONTROLLED MODEL ..... 4-10
   4.5 DECAY OF ISOTOPES DURING DIFFUSION AND TRANSPORT ..... 4-12
   4.6 RECURSION FORMULAS FOR MODEL CASE 2: GENERATION, DIFFUSION, AND DECAY ..... 4-12
   4.7 SUMMARY OF ASSUMPTIONS AND THEIR IMPACT ON THE ANALYSES ..... 4-13
   4.8 RESULTS OF DIFFUSION-CONTROLLED MODEL OF RELEASES FROM THE SNS SHIELD BERM ..... 4-14
   4.9 REFERENCES ..... 4-17
5. SESOIL BENCHMARK OF THE DIFFUSION-CONTROLLED MODEL WITH $^{14}C$ AND $^{22}Na$ ..... 5-1
   5.1 SESOIL MODEL DESCRIPTION ..... 5-1
      5.1.1 Limitations/Assumptions for SESOIL ..... 5-2
   5.2 SITE-SPECIFIC DATA USED FOR THE SNS FACILITY ON THE ORR ..... 5-3

5.2.1 Climatic Data ..... 5-3
5.2.2 Soil Data ..... 5-3
5.2.3 Contaminant Data ..... 5-5
5.2.4 Sediment Washload Data ..... 5-5
5.2.5 Application Data ..... 5-6
5.3 RESULTS ..... 5-7
5.4 REFERENCES ..... 5-8
6. CONCLUSION ..... 6-1
6.1 REFERENCE ..... 6-1
Appendix A. RESULTS OF ACTIVATION ANALYSES ..... A-1
Appendix B. SAMPLED CALCULATIONS OF $^{12}C$ AND $^{22}Na$ RELEASES FROM THE SNS SHIELD BERM ..... B-1

## LIST OF FIGURES


| Figure | | Page |
|---|---|---|
| 2.1 | SNS site location and features | 2-4 |
| 2.2 | Nitrogen (wt %) in SNS soil cores | 2-8 |
| 2.3 | Total carbon (wt %) in SNS soil cores | 2-8 |
| 3.1 | A flow diagram of the SNS activation analyses | 3-3 |
| 3.2 | Schematic diagram of accelerator tunnel calculation model | 3-6 |
| 3.3 | Schematic diagram of the HETC and MCNP models and their material zone radial boundaries | 3-7 |
| 3.4 | Layout and material information for the cable tray analysis of the activation products present in the insulation after 30-year irradiation at the nominal 1-nA/m (nano-Amp/meter) beam loss rate | 3-14 |
| 4.1 | If groundwater flows around rather than through the shield-berm matrix, releases will be diffusion controlled | 4-3 |
| 4.2 | Hydrologic cross section of the proposed SNS site used in the calculation of potential contaminant concentrations at the boundary of a 4-m zone of influence | 4-11 |
| 5.1 | Geometry of the proposed SNS site used in the SESOIL calculation | 5-6 |

## LIST OF TABLES


| Table | | Page |
|---|---|---|
| 2.1 | A summary of the SNS sections and their lengths | 2-2 |
| 2.2 | Concentration of metals and radionuclides in Copper Ridge dolomite | 2-6 |
| 2.3 | Overall composition of SNS soils | 2-7 |
| 2.4 | Results of nitrogen and total carbon analyses | 2-9 |
| 3.1 | Principal long-lived radioisotopes produced in the SNS shield berm and their characteristics | 3-1 |
| 3.2 | HETC and MCNP calculational model details | 3-6 |
| 3.3 | Calculational model material number densities (atoms/barn-cm) | 3-8 |
| 3.4 | Overall composition of Copper Ridge dolomite soil | 3-13 |
| 4.1 | Parameters used in this study to estimate $D_e$ | 4-6 |
| 4.2 | Nuclide partition coefficients from Tables 5 and 6 of D. H. Thibault and M. Shepard, 1990, *A Critical Compilation and Review of Default Soil Solid/Liquid Partition Coefficients*, AECL-10125, CAN/DN:1990:448145 | 4-7 |
| 4.3 | The distribution of activation nuclides over the radii of the SNS shield-berm components | 4-9 |
| 4.4 | Diameters and volumes of SNS shield-berm concrete, soil, and limestone zones used in the nucleonics model (Fig. 3.3) | 4-10 |
| 4.5 | Summary of activation product concentrations in the component layers of the current SNS shield-berm conceptual design | 4-16 |
| 4.6 | Comparison of two transport cases: In Case 1, the activity accumulates over the 30 years (360 months) of operation and then diffusion from the inner berm and radiogenic decay begin | 4-17 |
| 4.7 | Comparisons of the results of this diffusion model with those of SESOIL | 4-17 |
| 5.1 | SESOIL $^{14}C$ results for the two SESOIL calculated cases at the proposed SNS site | 5-7 |
| 5.2 | SESOIL $^{22}Na$ results for two $K_d$'s at the proposed SNS site at the conservative Case II calculated site hydrology | 5-8 |

## ACRONYMS

| | |
|---|---|
| AA | atomic adsorption |
| ADL | Arthur D. Little, Inc. |
| ANISN | Anisotropic Sn-Theory |
| ATDL | Atmospheric Turbulence Diffusion Laboratory |
| CCDTL | coupled-cavity drift-tube LINAC |
| CCL | coupled-cavity LINAC |
| CFR | *Code of Federal Regulations* |
| CNS | carbon-nitrogen-sulfur |
| DOE | U.S. Department of Energy |
| DORT | discrete ordinates deterministic transport |
| DTL | drift-tube LINAC |
| DWL | Drinking Water Limit |
| EIS | environmental impact statement |
| ENDF/B | evaluated nuclear data file/edition B |
| EPA | U.S. Environmental Protection Agency |
| ES&H | environment, safety, and health |
| FENDL | Fusion Evaluated Nuclear Data Library |
| HEBT | high-energy beam transport |
| HETC | High-Energy Transport Code |
| ICP | ion-coupled plasma |
| LEBT | low-energy beam transport |
| LINAC | linear accelerator |
| LMER | Lockheed Martin Energy Research Corp. |
| MCNP | Monte Carlo Neutron Photon |
| MEBT | medium-energy beam transport |
| NRC | U.S. Nuclear Regulatory Commission |
| 1-D | one-dimensional |
| ORIGEN | Oak Ridge Isotope GENeration and depletion code |
| ORIHET95 | Isotope Production and Decay Analysis Code (Fig. 3) |
| ORNL | Oak Ridge National Laboratory |
| ORR | Oak Ridge Reservation |
| OTS | Office of Toxic Substances (EPA) |
| RTBT | ring to target beam transport |
| SAIC | Science Applications International Corp. |
| SESOIL | Seasonal Soil |
| SNS | Spallation Neutron Source |
| SSC | Superconducting Super Collider |

# 1. EXECUTIVE SUMMARY

The purpose of this study was to estimate the potential groundwater concentrations of activation products that could migrate from the Oak Ridge Spallation Neutron Source (SNS) on top of Chestnut Ridge on the Oak Ridge Reservation (ORR). This Oak Ridge National Laboratory (ORNL) work follows a previous report, ORNL/TM-13665 (Dole, 1998), which had the same purpose.

However, this study uses updated data on the site's geology and hydrology (Sect. 2) and the site-specific revisions to the SNS conceptual design (NSNS/CDR-2/V1) (ORNL, 1997). This second effort was expanded to include the analyses of two diffusion-controlled cases (Sect. 4) and benchmarking with a standard one-dimensional (1-D) compartment, transport model, SESOIL (Seasonal Soil) (Sect. 5).

This work also uses revised estimates of the activation product generation rates and ultimate nuclide inventories within the SNS shield berm (Sect. 3). A normalization error in the original nuclide calculations has been corrected; this correction resulted in the prediction of significantly lower inventories in the SNS berm used for the source-term in these transport analyses.

The results show that the groundwater is protected by the nuclide retention capacity of the SNS shield berm. The Title 10 *Code of Federal Regulations* (CFR) Part 20 Drinking Water Limits (DLWs) are not exceeded even with the most conservative assumptions with regard to diffusion and transport (Sect. 4).

This study shows that the 4-m inner-soil layer of the SNS shield berm is sufficient such as to protect the site's groundwater without the need for additional migration barriers.

## 1.1 REFERENCES

Dole, L. R., September 1998, *Preliminary Assessment of the Nuclide Migration from the Activation Zone around the Proposed Spallation Neutron Source Facility*, ORNL/TM-13665, Lockheed Martin Energy Research Corp., Oak Ridge National Laboratory, Oak Ridge, Tennessee.

Oak Ridge National Laboratory, May 1997, *National Spallation Neutron Source (SNS) Conceptual Design Report*, Vol. 1, NSNS/CDR-2/V1, Lockheed Martin Energy Research Corp., Oak Ridge, Tennessee.

# 2. INTRODUCTION AND BACKGROUND

These studies are a continuation of the ORNL work reported in ORNL/TM-13665, *Preliminary Assessment of the Nuclide Migration from the Activation Zone around the Proposed Spallation Neutron Source Facility* (Dole, 1998). These subsequent studies repeat and expand on the previous analyses and include new information with regard to the site-specific design of the SNS facilities on the ORR. Also, these current studies correct the previous estimates of activation product generation rates in SNS shield berm. A programming flaw in the previous activation calculations (see Sect. 3) was found and corrected. The initial quantities of nuclides reported in ORNL 1998 were found to be high by as much as two orders of magnitude (100×). Therefore, in this study, the potential concentrations in the groundwater have become so low that the additional barriers proposed in the assessment (Dole, 1998) are no longer needed.

After publishing an ORNL 1998 assessment that also used a diffusion-controlled model, the standard transport code, SESOIL 1-D compartment model was used to benchmark the previous results. Analyses using this standard 1-D advective transport code are included in these studies. There is an order of magnitude agreement between these two modeling approaches, diffusion-controlled and 1-D compartment.

Also, both models and their analyses in this report are based on the recent ORR SNS site-specific geology and soil characteristics. Since the publishing of the preliminary report (Dole, 1998), the SNS site geotechnical exploration report by Law Engineering (1998) has been completed concerning the SNS site located on top of Chestnut Ridge. The current models and their analyses in this report have been updated to reflect these site-specific data and the revised conceptual design, NSNS/CDR-2/V1 (ORNL, 1997).

Subsequent to the completion of the SESOIL and diffusion model simulations, results of an additional phase of geotechnical studies have become available. The results of this study have been summarized in *Report of Phase II Additional Geotechnical Study* (Law Engineering, 1999). New hydraulic conductivity data from undisturbed core samples are generally lower than the previous data published in the 1998 Phase II Geotechnical report (1998), while moisture contents are generally higher. Based on a review of the new data, it was determined that rerunning the SESOIL and diffusion models using new input parameters (calculated using the new data) was not warranted because the basic conclusions regarding leaching would not change. Model input and output parameters (e.g., hydraulic conductivity and recharge rates) are believed to be conservative and representative of field-scale hydraulic parameters found at the site.

## 2.1 DESCRIPTION OF THE SNS FACILITY AND ITS INTENDED OPERATIONS

The U.S. Department of Energy (DOE) initiated a conceptual design study, NSNA-CDR-2/V1 (ORNL, May 1997), for the SNS and has given preliminary approval for the proposed facility to be built at ORNL. The conceptual design of the SNS consists of an accelerator system capable of delivering a 1-GeV proton beam with 1 MW of beam power in an approximate 0.5-μs pulse at a 60-Hz frequency into a single target station. During the conceptual design phase, the SNS was designed to be upgraded in stages to a 4-MW facility with two target stations (a 60-Hz station and a 10-Hz station). As a cost-saving measure, in Title I design, the upgrade path has been reduced to a 2-MW facility with two target sections.

The complete accelerator system consists of a front-end ion source, a linear accelerator (LINAC), an accumulator ring, and the associated transfer lines that link the complete system together. The primary function of the front-end systems is to produce a beam of $H^-$ ions to be injected into the LINAC at 2.5 MeV. This facility consists of the ion source, the low-energy beam

transport (LEBT) line, and the medium-energy beam transport (MEBT) line. Details of the front-end systems design can be found in Sect. 2 of the ORNL report, *National Spallation Neutron Source (SNS) Conceptual Design Report* (ORNL, May 1997).

The LINAC is coupled to the MEBT, accepts a beam from the front-end system, and accelerates it from 2.5 MeV to 1.0 GeV. The LINAC consists of a drift-tube LINAC (DTL), which accelerates the $H^-$ beam to 20 MeV; a coupled-cavity drift-tube LINAC (CCDTL), which further accelerates the $H^-$ beam to 93 MeV; and a coupled-cavity LINAC (CCL), which accelerates the $H^-$ beam to 1.0 GeV. The total length of the LINAC is ~492 m. A detailed discussion of the considerations that went into the design choices and the operating parameters for the various LINAC components is given in Sect. 3 of the *Conceptual Design Report* (ORNL, May 1997).

The remainder of the accelerator system is made up of the high-energy beam transport (HEBT) system from the LINAC to the ring, the accumulator ring, and the ring to target beam transport (RTBT) system. The lengths of these three components are 165 m (HEBT), 221 m (ring), and 167 m (RTBT). The HEBT system provides the beam transport between the LINAC and the accumulator ring. The ring accumulates beam pulses from the LINAC and bunches them into intense short pulses for delivery to the target. A 1-ms pulse of $H^-$ ions is delivered to the ring. The ions pass through a stripping foil to convert them to protons, wrap around the ring circumference ~1200 turns, and kick out in a single turn, making a sharp pulse of approximately 0.5 μs to be delivered to the mercury target. This process is repeated 60 times per second. The RTBT accepts the extracted beam from the accumulator ring and transports it to the mercury target. A detailed discussion of considerations leading to design choices and design parameters for the beam transport and accumulator rings can be found in Sect. 4 of the *Conceptual Design Report* (ORNL, May 1997). Table 2.1 summarizes these SNS components and their lengths.

**Table 2.1. A summary of the SNS sections and their lengths**

| Components | Length (m) |
|---|---|
| LINAC | 492 |
| HEBT | 165 |
| Ring | 221 |
| RTBT | 167 |
| Total length | 1045 |

The SNS target system has the basic function of converting the short pulse (<1 μs, 60 Hz, 17 kJ/pulse), high-average power (1 MW), 1-GeV proton beam delivered via the RTBT into 18 lower-energy (<1 eV), short-pulsed (~tens of microseconds) neutron beams that are optimized for use by neutron-scattering instruments. The proton beam target is liquid mercury flowing inside a stainless steel container. The proton beam enters horizontally at 2 m above the floor level. The target is positioned within a layered iron and/or lead and concrete shielding monolith ~12 m in diameter. Two ambient water moderators are positioned under the target, and two supercritical hydrogen cryogenic moderators are positioned above the target. A heavy-water-cooled beryllium reflector region surrounds the moderators. The core region, which includes the target, moderators, and beryllium reflector, is contained inside a 2-m-diam vessel filled with nickel and a helium atmosphere. Water-cooling is used to cool the mercury, shielding, vessels, reflectors, and other assemblies inside the shielding monolith. The target is installed and removed

horizontally using an adjacent service cell. The target service cell is located behind the target assembly and measures 10 m wide by 17.8 m long by 7.5 m high. Work will normally be performed via remote-handling techniques behind a 1-m-thick heavy concrete wall. The other core components are designed to be removed vertically and serviced in a second service maintenance cell adjacent to the target service cell. The general maintenance cell will be used to maintain the moderator/reflector/plug, proton-beam window, neutron-guide tubes, and shutters. This cell measures 10 m wide, 10.9 m long, and 9.5 m high. There are 18 neutron beam lines viewing the moderators, 9 on each side, and equally spaced in angle. Each beam line has an independently operable shielding shutter, which is controlled by the experimentalists. The beam lines are located at two levels: nine lines directed at the ambient water moderators under the target and nine at the cryogenic hydrogen moderators above the target. The shielding extends to a radius of 8 m at the beam-line level to provide a region for the neutron beam choppers with a vertical access hatch positioned at a radius of 7 m. More detailed discussions of the selection criteria and design considerations for the target systems in general are contained in Sect. 5 of the *Conceptual Design Report* (ORNL, May 1997).

## 2.2 SNS OAK RIDGE RESERVATION SITE DESCRIPTION

The proposed SNS site is located on top of Chestnut Ridge on the ORR, approximately 2.7 km northeast of ORNL (Fig. 2.1). The ORR lies in the Valley and Ridge Physiographic Province, ~32 km west of Knoxville, Tennessee (Solomon et al., 1992). The general topological features include:

- Parallel ridges and valleys oriented from northeast to southwest
- Topography influenced by alternating weak and strong strata
- Scarp (northwest-facing) slopes that are short, steep, and smooth
- Dip (southeast-facing) slopes that are long, shallow, and hummocky to dissected
- Elevations that range between 225–410 m above sea level

Elevations at the SNS site range from 357 to 305 m; there is about a 90-m elevation drop between the top of the ridge and Bethel Valley to the south and an 80-m drop to Bear Creek Valley to the north.

### 2.2.1 SNS Site Geology

Bedrock geology of Chestnut Ridge is composed entirely of sedimentary rocks that range in age from early Cambrian to early Mississippian (Hatcher et al., 1992). The total thickness of sections in the ORR is ~2.5 km. The Knox Group, the underlying Conasauga Group, and part of the overlying Chickamauga Group form the competent units within the major thrust sheets in the area (Solomon et al., 1992). The dip of bedrock is variable, but is commonly 45° SE, with a typical strike of N55E (Stockdale, 1951 and Hatcher et al., 1992). The primary stratigraphic unit underlying the site is the Copper Ridge Dolomite of the Knox Group. Other stratigraphic units present at or near the SNS site include the Maynardville Limestone, Chepultepec Dolomite, Longview Dolomite, and the Kingsport formation (see Fig. 2.1). Several sinkholes have been mapped at the proposed site (Fig. 2.1 shown as asterisk symbols). Karst geomorphic processes, which initiated the formation of the dolines, evidently started several million years ago. Analysis of doline soil stratigraphy suggests that most of the large dolines on the site have been stable for most of the past 10,000 to 100,000 years (Lietzke, Ketelle, and Lee, 1989). However,

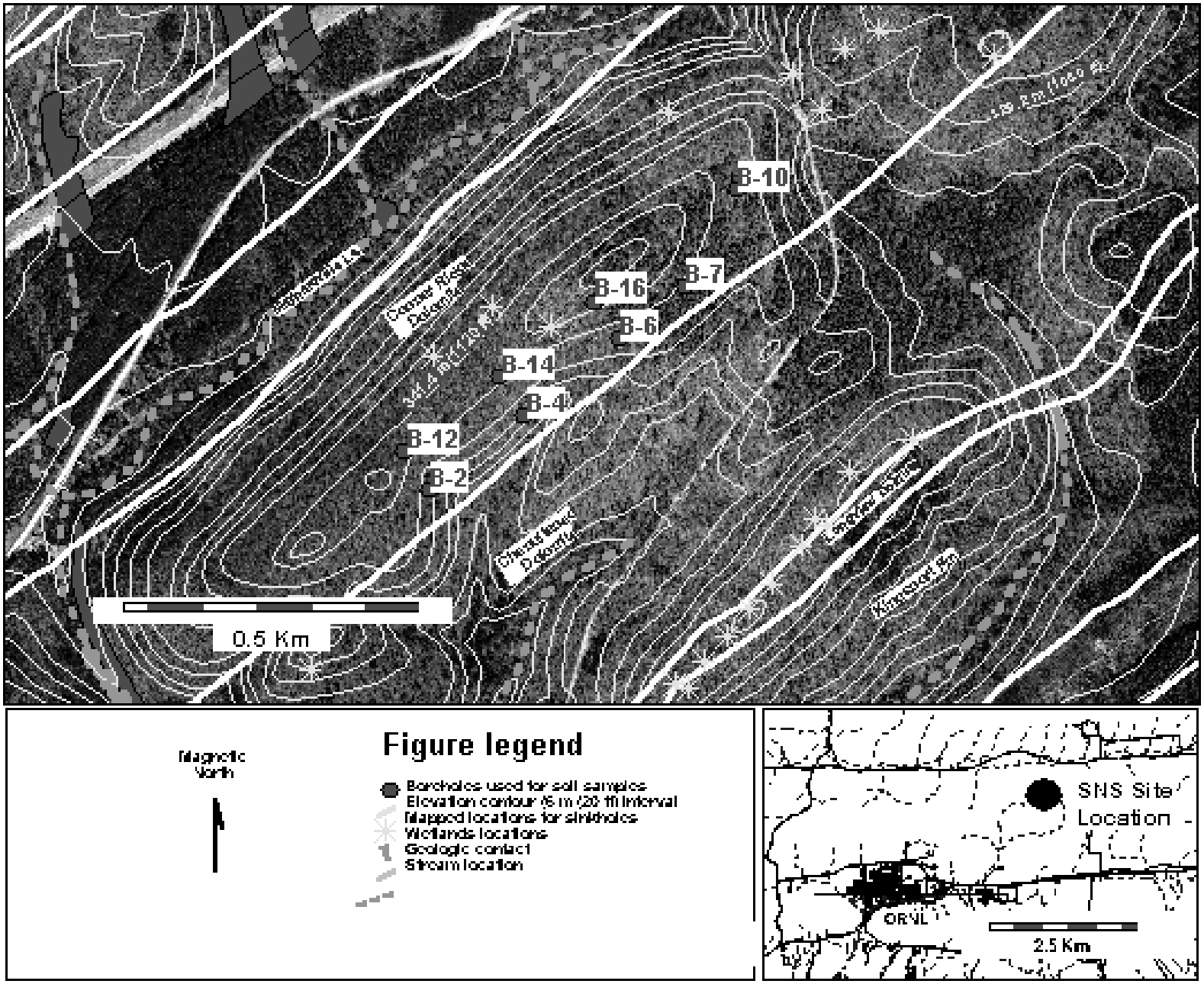


**Fig. 2.1. SNS site location and features.**

management of runoff from impervious areas and careful control of the cooling water pond at the SNS site are both very important to assuring that karst features are not enhanced; any enhancement could lead to problems with accelerated subsidence.

### 2.2.2 SNS Site Soils

Weathering processes have transformed hard rock into saprolite and residuum, and near-surface, soil-forming processes have transformed saprolite into soils with several soil horizons. Most soils in the area are of the Fullerton and Bodine series and are derived from dolomitic saprolite overlying the Copper Ridge Dolomite and have a high chert content (Harris, 1977). The Copper Ridge saprolite has a high clay and silt content and also contains abundant chert (Lietzke et al., 1989). The soils over the Copper Ridge Dolomite are well drained and deep ($\leq$15 m). Forest cover is oak and hickory. Data from the SNS phase II geotechnical report indicate that moisture contents are typically 24% by weight and soil densities are ~1.61 g/cm [Lockheed Martin Energy Research Corp. (LMER), 1998]. Data from Peters (1970) and Jardine, Wilson, and Luxmoore (1988) suggest that the soils beneath the proposed site consist of approximately 38% chert and 62% clay by weight. Based on the mineralogical data from Jardine et al. (1988) and Lee et al. (1984), the following mineralogical composition of the clay fraction of soil was assumed:

35% kaolinite
20% illite
14% smectite
10% vermiculite
5% interstratified minerals
16% quartz ($SiO_2$)

These clays are aluminum-silicates consisting mostly of $SiO_2$, $Al_2O_3$, mineral bound $H_2O$, and $K_2O$. Magnesium, Ca, and Fe can substitute in the clay structure for other cations (Lee et al., 1984). In addition to the clays, Fe, Al, Mn, Ti, and other oxides and possibly more mineral-bound $H_2O$ are present in the soils. Carbon, nitrogen, and phosphorus represent potential activation elements from potential SNS beam loss; hence, they are also of interest.

Martin Marietta Energy Systems, Inc. (1993) conducted a study to determine background concentrations of metals and radionuclides on the ORR. Background concentrations determined for metals and radionuclides in soils overlying the Copper Ridge dolomite are summarized in Table 2.2. The concentration of nitrogen was estimated to be 0.034%; carbon, 0.18%; and phosphorous, 0.02% (Peters, 1970; Johnson et al., 1981; Johnson et al., 1986). The estimated overall soil composition (assuming a bulk density of 1.61 g/cm$^3$ and a moisture content of 0.24) is summarized in Table 2.3.

To provide a better estimate of the background concentration of carbon and nitrogen in the residuum beneath the SNS site, 33 samples from soil cores collected during the SNS geotechnical studies (Fig. 2.1) were analyzed by a high-temperature combustion method using a Carlo-Erba NA 1500™ Carbon Nitrogen Sulfur (CNS) analyzer. The samples analyzed were from a range of depths; however, it was assumed that the depth of interest would not extend below 317 m (1040 ft). Table 2.4 summarizes the results of the analysis, and Figs. 2.2 and 2.3 show the distribution of nitrogen and carbon with depth. The percent carbon appears to decrease somewhat with depth. The mean weight percent of nitrogen and carbon was 0.010% and 0.048%, respectively. Based on these results, it was assumed that the dry weight percent for nitrogen and carbon estimated from the existing literature is a reasonable upper-bound concentration for these elements.

**Table 2.2. Concentration of metals and radionuclides in Copper Ridge dolomite**

| Sample No. | [45,60,75] | [51,55,62] | [54,64,83] | [58,59,91] | Average | Average composition |
|---|---|---|---|---|---|---|
| Constituent | | | (μg/g or ppm) | | | (wt %) |
| | | | *Neutron activation analysis data* | | | |
| Al | 72,400 | 79,900 | 92,200 | 113,000 | 89,375 | 8.94E–00 |
| Sb | 1.81 | 1.77 | 1.69 | 2.45 | 1.93 | 1.93E–04 |
| As | 84.9 | 59.5 | 71.8 | 107 | 80.8 | 8.08E–03 |
| Ba | 81.2 | 83.8 | 318 | 111 | 148.5 | 1.49E–02 |
| Ce | 41.3 | 46.2 | 54.9 | 45.7 | 47.025 | 4.70E–03 |
| Cs | 4.11 | 4.88 | 4.77 | 6.17 | 4.9825 | 4.98E–04 |
| Cr | 74.5 | 58.5 | 66.2 | 86.6 | 71.45 | 7.15E–03 |
| Co | 4.22 | 5.89 | 5.17 | 4.07 | 4.8375 | 4.84E–04 |
| Eu | 0.34 | 0.39 | 0.5 | 0.36 | 0.3975 | 3.98E–05 |
| Ga | 19.3 | 17 | 22.9 | 8.6 | 16.95 | 1.70E–03 |
| Au | 0.01 | 0.01 | 0.01 | 0.01 | 0.01 | 1.00E–06 |
| Hf | 2.28 | 3.8 | 2.36 | 3.23 | 2.9175 | 2.92E–04 |
| Fe | 41,400 | 45,100 | 44,300 | 53,500 | 46,075 | 4.61E–00 |
| La | 35.8 | 38.9 | 36.6 | 41.6 | 38.225 | 3.82E–03 |
| Lu | 0.1 | 0.27 | 0.19 | 0.24 | 0.2 | 2.00E–05 |
| Mg | 4,810 | 4,540 | 5,730 | 5,750 | 5207.5 | 5.21E–01 |
| Mn | 87.1 | 139 | 120 | 108 | 113.525 | 1.14E–02 |
| Hg | 0.94 | 0.9 | 1.02 | 1.48 | 1.085 | 1.09E–04 |
| K | 6,270 | 6,980 | 9,410 | 8,690 | 7837.5 | 7.84E–01 |
| Rb | 430 | 365 | 1350 | 403 | 637 | 6.37E–02 |
| Sc | 10.6 | 10.1 | 12.7 | 14.4 | 11.95 | 1.20E–03 |
| Ag | 1.67 | 1.54 | 1.83 | 2.66 | 1.925 | 1.93E–04 |
| Na | 128 | 157 | 151 | 169 | 151.25 | 1.51E–02 |
| Tb | 0.19 | 0.35 | 0.35 | 0.48 | 0.3425 | 3.43E–05 |
| $^{232}$Th | 12.1 | 13.5 | 12.2 | 15.8 | 13.4 | 1.34E–03 |
| Ti | 2,800 | 4,180 | 2,800 | 3,690 | 3367.5 | 3.37E–01 |
| $^{235}$U | 0.04 | 0.04 | 0.05 | 0.05 | 0.045 | 4.50E–06 |
| $^{238}$U | 2.96 | 4.97 | 6.36 | 6.42 | 5.1775 | 5.18E–04 |
| V | 108 | 124 | 126 | 168 | 131.5 | 1.32E–02 |
| Yb | 2.1 | 3.07 | 2.91 | 2.73 | 2.7025 | 2.70E–04 |
| Zn | 249 | 250 | 263 | 243 | 251.25 | 2.51E–02 |
| | | | *Inorganic analysis ion-coupled plasma (ICP) data* | | | |
| Be | 0.62 | 0.81 | 0.9 | 0.96 | 0.8225 | 8.23E–05 |
| B | 5 | 5.4 | 5.4 | 5.9 | 5.425 | 5.43E–04 |
| Cd | 0.21 | 0.22 | 0.22 | 0.24 | 0.2225 | 2.23E–05 |
| Ca | 154 | 219 | 185 | 151 | 177.25 | 1.77E–02 |
| Cu | 23.7 | 31.7 | 33.5 | 35.9 | 31.2 | 3.12E–03 |
| CN | 0 | 0.99 | 1 | 0.99 | 0.745 | 7.45E–05 |
| Pb | 30.8 | 39.2 | 31.2 | 34.9 | 34.025 | 3.40E–03 |
| Li | 2.5 | 4 | 6.6 | 4.9 | 4.5 | 4.50E–04 |
| Ni | 12.5 | 14.8 | 21.3 | 15.8 | 16.1 | 1.61E–03 |
| Se | 0.66 | 1 | 0.7 | 1.3 | 0.915 | 9.15E–05 |
| Sr | 0.25 | 0.68 | 0.45 | 0.52 | 0.475 | 4.75E–05 |
| $SO_4$ | 10.5 | 17.2 | 11.1 | 12.4 | 12.8 | 1.28E–03 |
| Tl | 0.41 | 0.45 | 0.44 | 0.48 | 0.445 | 4.45E–05 |
| Total | | | | | | 1.54E+01 |

**Table 2.3. Overall composition of SNS soils**

| Component | Wt fraction | Wt % | Component | Wt fraction | Wt % | Component | Wt fraction | Wt % |
|---|---|---|---|---|---|---|---|---|
| Si | 2.22E–01 | 22.20 | N | 2.58E–04 | 2.58E–02 | Tb | 2.60E–07 | 2.60E–05 |
| O | 3.43E–01 | 34.32 | P | 1.52E–04 | 1.52E–02 | $^{232}$Th | 1.02E–05 | 1.02E–03 |
| $H_2O$(total) | 3.16E–01 | 31.60 | Sb | 1.47E–06 | 1.47E–04 | $^{235}$U | 3.42E–08 | 3.42E–06 |
| Al | 6.79E–02 | 6.79 | As | 6.14E–05 | 6.14E–03 | $^{238}$U | 3.93E–06 | 3.93E–04 |
| Fe | 3.50E–02 | 3.50 | Ba | 1.13E–04 | 1.13E–02 | V | 9.99E–05 | 9.99E–03 |
| C | 1.37E–03 | 0.14 | Ce | 3.57E–05 | 3.57E–03 | Yb | 2.05E–06 | 2.05E–04 |
| Mg | 3.96E–03 | 0.40 | Cs | 3.79E–06 | 3.79E–04 | Zn | 1.91E–04 | 1.91E–02 |
| K | 5.96E–03 | 0.60 | Cr | 5.43E–05 | 5.43E–03 | Be | 6.25E–07 | 6.25E–05 |
| Ti | 2.56E–03 | 0.26 | Co | 3.68E–06 | 3.68E–04 | B | 4.12E–06 | 4.12E–04 |
| | | 99.81 | Eu | 3.02E–07 | 3.02E–05 | Cd | 1.69E–07 | 1.69E–05 |
| | | | Ga | 1.29E–05 | 1.29E–03 | Ca | 1.35E–04 | 1.35E–02 |
| | | | Au | 7.60E–09 | 7.60E–07 | Cu | 2.37E–05 | 2.37E–03 |
| | | | Hf | 2.22E–06 | 2.22E–04 | CN | 5.66E–07 | 5.66E–05 |
| | | | La | 2.91E–05 | 2.91E–03 | Pb | 2.59E–05 | 2.59E–03 |
| | | | Lu | 1.52E–07 | 1.52E–05 | Li | 3.42E–06 | 3.42E–04 |
| | | | Mn | 8.63E–05 | 8.63E–03 | Ni | 1.22E–05 | 1.22E–03 |
| | | | Hg | 8.25E–07 | 8.25E–05 | Se | 6.95E–07 | 6.95E–05 |
| | | | Rb | 4.84E–04 | 4.84E–02 | Sr | 3.61E–07 | 3.61E–05 |
| | | | Sc | 9.08E–06 | 9.08E–04 | $SO_4$ | 9.73E–06 | 9.73E–04 |
| | | | Ag | 1.46E–06 | 1.46E–04 | Tl | 3.38E–07 | 3.38E–05 |
| | | | Na | 1.15E–04 | 1.15E–02 | | | 5.24E–02 |
| | | | | | 1.42E–01 | | | |
| Total wt % | | 100.00 | | | | | | |

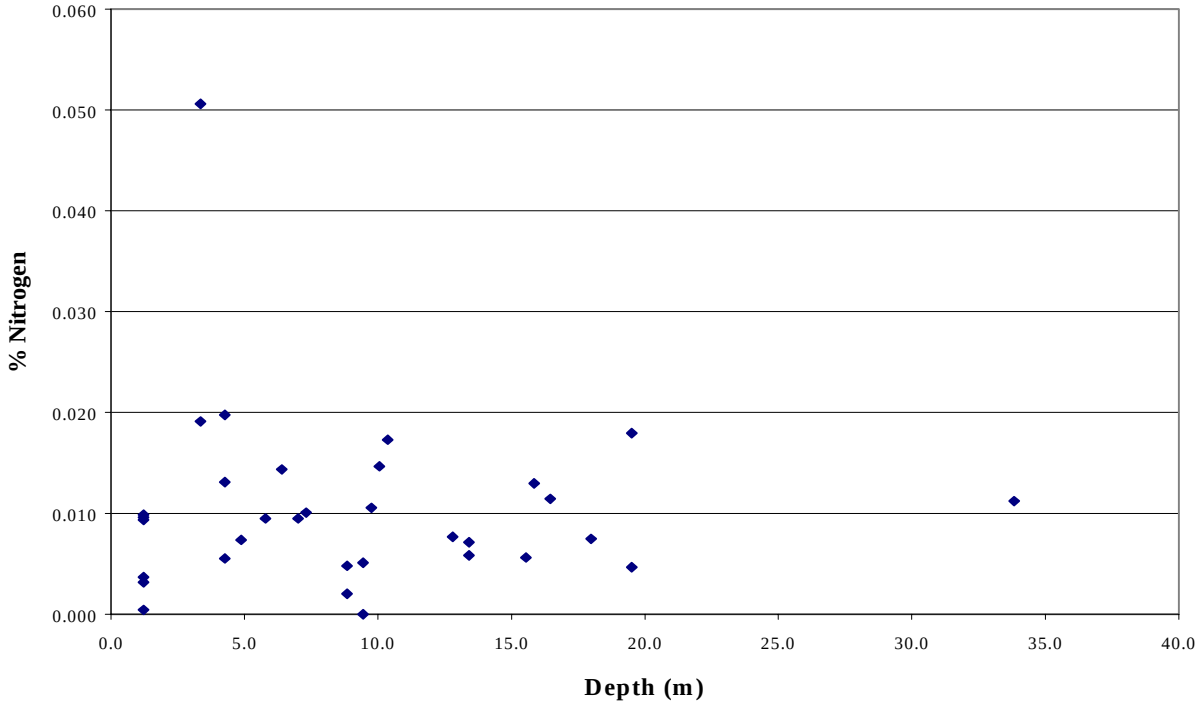


**Fig. 2.2. Nitrogen (wt %) in SNS soil cores.**

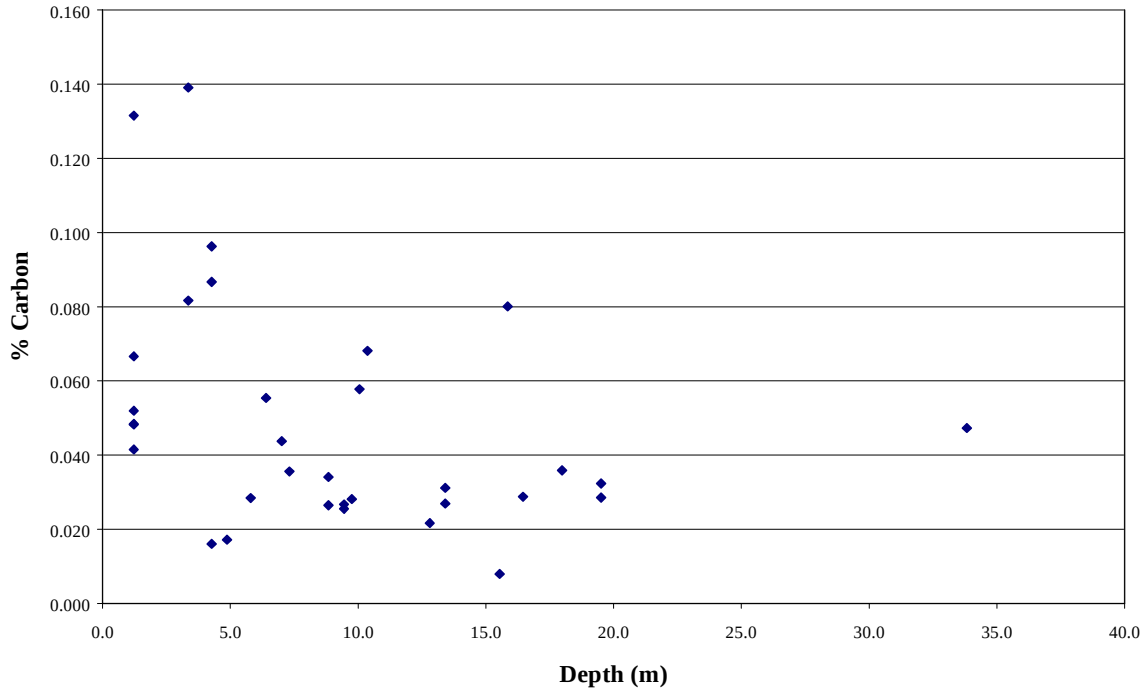


**Fig. 2.3. Total carbon (wt %) in SNS soil cores.**

**Table 2.4. Results of nitrogen and total carbon analyses**

| SNS core ID[a] | Depth | | Elevation | | Wt % | |
|---|---|---|---|---|---|---|
| | (m) | (ft) | (m) | (ft) | N | C |
| B10 S-1 TOP | 1.2 | 4 | 331.2 | 1086.8 | 0.000 | 0.132 |
| B10 S-3 TOP | 4.3 | 14 | 328.2 | 1076.8 | 0.020 | 0.096 |
| B10 S-4 TOP | 7.0 | 23 | 325.4 | 1067.8 | 0.009 | 0.044 |
| B10 S-6 TOP | 10.4 | 34 | 322.1 | 1056.8 | 0.017 | 0.068 |
| B10 S-8 TOP | 13.4 | 44 | 319.0 | 1046.8 | 0.007 | 0.027 |
| B12 S-1 BOT | 1.2 | 4 | 336.5 | 1103.9 | 0.004 | 0.042 |
| B12 S-3 TOP | 4.3 | 14 | 333.4 | 1093.9 | 0.006 | 0.016 |
| B12 S-6 TOP | 8.8 | 29 | 328.8 | 1078.9 | 0.005 | 0.034 |
| B12 S-13 TOP | 19.5 | 64 | 318.2 | 1043.9 | 0.018 | 0.032 |
| B14 S-2 TOP | 1.2 | 4 | 336.2 | 1103.0 | 0.010 | 0.067 |
| B14 S-4 TOP | 4.9 | 16 | 332.5 | 1091.0 | 0.007 | 0.017 |
| B14 S-7 TOP | 8.8 | 29 | 328.6 | 1078.0 | 0.002 | 0.026 |
| B14 S-10 TOP | 13.4 | 44 | 324.0 | 1063.0 | 0.006 | 0.031 |
| B14 S-13 TOP | 18.0 | 59 | 319.4 | 1048.0 | 0.007 | 0.036 |
| B16 S-3 TOP | 3.4 | 11 | 343.7 | 1127.8 | 0.051 | 0.139 |
| B16 S-7 TOP | 9.4 | 31 | 337.6 | 1107.8 | 0.000 | 0.026 |
| B16 S-11 TOP | 15.5 | 51 | 331.5 | 1087.8 | 0.006 | 0.008 |
| B16 S-23 TOP | 33.8 | 111 | 313.3 | 1027.8 | 0.011 | 0.047 |
| B2 S-3 TOP | 3.4 | 11 | 324.0 | 1062.9 | 0.019 | 0.082 |
| B2 S-5 TOP | 6.4 | 21 | 320.9 | 1052.9 | 0.014 | 0.055 |
| B2 S-7 TOP | 10.1 | 33 | 317.3 | 1040.9 | 0.015 | 0.058 |
| B4 S-1 | 1.2 | 4 | 320.4 | 1051.1 | 0.009 | 0.048 |
| B4 S-3 | 4.3 | 14 | 317.3 | 1041.1 | 0.013 | 0.087 |
| B6 S-2 | 1.2 | 4 | 334.8 | 1098.6 | 0.010 | 0.048 |
| B6 S-5 | 5.8 | 19 | 330.3 | 1083.6 | 0.010 | 0.028 |
| B6 S-7 | 9.8 | 32 | 326.3 | 1070.6 | 0.011 | 0.028 |
| B6 S-9B | 12.8 | 42 | 323.3 | 1060.6 | 0.008 | 0.022 |
| B6 S-11 | 15.8 | 52 | 320.2 | 1050.6 | 0.013 | 0.080 |
| B7 S-1 TOP | 1.2 | 4 | 337.9 | 1108.8 | 0.003 | 0.052 |
| B7 S-5 TOP | 7.3 | 24 | 331.9 | 1088.8 | 0.010 | 0.036 |
| B7 S-6 TOP | 9.4 | 31 | 329.7 | 1081.8 | 0.005 | 0.027 |
| B7 S-11 BOT | 16.5 | 54 | 322.7 | 1058.8 | 0.011 | 0.029 |
| B7 S-13 TOP | 19.5 | 64 | 319.7 | 1048.8 | 0.005 | 0.029 |
| Mean—all samples | | | | | 0.010 | 0.048 |
| Minimum | | | | | 0.000 | 0.008 |
| Maximum | | | | | 0.051 | 0.139 |
| Mean shallow samples, 1.2–1.7 m (4.0–5.5 ft) depth | | | | | 0.006 | 0.065 |
| Mean intermediate samples | | | | | 0.011 | 0.043 |
| Mean deep samples <373.7 m (1050 ft) elevation | | | | | 0.011 | 0.049 |

[a]ID = identifier.

### 2.2.3 SNS Site Hydrology

Studies for the ORR [e.g., Solomon et al., 1992 (pp. 1–5)] indicate that the mean annual precipitation in the period 1954 to 1983 was 133 cm, with extreme values of 90 and 190 cm during that same period. An average of 76 cm of water is consumed by evapotranspiration, and the remaining 57 cm is discharged as stream flow (combined surface runoff and groundwater flow). A hydraulic conductivity for the Knox shallow saturated zone was assumed to be ~24.4 cm/d (0.8 ft/d) based on a regional groundwater flow model developed for the Bear Creek Valley and Upper East Fork Poplar Creek Watershed remedial investigation and feasibility studies (DOE, 1997). The hydrologic gradient is 0.02 (dimensionless).

#### 2.2.3.1 Groundwater recharge

Hydrographic analyses and modeling results, which attempt to separate storm runoff from the much slower responding groundwater flow, indicate that between 47 and 35% of all stream flow is likely to be associated with groundwater in an average year (Huff, 1998; ORNL/GWPO-027, p. 6). This translates to a range from 20.0 to 26.8 cm of annual groundwater flow for an average year. It should be noted, however, that estimates of delayed flow, based only on hydrograph separation, represent as much as 86% of stream flow (Johnson et al., 1982). This places a possible upper limit of about 49 cm on annual groundwater recharge (if there were no perched zones of saturation), and all subsurface flow was assumed to move vertically downward to the water table before being discharged.

#### 2.2.3.2 Depth to groundwater

The depth to the saturated zone (perennial water table) on Chestnut Ridge has been studied. Monitoring wells that were installed at Walker Branch Watershed, ~2.5 km west of the SNS site, indicated a typical depth to permanent groundwater of about 30 m. This does not include transient zones of perched water, which may form during major storms and persist for up to a few weeks. These zones generally are believed to be associated with impeding layers and will discharge to springs or seeps and thus to the stream flow that is associated with storms or the recession of the hydrograph that follows a major storm event.

## 2.3 REFERENCES


Dole, L. R., September 1998, *Preliminary Assessment of the Nuclide Migration from the Activation Zone around the Proposed Spallation Neutron Source Facility*, ORNL/TM-13665, Lockheed Martin Energy Research Corp., Oak Ridge National Laboratory, Oak Ridge, Tennessee.

Harris, W. F., 1977, "Walker Branch Watershed: Site Description and Research Scope," pp. 4–17 in *Watershed Research in Eastern North America. A Workshop to Compare Results*, D. L. Correll, ed., Chesapeake Bay Center for Environmental Studies, Smithsonian Institution, Edgewater, Maryland.

Hatcher, R. D. Jr., et al., 1992, *Status Report on the Geology of the Oak Ridge Reservation*, ORNL/TM-12074, Lockheed Martin Energy Research Corp., Oak Ridge National Laboratory, Oak Ridge, Tennessee

Huff, D. D., 1998, *Environmental Sciences Division Groundwater Program Office Report for Fiscal Years 1995–1997*, ORNL/GWPO-027, Lockheed Martin Energy Research Corp., Oak Ridge National Laboratory, Oak Ridge, Tennessee.

Jardine, P. M., G. V. Wilson, and R. J. Luxmoore, 1988, "Modeling the Transport of Inorganic Ions Through Undisturbed Soil Columns from Two Contrasting Watersheds," *Soil Sci. Soc. Am. J.*, **52**, 1252–1259.

Johnson, D. W., et al., 1981, *Chemical Characteristics of Two Forested Ultisols and Two Forested Inceptisols Relevant to Anion Production and Mobility*, ORNL/TM-7646, Lockheed Martin Energy Research Corp., Oak Ridge National Laboratory, Oak Ridge, Tennessee.

Johnson, D. W., et al., 1986, "Factors Affecting Anion Movement and Retention in Four Forest Soils," *Soil Science Soc. Am. J.*, **50**, 776–783.

Johnson, D. W., et al., 1982, "Cycling of Organic and Inorganic Sulphur in a Chestnut Oak Forest," *Oecologia*, **54**, 141–148.

Law Engineering and Environmental Services, Inc., 1998, *Report of Phase II Geotechnical Exploration, The Spallation Neutron Source*, Oak Ridge, Tennessee.

Lee S. Y., O. C. Kopp, and D. A. Lietzke, 1984, *Mineralogical Characterization of West Chestnut Ridge Soils*, ORNL/TM-9361, Lockheed Martin Energy Research Corp., Oak Ridge National Laboratory, Oak Ridge, Tennessee.

Lietzke, D. A., R. H. Ketelle, and R. R. Lee, 1989, *Soils and Geomorphology of the East Chestnut Ridge Site*, ORNL/TM-11364, Lockheed Martin Energy Research Corp., Oak Ridge National Laboratory, Oak Ridge, Tennessee.

Martin Marietta Energy Systems, Inc., 1993, *Final Report on Background Soil Characterization Project at the Oak Ridge Reservation*, DOE/OR/01-1175, ES/ER/TM-84, Oak Ridge, Tennessee.

Oak Ridge National Laboratory, May 1997, *National Spallation Neutron Source (SNS) Conceptual Design Report*, Vol. 1, NSNS/CDR-2/V1, Oak Ridge, Tennessee.

Peters, L. N., et al., 1970, *Walker Branch Watershed Project: Chemical, Physical and Morphological Properties of the Soils of Walker Branch Watershed*, ORNL/TM-2968, Union Carbide Corp.–Nuclear Division, Oak Ridge National Laboratory, Oak Ridge, Tennessee.

Solomon, D. K., et al., 1992, *Status Report, A Hydrologic Framework for the Oak Ridge Reservation*, ORNL/TM-12026, Lockheed Martin Energy Research Corp., Oak Ridge National Laboratory, Oak Ridge, Tennessee.

Stockdale, P. B., 1951, *Geologic conditions at the Oak Ridge National Laboratory (X-10) area relevant to the disposal of radioactive waste*, ORO-58, U.S. Atomic Energy Commission, Washington, D.C.

U.S. Department of Energy, 1997, *Feasibility Study for Bear Creek Valley at the Oak Ridge Y-12 Plant, Oak Ridge, Tennessee*, DOE/OR/02-1525/D1, Oak Ridge Tennessee.

# 3. ACTIVATION PRODUCTS IN THE SNS SHIELD BERM

Accelerators produce particles that diffuse outward from the core of the beam and are periodically redirected by focusing magnets back into the core of the beam. These particles form a halo. These high-energy particles strike beam-line components, and, as these high-energy particles (GeV)* collide with the matter in magnets and other parts of the SNS structure, they initiate a series of nuclear interactions. These interactions are called "stars." These stars produce secondary particles, which also interact with their surrounding matter, producing more stars in a cascade until the stars' particle energies fall below the thresholds for further nuclear reactions (MeV).

Some of these secondary particles escape the beam-line components, causing star cascades in the accelerator tunnel structures and surrounding soil and activating the adjacent soils used for shielding. The quantities of activation products in the adjacent berm are proportional to the number of stars produced in the shield's soil minerals and pore water. Analyses have shown that 99.9% of the activation products in this activation zone are contained within the first 4 m perpendicular to the beam tunnel (Bull et al., November 1997) and beyond the outer surface of the tunnel's concrete structure. A general approximation is that the star density decreases by a factor of ten times ($10^{-1}$) for each meter of soil shielding.

Table 3.1 lists the principal long-lived isotopes that are estimated to build up in the shield-berm's activation zone assuming 30 years of continuous operations at 1 MW (see Sect. 3.1). These are very conservative estimates (i.e., high) because the beam does not operate continuously over its years of projected facility life. Therefore, these estimates of nuclide concentrations are much higher than actually expected. Also, one of the design goals for the facility is to significantly reduce beam leakage, which should in turn significantly reduce the actual concentrations of these activation products.

**Table 3.1. Principal long-lived radioisotopes produced in the SNS shield berm and their characteristics**

| Isotope | Half-life (year) | Specific activity (Ci/g-atom) | Gram-atomic weight (g) | Ci/g | g/Ci | Decay mode(s), energies in MeV |
|---|---|---|---|---|---|---|
| $^{3}$H | 1.26E+01 | 2.84E+04 | 3.016050 | 9.42E+03 | 1.06E–04 | –Beta = 0.0186 (max) |
| $^{10}$Be | 2.50E+06 | 1.43E–01 | 10.013534 | 1.43E–02 | 7.00E+01 | –Beta = 0.55 (max) |
| $^{14}$C | 5.73E+03 | 6.24E+01 | 14.003242 | 4.46E+00 | 2.24E–01 | –Beta = 0.156 (max_average) |
| $^{22}$Na | 2.62E+00 | 1.37E+05 | 21.994437 | 6.21E+03 | 1.61E–04 | +Beta = 1.82 (max, 0.05%), gamma = 1.275 (100%), 0.511 (180%) |
| $^{26}$Al | 7.40E+05 | 4.84E–01 | 25.986891 | 1.86E–02 | 5.37E+01 | +Beta = 1.17 (max) gamma = 0.511 (170%), 1.12 (4%), 1.81 (100%) |
| $^{36}$Cl | 3.08E+05 | 1.16E+00 | 35.968309 | 3.23E–02 | 3.10E+01 | –Beta = 0.714 (max) x-ray = 0.511 (0.003%) |
| $^{39}$Ar | 2.69E+02 | 1.33E+03 | 38.964317 | 3.41E+01 | 2.93E–02 | –Beta = 0.565 (max) |

*Giga electron volt » 1.60219 ´ $10^{-10}$ × J; J = N × m.

**Table 3.1. (continued)**

| Isotope | Half-life (year) | Specific activity (Ci/g-atom) | Gram-atomic weight (g) | Ci/g | g/Ci | Decay mode(s), energies in MeV |
|---|---|---|---|---|---|---|
| $^{40}$K | 1.26E+09 | 2.84E–04 | 39.964000 | 7.11E–06 | 1.41E+05 | -Beta = 1.314 (max)<br>+beta = 0.483 (max)<br>x-ray = 1.46 (11%) |
| $^{41}$Ca | 8.00E+04 | 4.47E+00 | 40.955000 | 1.09E–01 | 9.16E+00 | Potassium x-rays |
| $^{53}$Mn | 1.90E+06 | 1.88E–01 | 52.941295 | 3.56E–03 | 2.81E+02 | Cr x-rays |
| $^{54}$Mn | 8.30E–01 | 1.57E+08 | 53.940362 | 2.92E+06 | 3.43E–07 | Cr x-rays, 0.835 (100%)<br>electron = 0.829 |
| $^{55}$Fe | 2.60E+00 | 1.38E+05 | 54.938299 | 2.50E+03 | 3.99E–04 | Mn x-rays,<br>bremstrahlung to 0.23<br>(0.0004%) |

In one diffusion case (Sect. 4), this study assumes that these activation products remain in the matrix of the berm and do not begin to move until the end of the facilities' operations. This ensures that this study is based on the maximum credible or "incredible" starting concentrations of activation products. In a second diffusion case (Sect. 4) and two advective cases (Sect. 5), this study assumes that the nuclides begin to decay and diffuse immediately after generation. Also, this study assumes that the inventory of activation products within the tunnel's concrete structure does not contribute significantly to the inventory of mobile nuclides.

## 3.1 ACTIVATION ANALYSES

An analysis of the conceptual design of the proposed SNS proton beam transport system (LINAC, HEBT, ring, and RTBT) was performed to address the potential environmental impacts of operating the facility as planned. Neutron activation of soil in the earth berm shielding could lead to contamination of groundwater if a mechanism exists for migration of radioactive nuclides to occur. Nuclide production rate data were calculated for a wide range of buildup and decay steps to bracket the potential source terms that may affect the environment and address the many additional environmental impact statement (EIS) and environment, safety, and health (ES&H) analyses that have to be performed. Interpretation of these data requires an understanding of the uncertainty associated with the analyses.

The radiation transport analysis, which includes the accelerator and target station neutronics, shielding, and activation analyses, is important for the construction of the SNS. The potential activation products impact the conventional facility during maintenance operations. The costs associated with incorporating the results of the radiation transport analysis are a significant part of the total facility costs.

Therefore, activation analysis is one of the important components in the radiation transport analysis which will impact conventional facility design and all maintenance operations. Activation analyses are required to determine the radioactive waste streams, on-line material processing requirements (mercury, liquid hydrogen, cooling water, etc.), remote handling and maintenance requirements, and potential site contamination. The analyses are also required to determine background levels within all parts of the facility for normal operation and postulated accident scenarios. For the SNS proton beam transport systems, beam control and focus requirements are being designed to keep the activation of the structure low enough such as to allow hands-on maintenance in the LINAC and ring tunnels. The environmental impact of these

requirements needs to be assessed to be certain that site contamination is below regulatory concern. A strategy using coupled high-energy ($E$) ($E$ > 20 MeV) and low-energy ($E$ < 20 MeV) Monte Carlo calculations, along with a depletion and isotope production code, has been implemented to perform the activation analyses on the proton beam transport system conceptual design.

### 3.1.1 Activation Analysis Calculation Methodology

A flow diagram of the activation analysis methodology used in the conceptual design of the SNS is shown in Fig. 3.1. The analysis flow can be divided into two parts: (1) the radiation transport calculation; and (2) the activation calculation. These two components are described in the following subsections.

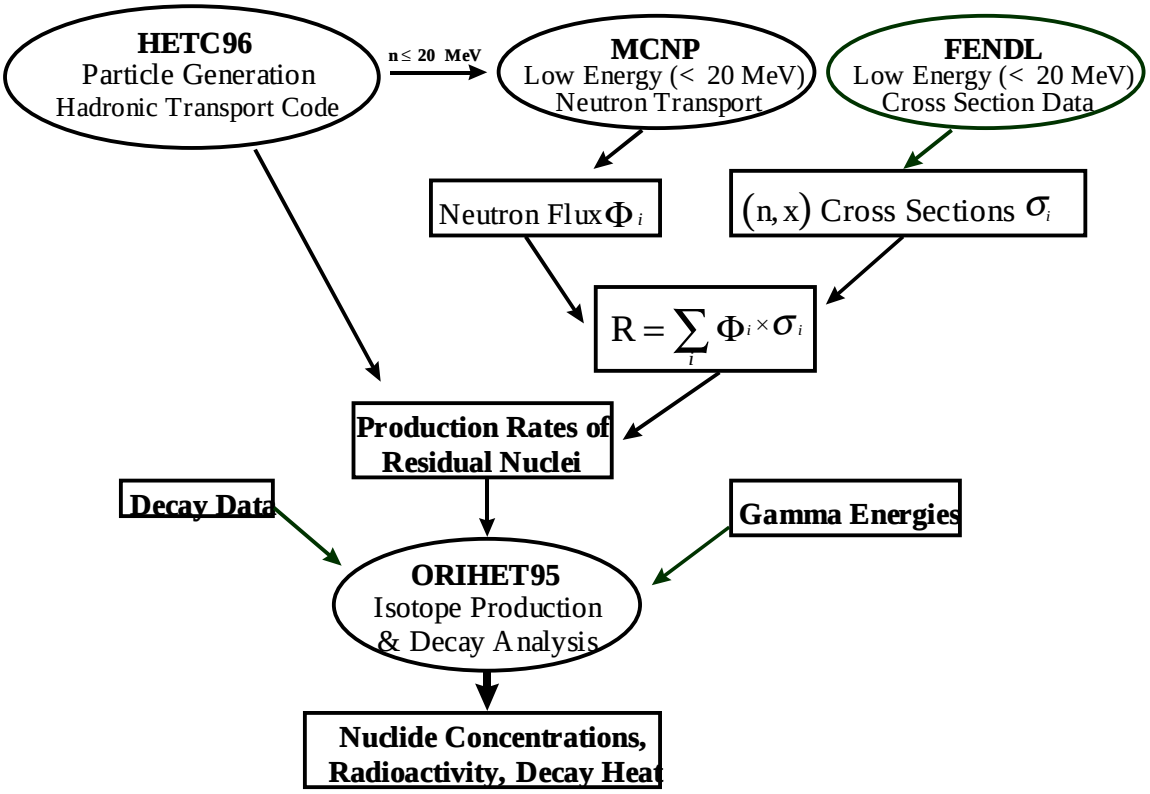


**Fig. 3.1. A flow diagram of the SNS activation analyses.**

### 3.1.2 Radiation Transport Calculations

The CALOR96 code system (Gabriel et al., 1997) is the main calculational tool used for the numerical radiation transport analysis. The three-dimensional, multimedia, High-Energy (nucleon-meson) Transport Code—HETC96—was used to obtain a detailed description of the nucleon-meson cascade. This Monte Carlo code takes into account the slowing down of charged particles via the continuous slowing-down approximation, the decay of charged pions and muons, and inelastic nucleon-nucleus and charged-pion-nucleus (excluding hydrogen) collisions through the use of a multitude of high-energy physics models.

In particular, HETC96 uses (1) an intermediate-energy, intranuclear-cascade evaporation model ($E$ < 3 GeV); (2) an intermediate-energy intranuclear-cascade-preequilibrium evaporation model ($E$ < 2 GeV); (3) a scaling model (3 GeV < $E$ < 5 GeV) and a multichain fragmentation model ($E$ > 5 GeV); and (4) inelastic nucleon-hydrogen and charged-pion-hydrogen collisions via the isobar model ($E$ < 3 GeV) and a fragmentation model ($E$ > 3 GeV). Also, this model accounts for elastic neutron-nucleus ($E$ < 100 MeV) collisions, and elastic nucleon and charged-pion collisions with hydrogen. The intranuclear-cascade-evaporation model and the intranuclear-cascade-preequilibrium evaporation model are the principal physics models in the HETC96 code used in these SNS analyses.

These models have been used for a variety of calculations and agree quite well with experimental results. For the SNS analyses, the Monte Carlo Neutron Photon (MCNP) code (Briesmeister, September 1986) was coupled to HETC96 in order to provide the proper source for the low-energy ($E$ < 20 MeV) neutron transport. MCNP is a general purpose, continuous-energy, generalized geometry, time-dependent, coupled neutron-photon-electron Monte Carlo transport code system. These transport code calculations provide the necessary information for the activation analyses such as nuclide production rates and neutron flux.

### 3.1.3 Activation Calculations

The HETC and MCNP codes provide the required input data for the isotope generation and depletion code, ORIGEN for HETC (ORIHET95) (Cloth et al., 1988), which uses a matrix-exponential method to study the buildup and decay of activity for any system for which the nuclide production rates are known. The combination of these two sources yield the radionuclide concentrations, radioactivity, and time-dependent decay gamma source spectra, as a function of generation (buildup) time and depletion (decay), for input into the Anisotropic Sn-Theory (ANISN) or discrete ordinates deterministic transport (DORT) codes.

The principal component of the activation analysis is the calculation by ORIHET95, an isotope generation and depletion code. As shown in the Fig. 3.1, HETC96 directly provides nuclide production rates as one of the calculation results. To obtain the nuclide production rates due to neutrons with energies below 20 MeV, reaction rates were calculated using the nuclear database, the Fusion Evaluated Nuclear Data Library (FENDL) Activation Library (Pashchenko and McLaughlin, 1995), and neutron fluxes calculated by MCNP. The FENDL Activation Library contains point-wise cross sections for all stable and unstable target nuclides with half-lives longer than 0.5 d and includes 636 target nuclides with ~11,000 reactions with nonzero cross sections below 20 MeV. Group-averaged cross sections were generated by an evaluated nuclear data file/edition B (ENDF/B) utility program, GROUPIE (Cullen, 1994), to match the energy bin structure of the MCNP calculations to calculate the nuclide production rates. Nuclide production rates for certain components were calculated by.

$$R_i = \Sigma_k \, \phi_j \, \sigma_k \, N_l \, V_j \, f_1 \, f_2 \, / \, A, \; k = 1,...,n \tag{3.1}$$

where

$R_i$ = production rate of nuclide $i$ ($g \cdot mol \cdot s^{-1}$),
$\phi_j$ = neutron flux in component $j$ ($cm^{-2}$),
$\sigma_k$ = group averaged cross section of $(n,x)$ reaction which produces nuclide $i$ ($cm^2$),
$N_l$ = number density of precursor of nuclide $i$ via $k$th reaction ($cm^{-3}$),
$V_j$ = volume of component $j$ ($cm^3$),
$f_1$ = number of protons per second ($s^{-1}$),
$f_2$ = normalization factor to get neutron flux per incident proton,

$A$ = Avogadro's number [$(g \cdot mol)^{-1}$],
$n$ = number of reactions which produce nuclide $i$ in component $j$.

In the activation analyses of the SNS, production rates of gaseous light nuclides ($^{1}H$, $^{2}H$, $^{3}H$, $^{3}He$, and $^{4}He$) were also required. These gas production rates were also calculated via Eq. (3.1) using cross sections of interactions that result in producing the gaseous light nuclides. The calculated gas production rates were included in the nuclide production rates. Nuclide production rates due to neutrons with energies below 20 MeV were combined with those calculated from HETC96 directly. The combined nuclide production rate data were used as input data to ORIHET95.

#### 3.1.3.1 ORIHET95 calculation

ORIHET95 was developed from the original Oak Ridge Isotope GENeration and depletion code, ORIGEN (Croff, 1980), which utilizes matrix-exponential methods to study the buildup and decay of nuclide in reactor cores. The ORIHET95 code was designed to study the buildup and decay of activity in any system for which the nuclide production rates are known. Nuclides treated in the code are constructed from input production rates of the problem and nuclide decay libraries.

The code uses a nuclide data library, which contains information on half-lives and decay modes of the nuclides, and a gamma data library, which contains the number of gamma lines and their energies. These libraries were accompanied with the distribution of the code. The nuclide library was taken from the original ORIGEN library and from the 7th edition of the *Table of Isotopes* (Leder et al., 1978). The gamma library was used to calculate gamma-ray spectra and was formed from an edited version of the Darmstadt gamma-ray atlas (Reuss et al., 1972).

Since the incident proton energy was 1 GeV in the present analyses, it was possible to produce nuclides which were not listed in the libraries. It was found that the production of unlisted nuclides could be ignored because their half-lives were always very short and they decayed into short-lived nuclides without emitting gamma rays. Also, production rates of these nuclides were smaller than were those of the main contributors to the activities by several orders of magnitude.

The output of the ORIHET95 calculation includes (1) nuclide concentrations in units of g·mol/s and curies (Ci), (2) gamma-ray spectra, and (3) energy deposition in units of joules (J) and watts (W). These outputs can be obtained for both buildup and decay and for arbitrary time sequences.

### 3.2 MODEL FOR ACTIVATION CALCULATIONS

To perform the activation analysis on the LINAC, HEBT, ring, and RTBT tunnels a simplified model was constructed. For the LINAC and HEBT components, a section of the tunnel was modeled as a cylindrical shell of concrete 2300 mm in radius, 460 mm thick, and 30 m long. The tunnel was filled with air and surrounded by ~9 m of earth berm for shielding. The earth berm was divided into segments to determine the distribution of radionuclide products in the soil as a function of radius. Within the berm, a 0.5-m-thick region of limestone rock was included as a capillary break.

This source would overestimate the neutron source entering the earth berm due to proton interactions in the accelerator structure. Consequently, the amount of ground activation due to this source would also be overestimated and yield an upper limit of the radionuclide production due to normal operation of the facility. An equivalent model for the ring and RTBT tunnels was

constructed—except the radius of the concrete shell was 3200 mm. The details of the calculational model are given in Table 3.2.

Schematic diagrams of the model are given in Figs. 3.2 and 3.3. The details of the material information (i.e., elements, number densities, and composition) are given in Tables 3.3 and 3.4 and Fig. 3.4. Activation analyses were performed with these models to assess the potential radioactive by-products generated in all of the components as a function of normal operation of the SNS facility using the methodology discussed in Sects. 3.1.1 and 3.1.2.

**Table 3.2. HETC and MCNP calculational model details**

| MCNP zone number | Inner radius (cm) | Outer radius (cm) | Volume ($cm^3$) | Material |
|---|---|---|---|---|
| 1002 | 0.00 | 7.50 | 1.76715E+04 | Copper |
| 1003 | 7.50 | 230.00 | 4.83245E+08 | Air |
| 1001 | | | 2.26005E+07 | Cable tray |
| 1004 | 230.00 | 275.72 | 2.20966E+08 | Concrete |
| 1005 | 275.72 | 325.72 | 2.87390E+08 | Soil |
| 1006 | 325.72 | 375.72 | 3.35173E+08 | Soil |
| 1007 | 375.72 | 475.72 | 8.13698E+08 | Soil |
| 1008 | 475.72 | 575.72 | 1.00483E+09 | Soil |
| 1009 | 575.72 | 675.72 | 1.19597E+09 | Soil |
| 1010 | 675.72 | 725.72 | 6.69659E+08 | Limestone |
| 1011 | 725.72 | 1101.00 | 6.55144E+09 | Soil |

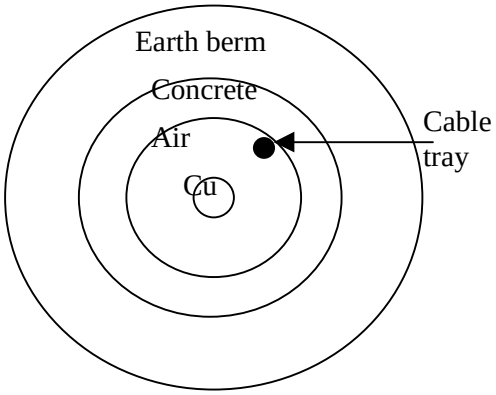


**Fig. 3.2. Schematic diagram of accelerator tunnel calculation model.**

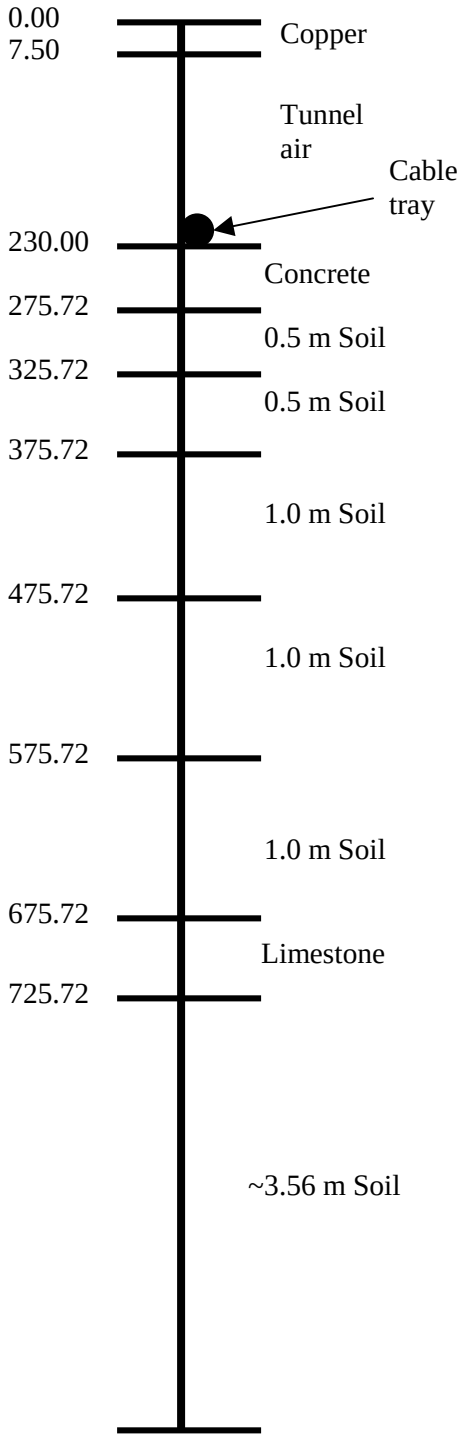


**Fig. 3.3. Schematic diagram of the HETC and MCNP models and their material zone radial boundaries.**

**Table 3.3. Calculational model material number densities (atoms/barn-cm)**

| Cross section type | Nuclide Z | Nuclide A | Number density | HETC/MCNP input |
|---|---|---|---|---|
| | | | | |
| *Copper Ridge dolomite soil* | | | | |
| Isotopic abundance | 1 | 1 | 2.5851E–02 | 2.5851E–02 |
| Isotopic abundance | 1 | 2 | 3.8782E–06 | 3.8782E–06 |
| Natural element | 6 | 12 | 1.2137E–04 | 1.2272E–04 |
| | 6 | 13 | 1.3499E–06 | |
| Isotopic abundance | 7 | 14 | 1.9804E–05 | 1.9804E–05 |
| Isotopic abundance | 7 | 15 | 7.3546E–08 | 7.3546E–08 |
| Isotopic abundance | 8 | 16 | 3.5956E–02 | 3.5956E–02 |
| Isotopic abundance | 8 | 17 | 1.4417E–05 | 1.4417E–05 |
| | 8 | 18 | 7.2085E–05 | |
| Isotopic abundance | 11 | 23 | 5.3873E–06 | 5.3873E–06 |
| Natural element | 12 | 24 | 1.3859E–04 | 1.7545E–04 |
| | 12 | 25 | 1.7545E–05 | |
| | 12 | 26 | 1.9317E–05 | |
| Isotopic abundance | 13 | 27 | 2.7125E–03 | 2.7125E–03 |
| Natural element | 14 | 28 | 7.8557E–03 | 8.5175E–03 |
| | 14 | 29 | 3.9777E–04 | |
| | 14 | 30 | 2.6404E–04 | |
| Isotopic abundance | 15 | 31 | 5.2875E–06 | 5.2875E–06 |
| Natural element | 19 | 39 | 1.5308E–04 | 1.6415E–04 |
| | 19 | 40 | 1.9205E–08 | |
| | 19 | 41 | 1.1047E–05 | |
| Natural element | 20 | 40 | 3.5108E–06 | 3.6216E–06 |
| | 20 | 42 | 2.3431E–08 | |
| | 20 | 43 | 4.8891E–09 | |
| | 20 | 44 | 7.5545E–08 | |
| | 20 | 46 | 1.4486E–10 | |
| | 20 | 48 | 6.7723E–09 | |
| Natural element | 22 | 46 | 4.7527E–06 | 5.7609E–05 |
| | 22 | 47 | 4.2861E–06 | |
| | 22 | 48 | 4.2469E–05 | |
| | 22 | 49 | 3.1166E–06 | |
| | 22 | 50 | 2.9841E–06 | |
| Natural element | 23 | 50 | 5.2845E–09 | 2.1138E–06 |
| | 23 | 51 | 2.1085E–06 | |
| Isotopic abundance | 25 | 55 | 1.6921E–06 | 1.6921E–06 |
| Natural element | 26 | 54 | 3.9523E–05 | 6.7561E–04 |
| | 26 | 56 | 6.1987E–04 | |
| | 26 | 57 | 1.4323E–05 | |
| | 26 | 58 | 1.8917E–06 | |
| | 30 | 64 | 1.5291E–06 | |
| | 30 | 66 | 8.7783E–07 | |
| | 30 | 67 | 1.2900E–07 | |
| | 30 | 68 | 5.9152E–07 | |

**Table 3.3. (continued)**

| Cross section type | Nuclide Z | Nuclide A | Number density | HETC/MCNP input |
|---|---|---|---|---|
| | | | | |
| | 30 | 70 | 1.8878E–08 | |
| Isotopic abundance | 37 | 85 | 4.4040E–06 | 4.4040E–06 |
| Isotopic abundance | 37 | 87 | 1.6991E–06 | 1.6991E–06 |
| | 56 | 130 | 9.3862E–10 | |
| | 56 | 132 | 8.9435E–10 | |
| | 56 | 134 | 2.1429E–08 | |
| | 56 | 135 | 5.8380E–08 | |
| | 56 | 136 | 6.9511E–08 | |
| | 56 | 137 | 9.9441E–08 | |
| Isotopic abundance | 56 | 138 | 6.3490E–07 | 6.3490E–07 |
| | 65 | 159 | 1.7647E–09 | |
| | | | **Soil total** | **T. (MCNP)** |
| | | | **7.4371E–02** | **7.4296E–02** |
| | | | | |
| **Cable tray** | | | | |
| Isotopic abundance | 1 | 1 | 5.9745E–03 | 5.9745E–03 |
| Isotopic abundance | 1 | 2 | 8.9631E–07 | 8.9631E–07 |
| Natural element | 6 | 12 | 3.8490E–03 | 3.8918E–03 |
| | 6 | 13 | 4.2820E–05 | |
| Isotopic abundance | 7 | 14 | 3.3580E–05 | 3.3580E–05 |
| Isotopic abundance | 7 | 15 | 1.2470E–07 | 1.2470E–07 |
| Isotopic abundance | 8 | 16 | 4.5800E–04 | 4.5800E–04 |
| Isotopic abundance | 8 | 17 | 1.8360E–07 | 1.8360E–07 |
| | 8 | 18 | 9.1820E–07 | |
| Natural element | 17 | 35 | 1.1660E–03 | 1.5388E–03 |
| | 17 | 37 | 3.7280E–04 | |
| Natural element | 18 | 36 | 6.7930E–10 | 2.0151E–07 |
| | 18 | 38 | 1.2700E–10 | |
| | 18 | 40 | 2.0070E–07 | |
| Natural element | 29 | 63 | 1.9620E–03 | 2.8365E–03 |
| | 29 | 65 | 8.7450E–04 | |
| | | | **Cable tray total** | **T. (MCNP)** |
| | | | **1.4736E–02** | **1.4735E–02** |
| | | | | |
| **Portland concrete** | | | | |
| Isotopic abundance | 1 | 1 | 7.9740E–03 | 7.9740E–03 |
| Isotopic abundance | 8 | 16 | 4.3860E–02 | 4.3860E–02 |
| Isotopic abundance | 11 | 23 | 1.3360E–03 | 1.3360E–03 |
| Natural element | 12 | 24 | 1.1740E–04 | 1.4862E–04 |
| | 12 | 25 | 1.4860E–05 | |
| | 12 | 26 | 1.6360E–05 | |
| Isotopic abundance | 13 | 27 | 2.3890E–03 | 2.3890E–03 |
| Natural element | 14 | 28 | 1.4570E–02 | 1.5801E–02 |
| | 14 | 29 | 7.4260E–04 | |

**Table 3.3. (continued)**

| Cross section type | Nuclide Z | Nuclide A | Number density | HETC/MCNP input |
|---|---|---|---|---|
| | | | | |
| | 14 | 30 | 4.8820E–04 | |
| Natural element | 19 | 39 | 6.4510E–04 | 6.9306E–04 |
| | 19 | 41 | 4.7960E–05 | |
| Natural element | 20 | 40 | 2.8270E–03 | 2.9155E–03 |
| | 20 | 42 | 1.8660E–05 | |
| | 20 | 43 | 4.2270E–06 | |
| | 20 | 44 | 6.0050E–05 | |
| | 20 | 46 | 9.6190E–08 | |
| | 20 | 48 | 5.4270E–06 | |
| Natural element | 26 | 54 | 1.8210E–05 | 3.1279E–04 |
| | 26 | 56 | 2.8670E–04 | |
| | 26 | 57 | 6.8500E–06 | |
| | 26 | 58 | 1.0320E–06 | |
| | | | **Concrete total** | **T. (MCNP)** |
| | | | **7.5430E–02** | **7.5430E–02** |
| | | | | |
| **Copper** | | | | |
| Natural element | 29 | 63 | 5.8750E–02 | 8.4940E–02 |
| | 29 | 65 | 2.6190E–02 | |
| | | | **Copper total** | **T. (MCNP)** |
| | | | **8.4940E–02** | **8.4940E–02** |
| | | | | |
| **Air** | | | | |
| Isotopic abundance | 1 | 1 | 6.1220E–07 | 6.1220E–07 |
| Natural element | 18 | 40 | 2.3834E–07 | 2.3834E–07 |
| Isotopic abundance | 7 | 14 | 3.9851E–05 | 3.9851E–05 |
| Isotopic abundance | 8 | 16 | 1.0957E–05 | 1.0957E–05 |
| | | | **Air total** | **T. (MCNP)** |
| | | | **5.1659E–05** | **5.1659E–05** |
| | | | | |
| **Limestone** | | | | |
| Natural element | 6 | 12 | 1.2430E–02 | 1.2568E–02 |
| | 6 | 13 | 1.3830E–04 | |
| Isotopic abundance | 8 | 16 | 3.7620E–02 | 3.7620E–02 |
| Isotopic abundance | 8 | 17 | 1.5090E–05 | 1.5090E–05 |
| | 8 | 18 | 7.5430E–05 | |
| Natural element | 20 | 40 | 1.2190E–02 | 1.2575E–02 |
| | 20 | 42 | 8.1340E–05 | |
| | 20 | 43 | 1.6970E–05 | |
| | 20 | 44 | 2.6220E–04 | |
| | 20 | 46 | 5.0290E–07 | |
| | 20 | 48 | 2.3510E–05 | |
| Natural element | 6 | 12 | 4.9730E–03 | 5.0283E–03 |
| | 6 | 13 | 5.5320E–05 | |

**Table 3.3. (continued)**

| Cross section type | Nuclide Z | Nuclide A | Number density | HETC/MCNP input |
|---|---|---|---|---|
| | | | | |
| Isotopic abundance | 8 | 16 | 1.5050E–02 | 1.5050E–02 |
| Isotopic abundance | 8 | 17 | 6.0340E–06 | 6.0340E–06 |
| | 8 | 18 | 3.0170E–05 | |
| Natural element | 12 | 24 | 3.9720E–03 | 5.0286E–03 |
| | 12 | 25 | 5.0290E–04 | |
| | 12 | 26 | 5.5370E–04 | |
| Isotopic abundance | 8 | 16 | 6.4980E–04 | 6.4980E–04 |
| Isotopic abundance | 8 | 17 | 2.6060E–07 | 2.6060E–07 |
| | 8 | 18 | 1.3030E–06 | |
| Natural element | 14 | 28 | 3.2490E–04 | 3.5021E–04 |
| | 14 | 29 | 1.5210E–05 | |
| | 14 | 30 | 1.0100E–05 | |
| Isotopic abundance | 8 | 16 | 1.2090E–04 | 1.2090E–04 |
| Isotopic abundance | 8 | 17 | 4.8490E–08 | 4.8490E–08 |
| | 8 | 18 | 2.4240E–07 | |
| Isotopic abundance | 13 | 27 | 8.0810E–05 | 8.0810E–05 |
| Isotopic abundance | 8 | 16 | 9.9730E–05 | 9.9730E–05 |
| Isotopic abundance | 8 | 17 | 3.9990E–08 | 3.9990E–08 |
| | 8 | 18 | 1.9990E–07 | |
| Natural element | 26 | 54 | 3.8990E–06 | 6.6649E–05 |
| | 26 | 56 | 6.1150E–05 | |
| | 26 | 57 | 1.4130E–06 | |
| | 26 | 58 | 1.8660E–07 | |
| Isotopic abundance | 8 | 16 | 3.3900E–05 | 3.3900E–05 |
| Isotopic abundance | 8 | 17 | 1.3590E–08 | 1.3590E–08 |
| | 8 | 18 | 6.7970E–08 | |
| Natural element | 19 | 39 | 6.3390E–05 | 6.7973E–05 |
| | 19 | 40 | 7.9530E–09 | |
| | 19 | 41 | 4.5750E–06 | |
| Isotopic abundance | 8 | 16 | 2.4140E–06 | 2.4140E–06 |
| Isotopic abundance | 8 | 17 | 9.6790E–10 | 9.6790E–10 |
| | 8 | 18 | 4.8400E–09 | |
| Isotopic abundance | 25 | 55 | 2.4200E–06 | 2.4200E–06 |
| Isotopic abundance | 8 | 16 | 3.2080E–05 | 3.2080E–05 |
| Isotopic abundance | 8 | 17 | 1.2860E–08 | 1.2860E–08 |
| | 8 | 18 | 6.4320E–08 | |
| Natural element | 16 | 32 | 1.0190E–05 | 1.0724E–05 |
| | 16 | 33 | 8.0400E–08 | |
| | 16 | 34 | 4.5130E–07 | |
| | 16 | 36 | 2.1440E–09 | |
| Isotopic abundance | 8 | 16 | 3.3050E–06 | 3.3050E–06 |
| Isotopic abundance | 8 | 17 | 1.3250E–09 | 1.3250E–09 |
| | 8 | 18 | 6.6260E–09 | |
| | 38 | 84 | 1.8550E–08 | |

**Table 3.3. (continued)**

| Cross section type | Nuclide Z | Nuclide A | Number density | HETC/MCNP input |
|---|---|---|---|---|
| | | | | |
| | 38 | 86 | 3.2670E–07 | |
| | 38 | 87 | 2.3190E–07 | |
| | 38 | 88 | 2.7360E–06 | |
| Isotopic abundance | 8 | 16 | 4.6730E–06 | 4.6730E–06 |
| Isotopic abundance | 8 | 17 | 1.8740E–09 | 1.8740E–09 |
| | 8 | 18 | 9.3680E–09 | |
| Isotopic abundance | 15 | 31 | 3.1230E–06 | 3.1230E–06 |
| Isotopic abundance | 8 | 16 | 4.2880E–06 | 4.2880E–06 |
| Isotopic abundance | 8 | 17 | 1.7190E–09 | 1.7190E–09 |
| | 8 | 18 | 8.5970E–09 | |
| Natural element | 22 | 46 | 1.7730E–07 | 2.1488E–06 |
| | 22 | 47 | 1.5990E–07 | |
| | 22 | 48 | 1.5840E–06 | |
| | 22 | 49 | 1.1630E–07 | |
| | 22 | 50 | 1.1130E–07 | |
| Isotopic abundance | 8 | 16 | 5.5260E–06 | 5.5260E–06 |
| Isotopic abundance | 8 | 17 | 2.2160E–09 | 2.2160E–09 |
| | 8 | 18 | 1.1080E–08 | |
| Isotopic abundance | 11 | 23 | 1.1080E–05 | 1.1080E–05 |
| | | | **Limestone total** | **T. (MCNP)** |
| | | | **8.9554E–02** | **8.9443E–02** |

**Table 3.4. Overall composition of Copper Ridge dolomite soil**

| | | | | | | | | | | |
|---|---|---|---|---|---|---|---|---|---|---|
| Basis: 1 $cm^3$ soil at density 1.61 $g/cm^3$, 24% bulk moisture | | | | | | | | | | |
| 1.61 g | soil | | | | | | | | | |
| 1.2236 g | dry soil | | | | | | | | | |
| | | | | | | | | | | |
| Component | Wt fraction | Wt % | | Component | Wt fraction | Wt % | | Component | Wt fraction | Wt % |
| Si | 2.22E–01 | 22.2021 | | N | 2.58E–04 | 2.5840E–02 | | Tb | 2.60E–07 | 2.6030E–05 |
| O | 3.43E–01 | 34.3246 | | P | 1.52E–04 | 1.5200E–02 | | $^{232}Th$ | 1.02E–05 | 1.0184E–03 |
| $H_2O$ | 3.16E–01 | 31.6000 | | Sb | 1.47E–06 | 1.4668E–04 | | $^{235}U$ | 3.42E–08 | 3.4200E–06 |
| Al | 6.79E–02 | 6.7925 | | As | 6.14E–05 | 6.1408E–03 | | $^{238}U$ | 3.93E–06 | 3.9349E–04 |
| Fe | 3.50E–02 | 3.5017 | | Ba | 1.13E–04 | 1.1286E–02 | | V | 9.99E–05 | 9.9940E–03 |
| C | 1.37E–03 | 0.1368 | | Ce | 3.57E–05 | 3.5739E–03 | | Yb | 2.05E–06 | 2.0539E–04 |
| Mg | 3.96E–03 | 0.3958 | | Cs | 3.79E–06 | 3.7867E–04 | | Zn | 1.91E–04 | 1.9095E–02 |
| K | 5.96E–03 | 0.5957 | | Cr | 5.43E–05 | 5.4302E–03 | | Be | 6.25E–07 | 6.2510E–05 |
| Ti | 2.56E–03 | 0.2559 | | Co | 3.68E–06 | 3.6765E–04 | | B | 4.12E–06 | 4.1230E–04 |
| | | | | Eu | 3.02E–07 | 3.0210E–05 | | Cd | 1.69E–07 | 1.6910E–05 |
| | | | | Ga | 1.29E–05 | 1.2882E–03 | | Ca | 1.35E–04 | 1.3471E–02 |
| | | | | Au | 7.60E–09 | 7.6000E–07 | | Cu | 2.37E–05 | 2.3712E–03 |
| | | | | Hf | 2.22E–06 | 2.2173E–04 | | CN | 5.66E–07 | 5.6620E–05 |
| | | | | La | 2.91E–05 | 2.9051E–03 | | Pb | 2.59E–05 | 2.5859E–03 |
| | | | | Lu | 1.52E–07 | 1.5200E–05 | | Li | 3.42E–06 | 3.4200E–04 |
| | | | | Mn | 8.63E–05 | 8.6279E–03 | | Ni | 1.22E–05 | 1.2236E–03 |
| | | | | Hg | 8.25E–07 | 8.2460E–05 | | Se | 6.95E–07 | 6.9540E–05 |
| | | | | Rb | 4.84E–04 | 4.8412E–02 | | Sr | 3.61E–07 | 3.6100E–05 |
| | | | | Sc | 9.08E–06 | 9.0820E–04 | | $SO_4$ | 9.73E–06 | 9.7280E–04 |
| | | | | Ag | 1.46E–06 | 1.4630E–04 | | Tl | 3.38E–07 | 3.3820E–05 |
| | | | | Na | 1.15E–04 | 1.1495E–02 | | | | |
| | | | | | | | | | | |
| | | | | | | | | Total | 9.98E–01 | 99.8051 |

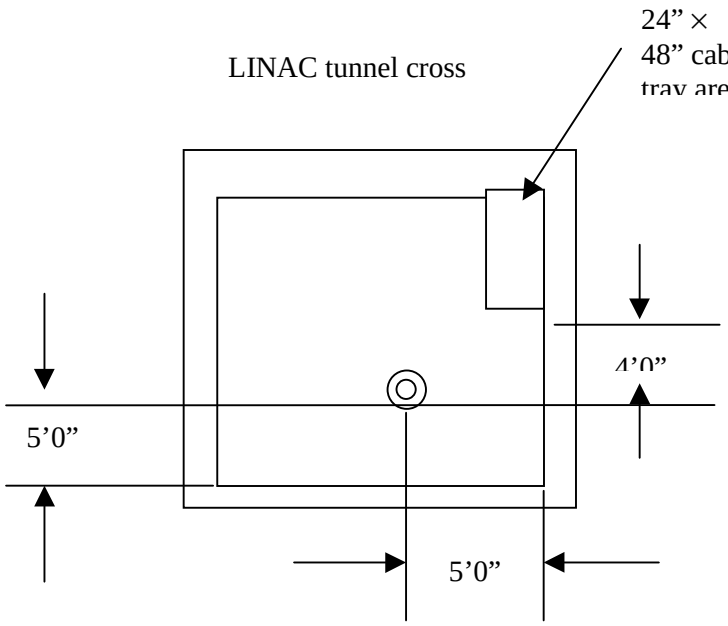


**Fig. 3.4. Layout and material information for the cable tray analysis of the activation products present in the insulation after 30-year irradiation at the nominal 1-nA/m (nano-Amp/meter) beam loss rate.**

The four cable trays are 16 in. high by 24 in. wide and are assumed to contain 566 cables of various sizes. The trays will require a 24 in. × 48 in. area for installation. The cable tray volumes per foot of tray length are as follows:

| | |
|---|---|
| Tray volume | 4608 $in.^3$/ft, |
| Cable volume | 788 $in.^3$/ft, |
| Insulation volume | 480 $in.^3$/ft, |
| Copper volume | 154 $in.^3$/ft, |
| Air volume | 3820 $in.^3$/ft, |
| Cable filler volume | 154 $in.^3$/ft. |

The volume percentages are as follows:

| | |
|---|---|
| Insulation | 10.42 |
| Copper wiring | 3.34 |
| Air | 82.9 |
| Cable filler | 3.34 |

Insulation composition is as follows:

| | |
|---|---|
| Polyvinyl chloride | 46 $in.^3$/ft (92.9%) |
| Nylon | 34.3 $in.^3$/ft (7.1%) |

Cable filler composition is as follows:

| | |
|---|---|
| Jute (cellulose) | 50% |
| Air | 50% |

## 3.3 DESCRIPTION OF THE RESULTS REPORTED IN APPENDIX A

The models described in Sect. 3.1.1 were used in the methodology in Sects. 3.1.2 and 3.1.3 to determine the radionuclide inventories for the various components associated with the simple accelerator tunnel model. A similar analysis was performed and documented in an earlier ORNL technical memorandum (ORNL, 1998). An investigation of the initial analysis indicated a normalization error in the contribution to the radioactive inventory due to low energy ($E <$ 20 MeV) neutron interactions. Consequently, a reinvestigation was initiated to ascertain the impact of the normalization error.

HETC calculations were run with 175,000 protons incident on the copper accelerator structure. The analysis was performed for 333-, 667-, and 1000-MeV incident proton beam energies. To accommodate the different requests for radionuclide inventory data at different buildup and decay time steps, the following sequence of analyses was performed.

For the copper, concrete, rock, and soil segments:

1. Buildup out to 30 years
2. Time steps: 3 months, 6 months, 9 months, 1 year, 2 years, 5 years, 10 years, 15 years, 20 years, 30 years
3. Decay out to 100 years, starting with 30-years buildup source
4. Time steps: 3 months, 6 months, 1 year, 5 years, 10 years, 20 years, 25 years, 50 years, 75 years, 100 years

For the air segment:

5. Buildup out to 30 min
6. Time steps: 10 s, 20 s, 30 s, 40 s, 50 s, 1 min, 5 min, 10 min, 20 min, 30 min
7. Decay out to 1 d, starting with 10-s, 20-s, 30-s, 40-s, 50-s, and 1-min buildup sources
8. Time steps: 30 s, 1 min, 5 min, 10 min, 30 min, 60 min, 6 h, 12 h, 24 h, 1 week

For the wire chase segment:

9. Buildup out to 30 years
10. Time steps: 1 month, 3 months, 6 months, 9 months, 1 year, 2 years, 5 years, 10 years, 20 years, 30 years
11. Decay out to 100 years, starting with 1-year, 5-years, 10-years, and 30-years buildup source(s)
12. Time steps: 3 months, 6 months, 1 year, 5 years, 10 years, 20 years, 25 years, 50 years, 75 years, 100 years

The results of these analyses have been archived as both hard-copy and in electronic file format. The nuclide production rate data for the anticipated accelerator normal operational loss scenario (1 nA/m) are documented in the appendix of this report for a proton beam energy of 1000 MeV. The data in the tables in the Appendix A are in units of gram-atoms/nA of beam current loss, integrated over the total volume of the material zone. Therefore, to renormalize to the overall berm length, the results need to be multiplied by the ratio of the total berm length to the 30-m berm length utilized in the model.

Similar results were obtained for the other energies, but were not included here due to the amount of data. Furthermore, as was noted above, there are data addressing both buildup and decay scenarios, activation levels, and decay gamma heat and spectra. The results were forwarded

on to the SNS design personnel working on the EIS and other ES&H issues for the SNS facility. With respect to the EIS, only the 1000-MeV data were used as radionuclide production rates in the concrete and soil to determine if there was risk to the public due to soil activation products leaching into the water supply.

### 3.3.1 Uncertainties in the Nuclide Production Rates in the SNS Components

The uncertainty associated with the calculated results can be attributed to three main sources: methodology, modeling, and statistical convergence. With respect to the methodology, there is a factor of 3 to 5 uncertainty in the determination of the neutron leakage source angular distribution. There is also the same uncertainty in energy distribution emanating from the copper structure. There is a factor of 5 to 10 uncertainty in the generation of the spallation products in the soil adjacent to the tunnel wall. Furthermore, the spallation product production becomes more uncertain as the atomic number of the spallation product decreases from target nuclei.

There is also a 15–20% uncertainty in the transport of this source through the thick earth berm shielding. Where the first source of methodology uncertainty could affect the answer by an amount similar to the uncertainty (i.e., a factor of 3 to 5), the second source of methodology uncertainty should only affect the distribution of the radionuclides close in to the accelerator tunnel by a small amount. In addition to the uncertainties in the source and transport processes, there is additional uncertainty in the nuclide production cross sections.

The model used in this analysis was simple. There was no attention given to the detailed structure in the accelerator tunnels since much of the detail had not been decided. Furthermore, the accelerator was placed in the center of the tunnel, and the tunnel was modeled as concentric cylinders. Adding the additional structure should reduce the amount of neutrons entering the earth berm thereby reducing the activation products being generated in the soil. An additional source of uncertainty in the analysis is the density of the soil. For this calculation, the soil was chosen to be 1.61 $g/cm^3$ with 24% bulk moisture, which are conservative numbers. When the berm is being built, the berm will be packed using heavy equipment and should be able to attain a density greater than that assumed in this analysis.

The last source of uncertainty in the calculations is the statistical convergence/accuracy of the results. The HETC calculations involved running 175,000 histories to generate the nuclide production data due to spallation. As stated previously, these results become increasingly more uncertain as the distribution of spallation product atomic number decreases from target nuclei. However, the spallation products are only part of the radionuclide production source terms. The second part is due to low-energy neutron interactions with the elemental constituents of the materials. The MCNP calculations typically had differential convergence results less than 5 to 10%. Consequently, the contribution to the problem uncertainty due to the MCNP calculation is minimal.

In the final result, if the radionuclide production source term is dominated by the spallation reactions, the uncertainty could be as high as an order of magnitude. If the low energy neutron absorption dominates the production, the uncertainty could be as low as a factor of 2.

Factoring all of these sources of uncertainty into a global uncertainty to assign the data is uncertain in its own right. Although a minimum level of confidence for this analysis is an order of magnitude, a factor of 20 to 30 uncertainty applied to the data would be more realistic for much of the results.

## 3.4 REFERENCES


Briesmeister, J. F., ed., September 1986, *MCNP-A General Purpose Monte Carlo Code for Neutron and Photon Transport*, LANL Report LA-7396-M, Rev. 2, Los Alamos National Laboratory, Los Alamos, New Mexico.

Bull, J. S., et al., November 1997, "Groundwater Activation at the Superconducting Super Collider: A New Design Model," *Health Physics*, **73**(5), 800–807.

Cloth, P., et al., 1988, *HERMES, A Monte Carlo Program System for Beam Material Interaction Studies*, KFA Jülich, Report Jul-2203.

Croff, A. G., 1980, *A User's Manual for the ORIGEN2 Computer Code*, ORNL/TM-7175, Union Carbide Corp.-Nuclear Division, Oak Ridge National Laboratory, Oak Ridge, Tennessee.

Croff, A. G., July 1980, *ORIGEN 2—A Revised and Updated Version of the Oak Ridge Isotope Generation and Depletion Code*, ORNL-5621, Union Carbide Corp.-Nuclear Division, Oak Ridge National Laboratory, Oak Ridge, Tennessee.

Cullen, D. E., January 1994, *The 1994 ENDF Pre-processing Codes (PRE–PRO 94)*, International Atomic Energy Agency Report IAEA-NDS-39, Rev. 8, Vienna.

Dole, L. R., September 1998, *Preliminary Assessment of the Nuclide Migration from the Activation Zone around the Proposed Spallation Neutron Source Facility*, ORNL/TM-13665, Lockheed Martin Energy Research Corp., Oak Ridge National Laboratory, Oak Ridge, Tennessee.

Engle, W. W. Jr., 1967, *A User's Manual for ANISN: A One-Dimensional Discrete Ordinates Transport Code with Anisotropic Scattering*, K-1693, Union Carbide Corp.- Nuclear Division, Oak Ridge, Tennessee.

Gabriel, T. A., et al., 1997 *CALOR: A Monte Carlo Program Package for the Design and Analysis of Calorimeter Systems*, ORNL/TM-5619, Lockheed Martin Energy Research Corp., Oak Ridge National Laboratory.

Leder, C. M., et al., 1978, *Table of Isotopes*, 7th ed., John Wiley & Sons Inc., New York.

Pashchenko, A. B., and P. K. McLaughlin, 1995, *FENDL/A-1.1, Neutron Activation Cross Section Data Library for Fusion Applications*, IAEA-NDS-148, Rev. 2, International Atomic Energy Agency, Vienna.

Reuss, U., et al., 1972, *Darmstadt Gamma-Ray Catalogue*, GSI 72-9, Germany.

Rhoades, W. A., and R. L. Childs, May 1988, "The DORT Two-Dimensional Discrete-Ordinates Transport Code" *Nucl. Sci. Eng*., **99**(1), 88–89.

Technical Report Series No. 283, 1988, *Radiological Safety Aspects of the Operation of Proton Accelerators*, ISBN 92-0-125`88-2, International Atomic Energy Agency, Vienna.

# 4. DIFFUSION-CONTROLLED RELEASES OF NUCLIDES FROM THE SNS SHIELD BERM

There are two conditions that make this study's cases of contaminant transport different from the usual transport analyses, which generally involve a spill or effluent that is carried through porous soils by percolating groundwater. First, the activation products in the shield berm are formed within the soils' mineral phases. Second, in the compacted shield berm, advective saturated groundwater is not the principal mechanism by which activation nuclides move.

This study addresses two cases of generation, diffusion, decay, and transport of the activation products that form in the SNS shield berm:

- *Case 1*. All nuclides stay in place and accumulate to their maximum concentration in the shield berm throughout the 30 years of operation. At the end of operations, this maximum inventory of activity (see Sect. 3) begins to diffuse and decay and to be transported toward the water table below the site.

- *Case 2*. The maximum inventory (see Sect. 3) of nuclides is distributed over 360 months (30 years) of operation. At the end of each month, the diffusion, decay, and transport processes begin for each of the 360 monthly packets of activity. Therefore, the total, potential nuclide source term is spread out over the 30 years of operations.

Because the shield berm has a significantly lower permeability than the surrounding, disturbed soils that were made looser during construction, the potential advective flow rate of water through the berm's mass is much lower than the rates of diffusion of contaminants through the berm's solid matrix to its surface. Detailed discussions of this study's major assumptions follow.

## 4.1 TOTAL CONTAMINANT AVAILABILITY FOR TRANSPORT

Because the radionuclides are produced through activation by high-energy particles scattered from the beam line, contaminants are produced within the crystalline structures of the soils' minerals. These minerals form the soils' finely divided primary soil phases. This process is the opposite of the classic spill scenario, during which the contaminants are carried by percolating water into clean soils and during which their migration potentials are predominantly controlled by the interactions with the surfaces of the soil minerals.

In the SNS activation case, the contaminants start out trapped inside the soils' minerals and must first diffuse through the crystalline solids to their surfaces before groundwater transport phenomena can begin. Therefore, transport in the case of the SNS shield berm is controlled by the rates of solid-solid diffusion out of the soil phases rather than by partitioning between mineral surfaces and moving, vadose groundwater.

However, there are few data that measure the behavior of these contaminants and their releases from the soils' phases of interest at the proposed SNS sites. There has been some work on soils and country rocks from the proposed Superconducting Super Collider (SSC) (Baker, Bull, and Gose, December 1997), and these experimental results show high rates of releases from the local Ellis County, Texas, materials.

These leaching experiments were very short term (hours and days), and these tests did not address diffusion-controlled release rates. The tests involved soluble mineral phases, calcium carbonate [$Ca(Mg)CO_3$], which were exposed to distilled water. These experiments did not use representative regional groundwaters that are at equilibrium with the local host soils through

which they must move. Real groundwaters would arrive already saturated with the local minerals' constituents, such as $SiO_2$, $Al_2O_3$, $Ca(Mg)CO_3$, $Fe_2O_3$, etc. These native saturated groundwaters will characteristically have 350 ppm or more total dissolved solids, which would substantially reduce the potential for solubilization of the berm-soils' minerals as a potential release mechanism.

Based on these few data, this study assumes that over the projected SNS facility life of 40 years and with the fine texture of the currently proposed shield-berm soils, that all of the activation products are immediately available for diffusion and subsequent hydraulic transport to the groundwater. Lacking sufficient data, this assumption is appropriate, but it is a conservative assumption.

## 4.2 NO ADVECTIVE FLOW THROUGH THE SHIELD BERM

The proposed SNS locations in Oak Ridge are in unsaturated surface soils located above the groundwater table (Sect. 2.2.3.2). The upper unsaturated soil is referred to as the vadose zone, where the pores are not completely filled with water. The soil particles may be covered with a more-or-less contiguous film of water, but there is also air in the rest of the pore spaces. Therefore, the water in the capillaries of the vadose soils is not pushed through the soil by a hydraulic pressure gradient; rather it is drawn through the soil by capillary "wicking." Since the capillary forces are greater in the smaller pores, the ground's moisture is drawn preferentially to the finer-grained soils.

In order for contaminant transport to occur, there must be some kind of water flow. Therefore, this study assumes that somehow there can be saturated flow around the outer surface of the shield berm to carry the contaminants to the water table below. This is a conservative assumption, and in this case, the difference in permeability between the berm and the surrounding native soils prevents advection through the berm's matrix.

The Darcy permeability of the compacted shield berm is estimated to be less than $1 \times 10^{-7}$cm/s to $1 \times 10^{-6}$ cm/s, and the adjacent, surrounding, disturbed native soils are estimated to have permeabilities greater than $1 \times 10^{-5}$cm/s to $3 \times 10^{-4}$ cm/s; the berm's conductivity is more than 100 times lower than that of the surrounding soils. While the undisturbed native soils show a wide range in permeabilities, the soils adjacent to the compacted shield-berm will be greatly disturbed during the construction of the tunnels and their shields. Under these conditions, advective water transport goes around the berm rather than through it (Atkins, May 1985). Figure 4.1 illustrates this effect.

So, even if the surrounding, disturbed soils could become saturated, there would be no significant advective transport through the berm matrix because of the relative difference in their permeabilities. Therefore, any releases to the surrounding groundwater transport system from the surface of the shield berm must then be controlled by diffusion through the shield-berm matrix to its surface contact with transportable vadose groundwater.

## 4.3 DIFFUSION FROM SHIELD BERM WITH NO RETARDATION INTO THE SURROUNDING SOIL

If the all of the nuclides are assumed to be available for transport within the shield-berm matrix, the individual rates of their diffusion will then depend on their interactions or partitioning constants between the berm's solid phases and the free porewater within the berm's pore structure. The most common expression for this liquid-solid partitioning coefficient is $K_{MB}$, which expresses the relative amount of a contaminant species adsorbed/absorbed on a soil mineral versus the amount of contaminant dissolved in the free water in contact with the soil.

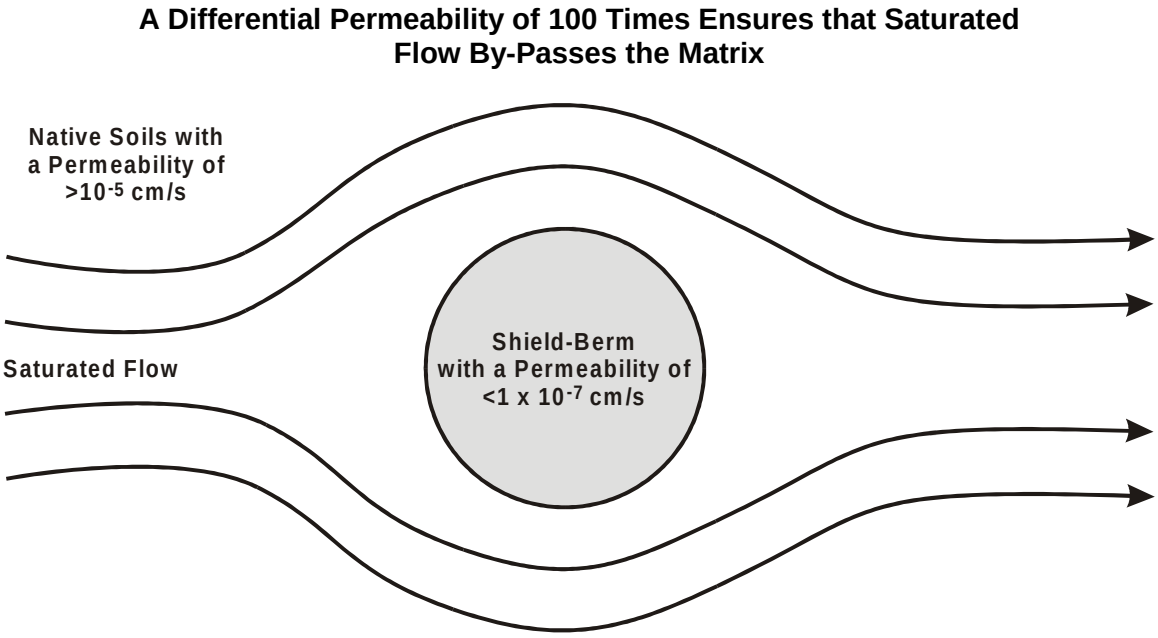


**Fig. 4.1. If groundwater flows around rather than through the shield-berm matrix, releases will be diffusion controlled.**

Equation (4.1) defines the $K_{MB}$ used most by researchers (Godbee et al., 1993), who measure these adsorption-absorption factors. The units of this definition of $K_{MB}$ are in milliliters per gram.

$$K_{MB} = \left[ \frac{\left( \frac{\text{mole of species}}{\text{mass of porous solid}} \right)}{\left( \frac{\text{mole of species}}{\text{volume of liquid}} \right)} \right] .$$

The $K_{MB}$ is measured by taking an aqueous solution with known initial concentrations of specific contaminants and mixing it with the known masses of soil particles to form an agitated slurry. After a few hours or days of equilibration, the solution is separated from the fine soil solids by filtering and/or centrifugation. The final concentrations of contaminants in the separated solution are measured, and the quantity adsorbed and/or absorbed is calculated by the difference between the initial and final concentrations.

The ubiquitous use of these static $K_{MB}$'s to describe both dynamic and nearly static contaminant transport in groundwater systems is fraught with difficulty and misconceptions. First, using $K_{MB}$ as an equilibrium constant in dynamic transport models is very tenuous because of the short contact times generally used in $K_{MB}$ measurements. While ion exchange with the surfaces of the mineral phases plays an important role in the adsorption of contaminants, many important, common minerals such as smectitic clays have even greater ion-exchange capacities in their internal structures. Since the access to these internal ion-exchange sites is limited by slow absorption into these minerals, short-term tests do not always measure their potentially significant contribution to the retardation of contaminant transport. Also, there are other relatively slow mechanisms, such as co-precipitation, mineral component substitution, and secondary mineral formation, that are not given enough time in these short-term measurements to influence the $K_{MB}$

results. Using a simple partition coefficient cannot adequately describe the complex interactions that contaminants can have with soil components (Dragun, 1988).

Furthermore, the measurement protocol itself has flaws. With fine-grained soils, particularly with silt and clay phases, the clean separation of the liquid from the soil slurry is very difficult. The silt and clay particles with high ion-exchange capacities form stubborn, stable colloids that can penetrate or blind most filters and that are also very difficult to centrifuge. Since these soil colloids adsorb a relatively larger fraction of the contaminants, a small contamination of the liquid phase by these soil colloids will strongly affect the analytical results. When these colloids are dissolved during analyses, they release their contaminants during the acid-oxidation digestion step of the samples preparation for ICP or atomic-adsorption (AA) analyses.

Also under the shear in this protocol's agitated slurry, the delicate, sometimes gossamer, secondary mineral coatings on the soils' primary minerals are torn off, dispersed, and dissolved in the water. These surface alteration phases, which may include gelatinous, hydrosilicate gels and mixed aluminosilicates, also have high-exchange capacities and contribute greatly to the retardation of contaminant transport.

As a result of these limitations, the "as measured" $K_{MB}$' s are usually lower than expected for the actual in situ soil conditions. Therefore, when they are used as equilibrium constants in transport models, the results are conservative in that they generally estimate greater contaminant mobilities than are actually to be expected.

### 4.3.1 Estimating the Retardation Factors and the Diffusion Coefficients

First, $K_{MB}$ is used to define a retardation coefficient that is a ratio of a contaminant's velocity relative to the velocity of the groundwater that carries it by advection through an open, porous soil. This simple model uses a dimensionless form of $K_{MB}$ as a formal partition coefficient ($K$) between the stationary soil's solids and its moving, free pore water. The contaminants are moving only when they are partitioned into the moving groundwater. So, $K$ is a measure of the relative amount of time that the contaminants spend on the sites' stationary soils or in their moving groundwaters. A higher $K$ means that the contaminant spends less time in the mobile, free, percolating water. Therefore, its migration is retarded more. Equation (4.2) describes the dimensionless retardation factor ($R$), and Eq. (4.3) defines $K$ in relationship to $K_{MB}$.

$$R = \left[ \frac{1}{1+K} \right], \tag{4.2}$$

where $K$ in terms of the measured $K_{MB}$ is

$$K = \left[ \frac{\dfrac{\textit{mole in species}}{\textit{volume of solid phase}}}{\dfrac{\textit{mole in species}}{\textit{volume of liquid}}} \right] = \left[ \rho_b \cdot \left( \frac{1-\epsilon}{\epsilon} \right) \cdot K_{MB} \right], \tag{4.3}$$

where

$\rho_b$ = bulk density of porous soil, g/cm$^3$
$\epsilon$ = average open-pore void fraction, dimensionless
$K$ = dimensionless contaminant species partition coefficient between pore water and soil-berm minerals.

This concept of a retardation factor also applies to diffusion processes. In a general sense, a diffusion coefficient, or diffusivity, is a statistical entity describing the relative shift in random molecular movement relative to a concentration gradient within a fluid or solid. Therefore, an "effective diffusion coefficient" ($D_e$) can legitimately be used to numerically summarize the collective result of simultaneous transport mechanisms in a complex matrix of soil minerals.

In the mineral matrixes of the shield berm, water is in at least four states. Some water is chemically bonded in the mineral structure or is in crystal waters-of-hydration. Other "clathrate" water is captured within the crystals or trapped in the silica-alumina hydrogels at the mineral surfaces. Some water is adsorbed onto the mineral surfaces or constrained within the hydrodynamic boundary of the minerals' ionic double layers. Finally, in the saturated, open pores, there is "free water." Within this stagnant, free pore water, the contaminants can diffuse from pore to pore, from higher to lower concentrations. The hydrodynamic radii of the ions with their hydration spheres control the diffusion rates of contaminant species in this free water.

As in the advection cases, the contaminants are partitioned between the free, pore water and the berm's mineral surfaces. So, the retardation factor in Eq. (4.2) can also be used to estimate the reduction in the pore diffusion ($D_f$) and to calculate an effective diffusion coefficient ($D_e$) that is described in:

$$D_e = \left[ \frac{D_f}{1+K} \right], \tag{4.4}$$

where

$D_e$ = effective diffusion coefficient, $cm^2/s$
$D_f$ = free diffusion coefficient of contaminate species within pore water, $cm^2/s$
$K$ = dimensionless contaminant species partition coefficient between pore water and soil, berm minerals [Eq. 4.3)].

In this study, an additional factor, tortuosity, is also considered to affect the estimates of contaminants' $D_e$. Tortuosity ($\tau$) is the ratio of the length of the actual diffusion path to the surface divided by the shortest geometric distance to the surface. In this study, the constrictivity of the connections between the berm's pores is not considered. It is set equal to one and does not appear as a parameter in Eq. (4.5), below. The soil-berm matrix is a tortuous diffusion labyrinth of diffusion detours around solid minerals. This porous labyrinth effectively creates obstructions in the direct path to the surface of the shield berm. In this study, the tortuosity was estimated to be 1.41 ($2^{1/2}$) for the compacted native-soil shield berm. The addition of tortuosity ($\tau$) factor and the full expansion of the definition of the effective diffusion coefficient results in:

$$D_e = \left[ \frac{D_f}{\tau^2 \cdot \left[ 1 + \rho_b \cdot \left[ \frac{(1-\epsilon)}{\epsilon} \right] \cdot K_{MB} \right]} \right], \tag{4.5}$$

where

$\tau$ = tortuosity, *dimensionless* (This study assumed that $\tau$ was equal to 1.47 for the compacted berm soils.)
$\rho_b$ = bulk density of porous soil, $g/cm^3$
$\epsilon$ = average *effective* open porosity, *dimensionless*.

Using estimates of $K_{MB}$ for the key isotopes, the effective diffusion coefficients ($D_e$) and the retardation factors ($R$) were calculated, using Eq. (4.5) and Eq. (4.2), respectively. Table 4.1 shows the values used to estimate $D_e$ in this diffusion-controlled study. Table 4.2 summarizes the results of these calculations.

The $K_{MB}$'s used in Table 4.1 are from the log averages of a critical compilation and review of the soil-solid/liquid partition coefficients of currently reported values for soils similar to the SNS site (Thibault and Shepard, 1990). The *Handbook of Chemistry and Physics* (1994) values for the self-diffusion coefficients ($D_f$) were used to estimate the effective diffusion coefficients ($D_e$). In general, this study's choices of $K_{MB}$'s and $D_f$'s were more conservative than in the previous TM-13665, resulting in significantly larger effective diffusion coefficients ($D_e$). Therefore, the estimated release rates in this study are conservatively higher.

The free water-particle travel time through the 10 m of soil from the bottom of the shield berm to the saturated water table, based on a recharge rate of 9.055 in./year and a porosity of 0.37 (see Sect. 2.2), is 16 years. With all of the previous caveats, the use of $K_{MB}$ to estimate the transport of these contaminates will result in a conservative overestimate of their mobilities and the rates of their releases.

**Table 4.1. Parameters used in this study to estimate $D_e$**

| | | |
|---|---|---|
| Dry soil density | 1.61 | $g/cm^3$ |
| Soil effective porosity | 37 | Percent |
| Tortuosity | 1.41 | Dimensionless |
| Constrictivity | 1 | Dimensionless |

### 4.3.2 Diffusion-Controlled Contaminant Releases from the Shield Berm

Using the derived effective diffusion coefficients ($D_e$) from the previous section, the following two diffusion models are applied to the internal transport of contaminants in the SNS shield berm. The first and simpler, semi-infinite medium model is used to calculate the initial release rates up until ~20% of a specific containment is released. After that, the remaining releases to complete depletion are calculated using a "geometry-specific" model.

#### 4.3.2.1 Semi-infinite medium diffusion model

The initial diffusion-controlled release of contaminants from the shield berm is based on the source-term model, which is shown in Eq. (4.6). As seen in this model, the surface-to-volume (S:V) ratio of the berm controls the "window" size of contaminant transport into the surrounding environment, and the effective $D_e$ controls the rate of transport from within the berm's matrix. This general "semi-infinite medium" equation (Spence et al., 1993) describes an ever decreasing release rate with time (Dole, 1989) as a depletion layer forms near the surface of the monolith. When this model's results are compared with more complex geometric models, the calculations based on Eq. (4.6) represent an upper bound on the potential release of contaminants.

$$F(t) = 2\left[\frac{S}{V}\right] \cdot \sqrt{\frac{D_e}{\pi} \cdot t} \qquad (4.6)$$

**Table 4.2. Nuclide partition coefficients from Tables 5 and 6 of D. H. Thibault and M. Shepard, 1990, *A Critical Compilation and Review of Default Soil Solid/Liquid Partition Coefficients*, AECL-10125, CAN/DN:1990:448145**

[*Water-particle travel time through the 10 m of soil from the bottom of the shield berm to the saturated water table, based on a recharge rate of 9.055 in./year and a porosity of 0.37 (see Sect. 2.2), is 16 years.*]

| Isotope | $K_{MB}$ from ORNL/ TM 13665 ($g/cm^3$) | Expected $K_{MB}$ clay ($g/cm^3$) | Expected $K_{MB}$ silt ($g/cm^3$) | $K_{MB}$ used in this study ($g/cm^3$) | Self-diffusion coefficient, ($D_f$) ($cm^2/s$) | Calculated effective diffusion coefficients, ($D_e$) ($cm^2/s$) | Calculated retardation coefficients, dimensionless | Expected nuclide travel time with retardation, year |
|---|---|---|---|---|---|---|---|---|
| 30 | 0 | 30 | 20 | | 9.31E–05 | 5.59E–07 | 3.23E–02 | 499 |
| $^{10}$Be | 20 | 1300 | 800 | 800 | 5.99E–06 | 1.37E–09 | 1.25E–03 | 12,886 |
| $^{14}$C | 10 | 1 | 20 | 1 | 1.19E–05 | 1.58E–06 | 5.00E–01 | 32 |
| $^{22}$Na | 15 | | | 15 | 1.33E–05 | 1.58E–07 | 6.25E–02 | 257 |
| $^{26}$Al | 3,000 | | | 3,000 | 5.41E–06 | 3.29E–10 | 3.33E–04 | 48,278 |
| $^{36}$Cl | 0 | | | 0 | 2.03E–05 | 1.02E–05 | 1.00E+00 | 16 |
| $^{39}$Ar | 0 | | | 0 | 2.40E–05 | 1.20E–05 | 1.00E+00 | 16 |
| $^{42}$Ar | 0 | | | 0 | 2.40E–05 | 1.20E–05 | 1.00E+00 | 16 |
| $^{40}$K | 15 | 75 | 55 | 75 | 1.96E–05 | 4.74E–08 | 1.32E–02 | 1,223 |
| $^{41}$Ca | 3,000 | 50 | 30 | 50 | 7.92E–06 | 2.87E–08 | 1.96E–02 | 820 |
| $^{53}$Mn | 25 | 180 | 750 | 180 | 7.12E–06 | 7.20E–09 | 5.52E–03 | 2,912 |
| $^{54}$Mn | 25 | 180 | 750 | 180 | 7.12E–06 | 7.20E–09 | 5.52E–03 | 2,912 |
| $^{55}$Fe | 486,000 | 165 | 800 | 165 | 7.19E–06 | 7.93E–09 | 6.02E–03 | 2,670 |

where

$F(t)$ = fractional contaminant release with time, $t$
$S$ = berm surface area, $cm^2$
$V$ = berm volume, $cm^3$
$D_e$ = contaminant's effective diffusion coefficient, $cm^2 s^{-1}$.

This semi-infinite medium model is accurate during the initial release scenario. It remains accurate up to a loss of up to about 20% of the initial contaminant inventory from within the berm. At higher percentages of release, a geometry-specific model, such as Eq. (4.7) should be used.

#### 4.3.2.2 Geometry-specific diffusion model

In this study's cases, more than 20% of the initial contaminant in the berm matrix is released during the period of interest. Therefore, a second geometry-specific model is used [Eq. (4.7)]. This cylinder and sphere diffusion model must be used for many of these cases because (a) all of the $D_e$ are large ($>10^{-11} cm^2/s$, see Table 4.3), (b) the shield-berm surface to volume ratio of the berm is large (S:V of 0.357 $cm^{-1}$), and (c) the period of the analysis is sufficiently long such as to release over 20% of specific contaminants.

$$F(t) = \left[1 - \frac{32}{\pi^2 a^2}\right] \cdot \sum_{n=1}^{n} \sum_{m=1}^{m} \exp\left[\frac{-D_e \cdot \left[\alpha_m^2 + (2n-1)^2 \frac{\pi^2}{4L^2}\right] \cdot t}{(2n-1)^2 \alpha_m^2}\right], \qquad (4.7)$$

where

$F(t)$ = fractional contaminant release with time, $t$
$D_e$ = effective diffusion coefficient, $cm^2\ s^{-1}$
$a$ = cylinder radius, cm
$\alpha_m$ = $m$th positive root of a zero-order Bessel function [$J_0(m)$]
$L$ = cylinder half-height, cm.

This geometry-specific model describes the diffusion from cylinders (Nestor, January 1980) and can be used successfully for approximated spheres* as well. This model results from Nestor's analytical solution in cylindrical coordinates. Representative MathCad© calculations using these models are presented in the attached Appendix B to this report.

The application of these models considerably overestimates the potential releases of the contaminants in Table 3.1. Based on conservative $K_{MB}$, these models assume the total availability of the nuclides for transport when many of them are trapped within the soils' minerals. Also, these models assume that throughout the berm matrix this system is always at equilibrium even though intuitively the complex mechanisms of the contaminants' retention cannot be.

The activation products are not formed uniformly across the radius of the berm, as shown in Table 4.3 Therefore, this study's assumption of uniform contaminant distributions within the shield berm at the end of the 30-year SNS operations is not expected. Based on the results from Sect. 3, Table 4.3 shows the uneven distribution of contaminants across the radius of the shield berm. These results show that 95% of the activity is within the inner 2 m of the 4-m-thick inner

*A cylinder, a sphere, and a cube may be related, if they have the same surface-to-volume ratio.

**Table 4.3. The distribution of activation nuclides over the radii of the SNS shield-berm components**

| Isotope | Nuclide activity in 30-m concrete section (Ci) | Nuclide activity in 30-m Soil-1 section (Ci) | Nuclide activity in 30-m Soil-2 section (Ci) | Nuclide activity in 30-m Soil-3 section (Ci) | Nuclide activity in 30-m Soil-4 section (Ci) | Nuclide activity in 30-m Soil-5 section (Ci) | Nuclide activity in 30-m limestone section (Ci) | Nuclide activity in 30-m Soil-6 section (Ci) | Total overall in 30-m section (Ci) | Total inner soil (between concrete and limestone) in 30-m section (Ci) | Total overall in total 1045-m berm (Ci) | Total inner soil (between concrete and limestone) in total berm (Ci) |
|---|---|---|---|---|---|---|---|---|---|---|---|---|
| $^{3}$H | 9.65E–03 | 1.83E–03 | 7.04E–04 | 4.40E–04 | 8.15E–05 | 1.55E–05 | 1.99E–06 | 1.91E–06 | 1.27E–02 | 3.07E–03 | 4.43E–01 | 1.07E–01 |
| $^{10}$Be | 3.84E–10 | 1.06E–10 | 4.94E–11 | 3.53E–11 | 7.06E–12 | 7.03E–12 | 1.57E–13 | 6.23E–16 | 5.89E–10 | 2.05E–10 | 2.05E–08 | 7.14E–09 |
| $^{14}$C | 1.50E–05 | 4.44E–06 | 1.79E–06 | 1.19E–06 | 2.29E–07 | 5.55E–08 | 1.66E–08 | 4.21E–09 | 2.27E–05 | 7.70E–06 | 7.91E–04 | 2.68E–04 |
| $^{22}$Na | 2.83E–03 | 3.77E–04 | 1.60E–04 | 9.59E–05 | 2.31E–05 | 5.95E–06 | 1.45E–07 | 6.51E–09 | 3.49E–03 | 6.62E–04 | 1.22E–01 | 2.30E–02 |
| $^{26}$Al | 4.21E–07 | 9.57E–08 | 3.86E–08 | 2.40E–08 | 5.03E–09 | 1.35E–09 | 3.59E–13 | 8.27E–11 | 5.85E–07 | 1.65E–07 | 2.04E–05 | 5.74E–06 |
| $^{36}$Cl | 1.29E–07 | 3.66E–09 | 1.89E–09 | 9.48E–10 | 1.68E–10 | 6.94E–11 | 1.15E–10 | 1.00E–12 | 1.36E–07 | 6.74E–09 | 4.73E–06 | 2.35E–07 |
| $^{39}$Ar | 2.90E–04 | 7.26E–06 | 2.70E–06 | 1.94E–06 | 2.97E–07 | 6.72E–08 | 2.69E–08 | 6.52E–09 | 3.02E–04 | 1.23E–05 | 1.05E–02 | 4.27E–04 |
| $^{42}$Ar | 1.99E–06 | 7.30E–12 | 2.78E–12 | 1.73E–12 | 3.43E–13 | 6.59E–14 | 2.89E–11 | 0.00E+00 | 1.99E–06 | 1.22E–11 | 6.95E–05 | 4.26E–10 |
| $^{40}$K | 3.78E–10 | 7.64E–13 | 1.80E–13 | 1.43E–13 | 4.60E–14 | 4.26E–15 | 3.95E–13 | 4.54E–16 | 3.79E–10 | 1.14E–12 | 1.32E–08 | 3.96E–11 |
| $^{41}$Ca | 5.28E–07 | 1.81E–09 | 6.71E–10 | 2.26E–10 | 1.40E–12 | 3.31E–13 | 4.19E–10 | 3.60E–14 | 5.31E–07 | 2.71E–09 | 1.85E–05 | 9.42E–08 |
| $^{53}$Mn | 3.84E–09 | 3.05E–09 | 1.33E–09 | 7.49E–10 | 1.74E–10 | 4.76E–11 | 1.84E–14 | 1.67E–13 | 9.19E–09 | 5.35E–09 | 3.20E–07 | 1.86E–07 |
| $^{54}$Mn | 1.40E–01 | 1.00E–01 | 3.67E–02 | 2.03E–02 | 6.55E–03 | 1.70E–03 | 2.58E–06 | 1.08E–05 | 3.05E–01 | 1.65E–01 | 1.06E+01 | 5.76E+00 |
| $^{55}$Fe | 9.14E–04 | 5.86E–04 | 1.93E–04 | 1.38E–04 | 2.28E–05 | 4.95E–06 | 8.92E–07 | 1.64E–07 | 1.86E–03 | 9.44E–04 | 6.48E–02 | 3.29E–02 |
| Total | 1.54E–01 | 1.03E–01 | 3.77E–02 | 2.10E–02 | 6.68E–03 | 1.73E–03 | 5.65E–06 | 1.29E–05 | 3.24E–01 | 1.70E–01 | 1.13E+01 | 5.92E+00 |
| Overall | 47.49% | 31.78% | 11.65% | 6.48% | 2.06% | 0.53% | 0.0017% | 0.0040% | | | | |
| Total berm | | 60.52% | 22.19% | 12.34% | 3.93% | 1.02% | 0.0033% | 0.0076% | | | | |
| Inner soil | | 60.52% | 22.19% | 12.34% | 3.93% | 1.02% | | | | | | |

berm (see Soil Zones 1 through 5 in Fig. 3.3 and Table 4.4). So, only about 5% of the activity forms in the outer 2-m layer of the inner shield berm.

With all of these conservative assumptions, if the conservative results show that the calculated potential concentrations of contaminants are still below the regulatory limits, then there is very high level of confidence that it is true.

**Table 4.4. Diameters and volumes of SNS shield-berm concrete, soil, and limestone zones used in the nucleonics model (Fig. 3.3)**

| Shield-berm zone | Zone thickness (m) | Inner radius (m) | Outer radius (m) | Volume over 1045 m (total SNS) ($m^3$) | Inner soil volume (between concrete and limestone) ($m^3$) |
|---|---|---|---|---|---|
| Concrete | 0.4572 | 2.3 | 2.7572 | 7,591 | |
| Soil Zone 1 | 0.5 | 2.7572 | 3.2572 | 9,873 | 9,873 |
| Soil Zone 2 | 0.5 | 3.2572 | 3.7572 | 11,514 | 11,514 |
| Soil Zone 3 | 1 | 3.7572 | 4.7572 | 27,952 | 27,952 |
| Soil Zone 4 | 1 | 4.7572 | 5.7572 | 34,518 | 34,518 |
| Soil Zone 5 | 1 | 5.7572 | 6.7572 | 41,084 | 41,084 |
| Limestone | 1 | 6.7572 | 7.7572 | 47,650 | |
| Soil Zone 6 | 3.0528 | 7.7572 | 10.81 | 186,085 | |
| Total volume | | | | 366,268 | 124,942 |

## 4.4 SITE-SPECIFIC SNS HYDROLOGICAL SETTING AND ASSUMPTIONS FOR THE DIFFUSION-CONTROLLED MODEL

Based on the site-specific data given in Sect. 2.2 of this report, Fig. 4.2 shows the ORR, SNS-site water balances used to calculate the pore water contaminant concentrations from the diffusion-controlled release and transport rates.

This model conservatively assumes a constant flux of water over the shield-berm surface. If contaminants at the berm's surface are not continually removed, the subsequent contaminant buildups at the surface will come to equilibrium, and transport out of the berm will stop.

Figure 4.2 depicts the hydrologic cross section used to calculate the flux of precipitation from above and the flux of groundwater below a proposed ORR SNS site. It assumes that the hydrologic cross section has a 4-m zone of influence beyond the 13.5-m-diam of the tunnel and its 4-m-thick inner berm. It assumes only 9.055 in. of annual groundwater recharge and that the cross section of the 1045-m SNS tunnel system has an effective area of 22,650 $m^2$ and an annual recharge flow of 5211 $m^3$/year. This represents the extreme low end of the site's recharge range and will result in a severe, conservatively high estimate of the concentrations of contaminants in the pore water below the shield berm.

The uncompacted soils have a porosity of 0.37 and a dry density of 1.61 $g/cm^3$. The mixing zone at the surface of the saturated groundwater table is assumed to be 3 m deep, and the groundwater velocity under this site is assumed to 2.9 m/year with a gradient of 0.02 (dimensionless). Then, the annual horizontal contribution to the flux of groundwater in the mixing zone under the SNS tunnels is 5631 $m^3$/year.

This brings the total annual water balance under the SNS facility and its adjacent 4-m zones of influence to an annual turnover of 10,840 $m^3$/year. Under these conservative assumptions, the

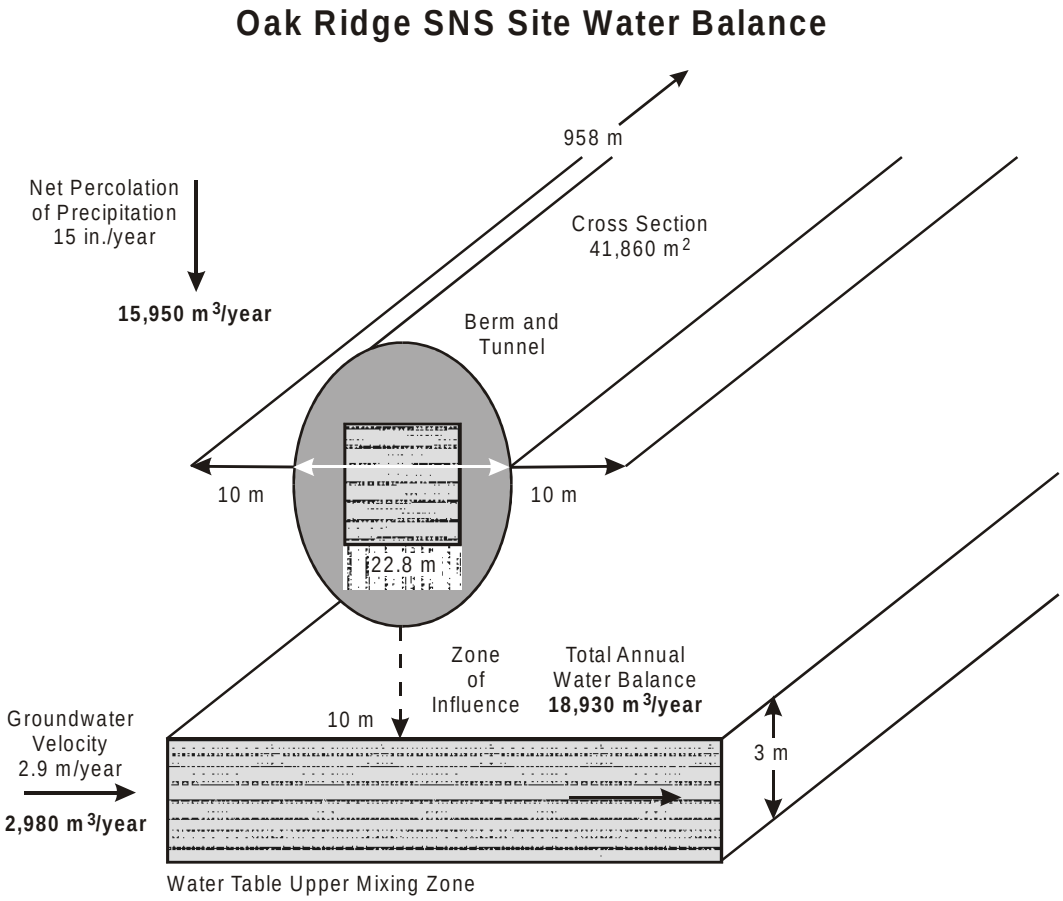


**Fig. 4.2. Hydrologic cross section of the proposed SNS site used in the calculation of potential contaminant concentrations at the boundary of a 4-m zone of influence.**

recharge: saturated-groundwater flow ratio is 0.925 (dimensionless). These turnover rates with the calculated transport rates of the contaminants to the outer surface of the berm can be used to calculate the dilution and potential concentrations of contaminants in the groundwater. However, in these diffusion studies, only the recharge rates were used to estimate conservatively high potential pore water concentrations.

The previous study, ORNL/TM-13665 (Dole, 1998), estimated the hydraulic velocity in the vadose zone to be 1 m/year, based on the general site assessment results of less than 0.2 m/year ("Performance Evaluation of the Technical Capabilities of DOE Sites for Disposal of Mixed Low-Level Waste," March 1996). This study used a downward water-particle velocity of 0.622 m/year based on the data in Sect. 2.2 of this report. From the very bottom of the shield berm, an unretarded packet of percolating water with contaminants from the berm's surface could reach the groundwater's upper boundary and mixing zone in 16 years. This study also assumes that there is no retardation of the contaminants' migrations by partitioning with the intervening soils, as would be expected from the results in Table 4.2. In this study all contaminants are assumed to travel continually with the water particles and take the 16 years to travel downward to the water table.

In general when compared to ORNL/TM-13665 (Dole, 1998), this current study uses more severe hydrologic and geometric boundary conditions for the ORR SNS site, which result in higher-relative pore-water concentrations.

## 4.5 DECAY OF ISOTOPES DURING DIFFUSION AND TRANSPORT

These analyses also applied isotopic decay factors to account for the radioactive decay of the contaminants in Table 3.1 starting at the end of the 30-year operation of the facility, as in Case 1, and after the first month, as in Case 2. In both cases, the reductions in nuclides are calculated over their diffusion and migration travel times. This becomes an important factor for those isotopes with high specific activities and short half-lives.

## 4.6 RECURSION FORMULAS FOR MODEL CASE 2: GENERATION, DIFFUSION, AND DECAY

In Case 2, the inventory of nuclides from Sect. 3 is divided into 360 equal packets representing the generation of each month of the 30-year SNS operation. Then, each packet begins to diffuse, decay, and migrate from the SNS shield berm as it is generated as opposed to Case 1, where the total inventory of nuclides accumulates in the shield berm over 30 years. Then the transport processes begin as described above. Case 1 is the more severe case because the accumulated nuclides result in the largest possible impulse source term for the transport model. In Case 2, the same models are used to describe the diffusion, decay, and transport (see Appendix B), but the source term is distributed. To collectively describe the cumulative release of the 360 packets, the following recursion formulas were used:

### Simultaneous Production and Diffusion Calculations

**month 1**

$$FT_1 := Fg_1 \cdot delta_FS_1$$

**month 2**

$$FT_2 := Fg_1 \cdot delta_FS_2 + Fg_2 \cdot delta_FS_1$$

**month 3**

$$FT_3 := Fg_1 \cdot delta_FS_3 + Fg_2 \cdot delta_FS_2 + Fg_3 \cdot delta_FS_1$$

**month 4**

$$FT_4 := Fg_4 \cdot delta_FS_1 + Fg_3 \cdot delta_FS_2 + Fg_2 \cdot delta_FS_3 + Fg_1 \cdot delta_FS_4$$

### Monthly Recursion Formula for Total Incremental Fractional Release

$$k := 1, 2 .. 724$$

$$FT_{k+4} := \sum_{n=1}^{k} Fg_n \cdot delta_FS_{k-n}$$

where

$FT_DF_i$ = the sums of the released packets of a specific nuclide at month$_k$ corrected for the decay time since its generation at month$_n$,

$Fg_i$ = the fraction of the total inventory generated during month$_k$ (This fraction is equal to 1/360 for the first 360 months; then it becomes zero.),

$delta_FS_i$ = the incremental fraction of nuclide packet released from the berm by diffusion during $month_k$, and
$C14_DF_I$ = the cumulative decay reduction factor for $month_k$ (decay factor for $^{14}C$ in this specific example).

In general for Case 2, the pore water nuclide concentrations are less than those for Case 1 because initial releases of the total nuclide inventories are spread over the 360 months of operations. The SNS operational period is almost twice the 16-year (196-month) travel time for water packets to reach the water table. Therefore, at month-196 from the generation and/or beginning of transport, the first and most concentrated contaminated pore water packet reaches the water table. This is why subsequent discussions in the conclusions focus on the pore water concentrations at the 196th monthly time-step.

## 4.7 SUMMARY OF ASSUMPTIONS AND THEIR IMPACT ON THE ANALYSES

This section summarizes the assumptions used in this study and attempts to estimate their impact on the final analysis. The assumptions follow:

- Thirty years of continuous operations, when the beam is actually operated intermittently over a projected life of 40 years. The Sect. 3 calculations result in maximum credible concentration of activation products.

- Only the 4-m-thick inner soil of the shield berm with 99.99% of the activity is considered in the release calculations with no barrier credit for the outer 3-m-thick portion of the berm of the proposed 1-m-thick limestone capillary break.

- Using only the inner-berm soil exaggerates the surface-to-volume ratio to 0.357 $cm^{-1}$ and exaggerates the diffusion-controlled releases of activation products.

- In Case 1, the buildup of activation products remains stationary until the end of operations, resulting in the highest possible source term.

- In Case 2, the releases of the final inventory are spread equally over 360 months.

- The shield berm is hydraulically connected to the local groundwater recharge and transport system, and diffusion can occur because the nuclides on the shield-berm surface are continually swept away.

- The activation rates are based on the highest energy section of the SNS beam at 1 GeV and a conservatively high beam-leakage rate (Sect. 3).

- These highest activation levels are distributed over the entire length of the SNS beam system and have both linear and axial homogeneity.

- Because of the fine primary particle sizes in the compacted soil shield berm, all activation products are immediately available for transport and are not bound in the soil minerals where they form.

- Movement of contaminants within the berm is controlled by diffusion, which is estimated using a conservative self-diffusion coefficient ($D_f$) and partition coefficients ($K_{MB}$).

- The diffusion models used in this study imply that within the berm matrix the contaminants are instantaneously at equilibrium everywhere within the system (using $K_{MB}$'s as if they were equilibrium constants).

- The tortuosity was estimated to be only 1.41 for the compacted soil berm.

- There is no retardation of the contaminants' transport through the native soils.

- The estimated 16-year travel time of the pore water from the bottom of the shield berm to the water table is based on 9.055 in. of recharge and an estimated regional effective porosity of 0.37. This site has very inhomogenous soils. Therefore, there will be specific areas where the travel times will be greater or less. Where greater, there will be more decay, and where less, there will be more dilution. Sixteen years represent a regional average applied to the kilometer-long SNS tunnels.

- The low end of the site's groundwater recharge rate range was chosen to maximize the quantities of contaminants that could diffuse into the slowly passing pore water and to minimize their dilution. Since this diffusion model and the subsequent advection model (Sect. 5) are based on different principles, what represents conservatism in their respective applications is choosing site conditions at opposite ends of this site's ranges of conditions. For example, choosing the lower recharge rate is more severe and conservative in the diffusion cases, and choosing the high end of the recharge range is conservative in the advection model. So, what looks like inconsistencies between the boundary conditions used for these two modeling approaches is actually a consistent choice of the most severe and conservative analyses.

The net effect of these assumptions throughout these analyses is to conservatively overestimate the potential concentrations in the groundwater below the SNS site by perhaps factors of between 25 to over 100 times. When the resulting predictions show that the nuclides are below NRC 10 CFR Part 20 DWLs, there is a very high confidence level that these limits will never be exceeded during the operation and postoperation periods of the SNS facility on the ORR.

## 4.8 RESULTS OF DIFFUSION-CONTROLLED MODEL OF RELEASES FROM THE SNS SHIELD BERM

Sample calculations using these diffusion models for Case 1 and Case 2 are presented in Appendix B.

These analyses are based on the SNS current conceptual design configuration and the g-mole quantities from the calculations in Sect. 3 (see Appendix A). This configuration is more compact than that used in the previous study. The berm layers and their volumes are shown in Table 4.4.

For the diffusion-controlling shield, this study considered only the layers between the outer surface of the tunnel concrete and the inner surface of the proposed limestone capillary break. Table 4.3 showed that Soil Zones 1 through 5 contain 99.997% of the activity in the shield berm.

Treating only this "inner-soil" portion as the only diffusion-controlling component is very conservative since it results in a larger surface-to-volume ratio, higher average concentrations of nuclides, and a smaller facility hydraulic cross section. All of these assumptions combine to estimate higher release rates and lower dilutions that result in high estimates of the pore water concentrations. These assumptions are much more severe than those used in the previous report, ORNL/TM-13665 (Dole, 1998).

Also, this analysis gives no barrier-credit to the "outer-soil" (3.05-m-thick Soil Zone 6) or proposed limestone (1-m-thick) layers. Another severe assumption in these analyses restricts the "zone of influence" with regard to infiltrating, recharge water to just the outer edge of Soil Zone 6. In report ORNL/TM-13665 (Dole, 1998), this zone of influence was extended 10 m beyond either side of the outermost edges of an earlier, larger-diameter shield berm. This study's assumption significantly reduces the hydraulic cross section and severely reduces the amount of vadose pore water available to dilute the berm's diffusing nuclides. Combining the volumes of the berm's components (Table 4.4) with the activities of activation products (Table 4.3) results in the concentrations shown in Table 4.5.

The masses of the total 30-year nuclide accumulations in Table 4.3 and the hydrologic data in Sect. 2.2 were used with the diffusion models to calculate the releases and the subsequent pore water concentrations. The pore water concentrations at the 196th month are reported in Table 4.6 because it represents the worst case, highest pore water concentration to arrive at the water table below the SNS facilities.

These analyses show that the DWLs are not exceeded in either Case 1 or Case 2.

These results for $^{14}C$ and $^{22}Na$ were compared to those of a standard 1-D transport code, SESOIL (see Sect. 5), as a benchmark. Table 4.7 shows that the results agree reasonably well, considering the wide range of different assumptions required to apply each of these models.

**Table 4.5. Summary of activation product concentrations in the component layers of the current SNS shield-berm conceptual design**

| Isotope | Nuclide activity in concrete section ($\mu Ci/cm^3$) | Nuclide activity in Soil-1 section ($\mu Ci/cm^3$) | Nuclide activity in Soil-2 section ($\mu Ci/cm^3$) | Nuclide activity in Soil-3 section ($\mu Ci/cm^3$) | Nuclide activity in Soil-4 section ($\mu Ci/cm^3$) | Nuclide activity in Soil-5 section, ($\mu Ci/cm^3$) | Nuclide activity in Limestone section ($\mu Ci/cm^3$) | Nuclide activity in 30 m Soil-6 section ($\mu Ci/cm^3$) | Total overall ($\mu Ci/cm^3$) |
|---|---|---|---|---|---|---|---|---|---|
| $^{3}H$ | 44.304 | 6.442241 | 2.13049 | 0.548487 | 0.08224 | 0.013121 | 0.00145307 | 0.000357 | 1.21E–06 |
| $^{10}Be$ | 1.76E–06 | 3.74E–07 | 1.49E–07 | 4.41E–08 | 7.12E–09 | 5.96E–09 | 1.1508E–10 | 1.17E–13 | 5.6E–14 |
| $^{14}C$ | 0.06877 | 0.015664 | 0.005422 | 0.001478 | 0.000231 | 4.71E–05 | 1.2142E–05 | 7.89E–07 | 2.16E–09 |
| $^{22}Na$ | 12.97214 | 1.329855 | 0.483374 | 0.119465 | 0.023289 | 0.005048 | 0.00010582 | 1.22E–06 | 3.32E–07 |
| $^{26}Al$ | 0.00193 | 0.000338 | 0.000117 | 2.99E–05 | 5.07E–06 | 1.15E–06 | 2.6261E–10 | 1.55E–08 | 5.57E–11 |
| $^{36}Cl$ | 0.000592 | 1.29E–05 | 5.73E–06 | 1.18E–06 | 1.7E–07 | 5.88E–08 | 8.3986E–08 | 1.88E–10 | 1.29E–11 |
| $^{39}Ar$ | 1.330598 | 0.025623 | 0.008168 | 0.00242 | 0.000299 | 5.69E–05 | 1.9641E–05 | 1.22E–06 | 2.87E–08 |
| $^{42}Ar$ | 0.009155 | 2.57E–08 | 8.4E–09 | 2.16E–09 | 3.46E–10 | 5.59E–11 | 2.1162E–08 | 0 | 1.9E–10 |
| $^{40}K$ | 1.73E–06 | 2.7E–09 | 5.44E–10 | 1.78E–10 | 4.64E–11 | 3.61E–12 | 2.8854E–10 | 8.5E–14 | 3.61E–14 |
| $^{41}Ca$ | 0.002422 | 6.38E–06 | 2.03E–06 | 2.82E–07 | 1.41E–09 | 2.81E–10 | 3.0602E–07 | 6.73E–12 | 5.05E–11 |
| $^{53}Mn$ | 1.76E–05 | 1.08E–05 | 4.01E–06 | 9.34E–07 | 1.75E–07 | 4.04E–08 | 1.3463E–11 | 3.13E–11 | 8.74E–13 |
| $^{54}Mn$ | 642.94 | 353.2597 | 110.9672 | 25.30667 | 6.60858 | 1.441495 | 0.00188731 | 0.002027 | 2.91E–05 |
| $^{55}Fe$ | 4.19312 | 2.068392 | 0.582845 | 0.171487 | 0.023052 | 0.0042 | 0.00065187 | 3.07E–05 | 1.77E–07 |
| Totals | 705.8273 | 363.1419 | 114.1776 | 26.15004 | 6.737698 | 1.46397 | 0.00413027 | 0.002418 | 3.08E–05 |

**Table 4.6. Comparison of two transport cases: In Case 1, the activity accumulates over the 30 years (360 months) of operation and then diffusion from the inner berm and radiogenic decay begin**

[*In Case 2, the generation of activity is equally divided in to 360 monthly packets, each with its own diffusion and radiogenic decay. The concentrations in the vadose zone pore water are those expected after 16 years (196 months) of travel from the bottom of the berm to the top of the water table.*]

| Isotope | Half-life (year) | Calculated effective diffusion coefficients ($cm^2/s$) | Total inner soil (between concrete and limestone) ($\mu Ci/cm^3$) | 16-year pore water: Case 1 ($\mu Ci/cm^3$) | 16-year pore water: Case 2 ($\mu Ci/cm^3$) | NRC 10 CFR Part 20 DWLs ($\mu Ci/cm^3$) |
|---|---|---|---|---|---|---|
| $^{3}H$ | 1.26E+01 | 5.59E–07 | 1.07E–01 | 5.26E–07 | 1.52E–09 | 1.E–03 |
| $^{10}Be$ | 2.50E+06 | 1.37E–09 | 7.14E–09 | 2.26E–14 | 7.91E–17 | 3.E–05 |
| $^{14}C$ | 5.73E+03 | 1.58E–06 | 2.68E–04 | 3.19E–09 | 8.56E–12 | 3.E–05 |
| $^{22}Na$ | 2.62E+00 | 1.58E–07 | 2.30E–02 | 3.86E–09 | 1.79E–11 | 6.E–06 |
| $^{26}Al$ | 7.40E+05 | 3.29E–10 | 5.74E–06 | 1.13E–11 | 3.10E–14 | 6.E–06 |
| $^{36}Cl$ | 3.08E+05 | 1.02E–05 | 2.35E–07 | 7.78E–15 | 2.80E–12 | 2.E–05 |
| $^{39}Ar$ | 2.69E+02 | 1.20E–05 | 4.27E–04 | 4.88E–09 | 1.36E–11 | |
| $^{42}Ar$ | 3.30E+01 | 1.20E–05 | 4.26E–10 | 4.91E–15 | 1.36E–17 | |
| $^{40}K$ | 1.26E+09 | 4.74E–08 | 3.96E–11 | 4.57E–16 | 1.27E–18 | 4.E–06 |
| $^{41}Ca$ | 8.00E+04 | 2.87E–08 | 9.42E–08 | 1.00E–12 | 2.84E–15 | |
| $^{53}Mn$ | 1.90E+06 | 7.20E–09 | 1.86E–07 | 1.23E–12 | 3.77E–15 | 7.E–04 |
| $^{54}Mn$ | 8.30E–01 | 7.20E–09 | 5.76E+00 | 5.53E–11 | 3.64E–09 | 3.E–05 |
| $^{55}Fe$ | 2.60E+00 | 7.93E–09 | 3.29E–02 | 3.10E–09 | 8.03E–11 | 1.E–04 |
| | | Totals | 5.92E+00 | 5.41E–07 | 5.28E–09 | |

**Table 4.7. Comparisons of the results of this diffusion model with those of SESOIL (see Sect. 5)**

| Isotope | Case 1 ($\mu Ci/cm^3$) | Case 2 ($\mu Ci/cm^3$) | SESOIL Case II ($\mu Ci/cm^3$) | DWL ($\mu Ci/cm^3$) |
|---|---|---|---|---|
| $^{14}C$ | 3.19E–09 | 8.86E–12 | 8.10E–10 | 3.00E–05 |
| $^{22}Na$ | 3.88E–09 | 1.79E–11 | 1.80E–11 | 6.00E–06 |

## 4.9 REFERENCES


Atkins, A., May 1985, "The Influence of Waste Form Permeability on the Release of Radionuclides from a Repository," *Nucl. Waste Manage.*, **5**, 203–214.

Baker, S. I., J. S. Bull, and D. L. Goss, December 1997, "Leaching of Accelerator-Produced Radionuclides," *Health Physics*, **73**(6), 912–819.

Dole, L. R., 1989, Sect. 2, "Report on Monolith Design and Performance," *Final Report on Remedial Action: Pepper's Steel and Alloys Superfund Site, Medley, Florida*, Florida Power and Light Company, Juno Beach, Florida.

Dole, L. R., September 1998, *Preliminary Assessment of the Nuclide Migration from the Activation Zone around the Proposed Spallation Neutron Source Facility*, ORNL/TM-13665, Lockheed Martin Energy Research Corp., Oak Ridge National Laboratory, Oak Ridge, Tennessee.

Dragun, J., 1988, Chapter 1, "Overview: How Soil Governs Water Quality," pp. 1–15 in *The Soil Chemistry of Hazardous Materials*, Hazardous Materials Control Research Institute, Silver Springs, Maryland.

Godbee, H. W., et al., 1993, *Waste Confinement Systems and Waste-Form Durability*, pp. 125-141 in *Effective Waste Management: Interfacing Sciences and Engineering with Monitoring and Risk Analysis*, eds., R. L. Jolley and R. G. M. Wang, Lewis Publishers, Boca Raton, Florida.

*Handbook of Chemistry and Physics*, 1993–1994, CRC Press, 74th ed., New York.

Nestor, C. W., Jr., January 1980, *Diffusion from Solid Cylinders*, ORNL/SDTM-84, Lockheed Martin Energy Research Corp., Oak Ridge National Laboratory, Oak Ridge, Tennessee.

"Performance Evaluation of the Technical Capabilities of DOE Sites for Disposal of Mixed Low-Level Waste," March 1996, Chapter 14, Vol. 3, *Site Evaluations*, DOE/ID-10521/3, Sandia National Laboratories, Albuquerque, New Mexico.

Spence, R. D., et al., 1993, Chapter 14, "Interpretation of Leaching Data for Cementitious Waste Forms Using Analytical Solutions Based on Mass Transport Theory and Empiricism," pp. 143–161 in *Effective Safe Waste Management: Interfacing Sciences and Engineering with Monitoring and Risk Analysis*, eds., R. L. Jolley and R. G. Wang, Lewis Publishers, Boca Raton, Florida.

Thibault, D. H., and M. Shepard, 1990, "A Critical Compilation and Review of Default Soil Solid/Liquid Partition Coefficients," Nuclide Partition Coefficients from Tables 5 and 6, AECL-10125, CAN/DN:1990:448145.

# 5. SESOIL BENCHMARK OF THE DIFFUSION-CONTROLLED MODEL WITH $^{14}C$ AND $^{22}Na$

The purpose of this part of the study is to compare the results of the diffusion-controlled transport model with those of a standard transport model. It is an independent investigation of the potential impacts of migrating isotopes from the activation zone around the proposed SNS at the ORR using the unsaturated soil zone model SESOIL.

In Sect. 4 a diffusion-transport model predicted that concentrations in the groundwater under the SNS site would not exceed the U.S. Nuclear Regulatory Commission (NRC) Title 10 CFR Part 20 DWLs. The diffusion-model used conservatively high estimates of the potential inventories of several radionuclides that could form in the shield berm around the SNS facility.

This part of the study uses the fate and transport model SESOIL to predict time-dependent concentrations in the unsaturated zone as well as the groundwater below the site. This study can be considered to be an independent analysis to support and compare the diffusion assessment with this standard 1-D advective transport model in order to confirm that DWLs will not be exceeded. The hydrology of SESOIL was calibrated to data from the ORR (see Sect. 2.2). Two cases are simulated for migration-contamination at the SNS site ($^{14}C$ and $^{22}Na$). In each case, conservative assumptions were made that were tailored for the SESOIL model (e.g., geometry of the site, contaminant loading, etc.). The following describes the SESOIL model and data used and presents the results.

## 5.1 SESOIL MODEL DESCRIPTION

SESOIL is an acronym for Seasonal Soil Compartment Model and is a 1-D vertical advective transport code for the unsaturated soil zone. It is an integrated screening-level soil compartment model and is designed to simultaneously model water transport, sediment transport, and pollutant fate.

The program was developed for the U.S. Environmental Protection Agency (EPA) Office of Water and the Office of Toxic Substances (OTS) in 1981 by Arthur D. Little, Inc. (ADL). ADL updated the SESOIL model in 1984 to include a fourth soil compartment (the original model included up to three layers) and the soil erosion algorithms (Bonazountas and Wagner, 1984). A comprehensive evaluation of SESOIL performed by Watson and Brown (1985) uncovered numerous deficiencies in the model, and subsequently SESOIL was modified extensively by Hetrick et al. at ORNL to enhance its capabilities (Hetrick et al., 1986; Hetrick and Travis, 1988; Hetrick et al., 1989; Hetrick et al., 1993, and Hetrick and Luxmoore, 1997).

SESOIL considers only one compound at a time, and the model is based on mass balance and equilibrium partitioning of the contaminant between different phases (dissolved, sorbed, vapor, and pure). The SESOIL model was designed to perform long-term simulations of chemical transport and transformations in the soil. The model uses theoretically derived equations to represent water transport, sediment transport on the land surface, pollutant transformation, and migration of the pollutant to the atmosphere and groundwater. Climatic data, compartment geometry, and soil and contaminant property data are the major components used in the equations.

The soil column in SESOIL is a user-defined compartment extending from the surface through the unsaturated zone to the groundwater table. Typically, SESOIL is used to estimate the rate of migration of a chemical through soil and the concentration of the chemical in soil layers following chemical release to the soil environment. The model can accept time-varying pollutant loading. SESOIL's simulation of chemical persistence considers mobility, volatility, and

degradation. The model performs calculations on a monthly basis, and can simulate chemical transport for as many years as the user desires.

SESOIL was developed as a screening-level model, utilizing less soil, chemical, and meteorological values as input than most other similar models. The model requires several types of chemical- and site-specific data to estimate the concentration of the chemical in the soil, its rate of leaching toward groundwater, and the impact of other environmental pathways. The user is required to provide chemical properties and release rate, and soil and climate data. Output of the SESOIL model includes time-varying pollutant concentrations at various soil depths and pollutant loss from the unsaturated zone in terms of surface runoff, percolation to the groundwater, volatilization, and degradation.

### 5.1.1 Limitations/Assumptions for SESOIL

The attributes of SESOIL that make it particularly attractive and suitable for vadose zone soil leaching studies are given below:

- SESOIL has been extensively validated and shown to work under a number of scenarios [Bonazountas, Wagner, and Goodwin, 1982; Wagner, Bonazountas, and Altersberg, 1983; Hetrick, 1984; Kincaid et al., 1984; Watson and Brown, 1985; Hetrick et al., 1986; Melancon, Pollard, and Hern, 1986; Hetrick and Travis, 1988; Hetrick et al., 1989; Hetrick, Luxmoore, and Tharp, 1997; Ladwig and Hensel, 1993; Odencrantz, Farr, and Robinson, 1992; Science Applications International Corporation (SAIC), 1994].

- SESOIL is a 1-D soil compartment model that considers adsorption, volatilization, degradation-decay, and convective transport. At the same time, the input data requirements are not extensive, making it simpler than more complex models, while still maintaining considerable resolution of the pollutant front in both time and space.

- Documentation of SESOIL is readily available, including numerous publications on the subject and a user's guide recently developed by Hetrick and Scott (1993).

- The model can be divided into as few as two layers and as many as four layers, with options of up to ten sublayers per layer. This compartmental nature of the model allows for user-specified tailoring to suit a particular site.

SESOIL, like any other vadose-zone, soil-leaching model, has some built-in assumptions and limitations:

- A contaminant in SESOIL can partition in up to four phases (liquid, adsorbed, air, and pure) and is at equilibrium within the soil system. However, transport of the pure phase is not considered.

- SESOIL can be used to model the transport of only one contaminant at a time through the vadose zone. Consequently, the effect of various contaminants on one another in different phases (solid, liquid, and gaseous) can not be simulated or studied.

- No provision is made in the SESOIL code to handle the presence of a perched water table.

- SESOIL does include the process of biodegradation-decay in its pollutant cycle, but does not keep track of the daughter products. For example, if trichloroethylene (TCE) were to degrade

to vinyl chloride, it is expected that the modeler would conduct another simulation to study the transport of vinyl chloride.

- SESOIL does not take the process of dispersion into account. Hence, the contaminant could migrate at a slower pace through the vadose zone to the groundwater, as compared to real systems.

- Only one value of the water content is computed in the hydrologic cycle for each month.

- Seasonal fluctuations of the groundwater table cannot be addressed in SESOIL. Moreover, there is no upward movement of contaminant from the groundwater to the soil column, nor does SESOIL consider the potential upward movement of contaminant with the upward movement of water due to soil evaporation losses.

## 5.2 SITE-SPECIFIC DATA USED FOR THE SNS FACILITY ON THE ORR

Selection of input parameters for a specific site is a critical factor in evaluating the exposure assessment relating to any modeling effort. The input parameters for SESOIL can be divided into five major data types:

- climatic
- soil
- chemical
- sediment washload
- application

This section describes the data needed and used for this study for each of these categories. Assumptions are discussed.

### 5.2.1 Climatic Data

The climatic data file of SESOIL consists of arrays of mean monthly temperature, cloud-cover fraction, relative humidity, shortwave albedo, evapotranspiration, precipitation, number of storm events, duration of rainfall, and length of rainy season. Climatic data sets for weather stations located throughout the country are available for SESOIL from General Sciences Corporation, the proprietors of the RISKPRO$^{TM}$ system that contains the SESOIL program (General Sciences Corp., 1987). The climatic data for the weather station at the Atmospheric Turbulence and Diffusion Laboratory (ATDL) in Oak Ridge, Tennessee, are the closest to the SNS site and thus were chosen for this study.

### 5.2.2 Soil Data

The soil data file of SESOIL contains input parameters describing the physical characteristics of the subsurface soil. These parameters include dry soil bulk density, intrinsic permeability,* soil disconnectedness index, effective soil porosity, and the Freundlich exponent. Dry soil bulk density, intrinsic permeability, and effective porosity should be measured for the site. There is, however, no measurement method for the soil disconnectedness index or estimation techniques for determining the Freundlich exponent. Default values for these parameters are

*Intrinsic permeability ($cm^2$) = [$1 \times 10^{-5} \times$ Darcy permeability (cm/s)].

suggested in the user's guide (Hetrick and Scott, 1993). When hydrologic measurements at the site are available, the soil parameters should be calibrated within measured limits to optimize agreement between SESOIL hydrologic results and the measurements. Two hydrologic cases were modeled with SESOIL.

Intrinsic permeability measured in the laboratory (Table 15 of *Geotechnical Report, 1998*) varied from 8.55E–9 to 3.5E–13 $cm^2$ with an average of 1.29E–9 $cm^2$. The soil density at the site ranges from 1.51–1.69 $g/cm^3$ with an average of 1.61 $g/cm^3$ (Table 9 of *Geotechnical Report*). Studies for the ORR (see Sect. 2.2.3) indicate that the mean annual precipitation in the period 1954 to 1983 was 133 cm, with extreme values of 90 and 190 cm during that same period. An average of 76 cm of water is consumed by evapotranspiration, and the remaining 57 cm is discharged as stream flow. Hydrograph analyses and modeling results, which attempt to separate storm runoff from the much slower responding groundwater flow, indicate that between 47 and 35% of all runoff is likely to be associated with groundwater in an average year (see Sect. 2.2.3). This translates to a range from 20.0 to 26.8 cm of annual groundwater flow for an average year in Case I.

It should be noted, however, that estimates of delayed flow, based only on hydrograph separation, represent as much as 86% of runoff (see Sect. 2.2.3.1). This places a possible upper limit of about 49 cm on annual groundwater recharge for Case II. In both cases, there were no assumptions of perched zones of saturation, and all subsurface flow was assumed to move vertically downward to the water table before being discharged.

Using the evapotranspiration, and groundwater recharge as calibration endpoints, SESOIL parameters were calibrated to compute the following annual hydrology [annual average rainfall at ATDL in Oak Ridge, used in this study, is 138.8 cm (54.6 in.), which is slightly more than the ORR].

SESOIL Case I Calculated Parameters:

Volumetric soil moisture content—annual average = 24.4% (varies from 21.7% in September to 27.7% in February)
Infiltration—98.3 cm (38.7 in.)
Evapotranspiration—75.0 cm (29.5 in.)
Surface runoff—40.4 cm (15.9 in.)
Groundwater runoff—23.4 cm (9.2 in.)

Final Case I calculated SESOIL soil parameters used at the SNS site are:

Dry soil bulk density—1.61 $g/cm^3$
Intrinsic permeability—1.8E–10 $cm^2$
Effective porosity—0.37
Disconnectedness index—7.5 (for clay loam soil)
Freundlich exponent—1.0

The calibrated parameters (intrinsic permeability, effective porosity, and disconnectedness index) are very reasonable for the clay loam soil at the SNS site. Note that if the intrinsic permeability is raised to 7.5E–10 $cm^2$, SESOIL computes the following hydrology (i.e., SESOIL was calibrated in a separate analysis until the groundwater runoff reached 49 cm/year):

Case II Calculated SESOIL Parameters:

Volumetric soil moisture content—annual average = 22.3% (varies from 19.8% in August to 25.3% in February)
Infiltration—124.9 cm (49.2 in.)
Evapotranspiration—76.2 cm (30.0 in.)
Surface runoff—13.8 cm (5.4 in.)
Groundwater runoff—48.8 cm (19.2 in.)

Both Case I and Case II hydrologies were used in this study to give a range of results. It should be noted, however, that these computed hydrologies assume the site has not been altered (i.e., there is no tunnel or buildings obstructing infiltration and flow).

Subsequent to the completion of the SESOIL and diffusion model simulations, results of an additional phase of geotechnical studies have become available. The results of this study have been summarized in *Report of Phase II Additional Geotechnical Study* (Law Engineering, 1999). New hydraulic conductivity data from undisturbed core samples are generally lower than the previous data published in the 1998 Phase II Geotechnical report (1998), while moisture contents are generally higher. Based on a review of the new data , it was determined that rerunning the SESOIL and diffusion models using new input parameters (calculated using the new data) was not warranted because the basic conclusions regarding leaching would not change. Model input and output parameters (e.g., hydraulic conductivity and recharge rates) are believed to be conservative and representative of field-scale hydraulic parameters found at the site.

### 5.2.3 Contaminant Data

The pollutant fate cycle of SESOIL focuses on the various chemical transport and transformation processes that may occur in the soil zone. These processes include volatilization-diffusion, adsorption-desorption, and biodegradation. Two isotopes were included in this study ($^{14}C$ and $^{22}Na$). The data used for $^{14}C$ in SESOIL for the SNS site are as follows (given the uncertainty in the soil adsorption coefficient $K_d$ for $^{14}C$, the conservative value of 1.0 was used):

Solubility in water—1.69E5 µg/mL
Air diffusion coefficient—0.139 $cm^2/s$
Henry's Law constant—0.022 $m^3$-atm/mole
Soil adsorption coefficient—1.0 (µg/g)/(µg/mL)
Biodegradation rate—3.3E–7 $day^{-1}$ (half-life is 5730 years)

The data used for $^{22}Na$ in SESOIL for the SNS site are as follows (given the uncertainty in the soil adsorption coefficient $K_d$ for $^{22}Na$, values of 15.0 and 1.0 were used):

Solubility in water—6.9E–4 µg/mL
Air diffusion coefficient—0.0 $cm^2/s$
Henry's Law constant—0.0 $m^3$-atm/mole
Soil adsorption coefficient—1.0 and 15.0 (µg/g)/(µg/mL)
Biodegradation rate—7.29E–4 $day^{-1}$ (half-life is 2.604 years)

### 5.2.4 Sediment Washload Data

The sediment washload cycle of SESOIL is optional; it can be turned on or off by the user. Additional data needed for the sediment cycle include the washload area; the fraction of sand, silt,

and clay in the soil; the average slope and slope length of the representative overland flow profile; the soil erodibility factor; the soil loss ratio; the contouring factor; and Manning's n coefficient for soil cover and surface roughness (Hetrick and Scott, 1993). This cycle was not used in this study since the contaminant source was deep and pollutant eroded with sediment particles at the surface would be negligible.

### 5.2.5 Application Data

The application data file of SESOIL contains the general information describing the specifics of the chemical releases or application to the soil column. This information includes the dimensions of the soil column and definition of soil layers (i.e., depths).

The geometry of the site used for the SESOIL model is shown in Fig. 5.1. Borehole data determined that the average depth from below the tunnel base to the groundwater was 16.7 m (54.8 ft) (Joe DeVore, LMER, private communication, 1999). The total depth from surface to groundwater was set to 28.75 m (94.3 ft). The unsaturated zone was divided into four layers for input to SESOIL, with depths of 6.71 m (22 ft), 5.34 m (17.5 ft), 4.0 m (13.1 ft), and 12.7 m (41.7 ft), respectively. The third layer was divided into four sublayers, and the contaminant source was loaded into the first 1.0-m sublayer of this layer (considered to be a conservative approach). The calculated quantities of $^{14}C$ and $^{22}Na$ for the entire soil berm were 2.5E–4 Ci (56 μg) and 2.1E–2 Ci (3.4 μg), respectively. These activation rates were based on the highest-energy section of the SNS beam at 1 GeV and were distributed over the entire length of the SNS beam. These values were each divided by 360 months (30 years of operation) and input to SESOIL monthly over this time period. The area used for the source contamination was the width of the tunnel (~5.5 m) plus a 4.0-m spread on each side of the tunnel, multiplied by the entire tunnel length (958 m). The fourth layer was divided into ten sublayers for increased resolution.

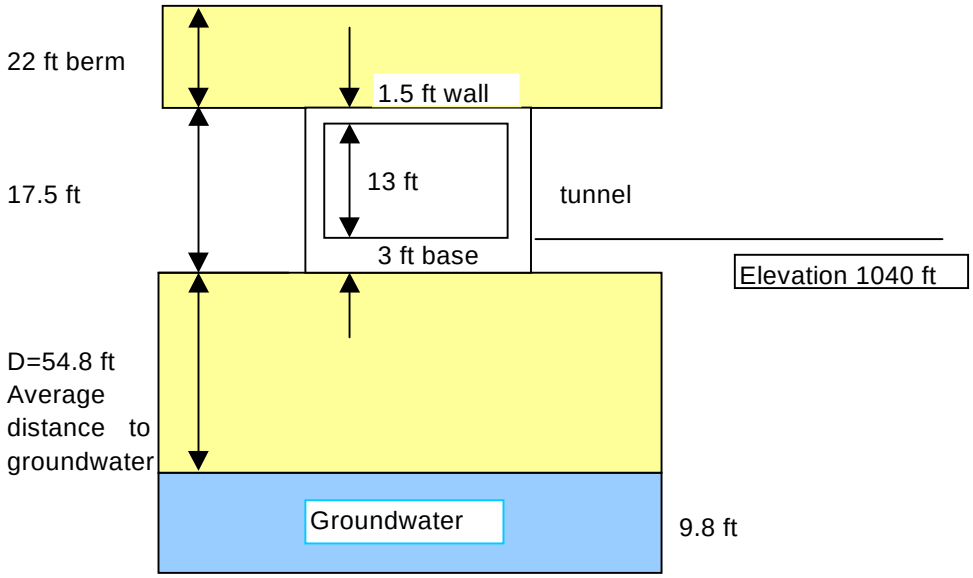


**Fig. 5.1. Geometry of the proposed SNS site used in the SESOIL calculation.**

Summers, Gherini, and Chen's model (1980) is used in SESOIL to compute the concentration of the contaminant in the groundwater directly below the source (Fig. 5.1). The thickness of the saturated zone (groundwater) was set to 3 m (9.8 ft) with a saturated hydraulic conductivity equal to 24.4 cm/d (0.8 ft/d) and hydraulic gradient of 0.02. These values are typical for the ORR (see Sect. 2.2.3). The width of the contaminated zone perpendicular to the flow was input as 958 m.

## 5.3 RESULTS

Due to the uncertainty in the soil adsorption coefficient $K_d$ for $^{14}C$, $K_d$ was set to the conservative value of 1.0 (μg/g)/(μg/mL). Table 5.1 shows the results for $^{14}C$ using the average hydrology, including the year in which the contaminant reached the groundwater, the year in which the maximum dissolved concentration occurred in groundwater, and the computed maximum dissolved concentration. In the more conservative Case II, the calculated maximum groundwater concentration is several orders of magnitude below the DWL. An additional case was simulated with $K_d$ = 1.0 using the hydrology computed by SESOIL when the model was calibrated to a conservative maximum groundwater recharge rate of 49 cm/year. It was also assumed that there was no gaseous phase (and thus no diffusion-volatilization upward of the contaminant—that is, the air diffusion coefficient and the Henry's Law constant were both set to 0.0). Case II is considered the most conservative that could be simulated since all contaminant would be allowed to go in the vertical, downward direction only in SESOIL, and the contaminant would be in the adsorbed and dissolved phases only. Results are shown in Table 5.1; the maximum computed concentration is still several orders of magnitude below the DWL for $^{14}C$.

The isotope $^{22}Na$ has a relatively short half-life and thus would be expected to be depleted from the soil system before reaching the groundwater. The SESOIL results confirmed this expectation when using the adsorption coefficient $K_d$ of 15 (μg/g)/(μg/mL), even when using the maximum groundwater recharge rate of 49 cm/year (see Table 5.2). Due to the uncertainty in the $K_d$ value, another case was simulated where this parameter was set to 1.0 (μg/g)/(μg/mL). These results are also shown in Table 5.2 and are several orders of magnitude below the DWL for $^{22}Na$.

**Table 5.1. SESOIL $^{14}C$ results for the two SESOIL calculated cases at the proposed SNS site**

| SESOIL calculated hydrology Cases | Year reached groundwater | Year of maximum concentration | Computed maximum concentration (μCi/cm$^3$) | DWL (μCi/cm$^3$) |
|---|---|---|---|---|
| **Case I:** $K_d$ = 1 (average hydrology) | 74 | 88 | 2.7E–10 | 3.0E–5 |
| **Case II:** $K_d$ = 1 (maximum groundwater recharge = 49 cm/year; no gaseous phase) | 43 | 57 | 8.1E–10 | 3.0E–5 |

**Table 5.2. SESOIL $^{22}$Na results for two $K_d$'s at the proposed SNS site at the conservative Case II calculated site hydrology**

| Case II (Maximum groundwater recharge) | Year reached groundwater | Year of maximum concentration | Computed maximum concentration (μCi/cm$^3$) | DWL (μCi/cm$^3$) |
|---|---|---|---|---|
| $K_d$ = 15 (groundwater recharge = 49 cm/year) | 569 | NA | 0.0 | 6.0E–6 |
| $K_d$ = 1 (groundwater recharge = 49 cm/year) | 43 | 44 | 1.8E–11 | 6.0E–6 |

## 5.4 REFERENCES


Bonazountas, M., J. Wagner, and B. Goodwin, 1982, *Evaluation of Seasonal Soil/Groundwater Pollutant Pathways*, EPA Contract No. 68-01-5949 (9), Arthur D. Little, Inc., Cambridge, Massachusetts.

Bonazountas, M., and J. Wagner, 1984, *SESOIL: A Seasonal Soil Compartment Model*, Arthur D. Little, Inc., Cambridge, Massachusetts.

Devore, J. R., July 1999, SNS Project Manager, LMER, private communication to D. M. Hetrick.

General Sciences Corporation, 1987, *User's Guide to SESOIL Execution in GEMS*, Laurel, Maryland.

Hetrick, D. M., 1984, *Simulation of the Hydrologic Cycle for Watersheds*, Proc. 10th IASTED International Symposium: Applied Simulation and Modeling, San Francisco, California.

Hetrick, D. M. et al., 1986, "Model Predictions of Watershed Hydrologic Components: Comparison and Verification," *Water Resour. Bull.*, **22**(5), 803–810.

Hetrick, D. M., and C. C. Travis, 1988, "Model Predictions of Watershed Erosion Components," *Water Resour. Bull.*, **24**(2), 413–419.

Hetrick, D. M., et al., 1989, *Qualitative Validation of Pollutant Transport Components of an Unsaturated Soil Zone Model (SESOIL)*, ORNL/TM-10672, Lockheed Martin Energy Research Corp., Oak Ridge National Laboratory, Oak Ridge, Tennessee.

Hetrick, D. M., and S. J. Scott, 1993, *The New SESOIL User's Guide*, Wisconsin Department of Natural Resources, PUBL-SW-200, Madison, Wisconsin.

Hetrick, D. M., R. J. Luxmoore, and M. L. Tharp, 1997, Chapter 12, "Latin Hypercube Sampling with the SESOIL Model," pp. 293–309 in *SESOIL in Environmental Fate and Risk Modeling*, eds., M. Bonazountas, D. M. Hetrick, P. T. Kostecki, and E. J. Calabrese, Amherst Scientific Publishers, Amherst, Massachusetts.

Kincaid, C. T., et al., 1984, "Geohydrochemical Models for Solute Migration," *Vol. 2: Preliminary Evaluation of Selected Computer Codes for Modeling Aqueous Solution and Solute Migration in Soils and Geologic Media*, EA-3477, Electric Power Research Institute, Palo Alto, California.

Ladwig, K. J., and B. R. Hensel, 1993, *Groundwater Contamination Susceptibility Evaluation, SESOIL Modeling Results*, Madison, Wisconsin.

Law Engineering and Environmental Services, Inc., December 1998, *Report of Phase II Geotechnical Exploration, The Spallation Neutron Source*, Project 50300-8-1020/0002/0800, Knoxville, Tennessee.

Melancon, S. M., J. E. Pollard, and S. C. Hern, 1986, "Evaluation of SESOIL, PRZM, and PESTAN in a Laboratory Column Leaching Experiment," *Environ. Toxicol. Chem*., **5**(10), 865–878.

Odencrantz, J. E., J. M. Farr, and C. E. Robinson, 1992, "Transport Model Parameter Sensitivity for Soil Cleanup Level Determinations Using SESOIL and AT123D in the Context of the California Leaking Underground Fuel Tank Manual," *J. Soil Contamination*, **1**(2), 159–182.

Science Applications International Corporation, 1994, *Vadose Zone Soil Leaching Report (Model and PRG Development)*, U.S. Department of Energy, DOE/OR/12-1249&D1, POEF-ER-4591&D1, Piketon, Ohio.

Summers, K., S. Gherini, and C. Chen, 1980, *Methodology to Evaluate the Potential for Groundwater Contamination from Geothermal Fluid Release*, EPA-600/7-80-117, as modified by U.S. EPA Region IV, Atlanta, Georgia.

Wagner, J., M. Bonazountas, and M. Alsterberg, 1983, *Potential Fate of Buried Halogenated Solvents via SESOIL*, Arthur D. Little, Inc., Cambridge, Massachusetts.

Watson, D. B., and S. N. Brown, 1985, *Testing and Evaluation of the SESOIL Model*, Anderson-Nichols and Co., Inc., Palo Alto, California.

# 6. CONCLUSION

Alone, the 4-m-thick inner-soil of the SNS shield berm, which contains 99.997% of the activation products, has sufficient retention of the major nuclides to ensure that the groundwater directly under this facility on top of Chestnut Ridge on the ORR cannot exceed the 10 CFR Part 20 DWLs.

The diffusion-controlled models used very conservative assumptions with regard to diffusion coefficients and the site's transport conditions. Case I of the diffusion-controlled model cases used the maximum credible source term for the initial nuclide inventories. Case II of the diffusion-controlled models agrees with the results of the standard advective 1-D compartment model, SESOIL Case II (maximum groundwater recharge). In these cases, the inventory of activation products was released in increments as the products were generated, and there is excellent agreement between the two models. In comparing these results, even the sums of all the major nuclides (see Table 4.6) do not exceed the lowest DWL.

The most significant impact on these analyses was the corrected calculation of activation products within the SNS shield berm. These corrected nuclide generation rates resulted in significant reduction in the estimates of its nuclide inventories. Subsequently, this resulted in lowering the estimated activity concentrations in the vadose pore water beneath the Oak Ridge SNS Facility on Chestnut Ridge.

These results show that just the inner-soil portion of the SNS shield berm is sufficient to protect the site's groundwater without additional barriers or the limestone capillary-break that was suggested in the previous report, ORNL/TM-13665 (Dole, 1998).

## 6.1 REFERENCE

Dole, L. R., September 1998, *Preliminary Assessment of the Nuclide Migration from the Activation Zone around the Proposed Spallation Neutron Source Facility*, ORNL/TM-13665, Lockheed Martin Energy Research Corp., Oak Ridge National Laboratory, Oak Ridge, Tennessee.

# Appendix A

# RESULTS OF ACTIVATION ANALYSES

| Table A.1. SNS nuclide production during normal proton beam operation: beam transport line copper | | | | | | | | | | | | |
|---|---|---|---|---|---|---|---|---|---|---|---|---|
| Proton beam energy: 1 GeV | | | | | | | Operational line loss assumption: 1 nA/m (continuous) | | | | | |
| Nuclide masses integrated over the material zone volume in the HETC & MCNP calculational model | | | | | | | | | | | | |
| Nuclide concentration | | Time (s) | 7.88E+06 | 1.58E+07 | 2.37E+07 | 3.15E+07 | 6.31E+07 | 1.58E+08 | 3.15E+08 | 4.73E+08 | 6.31E+08 | 9.46E+08 |
| (gram-atoms) | | Initial | 3 months | 6 months | 9 months | 1 year | 2 years | 5 years | 10 years | 15 years | 20 years | 30 years |
| H | 1 | 0.00E+00 | 4.93E-07 | 1.00E-06 | 1.50E-06 | 2.00E-06 | 4.00E-06 | 1.00E-05 | 2.00E-05 | 3.00E-05 | 4.00E-05 | 5.99E-05 |
| H | 2 | 0.00E+00 | 3.35E-08 | 6.81E-08 | 1.02E-07 | 1.36E-07 | 2.72E-07 | 6.81E-07 | 1.36E-06 | 2.04E-06 | 2.72E-06 | 4.08E-06 |
| H | 3 | 0.00E+00 | 1.22E-08 | 2.47E-08 | 3.68E-08 | 4.85E-08 | 9.45E-08 | 2.18E-07 | 3.82E-07 | 5.06E-07 | 6.00E-07 | 7.23E-07 |
| HE | 3 | 0.00E+00 | 7.85E-09 | 1.61E-08 | 2.44E-08 | 3.28E-08 | 6.84E-08 | 1.90E-07 | 4.32E-07 | 7.15E-07 | 1.03E-06 | 1.72E-06 |
| HE | 4 | 0.00E+00 | 3.55E-08 | 7.21E-08 | 1.08E-07 | 1.44E-07 | 2.88E-07 | 7.21E-07 | 1.44E-06 | 2.16E-06 | 2.88E-06 | 4.32E-06 |
| LI | 6 | 0.00E+00 | 5.25E-12 | 1.07E-11 | 1.60E-11 | 2.12E-11 | 4.26E-11 | 1.07E-10 | 2.12E-10 | 3.19E-10 | 4.26E-10 | 6.38E-10 |
| LI | 7 | 0.00E+00 | 1.66E-13 | 5.07E-13 | 8.95E-13 | 1.29E-12 | 2.93E-12 | 8.20E-12 | 1.67E-11 | 2.52E-11 | 3.38E-11 | 5.05E-11 |
| BE | 7 | 0.00E+00 | 2.38E-13 | 3.13E-13 | 3.35E-13 | 3.42E-13 | 3.45E-13 | 3.45E-13 | 3.45E-13 | 3.45E-13 | 3.45E-13 | 3.45E-13 |
| BE | 9 | 0.00E+00 | 2.02E-12 | 4.10E-12 | 6.15E-12 | 8.17E-12 | 1.64E-11 | 4.10E-11 | 8.17E-11 | 1.23E-10 | 1.64E-10 | 2.45E-10 |
| B | 10 | 0.00E+00 | 6.86E-12 | 1.39E-11 | 2.09E-11 | 2.78E-11 | 5.57E-11 | 1.39E-10 | 2.78E-10 | 4.17E-10 | 5.57E-10 | 8.34E-10 |
| B | 11 | 0.00E+00 | 6.46E-12 | 1.31E-11 | 1.97E-11 | 2.62E-11 | 5.24E-11 | 1.31E-10 | 2.62E-10 | 3.93E-10 | 5.24E-10 | 7.85E-10 |
| C | 11 | 0.00E+00 | 4.58E-16 | 4.58E-16 | 4.58E-16 | 4.58E-16 | 4.58E-16 | 4.58E-16 | 4.58E-16 | 4.58E-16 | 4.58E-16 | 4.58E-16 |
| C | 12 | 0.00E+00 | 5.09E-11 | 1.03E-10 | 1.55E-10 | 2.06E-10 | 4.13E-10 | 1.03E-09 | 2.06E-09 | 3.09E-09 | 4.13E-09 | 6.18E-09 |
| C | 13 | 0.00E+00 | 3.19E-11 | 6.48E-11 | 9.71E-11 | 1.29E-10 | 2.59E-10 | 6.48E-10 | 1.29E-09 | 1.94E-09 | 2.59E-09 | 3.88E-09 |
| C | 14 | 0.00E+00 | 1.21E-12 | 2.46E-12 | 3.69E-12 | 4.90E-12 | 9.82E-12 | 2.46E-11 | 4.90E-11 | 7.36E-11 | 9.81E-11 | 1.47E-10 |
| N | 13 | 0.00E+00 | 5.82E-16 | 5.82E-16 | 5.82E-16 | 5.82E-16 | 5.82E-16 | 5.82E-16 | 5.82E-16 | 5.82E-16 | 5.82E-16 | 5.82E-16 |
| N | 14 | 0.00E+00 | 8.96E-11 | 1.82E-10 | 2.73E-10 | 3.63E-10 | 7.27E-10 | 1.82E-09 | 3.63E-09 | 5.45E-09 | 7.27E-09 | 1.09E-08 |
| N | 15 | 0.00E+00 | 5.29E-11 | 1.07E-10 | 1.61E-10 | 2.14E-10 | 4.29E-10 | 1.07E-09 | 2.14E-09 | 3.21E-09 | 4.29E-09 | 6.43E-09 |
| N | 16 | 0.00E+00 | 5.85E-18 | 5.85E-18 | 5.85E-18 | 5.85E-18 | 5.85E-18 | 5.85E-18 | 5.85E-18 | 5.85E-18 | 5.85E-18 | 5.85E-18 |
| N | 17 | 0.00E+00 | 9.36E-19 | 9.36E-19 | 9.36E-19 | 9.36E-19 | 9.36E-19 | 9.36E-19 | 9.36E-19 | 9.36E-19 | 9.36E-19 | 9.36E-19 |
| O | 15 | 0.00E+00 | 1.28E-16 | 1.28E-16 | 1.28E-16 | 1.28E-16 | 1.28E-16 | 1.28E-16 | 1.28E-16 | 1.28E-16 | 1.28E-16 | 1.28E-16 |
| O | 16 | 0.00E+00 | 1.11E-10 | 2.25E-10 | 3.37E-10 | 4.48E-10 | 8.97E-10 | 2.25E-09 | 4.48E-09 | 6.72E-09 | 8.97E-09 | 1.34E-08 |
| O | 17 | 0.00E+00 | 3.07E-11 | 6.23E-11 | 9.35E-11 | 1.24E-10 | 2.49E-10 | 6.23E-10 | 1.24E-09 | 1.87E-09 | 2.49E-09 | 3.73E-09 |
| O | 18 | 0.00E+00 | 7.67E-11 | 1.56E-10 | 2.34E-10 | 3.11E-10 | 6.22E-10 | 1.56E-09 | 3.11E-09 | 4.66E-09 | 6.22E-09 | 9.33E-09 |
| O | 19 | 0.00E+00 | 6.51E-18 | 6.51E-18 | 6.51E-18 | 6.51E-18 | 6.51E-18 | 6.51E-18 | 6.51E-18 | 6.51E-18 | 6.51E-18 | 6.51E-18 |
| F | 17 | 0.00E+00 | 2.90E-17 | 2.90E-17 | 2.90E-17 | 2.90E-17 | 2.90E-17 | 2.90E-17 | 2.90E-17 | 2.90E-17 | 2.90E-17 | 2.90E-17 |
| F | 18 | 0.00E+00 | 8.18E-14 | 8.18E-14 | 8.18E-14 | 8.18E-14 | 8.18E-14 | 8.18E-14 | 8.18E-14 | 8.18E-14 | 8.18E-14 | 8.18E-14 |
| F | 19 | 0.00E+00 | 5.05E-11 | 1.02E-10 | 1.54E-10 | 2.04E-10 | 4.09E-10 | 1.02E-09 | 2.04E-09 | 3.07E-09 | 4.09E-09 | 6.14E-09 |
| F | 20 | 0.00E+00 | 9.88E-18 | 9.88E-18 | 9.88E-18 | 9.88E-18 | 9.88E-18 | 9.88E-18 | 9.88E-18 | 9.88E-18 | 9.88E-18 | 9.88E-18 |
| F | 21 | 0.00E+00 | 6.51E-19 | 6.51E-19 | 6.51E-19 | 6.51E-19 | 6.51E-19 | 6.51E-19 | 6.51E-19 | 6.51E-19 | 6.51E-19 | 6.51E-19 |
| F | 22 | 0.00E+00 | 3.17E-19 | 3.17E-19 | 3.17E-19 | 3.17E-19 | 3.17E-19 | 3.17E-19 | 3.17E-19 | 3.17E-19 | 3.17E-19 | 3.17E-19 |
| NE | 19 | 0.00E+00 | 1.03E-17 | 1.03E-17 | 1.03E-17 | 1.03E-17 | 1.03E-17 | 1.03E-17 | 1.03E-17 | 1.03E-17 | 1.03E-17 | 1.03E-17 |
| NE | 20 | 0.00E+00 | 5.05E-11 | 1.02E-10 | 1.54E-10 | 2.04E-10 | 4.09E-10 | 1.02E-09 | 2.04E-09 | 3.07E-09 | 4.09E-09 | 6.14E-09 |
| NE | 21 | 0.00E+00 | 3.19E-11 | 6.48E-11 | 9.71E-11 | 1.29E-10 | 2.59E-10 | 6.48E-10 | 1.29E-09 | 1.94E-09 | 2.59E-09 | 3.88E-09 |

**Table A.1. (continued)**

| Proton beam energy: 1 GeV | | | | | | | Operational line loss assumption: 1 nA/m (continuous) | | | | | |
|---|---|---|---|---|---|---|---|---|---|---|---|---|
| Nuclide masses integrated over the material zone volume in the HETC & MCNP calculational model | | | | | | | | | | | | |
| Nuclide concentration | | Time (s) | 7.88E+06 | 1.58E+07 | 2.37E+07 | 3.15E+07 | 6.31E+07 | 1.58E+08 | 3.15E+08 | 4.73E+08 | 6.31E+08 | 9.46E+08 |
| (gram-atoms) | | Initial | 3 months | 6 months | 9 months | 1 year | 2 years | 5 years | 10 years | 15 years | 20 years | 30 years |
| NE | 22 | 0.00E+00 | 2.13E-11 | 4.72E-11 | 7.63E-11 | 1.08E-10 | 2.68E-10 | 9.45E-10 | 2.38E-09 | 3.97E-09 | 5.59E-09 | 8.83E-09 |
| NE | 23 | 0.00E+00 | 2.25E-17 | 2.25E-17 | 2.25E-17 | 2.25E-17 | 2.25E-17 | 2.25E-17 | 2.25E-17 | 2.25E-17 | 2.25E-17 | 2.25E-17 |
| NE | 24 | 0.00E+00 | 4.55E-17 | 4.55E-17 | 4.55E-17 | 4.55E-17 | 4.55E-17 | 4.55E-17 | 4.55E-17 | 4.55E-17 | 4.55E-17 | 4.55E-17 |
| NA | 21 | 0.00E+00 | 5.05E-18 | 5.05E-18 | 5.05E-18 | 5.05E-18 | 5.05E-18 | 5.05E-18 | 5.05E-18 | 5.05E-18 | 5.05E-18 | 5.05E-18 |
| NA | 22 | 0.00E+00 | 5.90E-11 | 1.16E-10 | 1.68E-10 | 2.17E-10 | 3.84E-10 | 6.86E-10 | 8.68E-10 | 9.17E-10 | 9.30E-10 | 9.34E-10 |
| NA | 23 | 0.00E+00 | 1.42E-10 | 2.88E-10 | 4.32E-10 | 5.74E-10 | 1.15E-09 | 2.88E-09 | 5.74E-09 | 8.61E-09 | 1.15E-08 | 1.72E-08 |
| NA | 24 | 0.00E+00 | 1.86E-13 | 1.86E-13 | 1.86E-13 | 1.86E-13 | 1.86E-13 | 1.86E-13 | 1.86E-13 | 1.86E-13 | 1.86E-13 | 1.86E-13 |
| NA | 25 | 0.00E+00 | 3.59E-17 | 3.59E-17 | 3.59E-17 | 3.59E-17 | 3.59E-17 | 3.59E-17 | 3.59E-17 | 3.59E-17 | 3.59E-17 | 3.59E-17 |
| NA | 26 | 0.00E+00 | 3.20E-19 | 3.20E-19 | 3.20E-19 | 3.20E-19 | 3.20E-19 | 3.20E-19 | 3.20E-19 | 3.20E-19 | 3.20E-19 | 3.20E-19 |
| MG | 23 | 0.00E+00 | 7.63E-18 | 7.63E-18 | 7.63E-18 | 7.63E-18 | 7.63E-18 | 7.63E-18 | 7.63E-18 | 7.63E-18 | 7.63E-18 | 7.63E-18 |
| MG | 24 | 0.00E+00 | 1.47E-10 | 2.99E-10 | 4.48E-10 | 5.95E-10 | 1.19E-09 | 2.98E-09 | 5.95E-09 | 8.93E-09 | 1.19E-08 | 1.79E-08 |
| MG | 25 | 0.00E+00 | 1.37E-10 | 2.79E-10 | 4.18E-10 | 5.56E-10 | 1.11E-09 | 2.79E-09 | 5.56E-09 | 8.34E-09 | 1.11E-08 | 1.67E-08 |
| MG | 26 | 0.00E+00 | 6.34E-11 | 1.29E-10 | 1.93E-10 | 2.57E-10 | 5.14E-10 | 1.29E-09 | 2.57E-09 | 3.85E-09 | 5.14E-09 | 7.71E-09 |
| MG | 27 | 0.00E+00 | 1.02E-15 | 1.02E-15 | 1.02E-15 | 1.02E-15 | 1.02E-15 | 1.02E-15 | 1.02E-15 | 1.02E-15 | 1.02E-15 | 1.02E-15 |
| AL | 25 | 0.00E+00 | 1.07E-18 | 1.07E-18 | 1.07E-18 | 1.07E-18 | 1.07E-18 | 1.07E-18 | 1.07E-18 | 1.07E-18 | 1.07E-18 | 1.07E-18 |
| AL | 26 | 0.00E+00 | 1.51E-10 | 3.07E-10 | 4.61E-10 | 6.13E-10 | 1.23E-09 | 3.07E-09 | 6.13E-09 | 9.20E-09 | 1.23E-08 | 1.84E-08 |
| AL | 27 | 0.00E+00 | 3.23E-10 | 6.57E-10 | 9.85E-10 | 1.31E-09 | 2.62E-09 | 6.57E-09 | 1.31E-08 | 1.97E-08 | 2.62E-08 | 3.93E-08 |
| AL | 28 | 0.00E+00 | 2.52E-15 | 2.52E-15 | 2.52E-15 | 2.52E-15 | 2.52E-15 | 2.52E-15 | 2.52E-15 | 2.52E-15 | 2.52E-15 | 2.52E-15 |
| AL | 29 | 0.00E+00 | 1.25E-15 | 1.25E-15 | 1.25E-15 | 1.25E-15 | 1.25E-15 | 1.25E-15 | 1.25E-15 | 1.25E-15 | 1.25E-15 | 1.25E-15 |
| AL | 30 | 0.00E+00 | 1.93E-18 | 1.93E-18 | 1.93E-18 | 1.93E-18 | 1.93E-18 | 1.93E-18 | 1.93E-18 | 1.93E-18 | 1.93E-18 | 1.93E-18 |
| AL | 31 | 0.00E+00 | 9.58E-20 | 9.58E-20 | 9.58E-20 | 9.58E-20 | 9.58E-20 | 9.58E-20 | 9.58E-20 | 9.58E-20 | 9.58E-20 | 9.58E-20 |
| SI | 27 | 0.00E+00 | 4.61E-18 | 4.61E-18 | 4.61E-18 | 4.61E-18 | 4.61E-18 | 4.61E-18 | 4.61E-18 | 4.61E-18 | 4.61E-18 | 4.61E-18 |
| SI | 28 | 0.00E+00 | 3.79E-10 | 7.70E-10 | 1.15E-09 | 1.53E-09 | 3.07E-09 | 7.70E-09 | 1.53E-08 | 2.30E-08 | 3.07E-08 | 4.61E-08 |
| SI | 29 | 0.00E+00 | 4.76E-10 | 9.67E-10 | 1.45E-09 | 1.93E-09 | 3.86E-09 | 9.67E-09 | 1.93E-08 | 2.90E-08 | 3.86E-08 | 5.79E-08 |
| SI | 30 | 0.00E+00 | 2.12E-10 | 4.30E-10 | 6.46E-10 | 8.58E-10 | 1.72E-09 | 4.30E-09 | 8.58E-09 | 1.29E-08 | 1.72E-08 | 2.58E-08 |
| SI | 31 | 0.00E+00 | 6.99E-14 | 6.99E-14 | 6.99E-14 | 6.99E-14 | 6.99E-14 | 6.99E-14 | 6.99E-14 | 6.99E-14 | 6.99E-14 | 6.99E-14 |
| SI | 32 | 0.00E+00 | 5.65E-12 | 1.15E-11 | 1.72E-11 | 2.29E-11 | 4.58E-11 | 1.14E-10 | 2.28E-10 | 3.41E-10 | 4.53E-10 | 6.76E-10 |
| SI | 33 | 0.00E+00 | 9.28E-19 | 9.28E-19 | 9.28E-19 | 9.28E-19 | 9.28E-19 | 9.28E-19 | 9.28E-19 | 9.28E-19 | 9.28E-19 | 9.28E-19 |
| P | 31 | 0.00E+00 | 6.56E-10 | 1.33E-09 | 2.00E-09 | 2.65E-09 | 5.32E-09 | 1.33E-08 | 2.65E-08 | 3.99E-08 | 5.32E-08 | 7.97E-08 |
| P | 32 | 0.00E+00 | 9.00E-11 | 9.12E-11 | 9.12E-11 | 9.12E-11 | 9.12E-11 | 9.12E-11 | 9.12E-11 | 9.12E-11 | 9.12E-11 | 9.12E-11 |
| P | 33 | 0.00E+00 | 3.23E-11 | 3.50E-11 | 3.52E-11 | 3.52E-11 | 3.52E-11 | 3.52E-11 | 3.52E-11 | 3.52E-11 | 3.52E-11 | 3.52E-11 |
| P | 34 | 0.00E+00 | 3.90E-17 | 3.90E-17 | 3.90E-17 | 3.90E-17 | 3.90E-17 | 3.90E-17 | 3.90E-17 | 3.90E-17 | 3.90E-17 | 3.90E-17 |
| P | 35 | 0.00E+00 | 2.11E-17 | 2.11E-17 | 2.11E-17 | 2.11E-17 | 2.11E-17 | 2.11E-17 | 2.11E-17 | 2.11E-17 | 2.11E-17 | 2.11E-17 |
| S | 31 | 0.00E+00 | 4.29E-18 | 4.29E-18 | 4.29E-18 | 4.29E-18 | 4.29E-18 | 4.29E-18 | 4.29E-18 | 4.29E-18 | 4.29E-18 | 4.29E-18 |

**Table A.1. (continued)**

| Proton beam energy: 1 GeV | | | | | | | Operational line loss assumption: 1 nA/m (continuous) | | | | | |
|---|---|---|---|---|---|---|---|---|---|---|---|---|
| Nuclide masses integrated over the material zone volume in the HETC & MCNP calculational model | | | | | | | | | | | | |
| Nuclide concentration | | Time (s) | 7.88E+06 | 1.58E+07 | 2.37E+07 | 3.15E+07 | 6.31E+07 | 1.58E+08 | 3.15E+08 | 4.73E+08 | 6.31E+08 | 9.46E+08 |
| (gram-atoms) | | Initial | 3 months | 6 months | 9 months | 1 year | 2 years | 5 years | 10 years | 15 years | 20 years | 30 years |
| S | 32 | 0.00E+00 | 4.44E-10 | 9.93E-10 | 1.53E-09 | 2.07E-09 | 4.33E-09 | 1.09E-08 | 2.18E-08 | 3.27E-08 | 4.37E-08 | 6.54E-08 |
| S | 33 | 0.00E+00 | 5.07E-10 | 1.06E-09 | 1.61E-09 | 2.15E-09 | 4.37E-09 | 1.10E-08 | 2.19E-08 | 3.29E-08 | 4.39E-08 | 6.58E-08 |
| S | 34 | 0.00E+00 | 5.69E-10 | 1.16E-09 | 1.73E-09 | 2.30E-09 | 4.62E-09 | 1.16E-08 | 2.30E-08 | 3.46E-08 | 4.62E-08 | 6.92E-08 |
| S | 35 | 0.00E+00 | 1.21E-10 | 1.82E-10 | 2.11E-10 | 2.25E-10 | 2.38E-10 | 2.39E-10 | 2.39E-10 | 2.39E-10 | 2.39E-10 | 2.39E-10 |
| S | 36 | 0.00E+00 | 3.71E-11 | 7.54E-11 | 1.13E-10 | 1.50E-10 | 3.01E-10 | 7.54E-10 | 1.50E-09 | 2.26E-09 | 3.01E-09 | 4.52E-09 |
| S | 37 | 0.00E+00 | 2.50E-16 | 2.50E-16 | 2.50E-16 | 2.50E-16 | 2.50E-16 | 2.50E-16 | 2.50E-16 | 2.50E-16 | 2.50E-16 | 2.50E-16 |
| S | 38 | 0.00E+00 | 7.62E-16 | 7.62E-16 | 7.62E-16 | 7.62E-16 | 7.62E-16 | 7.62E-16 | 7.62E-16 | 7.62E-16 | 7.62E-16 | 7.62E-16 |
| CL | 35 | 0.00E+00 | 8.26E-10 | 1.74E-09 | 2.67E-09 | 3.61E-09 | 7.44E-09 | 1.92E-08 | 3.86E-08 | 5.81E-08 | 7.75E-08 | 1.16E-07 |
| CL | 36 | 0.00E+00 | 9.39E-10 | 1.91E-09 | 2.86E-09 | 3.80E-09 | 7.62E-09 | 1.91E-08 | 3.80E-08 | 5.71E-08 | 7.62E-08 | 1.14E-07 |
| CL | 37 | 0.00E+00 | 7.64E-10 | 1.92E-09 | 3.11E-09 | 4.30E-09 | 9.62E-09 | 2.46E-08 | 4.91E-08 | 7.37E-08 | 9.83E-08 | 1.47E-07 |
| CL | 38 | 0.00E+00 | 1.42E-14 | 1.42E-14 | 1.42E-14 | 1.42E-14 | 1.42E-14 | 1.42E-14 | 1.42E-14 | 1.42E-14 | 1.42E-14 | 1.42E-14 |
| CL | 39 | 0.00E+00 | 5.30E-15 | 5.30E-15 | 5.30E-15 | 5.30E-15 | 5.30E-15 | 5.30E-15 | 5.30E-15 | 5.30E-15 | 5.30E-15 | 5.30E-15 |
| CL | 40 | 0.00E+00 | 2.96E-17 | 2.96E-17 | 2.96E-17 | 2.96E-17 | 2.96E-17 | 2.96E-17 | 2.96E-17 | 2.96E-17 | 2.96E-17 | 2.96E-17 |
| AR | 36 | 0.00E+00 | 1.81E-10 | 3.67E-10 | 5.51E-10 | 7.32E-10 | 1.47E-09 | 3.67E-09 | 7.32E-09 | 1.10E-08 | 1.47E-08 | 2.20E-08 |
| AR | 37 | 0.00E+00 | 4.23E-10 | 4.95E-10 | 5.06E-10 | 5.08E-10 | 5.09E-10 | 5.08E-10 | 5.08E-10 | 5.08E-10 | 5.08E-10 | 5.08E-10 |
| AR | 38 | 0.00E+00 | 1.20E-09 | 2.43E-09 | 3.64E-09 | 4.84E-09 | 9.70E-09 | 2.43E-08 | 4.84E-08 | 7.27E-08 | 9.70E-08 | 1.45E-07 |
| AR | 39 | 0.00E+00 | 2.31E-10 | 4.69E-10 | 7.03E-10 | 9.34E-10 | 1.87E-09 | 4.66E-09 | 9.23E-09 | 1.38E-08 | 1.83E-08 | 2.70E-08 |
| AR | 40 | 0.00E+00 | 8.28E-11 | 1.68E-10 | 2.52E-10 | 3.35E-10 | 6.71E-10 | 1.68E-09 | 3.35E-09 | 5.03E-09 | 6.71E-09 | 1.01E-08 |
| AR | 41 | 0.00E+00 | 3.45E-14 | 3.45E-14 | 3.45E-14 | 3.45E-14 | 3.45E-14 | 3.45E-14 | 3.45E-14 | 3.45E-14 | 3.45E-14 | 3.45E-14 |
| AR | 42 | 0.00E+00 | 4.43E-12 | 8.97E-12 | 1.34E-11 | 1.78E-11 | 3.53E-11 | 8.56E-11 | 1.62E-10 | 2.31E-10 | 2.94E-10 | 4.00E-10 |
| K | 38 | 0.00E+00 | 1.36E-14 | 1.36E-14 | 1.36E-14 | 1.36E-14 | 1.36E-14 | 1.36E-14 | 1.36E-14 | 1.36E-14 | 1.36E-14 | 1.36E-14 |
| K | 39 | 0.00E+00 | 1.07E-09 | 2.18E-09 | 3.27E-09 | 4.34E-09 | 8.70E-09 | 2.18E-08 | 4.35E-08 | 6.54E-08 | 8.74E-08 | 1.31E-07 |
| K | 40 | 0.00E+00 | 1.01E-09 | 2.04E-09 | 3.07E-09 | 4.08E-09 | 8.17E-09 | 2.04E-08 | 4.08E-08 | 6.12E-08 | 8.17E-08 | 1.22E-07 |
| K | 41 | 0.00E+00 | 4.74E-10 | 9.62E-10 | 1.44E-09 | 1.92E-09 | 3.84E-09 | 9.62E-09 | 1.92E-08 | 2.88E-08 | 3.84E-08 | 5.76E-08 |
| K | 42 | 0.00E+00 | 1.68E-12 | 1.68E-12 | 1.68E-12 | 1.68E-12 | 1.68E-12 | 1.68E-12 | 1.68E-12 | 1.69E-12 | 1.69E-12 | 1.69E-12 |
| K | 43 | 0.00E+00 | 6.76E-13 | 6.76E-13 | 6.76E-13 | 6.76E-13 | 6.76E-13 | 6.76E-13 | 6.76E-13 | 6.76E-13 | 6.76E-13 | 6.76E-13 |
| K | 44 | 0.00E+00 | 1.69E-15 | 1.69E-15 | 1.69E-15 | 1.69E-15 | 1.69E-15 | 1.69E-15 | 1.69E-15 | 1.69E-15 | 1.69E-15 | 1.69E-15 |
| K | 45 | 0.00E+00 | 2.69E-16 | 2.69E-16 | 2.69E-16 | 2.69E-16 | 2.69E-16 | 2.69E-16 | 2.69E-16 | 2.69E-16 | 2.69E-16 | 2.69E-16 |
| CA | 40 | 0.00E+00 | 3.47E-10 | 7.05E-10 | 1.06E-09 | 1.41E-09 | 2.82E-09 | 7.05E-09 | 1.41E-08 | 2.11E-08 | 2.82E-08 | 4.22E-08 |
| CA | 41 | 0.00E+00 | 1.27E-09 | 2.57E-09 | 3.86E-09 | 5.13E-09 | 1.03E-08 | 2.57E-08 | 5.13E-08 | 7.71E-08 | 1.03E-07 | 1.54E-07 |
| CA | 42 | 0.00E+00 | 1.80E-09 | 3.67E-09 | 5.50E-09 | 7.31E-09 | 1.46E-08 | 3.67E-08 | 7.31E-08 | 1.10E-07 | 1.46E-07 | 2.20E-07 |
| CA | 43 | 0.00E+00 | 1.50E-09 | 3.04E-09 | 4.57E-09 | 6.07E-09 | 1.22E-08 | 3.04E-08 | 6.07E-08 | 9.11E-08 | 1.22E-07 | 1.82E-07 |
| CA | 44 | 0.00E+00 | 1.21E-09 | 2.46E-09 | 3.69E-09 | 4.90E-09 | 9.81E-09 | 2.46E-08 | 4.91E-08 | 7.39E-08 | 9.88E-08 | 1.49E-07 |
| CA | 45 | 0.00E+00 | 6.18E-11 | 1.05E-10 | 1.34E-10 | 1.54E-10 | 1.87E-10 | 1.96E-10 | 1.97E-10 | 1.97E-10 | 1.97E-10 | 1.96E-10 |

**Table A.1. (continued)**

| Proton beam energy: 1 GeV | | | | | | | Operational line loss assumption: 1 nA/m (continuous) | | | | | |
|---|---|---|---|---|---|---|---|---|---|---|---|---|
| Nuclide masses integrated over the material zone volume in the HETC & MCNP calculational model | | | | | | | | | | | | |
| Nuclide concentration | | Time (s) | 7.88E+06 | 1.58E+07 | 2.37E+07 | 3.15E+07 | 6.31E+07 | 1.58E+08 | 3.15E+08 | 4.73E+08 | 6.31E+08 | 9.46E+08 |
| (gram-atoms) | | Initial | 3 months | 6 months | 9 months | 1 year | 2 years | 5 years | 10 years | 15 years | 20 years | 30 years |
| CA | 46 | 0.00E+00 | 2.38E-11 | 4.84E-11 | 7.26E-11 | 9.64E-11 | 1.93E-10 | 4.84E-10 | 9.64E-10 | 1.45E-09 | 1.93E-09 | 2.90E-09 |
| CA | 47 | 0.00E+00 | 3.52E-13 | 3.52E-13 | 3.52E-13 | 3.52E-13 | 3.52E-13 | 3.52E-13 | 3.52E-13 | 3.52E-13 | 3.52E-13 | 3.52E-13 |
| CA | 48 | 0.00E+00 | 8.07E-13 | 1.64E-12 | 2.46E-12 | 3.27E-12 | 6.55E-12 | 1.64E-11 | 3.27E-11 | 4.91E-11 | 6.55E-11 | 9.82E-11 |
| SC | 41 | 0.00E+00 | 4.46E-20 | 4.46E-20 | 4.46E-20 | 4.46E-20 | 4.46E-20 | 4.46E-20 | 4.46E-20 | 4.46E-20 | 4.46E-20 | 4.46E-20 |
| SC | 42 | 0.00E+00 | 1.30E-17 | 1.30E-17 | 1.30E-17 | 1.30E-17 | 1.30E-17 | 1.30E-17 | 1.30E-17 | 1.30E-17 | 1.30E-17 | 1.30E-17 |
| SC | 43 | 0.00E+00 | 1.15E-12 | 1.15E-12 | 1.15E-12 | 1.15E-12 | 1.15E-12 | 1.15E-12 | 1.15E-12 | 1.15E-12 | 1.15E-12 | 1.15E-12 |
| SC | 44 | 0.00E+00 | 2.47E-12 | 2.47E-12 | 2.47E-12 | 2.47E-12 | 2.48E-12 | 2.48E-12 | 2.50E-12 | 2.51E-12 | 2.52E-12 | 2.54E-12 |
| SC | 45 | 0.00E+00 | 1.03E-09 | 2.11E-09 | 3.19E-09 | 4.26E-09 | 8.66E-09 | 2.20E-08 | 4.42E-08 | 6.65E-08 | 8.89E-08 | 1.33E-07 |
| SC | 46 | 0.00E+00 | 2.38E-10 | 3.53E-10 | 4.06E-10 | 4.31E-10 | 4.52E-10 | 4.53E-10 | 4.53E-10 | 4.53E-10 | 4.53E-10 | 4.53E-10 |
| SC | 47 | 0.00E+00 | 8.17E-12 | 8.17E-12 | 8.17E-12 | 8.17E-12 | 8.17E-12 | 8.17E-12 | 8.17E-12 | 8.17E-12 | 8.17E-12 | 8.17E-12 |
| SC | 48 | 0.00E+00 | 1.21E-12 | 1.21E-12 | 1.21E-12 | 1.21E-12 | 1.21E-12 | 1.21E-12 | 1.21E-12 | 1.21E-12 | 1.21E-12 | 1.21E-12 |
| SC | 49 | 0.00E+00 | 2.30E-15 | 2.30E-15 | 2.30E-15 | 2.30E-15 | 2.30E-15 | 2.30E-15 | 2.30E-15 | 2.30E-15 | 2.30E-15 | 2.30E-15 |
| SC | 50 | 0.00E+00 | 7.68E-18 | 7.68E-18 | 7.68E-18 | 7.68E-18 | 7.68E-18 | 7.68E-18 | 7.68E-18 | 7.68E-18 | 7.68E-18 | 7.68E-18 |
| TI | 43 | 0.00E+00 | 7.34E-20 | 7.34E-20 | 7.34E-20 | 7.34E-20 | 7.34E-20 | 7.34E-20 | 7.34E-20 | 7.34E-20 | 7.34E-20 | 7.34E-20 |
| TI | 44 | 0.00E+00 | 7.45E-11 | 1.51E-10 | 2.26E-10 | 3.00E-10 | 5.97E-10 | 1.46E-09 | 2.82E-09 | 4.08E-09 | 5.26E-09 | 7.38E-09 |
| TI | 45 | 0.00E+00 | 6.91E-13 | 6.91E-13 | 6.91E-13 | 6.91E-13 | 6.91E-13 | 6.91E-13 | 6.91E-13 | 6.91E-13 | 6.91E-13 | 6.91E-13 |
| TI | 46 | 0.00E+00 | 1.37E-09 | 2.92E-09 | 4.50E-09 | 6.09E-09 | 1.26E-08 | 3.27E-08 | 6.56E-08 | 9.88E-08 | 1.32E-07 | 1.98E-07 |
| TI | 47 | 0.00E+00 | 2.17E-09 | 4.42E-09 | 6.64E-09 | 8.83E-09 | 1.77E-08 | 4.42E-08 | 8.81E-08 | 1.32E-07 | 1.76E-07 | 2.64E-07 |
| TI | 48 | 0.00E+00 | 2.47E-09 | 5.62E-09 | 8.73E-09 | 1.18E-08 | 2.49E-08 | 6.29E-08 | 1.25E-07 | 1.88E-07 | 2.51E-07 | 3.76E-07 |
| TI | 49 | 0.00E+00 | 4.86E-10 | 1.49E-09 | 2.90E-09 | 4.62E-09 | 1.39E-08 | 5.08E-08 | 1.17E-07 | 1.83E-07 | 2.50E-07 | 3.98E-07 |
| TI | 50 | 0.00E+00 | 4.52E-11 | 9.18E-11 | 1.38E-10 | 1.83E-10 | 3.67E-10 | 9.18E-10 | 1.83E-09 | 2.75E-09 | 3.67E-09 | 5.50E-09 |
| TI | 51 | 0.00E+00 | 2.34E-16 | 2.34E-16 | 2.34E-16 | 2.34E-16 | 2.34E-16 | 2.34E-16 | 2.34E-16 | 2.34E-16 | 2.34E-16 | 2.34E-16 |
| TI | 52 | 0.00E+00 | 7.64E-18 | 7.64E-18 | 7.64E-18 | 7.64E-18 | 7.64E-18 | 7.64E-18 | 7.64E-18 | 7.64E-18 | 7.64E-18 | 7.64E-18 |
| V | 46 | 0.00E+00 | 4.71E-18 | 4.71E-18 | 4.71E-18 | 4.71E-18 | 4.71E-18 | 4.71E-18 | 4.71E-18 | 4.71E-18 | 4.71E-18 | 4.71E-18 |
| V | 47 | 0.00E+00 | 2.07E-13 | 2.07E-13 | 2.07E-13 | 2.07E-13 | 2.07E-13 | 2.07E-13 | 2.07E-13 | 2.07E-13 | 2.07E-13 | 2.07E-13 |
| V | 48 | 0.00E+00 | 6.00E-10 | 6.12E-10 | 6.12E-10 | 6.12E-10 | 6.12E-10 | 6.12E-10 | 6.12E-10 | 6.12E-10 | 6.12E-10 | 6.12E-10 |
| V | 49 | 0.00E+00 | 2.79E-09 | 5.16E-09 | 7.08E-09 | 8.65E-09 | 1.26E-08 | 1.57E-08 | 1.61E-08 | 1.61E-08 | 1.61E-08 | 1.61E-08 |
| V | 50 | 0.00E+00 | 1.26E-09 | 2.57E-09 | 3.85E-09 | 5.11E-09 | 1.02E-08 | 2.57E-08 | 5.11E-08 | 7.68E-08 | 1.02E-07 | 1.54E-07 |
| V | 51 | 0.00E+00 | 3.19E-09 | 8.19E-09 | 1.33E-08 | 1.83E-08 | 4.09E-08 | 1.04E-07 | 2.08E-07 | 3.12E-07 | 4.17E-07 | 6.23E-07 |
| V | 52 | 0.00E+00 | 2.59E-15 | 2.59E-15 | 2.59E-15 | 2.59E-15 | 2.59E-15 | 2.59E-15 | 2.59E-15 | 2.59E-15 | 2.59E-15 | 2.59E-15 |
| V | 53 | 0.00E+00 | 1.72E-16 | 1.72E-16 | 1.72E-16 | 1.72E-16 | 1.72E-16 | 1.72E-16 | 1.72E-16 | 1.72E-16 | 1.72E-16 | 1.72E-16 |
| V | 54 | 0.00E+00 | 1.93E-17 | 1.93E-17 | 1.93E-17 | 1.93E-17 | 1.93E-17 | 1.93E-17 | 1.93E-17 | 1.93E-17 | 1.93E-17 | 1.93E-17 |
| CR | 48 | 0.00E+00 | 9.93E-13 | 9.93E-13 | 9.93E-13 | 9.93E-13 | 9.93E-13 | 9.93E-13 | 9.93E-13 | 9.93E-13 | 9.93E-13 | 9.93E-13 |
| CR | 49 | 0.00E+00 | 3.57E-13 | 3.57E-13 | 3.57E-13 | 3.57E-13 | 3.57E-13 | 3.57E-13 | 3.57E-13 | 3.57E-13 | 3.57E-13 | 3.57E-13 |

**Table A.1. (continued)**

| Proton beam energy: 1 GeV | | | | | | | Operational line loss assumption: 1 nA/m (continuous) | | | | | |
|---|---|---|---|---|---|---|---|---|---|---|---|---|
| Nuclide masses integrated over the material zone volume in the HETC & MCNP calculational model | | | | | | | | | | | | |
| Nuclide concentration | | Time (s) | 7.88E+06 | 1.58E+07 | 2.37E+07 | 3.15E+07 | 6.31E+07 | 1.58E+08 | 3.15E+08 | 4.73E+08 | 6.31E+08 | 9.46E+08 |
| (gram-atoms) | | Initial | 3 months | 6 months | 9 months | 1 year | 2 years | 5 years | 10 years | 15 years | 20 years | 30 years |
| CR | 50 | 0.00E+00 | 2.90E-09 | 5.89E-09 | 8.84E-09 | 1.17E-08 | 2.35E-08 | 5.89E-08 | 1.17E-07 | 1.76E-07 | 2.35E-07 | 3.53E-07 |
| CR | 51 | 0.00E+00 | 1.84E-09 | 2.04E-09 | 2.06E-09 | 2.06E-09 | 2.06E-09 | 2.06E-09 | 2.06E-09 | 2.06E-09 | 2.06E-09 | 2.06E-09 |
| CR | 52 | 0.00E+00 | 6.29E-09 | 1.31E-08 | 1.99E-08 | 2.66E-08 | 5.25E-08 | 1.30E-07 | 2.57E-07 | 3.85E-07 | 5.13E-07 | 7.68E-07 |
| CR | 53 | 0.00E+00 | 6.23E-10 | 1.27E-09 | 1.90E-09 | 2.52E-09 | 5.05E-09 | 1.27E-08 | 2.52E-08 | 3.79E-08 | 5.05E-08 | 7.58E-08 |
| CR | 54 | 0.00E+00 | 3.79E-10 | 1.28E-09 | 2.57E-09 | 4.18E-09 | 1.29E-08 | 4.76E-08 | 1.09E-07 | 1.71E-07 | 2.33E-07 | 3.72E-07 |
| CR | 55 | 0.00E+00 | 7.27E-16 | 7.27E-16 | 7.27E-16 | 7.27E-16 | 7.27E-16 | 7.27E-16 | 7.27E-16 | 7.27E-16 | 7.27E-16 | 7.27E-16 |
| CR | 56 | 0.00E+00 | 4.00E-16 | 4.00E-16 | 4.00E-16 | 4.00E-16 | 4.00E-16 | 4.00E-16 | 4.00E-16 | 4.00E-16 | 4.00E-16 | 4.00E-16 |
| MN | 50 | 0.00E+00 | 3.30E-18 | 3.30E-18 | 3.30E-18 | 3.30E-18 | 3.30E-18 | 3.30E-18 | 3.30E-18 | 3.30E-18 | 3.30E-18 | 3.30E-18 |
| MN | 51 | 0.00E+00 | 5.02E-13 | 5.02E-13 | 5.02E-13 | 5.02E-13 | 5.02E-13 | 5.02E-13 | 5.02E-13 | 5.02E-13 | 5.02E-13 | 5.02E-13 |
| MN | 52 | 0.00E+00 | 3.71E-10 | 3.71E-10 | 3.71E-10 | 3.71E-10 | 3.71E-10 | 3.71E-10 | 3.71E-10 | 3.71E-10 | 3.71E-10 | 3.71E-10 |
| MN | 53 | 0.00E+00 | 6.50E-09 | 1.32E-08 | 1.98E-08 | 2.63E-08 | 5.27E-08 | 1.32E-07 | 2.63E-07 | 3.95E-07 | 5.27E-07 | 7.91E-07 |
| MN | 54 | 0.00E+00 | 2.68E-09 | 4.93E-09 | 6.74E-09 | 8.20E-09 | 1.19E-08 | 1.45E-08 | 1.48E-08 | 1.48E-08 | 1.48E-08 | 1.48E-08 |
| MN | 55 | 0.00E+00 | 8.94E-10 | 2.22E-09 | 3.91E-09 | 5.92E-09 | 1.71E-08 | 7.19E-08 | 1.97E-07 | 3.37E-07 | 4.81E-07 | 7.72E-07 |
| MN | 56 | 0.00E+00 | 3.56E-13 | 3.56E-13 | 3.56E-13 | 3.56E-13 | 3.56E-13 | 3.56E-13 | 3.56E-13 | 3.56E-13 | 3.56E-13 | 3.56E-13 |
| MN | 57 | 0.00E+00 | 8.09E-16 | 8.09E-16 | 8.09E-16 | 8.09E-16 | 8.09E-16 | 8.09E-16 | 8.09E-16 | 8.09E-16 | 8.09E-16 | 8.09E-16 |
| MN | 58 | 0.00E+00 | 2.98E-16 | 2.98E-16 | 2.98E-16 | 2.98E-16 | 2.98E-16 | 2.98E-16 | 2.98E-16 | 2.98E-16 | 2.98E-16 | 2.98E-16 |
| FE | 52 | 0.00E+00 | 3.92E-13 | 3.92E-13 | 3.92E-13 | 3.92E-13 | 3.92E-13 | 3.92E-13 | 3.92E-13 | 3.92E-13 | 3.92E-13 | 3.92E-13 |
| FE | 53 | 0.00E+00 | 7.48E-14 | 7.48E-14 | 7.48E-14 | 7.48E-14 | 7.48E-14 | 7.48E-14 | 7.48E-14 | 7.48E-14 | 7.48E-14 | 7.48E-14 |
| FE | 54 | 0.00E+00 | 4.27E-09 | 8.68E-09 | 1.30E-08 | 1.73E-08 | 3.46E-08 | 8.68E-08 | 1.73E-07 | 2.60E-07 | 3.46E-07 | 5.19E-07 |
| FE | 55 | 0.00E+00 | 6.29E-09 | 1.24E-08 | 1.80E-08 | 2.32E-08 | 4.12E-08 | 7.40E-08 | 9.43E-08 | 9.99E-08 | 1.01E-07 | 1.02E-07 |
| FE | 56 | 0.00E+00 | 4.30E-09 | 1.04E-08 | 1.73E-08 | 2.43E-08 | 5.38E-08 | 1.48E-07 | 3.01E-07 | 4.55E-07 | 6.09E-07 | 9.11E-07 |
| FE | 57 | 0.00E+00 | 2.06E-09 | 5.58E-09 | 1.01E-08 | 1.55E-08 | 4.25E-08 | 1.42E-07 | 3.13E-07 | 4.86E-07 | 6.58E-07 | 1.03E-06 |
| FE | 58 | 0.00E+00 | 2.50E-09 | 7.37E-09 | 1.31E-08 | 1.91E-08 | 4.44E-08 | 1.27E-07 | 2.60E-07 | 3.94E-07 | 5.27E-07 | 7.87E-07 |
| FE | 59 | 0.00E+00 | 1.29E-10 | 1.62E-10 | 1.69E-10 | 1.71E-10 | 1.72E-10 | 1.72E-10 | 1.72E-10 | 1.72E-10 | 1.72E-10 | 1.72E-10 |
| FE | 60 | 0.00E+00 | 1.07E-10 | 2.16E-10 | 3.25E-10 | 4.31E-10 | 8.64E-10 | 2.16E-09 | 4.31E-09 | 6.48E-09 | 8.64E-09 | 1.30E-08 |
| FE | 61 | 0.00E+00 | 2.90E-15 | 2.90E-15 | 2.90E-15 | 2.90E-15 | 2.90E-15 | 2.90E-15 | 2.90E-15 | 2.90E-15 | 2.90E-15 | 2.90E-15 |
| FE | 62 | 0.00E+00 | 1.88E-16 | 1.88E-16 | 1.88E-16 | 1.88E-16 | 1.88E-16 | 1.88E-16 | 1.88E-16 | 1.88E-16 | 1.88E-16 | 1.88E-16 |
| CO | 53 | 0.00E+00 | 5.88E-20 | 5.88E-20 | 5.88E-20 | 5.88E-20 | 5.88E-20 | 5.88E-20 | 5.88E-20 | 5.88E-20 | 5.88E-20 | 5.88E-20 |
| CO | 54 | 0.00E+00 | 2.46E-18 | 2.46E-18 | 2.46E-18 | 2.46E-18 | 2.46E-18 | 2.46E-18 | 2.46E-18 | 2.46E-18 | 2.46E-18 | 2.46E-18 |
| CO | 55 | 0.00E+00 | 1.11E-11 | 1.11E-11 | 1.11E-11 | 1.11E-11 | 1.11E-11 | 1.11E-11 | 1.11E-11 | 1.11E-11 | 1.11E-11 | 1.11E-11 |
| CO | 56 | 0.00E+00 | 3.01E-09 | 4.41E-09 | 5.01E-09 | 5.29E-09 | 5.49E-09 | 5.50E-09 | 5.50E-09 | 5.50E-09 | 5.50E-09 | 5.50E-09 |
| CO | 57 | 0.00E+00 | 6.44E-09 | 1.17E-08 | 1.58E-08 | 1.90E-08 | 2.65E-08 | 3.11E-08 | 3.13E-08 | 3.13E-08 | 3.13E-08 | 3.13E-08 |
| CO | 58 | 0.00E+00 | 3.76E-09 | 5.35E-09 | 5.99E-09 | 6.24E-09 | 6.42E-09 | 6.42E-09 | 6.42E-09 | 6.42E-09 | 6.42E-09 | 6.42E-09 |
| CO | 59 | 0.00E+00 | 4.79E-09 | 9.84E-09 | 1.48E-08 | 1.98E-08 | 3.98E-08 | 1.00E-07 | 2.00E-07 | 3.00E-07 | 4.00E-07 | 5.99E-07 |

**Table A.1. (continued)**

| Proton beam energy: 1 GeV | | | | | | | Operational line loss assumption: 1 nA/m (continuous) | | | | | |
|---|---|---|---|---|---|---|---|---|---|---|---|---|
| Nuclide masses integrated over the material zone volume in the HETC & MCNP calculational model | | | | | | | | | | | | |
| Nuclide concentration | | Time (s) | 7.88E+06 | 1.58E+07 | 2.37E+07 | 3.15E+07 | 6.31E+07 | 1.58E+08 | 3.15E+08 | 4.73E+08 | 6.31E+08 | 9.46E+08 |
| (gram-atoms) | | Initial | 3 months | 6 months | 9 months | 1 year | 2 years | 5 years | 10 years | 15 years | 20 years | 30 years |
| CO | 60 | 0.00E+00 | 2.68E-09 | 5.36E-09 | 7.91E-09 | 1.04E-08 | 1.95E-08 | 4.06E-08 | 6.15E-08 | 7.24E-08 | 7.81E-08 | 8.25E-08 |
| CO | 61 | 0.00E+00 | 1.68E-12 | 1.68E-12 | 1.68E-12 | 1.68E-12 | 1.68E-12 | 1.68E-12 | 1.68E-12 | 1.68E-12 | 1.68E-12 | 1.68E-12 |
| CO | 62 | 0.00E+00 | 1.18E-14 | 1.18E-14 | 1.18E-14 | 1.18E-14 | 1.18E-14 | 1.18E-14 | 1.18E-14 | 1.18E-14 | 1.18E-14 | 1.18E-14 |
| CO | 63 | 0.00E+00 | 1.54E-15 | 1.54E-15 | 1.54E-15 | 1.54E-15 | 1.54E-15 | 1.54E-15 | 1.54E-15 | 1.54E-15 | 1.54E-15 | 1.54E-15 |
| CO | 64 | 0.00E+00 | 1.23E-18 | 1.23E-18 | 1.23E-18 | 1.23E-18 | 1.23E-18 | 1.23E-18 | 1.23E-18 | 1.23E-18 | 1.23E-18 | 1.23E-18 |
| NI | 56 | 0.00E+00 | 7.34E-12 | 7.34E-12 | 7.34E-12 | 7.34E-12 | 7.34E-12 | 7.34E-12 | 7.34E-12 | 7.34E-12 | 7.34E-12 | 7.34E-12 |
| NI | 57 | 0.00E+00 | 2.24E-11 | 2.24E-11 | 2.24E-11 | 2.24E-11 | 2.24E-11 | 2.24E-11 | 2.24E-11 | 2.24E-11 | 2.24E-11 | 2.24E-11 |
| NI | 58 | 0.00E+00 | 5.38E-09 | 1.09E-08 | 1.64E-08 | 2.18E-08 | 4.37E-08 | 1.09E-07 | 2.18E-07 | 3.27E-07 | 4.37E-07 | 6.54E-07 |
| NI | 59 | 0.00E+00 | 1.17E-08 | 2.38E-08 | 3.57E-08 | 4.74E-08 | 9.50E-08 | 2.38E-07 | 4.74E-07 | 7.12E-07 | 9.50E-07 | 1.42E-06 |
| NI | 60 | 0.00E+00 | 1.80E-08 | 3.67E-08 | 5.52E-08 | 7.36E-08 | 1.49E-07 | 3.80E-07 | 7.78E-07 | 1.19E-06 | 1.60E-06 | 2.44E-06 |
| NI | 61 | 0.00E+00 | 2.81E-08 | 5.71E-08 | 8.57E-08 | 1.14E-07 | 2.28E-07 | 5.71E-07 | 1.14E-06 | 1.71E-06 | 2.28E-06 | 3.42E-06 |
| NI | 62 | 0.00E+00 | 6.86E-08 | 1.39E-07 | 2.09E-07 | 2.78E-07 | 5.56E-07 | 1.39E-06 | 2.78E-06 | 4.17E-06 | 5.56E-06 | 8.34E-06 |
| NI | 63 | 0.00E+00 | 1.89E-08 | 3.84E-08 | 5.75E-08 | 7.63E-08 | 1.52E-07 | 3.78E-07 | 7.40E-07 | 1.09E-06 | 1.43E-06 | 2.08E-06 |
| NI | 64 | 0.00E+00 | 2.28E-08 | 4.65E-08 | 6.98E-08 | 9.29E-08 | 1.86E-07 | 4.64E-07 | 9.25E-07 | 1.39E-06 | 1.85E-06 | 2.78E-06 |
| NI | 65 | 0.00E+00 | 1.74E-12 | 1.74E-12 | 1.74E-12 | 1.74E-12 | 1.74E-12 | 1.74E-12 | 1.74E-12 | 1.74E-12 | 1.74E-12 | 1.74E-12 |
| CU | 58 | 0.00E+00 | 8.39E-18 | 8.39E-18 | 8.39E-18 | 8.39E-18 | 8.39E-18 | 8.39E-18 | 8.39E-18 | 8.39E-18 | 8.39E-18 | 8.39E-18 |
| CU | 59 | 0.00E+00 | 3.76E-15 | 3.76E-15 | 3.76E-15 | 3.76E-15 | 3.76E-15 | 3.76E-15 | 3.76E-15 | 3.76E-15 | 3.76E-15 | 3.76E-15 |
| CU | 60 | 0.00E+00 | 6.92E-13 | 6.92E-13 | 6.92E-13 | 6.92E-13 | 6.92E-13 | 6.92E-13 | 6.92E-13 | 6.92E-13 | 6.92E-13 | 6.92E-13 |
| CU | 61 | 0.00E+00 | 2.91E-11 | 2.91E-11 | 2.91E-11 | 2.91E-11 | 2.91E-11 | 2.91E-11 | 2.91E-11 | 2.91E-11 | 2.91E-11 | 2.91E-11 |
| CU | 62 | 0.00E+00 | 4.71E-12 | 4.71E-12 | 4.71E-12 | 4.71E-12 | 4.71E-12 | 4.71E-12 | 4.71E-12 | 4.71E-12 | 4.71E-12 | 4.71E-12 |
| CU | 63 | 0.00E+00 | 1.44E-08 | 2.92E-08 | 4.39E-08 | 5.84E-08 | 1.18E-07 | 2.98E-07 | 6.07E-07 | 9.31E-07 | 1.27E-06 | 1.97E-06 |
| CU | 64 | 0.00E+00 | 2.35E-10 | 2.35E-10 | 2.35E-10 | 2.35E-10 | 2.35E-10 | 2.35E-10 | 2.35E-10 | 2.35E-10 | 2.35E-10 | 2.35E-10 |
| CU | 65 | 0.00E+00 | 3.66E-09 | 7.54E-09 | 1.15E-08 | 1.54E-08 | 3.17E-08 | 8.19E-08 | 1.65E-07 | 2.49E-07 | 3.33E-07 | 5.03E-07 |
| CU | 66 | 0.00E+00 | 1.16E-13 | 1.16E-13 | 1.16E-13 | 1.16E-13 | 1.16E-13 | 1.16E-13 | 1.16E-13 | 1.16E-13 | 1.16E-13 | 1.16E-13 |
| ZN | 60 | 0.00E+00 | 5.43E-17 | 5.43E-17 | 5.43E-17 | 5.43E-17 | 5.43E-17 | 5.43E-17 | 5.43E-17 | 5.43E-17 | 5.43E-17 | 5.43E-17 |
| ZN | 61 | 0.00E+00 | 9.80E-16 | 9.80E-16 | 9.80E-16 | 9.80E-16 | 9.80E-16 | 9.80E-16 | 9.80E-16 | 9.80E-16 | 9.80E-16 | 9.80E-16 |
| ZN | 62 | 0.00E+00 | 3.38E-12 | 3.38E-12 | 3.38E-12 | 3.38E-12 | 3.38E-12 | 3.38E-12 | 3.38E-12 | 3.38E-12 | 3.38E-12 | 3.38E-12 |
| ZN | 63 | 0.00E+00 | 5.33E-13 | 5.33E-13 | 5.33E-13 | 5.33E-13 | 5.33E-13 | 5.33E-13 | 5.33E-13 | 5.33E-13 | 5.33E-13 | 5.33E-13 |
| ZN | 64 | 0.00E+00 | 1.19E-08 | 2.43E-08 | 3.65E-08 | 4.86E-08 | 9.71E-08 | 2.43E-07 | 4.83E-07 | 7.26E-07 | 9.68E-07 | 1.45E-06 |
| ZN | 65 | 0.00E+00 | 4.81E-10 | 8.64E-10 | 1.15E-09 | 1.37E-09 | 1.86E-09 | 2.12E-09 | 2.13E-09 | 2.13E-09 | 2.13E-09 | 2.13E-09 |
| ZN | 66 | 0.00E+00 | 2.10E-09 | 4.27E-09 | 6.40E-09 | 8.50E-09 | 1.70E-08 | 4.27E-08 | 8.50E-08 | 1.28E-07 | 1.70E-07 | 2.55E-07 |
| Total | | 0.00E+00 | 8.85E-07 | 1.80E-06 | 2.70E-06 | 3.59E-06 | 7.18E-06 | 1.80E-05 | 3.59E-05 | 5.38E-05 | 7.18E-05 | 1.08E-04 |

| Table A.2. SNS nuclide production during normal proton beam operation: tunnel air | | | | | | | | | | | | |
|---|---|---|---|---|---|---|---|---|---|---|---|---|
| Proton beam energy: 1 GeV | | | | | | | Operational line loss assumption: 1 nA/m (continuous) | | | | | |
| Nuclide masses integrated over the material zone volume in the HETC & MCNP calculational model | | | | | | | | | | | | |
| Nuclide concentration | | Time (s) | 1.00E+01 | 2.00E+01 | 3.00E+01 | 4.00E+01 | 5.00E+01 | 6.00E+01 | 3.00E+02 | 6.00E+02 | 1.20E+03 | 1.80E+03 |
| (gram-atoms) | | Initial | 10 seconds | 20 seconds | 30 seconds | 40 seconds | 50 seconds | 1 minute | 5 minutes | 10 minutes | 20 minutes | 30 minutes |
| H | 1 | 0.00E+00 | 3.86E-15 | 7.72E-15 | 1.16E-14 | 1.54E-14 | 1.93E-14 | 2.31E-14 | 1.16E-13 | 2.31E-13 | 4.63E-13 | 6.94E-13 |
| H | 2 | 0.00E+00 | 5.72E-17 | 1.14E-16 | 1.72E-16 | 2.29E-16 | 2.86E-16 | 3.43E-16 | 1.72E-15 | 3.43E-15 | 6.87E-15 | 1.03E-14 |
| H | 3 | 0.00E+00 | 4.67E-17 | 9.34E-17 | 1.40E-16 | 1.87E-16 | 2.33E-16 | 2.80E-16 | 1.40E-15 | 2.80E-15 | 5.60E-15 | 8.40E-15 |
| HE | 3 | 0.00E+00 | 8.95E-18 | 1.79E-17 | 2.68E-17 | 3.58E-17 | 4.47E-17 | 5.37E-17 | 2.68E-16 | 5.37E-16 | 1.07E-15 | 1.61E-15 |
| HE | 4 | 0.00E+00 | 1.52E-15 | 3.04E-15 | 4.56E-15 | 6.08E-15 | 7.60E-15 | 9.12E-15 | 4.56E-14 | 9.12E-14 | 1.82E-13 | 2.74E-13 |
| LI | 6 | 0.00E+00 | 2.06E-17 | 4.12E-17 | 6.18E-17 | 8.25E-17 | 1.03E-16 | 1.24E-16 | 6.18E-16 | 1.24E-15 | 2.47E-15 | 3.71E-15 |
| LI | 7 | 0.00E+00 | 1.56E-18 | 3.11E-18 | 4.67E-18 | 6.23E-18 | 7.78E-18 | 9.34E-18 | 4.67E-17 | 9.34E-17 | 1.87E-16 | 2.80E-16 |
| BE | 7 | 0.00E+00 | 1.04E-18 | 2.08E-18 | 3.11E-18 | 4.15E-18 | 5.19E-18 | 6.23E-18 | 3.11E-17 | 6.23E-17 | 1.25E-16 | 1.87E-16 |
| BE | 9 | 0.00E+00 | 6.23E-18 | 1.25E-17 | 1.87E-17 | 2.49E-17 | 3.11E-17 | 3.74E-17 | 1.87E-16 | 3.74E-16 | 7.47E-16 | 1.12E-15 |
| BE | 10 | 0.00E+00 | 2.08E-18 | 4.15E-18 | 6.23E-18 | 8.30E-18 | 1.04E-17 | 1.25E-17 | 6.23E-17 | 1.25E-16 | 2.49E-16 | 3.74E-16 |
| B | 10 | 0.00E+00 | 3.84E-17 | 7.68E-17 | 1.15E-16 | 1.54E-16 | 1.92E-16 | 2.30E-16 | 1.15E-15 | 2.30E-15 | 4.61E-15 | 6.91E-15 |
| B | 11 | 0.00E+00 | 1.33E-15 | 2.66E-15 | 3.99E-15 | 5.32E-15 | 6.65E-15 | 7.98E-15 | 3.99E-14 | 8.00E-14 | 1.60E-13 | 2.40E-13 |
| B | 12 | 0.00E+00 | 2.74E-20 | 2.74E-20 | 2.74E-20 | 2.74E-20 | 2.74E-20 | 2.74E-20 | 2.74E-20 | 2.74E-20 | 2.74E-20 | 2.74E-20 |
| C | 11 | 0.00E+00 | 1.53E-17 | 3.05E-17 | 4.56E-17 | 6.07E-17 | 7.56E-17 | 9.05E-17 | 4.23E-16 | 7.80E-16 | 1.34E-15 | 1.73E-15 |
| C | 12 | 0.00E+00 | 2.79E-16 | 5.59E-16 | 8.38E-16 | 1.12E-15 | 1.40E-15 | 1.68E-15 | 8.38E-15 | 1.68E-14 | 3.35E-14 | 5.03E-14 |
| C | 13 | 0.00E+00 | 3.91E-16 | 7.83E-16 | 1.18E-15 | 1.57E-15 | 1.96E-15 | 2.36E-15 | 1.21E-14 | 2.47E-14 | 5.12E-14 | 7.85E-14 |
| C | 14 | 0.00E+00 | 7.66E-16 | 1.53E-15 | 2.30E-15 | 3.06E-15 | 3.83E-15 | 4.60E-15 | 2.30E-14 | 4.60E-14 | 9.19E-14 | 1.38E-13 |
| N | 13 | 0.00E+00 | 7.86E-17 | 1.56E-16 | 2.33E-16 | 3.09E-16 | 3.84E-16 | 4.58E-16 | 2.00E-15 | 3.42E-15 | 5.12E-15 | 5.97E-15 |
| N | 14 | 0.00E+00 | 1.27E-16 | 2.55E-16 | 3.83E-16 | 5.12E-16 | 6.40E-16 | 7.69E-16 | 3.88E-15 | 7.80E-15 | 1.56E-14 | 2.35E-14 |
| N | 15 | 0.00E+00 | 6.03E-17 | 1.21E-16 | 1.83E-16 | 2.46E-16 | 3.09E-16 | 3.73E-16 | 2.03E-15 | 4.22E-15 | 8.69E-15 | 1.32E-14 |
| N | 16 | 0.00E+00 | 4.12E-18 | 5.67E-18 | 6.25E-18 | 6.47E-18 | 6.56E-18 | 6.59E-18 | 6.61E-18 | 6.61E-18 | 6.61E-18 | 6.61E-18 |
| O | 14 | 0.00E+00 | 2.97E-18 | 5.65E-18 | 8.09E-18 | 1.03E-17 | 1.23E-17 | 1.41E-17 | 3.00E-17 | 3.16E-17 | 3.17E-17 | 3.17E-17 |
| O | 15 | 0.00E+00 | 1.43E-17 | 2.77E-17 | 4.05E-17 | 5.25E-17 | 6.38E-17 | 7.46E-17 | 2.11E-16 | 2.50E-16 | 2.58E-16 | 2.58E-16 |
| O | 16 | 0.00E+00 | 1.53E-17 | 3.32E-17 | 5.20E-17 | 7.12E-17 | 9.05E-17 | 1.10E-16 | 5.83E-16 | 1.17E-15 | 2.34E-15 | 3.52E-15 |
| O | 17 | 0.00E+00 | 8.87E-18 | 1.77E-17 | 2.66E-17 | 3.55E-17 | 4.43E-17 | 5.32E-17 | 2.66E-16 | 5.32E-16 | 1.06E-15 | 1.60E-15 |
| S | 36 | 0.00E+00 | 2.13E-19 | 4.26E-19 | 6.39E-19 | 8.51E-19 | 1.06E-18 | 1.28E-18 | 6.39E-18 | 1.28E-17 | 2.55E-17 | 3.83E-17 |
| S | 37 | 0.00E+00 | 4.41E-20 | 8.71E-20 | 1.29E-19 | 1.70E-19 | 2.11E-19 | 2.50E-19 | 9.68E-19 | 1.46E-18 | 1.83E-18 | 1.92E-18 |
| CL | 40 | 0.00E+00 | 5.96E-20 | 1.14E-19 | 1.64E-19 | 2.10E-19 | 2.52E-19 | 2.90E-19 | 6.60E-19 | 7.07E-19 | 7.11E-19 | 7.11E-19 |
| AR | 38 | 0.00E+00 | 1.97E-19 | 3.94E-19 | 5.91E-19 | 7.89E-19 | 9.86E-19 | 1.18E-18 | 5.92E-18 | 1.19E-17 | 2.38E-17 | 3.57E-17 |
| AR | 39 | 0.00E+00 | 2.34E-18 | 4.68E-18 | 7.01E-18 | 9.35E-18 | 1.17E-17 | 1.40E-17 | 7.02E-17 | 1.40E-16 | 2.81E-16 | 4.21E-16 |
| AR | 41 | 0.00E+00 | 4.92E-19 | 9.83E-19 | 1.47E-18 | 1.96E-18 | 2.45E-18 | 2.94E-18 | 1.45E-17 | 2.86E-17 | 5.54E-17 | 8.06E-17 |
| Total | | 0.00E+00 | 8.66E-15 | 1.73E-14 | 2.60E-14 | 3.46E-14 | 4.33E-14 | 5.20E-14 | 2.60E-13 | 5.20E-13 | 1.04E-12 | 1.56E-12 |

| Table A.3. SNS nuclide production during normal proton beam operation: wiring cable tray material | | | | | | | | | | | | |
|---|---|---|---|---|---|---|---|---|---|---|---|---|
| Proton beam energy: 1 GeV | | | | | | | Operational line loss assumption: 1 nA/m (continuous) | | | | | |
| Nuclide masses integrated over the material zone volume in the HETC & MCNP calculational model | | | | | | | | | | | | |
| Nuclide concentration | | Time (s) | 7.88E+06 | 1.58E+07 | 2.37E+07 | 3.15E+07 | 6.31E+07 | 1.58E+08 | 3.15E+08 | 4.73E+08 | 6.31E+08 | 9.46E+08 |
| (gram-atoms) | | Initial | 3 months | 6 months | 9 months | 1 year | 2 years | 5 years | 10 years | 15 years | 20 years | 30 years |
| H | 1 | 0.00E+00 | 2.14E-09 | 6.43E-09 | 1.31E-08 | 1.96E-08 | 2.60E-08 | 5.21E-08 | 1.31E-07 | 2.60E-07 | 5.21E-07 | 7.82E-07 |
| H | 2 | 0.00E+00 | 7.36E-11 | 2.21E-10 | 4.49E-10 | 6.73E-10 | 8.95E-10 | 1.79E-09 | 4.49E-09 | 8.95E-09 | 1.79E-08 | 2.69E-08 |
| H | 3 | 0.00E+00 | 2.41E-11 | 7.19E-11 | 1.45E-10 | 2.16E-10 | 2.85E-10 | 5.55E-10 | 1.28E-09 | 2.24E-09 | 3.52E-09 | 4.25E-09 |
| HE | 3 | 0.00E+00 | 7.62E-12 | 2.32E-11 | 4.82E-11 | 7.39E-11 | 1.00E-10 | 2.16E-10 | 6.51E-10 | 1.61E-09 | 4.19E-09 | 7.32E-09 |
| HE | 4 | 0.00E+00 | 2.33E-10 | 7.00E-10 | 1.42E-09 | 2.13E-09 | 2.83E-09 | 5.67E-09 | 1.42E-08 | 2.83E-08 | 5.67E-08 | 8.51E-08 |
| LI | 6 | 0.00E+00 | 5.33E-12 | 1.60E-11 | 3.25E-11 | 4.88E-11 | 6.48E-11 | 1.30E-10 | 3.25E-10 | 6.48E-10 | 1.30E-09 | 1.95E-09 |
| LI | 7 | 0.00E+00 | 1.69E-12 | 5.08E-12 | 1.03E-11 | 1.55E-11 | 2.06E-11 | 4.12E-11 | 1.03E-10 | 2.06E-10 | 4.12E-10 | 6.18E-10 |
| LI | 8 | 0.00E+00 | 4.26E-19 | 4.26E-19 | 4.26E-19 | 4.26E-19 | 4.26E-19 | 4.26E-19 | 4.26E-19 | 4.26E-19 | 4.26E-19 | 4.26E-19 |
| BE | 9 | 0.00E+00 | 4.87E-11 | 1.46E-10 | 2.97E-10 | 4.46E-10 | 5.93E-10 | 1.19E-09 | 2.97E-09 | 5.93E-09 | 1.19E-08 | 1.78E-08 |
| BE | 10 | 0.00E+00 | 4.81E-12 | 1.44E-11 | 2.93E-11 | 4.40E-11 | 5.85E-11 | 1.17E-10 | 2.93E-10 | 5.85E-10 | 1.17E-09 | 1.76E-09 |
| BE | 11 | 0.00E+00 | 3.87E-17 | 3.87E-17 | 3.87E-17 | 3.87E-17 | 3.87E-17 | 3.87E-17 | 3.87E-17 | 3.87E-17 | 3.87E-17 | 3.87E-17 |
| B | 10 | 0.00E+00 | 7.88E-12 | 2.37E-11 | 4.81E-11 | 7.21E-11 | 9.58E-11 | 1.92E-10 | 4.81E-10 | 9.58E-10 | 1.92E-09 | 2.88E-09 |
| B | 11 | 0.00E+00 | 5.05E-11 | 1.52E-10 | 3.08E-10 | 4.62E-10 | 6.15E-10 | 1.23E-09 | 3.08E-09 | 6.15E-09 | 1.23E-08 | 1.85E-08 |
| B | 12 | 0.00E+00 | 4.67E-19 | 4.67E-19 | 4.67E-19 | 4.67E-19 | 4.67E-19 | 4.67E-19 | 4.67E-19 | 4.67E-19 | 4.67E-19 | 4.67E-19 |
| B | 13 | 0.00E+00 | 2.54E-19 | 2.54E-19 | 2.54E-19 | 2.54E-19 | 2.54E-19 | 2.54E-19 | 2.54E-19 | 2.54E-19 | 2.54E-19 | 2.54E-19 |
| B | 14 | 0.00E+00 | 3.38E-19 | 3.38E-19 | 3.38E-19 | 3.38E-19 | 3.38E-19 | 3.38E-19 | 3.38E-19 | 3.38E-19 | 3.38E-19 | 3.38E-19 |
| C | 11 | 0.00E+00 | 7.08E-16 | 7.08E-16 | 7.08E-16 | 7.08E-16 | 7.08E-16 | 7.08E-16 | 7.08E-16 | 7.08E-16 | 7.08E-16 | 7.08E-16 |
| C | 12 | 0.00E+00 | 8.21E-11 | 2.47E-10 | 5.01E-10 | 7.51E-10 | 9.99E-10 | 2.00E-09 | 5.01E-09 | 9.99E-09 | 2.00E-08 | 3.00E-08 |
| C | 13 | 0.00E+00 | 9.98E-11 | 3.00E-10 | 6.09E-10 | 9.13E-10 | 1.21E-09 | 2.43E-09 | 6.09E-09 | 1.21E-08 | 2.43E-08 | 3.64E-08 |
| C | 14 | 0.00E+00 | 1.44E-10 | 4.34E-10 | 8.81E-10 | 1.32E-09 | 1.76E-09 | 3.52E-09 | 8.81E-09 | 1.76E-08 | 3.51E-08 | 5.27E-08 |
| C | 16 | 0.00E+00 | 6.57E-18 | 6.57E-18 | 6.57E-18 | 6.57E-18 | 6.57E-18 | 6.57E-18 | 6.57E-18 | 6.57E-18 | 6.57E-18 | 6.57E-18 |
| N | 13 | 0.00E+00 | 7.68E-16 | 7.68E-16 | 7.68E-16 | 7.68E-16 | 7.68E-16 | 7.68E-16 | 7.68E-16 | 7.68E-16 | 7.68E-16 | 7.68E-16 |
| N | 14 | 0.00E+00 | 1.83E-11 | 5.49E-11 | 1.12E-10 | 1.67E-10 | 2.22E-10 | 4.46E-10 | 1.12E-09 | 2.23E-09 | 4.50E-09 | 6.77E-09 |
| N | 15 | 0.00E+00 | 2.80E-11 | 8.40E-11 | 1.71E-10 | 2.56E-10 | 3.40E-10 | 6.81E-10 | 1.71E-09 | 3.40E-09 | 6.81E-09 | 1.02E-08 |
| N | 16 | 0.00E+00 | 7.23E-17 | 7.23E-17 | 7.23E-17 | 7.23E-17 | 7.23E-17 | 7.23E-17 | 7.23E-17 | 7.23E-17 | 7.23E-17 | 7.23E-17 |
| O | 14 | 0.00E+00 | 1.59E-17 | 1.59E-17 | 1.59E-17 | 1.59E-17 | 1.59E-17 | 1.59E-17 | 1.59E-17 | 1.59E-17 | 1.59E-17 | 1.59E-17 |
| O | 15 | 0.00E+00 | 3.83E-16 | 3.83E-16 | 3.83E-16 | 3.83E-16 | 3.83E-16 | 3.83E-16 | 3.83E-16 | 3.83E-16 | 3.83E-16 | 3.83E-16 |
| O | 16 | 0.00E+00 | 2.47E-11 | 7.42E-11 | 1.51E-10 | 2.26E-10 | 3.00E-10 | 6.02E-10 | 1.51E-09 | 3.00E-09 | 6.02E-09 | 9.02E-09 |
| O | 17 | 0.00E+00 | 2.84E-12 | 8.53E-12 | 1.73E-11 | 2.60E-11 | 3.45E-11 | 6.91E-11 | 1.73E-10 | 3.45E-10 | 6.91E-10 | 1.04E-09 |
| O | 18 | 0.00E+00 | 6.72E-13 | 2.02E-12 | 4.11E-12 | 6.16E-12 | 8.19E-12 | 1.64E-11 | 4.10E-11 | 8.18E-11 | 1.64E-10 | 2.46E-10 |
| O | 19 | 0.00E+00 | 7.19E-20 | 7.19E-20 | 7.19E-20 | 7.19E-20 | 7.19E-20 | 7.19E-20 | 7.19E-20 | 7.19E-20 | 7.19E-20 | 7.19E-20 |
| F | 18 | 0.00E+00 | 2.46E-15 | 2.46E-15 | 2.46E-15 | 2.46E-15 | 2.46E-15 | 2.46E-15 | 2.46E-15 | 2.46E-15 | 2.46E-15 | 2.46E-15 |
| F | 19 | 0.00E+00 | 8.11E-13 | 2.44E-12 | 4.95E-12 | 7.42E-12 | 9.86E-12 | 1.98E-11 | 4.95E-11 | 9.86E-11 | 1.98E-10 | 2.96E-10 |

| Table A.3. (continued) | | | | | | | | | | | | |
|---|---|---|---|---|---|---|---|---|---|---|---|---|
| Proton beam energy: 1 GeV | | | | | | | Operational line loss assumption: 1 nA/m (continuous) | | | | | |
| Nuclide masses integrated over the material zone volume in the HETC & MCNP calculational model | | | | | | | | | | | | |
| Nuclide concentration | | Time (s) | 7.88E+06 | 1.58E+07 | 2.37E+07 | 3.15E+07 | 6.31E+07 | 1.58E+08 | 3.15E+08 | 4.73E+08 | 6.31E+08 | 9.46E+08 |
| (gram-atoms) | | Initial | 3 months | 6 months | 9 months | 1 year | 2 years | 5 years | 10 years | 15 years | 20 years | 30 years |
| NE | 20 | 0.00E+00 | 5.99E-13 | 1.80E-12 | 3.65E-12 | 5.48E-12 | 7.28E-12 | 1.46E-11 | 3.65E-11 | 7.28E-11 | 1.46E-10 | 2.19E-10 |
| NE | 22 | 0.00E+00 | 1.37E-13 | 4.29E-13 | 9.24E-13 | 1.46E-12 | 2.03E-12 | 4.74E-12 | 1.55E-11 | 3.75E-11 | 8.59E-11 | 1.35E-10 |
| NA | 22 | 0.00E+00 | 2.66E-13 | 7.82E-13 | 1.54E-12 | 2.23E-12 | 2.87E-12 | 5.08E-12 | 9.09E-12 | 1.15E-11 | 1.23E-11 | 1.24E-11 |
| NA | 23 | 0.00E+00 | 1.53E-12 | 4.59E-12 | 9.32E-12 | 1.40E-11 | 1.86E-11 | 3.72E-11 | 9.32E-11 | 1.86E-10 | 3.72E-10 | 5.58E-10 |
| MG | 24 | 0.00E+00 | 1.18E-12 | 3.56E-12 | 7.23E-12 | 1.08E-11 | 1.44E-11 | 2.89E-11 | 7.23E-11 | 1.44E-10 | 2.89E-10 | 4.33E-10 |
| MG | 25 | 0.00E+00 | 1.66E-12 | 5.00E-12 | 1.02E-11 | 1.52E-11 | 2.02E-11 | 4.06E-11 | 1.02E-10 | 2.02E-10 | 4.06E-10 | 6.08E-10 |
| MG | 26 | 0.00E+00 | 8.96E-13 | 2.69E-12 | 5.47E-12 | 8.20E-12 | 1.09E-11 | 2.18E-11 | 5.47E-11 | 1.09E-10 | 2.18E-10 | 3.27E-10 |
| AL | 25 | 0.00E+00 | 5.37E-19 | 5.37E-19 | 5.37E-19 | 5.37E-19 | 5.37E-19 | 5.37E-19 | 5.37E-19 | 5.37E-19 | 5.37E-19 | 5.37E-19 |
| AL | 26 | 0.00E+00 | 1.51E-12 | 4.54E-12 | 9.22E-12 | 1.38E-11 | 1.84E-11 | 3.68E-11 | 9.22E-11 | 1.84E-10 | 3.68E-10 | 5.52E-10 |
| AL | 27 | 0.00E+00 | 4.52E-12 | 1.36E-11 | 2.76E-11 | 4.14E-11 | 5.50E-11 | 1.10E-10 | 2.76E-10 | 5.50E-10 | 1.10E-09 | 1.65E-09 |
| AL | 28 | 0.00E+00 | 8.30E-17 | 8.30E-17 | 8.30E-17 | 8.30E-17 | 8.30E-17 | 8.30E-17 | 8.30E-17 | 8.30E-17 | 8.30E-17 | 8.30E-17 |
| AL | 29 | 0.00E+00 | 8.89E-17 | 8.89E-17 | 8.89E-17 | 8.89E-17 | 8.89E-17 | 8.89E-17 | 8.89E-17 | 8.89E-17 | 8.89E-17 | 8.89E-17 |
| SI | 27 | 0.00E+00 | 3.08E-19 | 3.08E-19 | 3.08E-19 | 3.08E-19 | 3.08E-19 | 3.08E-19 | 3.08E-19 | 3.08E-19 | 3.08E-19 | 3.08E-19 |
| SI | 28 | 0.00E+00 | 5.28E-12 | 1.59E-11 | 3.22E-11 | 4.84E-11 | 6.43E-11 | 1.29E-10 | 3.22E-10 | 6.43E-10 | 1.29E-09 | 1.93E-09 |
| SI | 29 | 0.00E+00 | 1.27E-11 | 3.83E-11 | 7.77E-11 | 1.17E-10 | 1.55E-10 | 3.10E-10 | 7.77E-10 | 1.55E-09 | 3.10E-09 | 4.65E-09 |
| SI | 30 | 0.00E+00 | 5.04E-12 | 1.51E-11 | 3.07E-11 | 4.61E-11 | 6.13E-11 | 1.23E-10 | 3.07E-10 | 6.13E-10 | 1.23E-09 | 1.84E-09 |
| SI | 31 | 0.00E+00 | 6.93E-15 | 6.93E-15 | 6.93E-15 | 6.93E-15 | 6.93E-15 | 6.93E-15 | 6.93E-15 | 6.93E-15 | 6.93E-15 | 6.93E-15 |
| SI | 32 | 0.00E+00 | 1.34E-13 | 4.04E-13 | 8.20E-13 | 1.23E-12 | 1.63E-12 | 3.27E-12 | 8.18E-12 | 1.63E-11 | 3.24E-11 | 4.83E-11 |
| P | 31 | 0.00E+00 | 3.04E-11 | 9.12E-11 | 1.85E-10 | 2.78E-10 | 3.69E-10 | 7.40E-10 | 1.85E-09 | 3.69E-09 | 7.40E-09 | 1.11E-08 |
| P | 32 | 0.00E+00 | 3.34E-11 | 4.30E-11 | 4.36E-11 | 4.36E-11 | 4.36E-11 | 4.36E-11 | 4.36E-11 | 4.36E-11 | 4.36E-11 | 4.36E-11 |
| P | 33 | 0.00E+00 | 4.67E-12 | 7.59E-12 | 8.22E-12 | 8.27E-12 | 8.27E-12 | 8.27E-12 | 8.27E-12 | 8.27E-12 | 8.27E-12 | 8.27E-12 |
| P | 34 | 0.00E+00 | 3.14E-17 | 3.14E-17 | 3.14E-17 | 3.14E-17 | 3.14E-17 | 3.14E-17 | 3.14E-17 | 3.14E-17 | 3.14E-17 | 3.14E-17 |
| P | 35 | 0.00E+00 | 1.00E-17 | 1.00E-17 | 1.00E-17 | 1.00E-17 | 1.00E-17 | 1.00E-17 | 1.00E-17 | 1.00E-17 | 1.00E-17 | 1.00E-17 |
| S | 31 | 0.00E+00 | 1.95E-19 | 1.95E-19 | 1.95E-19 | 1.95E-19 | 1.95E-19 | 1.95E-19 | 1.95E-19 | 1.95E-19 | 1.95E-19 | 1.95E-19 |
| S | 32 | 0.00E+00 | 4.13E-11 | 1.81E-10 | 4.12E-10 | 6.40E-10 | 8.65E-10 | 1.82E-09 | 4.60E-09 | 9.17E-09 | 1.83E-08 | 2.75E-08 |
| S | 33 | 0.00E+00 | 4.68E-11 | 1.47E-10 | 3.06E-10 | 4.63E-10 | 6.18E-10 | 1.25E-09 | 3.15E-09 | 6.28E-09 | 1.26E-08 | 1.88E-08 |
| S | 34 | 0.00E+00 | 9.11E-11 | 2.74E-10 | 5.56E-10 | 8.34E-10 | 1.11E-09 | 2.22E-09 | 5.56E-09 | 1.11E-08 | 2.22E-08 | 3.33E-08 |
| S | 35 | 0.00E+00 | 9.97E-11 | 2.41E-10 | 3.62E-10 | 4.20E-10 | 4.47E-10 | 4.73E-10 | 4.74E-10 | 4.74E-10 | 4.74E-10 | 4.74E-10 |
| S | 36 | 0.00E+00 | 1.13E-11 | 3.39E-11 | 6.88E-11 | 1.03E-10 | 1.37E-10 | 2.75E-10 | 6.88E-10 | 1.37E-09 | 2.75E-09 | 4.12E-09 |
| S | 37 | 0.00E+00 | 3.49E-16 | 3.49E-16 | 3.49E-16 | 3.49E-16 | 3.49E-16 | 3.49E-16 | 3.49E-16 | 3.49E-16 | 3.49E-16 | 3.49E-16 |
| S | 38 | 0.00E+00 | 2.82E-20 | 2.82E-20 | 2.82E-20 | 2.82E-20 | 2.82E-20 | 2.82E-20 | 2.82E-20 | 2.82E-20 | 2.82E-20 | 2.82E-20 |
| CL | 35 | 0.00E+00 | 3.38E-11 | 1.60E-10 | 4.53E-10 | 8.02E-10 | 1.18E-09 | 2.78E-09 | 8.15E-09 | 1.67E-08 | 3.35E-08 | 5.02E-08 |
| CL | 36 | 0.00E+00 | 2.81E-11 | 8.43E-11 | 1.71E-10 | 2.57E-10 | 3.41E-10 | 6.84E-10 | 1.71E-09 | 3.41E-09 | 6.84E-09 | 1.03E-08 |
| CL | 37 | 0.00E+00 | 9.11E-12 | 2.78E-11 | 5.72E-11 | 8.62E-11 | 1.15E-10 | 2.32E-10 | 5.81E-10 | 1.16E-09 | 2.32E-09 | 3.48E-09 |

**Table A.3. (continued)**

| Proton beam energy: 1 GeV | | | | | | | Operational line loss assumption: 1 nA/m (continuous) | | | | | |
|---|---|---|---|---|---|---|---|---|---|---|---|---|
| Nuclide masses integrated over the material zone volume in the HETC & MCNP calculational model | | | | | | | | | | | | |
| Nuclide concentration | | Time (s) | 7.88E+06 | 1.58E+07 | 2.37E+07 | 3.15E+07 | 6.31E+07 | 1.58E+08 | 3.15E+08 | 4.73E+08 | 6.31E+08 | 9.46E+08 |
| (gram-atoms) | | Initial | 3 months | 6 months | 9 months | 1 year | 2 years | 5 years | 10 years | 15 years | 20 years | 30 years |
| CL | 38 | 0.00E+00 | 2.01E-15 | 2.01E-15 | 2.01E-15 | 2.01E-15 | 2.01E-15 | 2.01E-15 | 2.01E-15 | 2.01E-15 | 2.01E-15 | 2.01E-15 |
| CL | 39 | 0.00E+00 | 6.56E-20 | 6.56E-20 | 6.56E-20 | 6.56E-20 | 6.56E-20 | 6.56E-20 | 6.56E-20 | 6.56E-20 | 6.56E-20 | 6.56E-20 |
| CL | 40 | 0.00E+00 | 1.32E-20 | 1.32E-20 | 1.32E-20 | 1.32E-20 | 1.32E-20 | 1.32E-20 | 1.32E-20 | 1.32E-20 | 1.32E-20 | 1.32E-20 |
| AR | 36 | 0.00E+00 | 2.53E-18 | 2.28E-17 | 9.40E-17 | 2.12E-16 | 3.74E-16 | 1.50E-15 | 9.40E-15 | 3.74E-14 | 1.50E-13 | 3.37E-13 |
| AR | 37 | 0.00E+00 | 4.05E-13 | 7.53E-13 | 8.81E-13 | 9.02E-13 | 9.05E-13 | 9.06E-13 | 9.05E-13 | 9.05E-13 | 9.05E-13 | 9.05E-13 |
| AR | 38 | 0.00E+00 | 2.15E-12 | 6.46E-12 | 1.31E-11 | 1.97E-11 | 2.62E-11 | 5.24E-11 | 1.31E-10 | 2.62E-10 | 5.24E-10 | 7.86E-10 |
| AR | 39 | 0.00E+00 | 1.13E-14 | 3.40E-14 | 6.89E-14 | 1.03E-13 | 1.37E-13 | 2.75E-13 | 6.85E-13 | 1.36E-12 | 2.69E-12 | 3.97E-12 |
| AR | 40 | 0.00E+00 | 2.99E-16 | 8.99E-16 | 1.83E-15 | 2.74E-15 | 3.64E-15 | 7.29E-15 | 1.83E-14 | 3.64E-14 | 7.29E-14 | 1.09E-13 |
| AR | 41 | 0.00E+00 | 8.90E-18 | 8.90E-18 | 8.90E-18 | 8.90E-18 | 8.90E-18 | 8.90E-18 | 8.90E-18 | 8.90E-18 | 8.90E-18 | 8.90E-18 |
| K | 38 | 0.00E+00 | 6.84E-17 | 6.84E-17 | 6.84E-17 | 6.84E-17 | 6.84E-17 | 6.84E-17 | 6.84E-17 | 6.84E-17 | 6.84E-17 | 6.84E-17 |
| K | 39 | 0.00E+00 | 1.34E-13 | 4.04E-13 | 8.20E-13 | 1.23E-12 | 1.63E-12 | 3.27E-12 | 8.20E-12 | 1.64E-11 | 3.28E-11 | 4.92E-11 |
| K | 40 | 0.00E+00 | 4.03E-13 | 1.21E-12 | 2.46E-12 | 3.69E-12 | 4.90E-12 | 9.82E-12 | 2.46E-11 | 4.90E-11 | 9.82E-11 | 1.47E-10 |
| K | 41 | 0.00E+00 | 1.37E-13 | 4.11E-13 | 8.35E-13 | 1.25E-12 | 1.66E-12 | 3.33E-12 | 8.35E-12 | 1.66E-11 | 3.33E-11 | 5.00E-11 |
| K | 42 | 0.00E+00 | 3.33E-15 | 3.33E-15 | 3.33E-15 | 3.33E-15 | 3.33E-15 | 3.33E-15 | 3.33E-15 | 3.33E-15 | 3.33E-15 | 3.33E-15 |
| CA | 41 | 0.00E+00 | 2.69E-13 | 8.07E-13 | 1.64E-12 | 2.46E-12 | 3.27E-12 | 6.55E-12 | 1.64E-11 | 3.27E-11 | 6.55E-11 | 9.82E-11 |
| CA | 42 | 0.00E+00 | 1.08E-12 | 3.23E-12 | 6.56E-12 | 9.85E-12 | 1.31E-11 | 2.62E-11 | 6.56E-11 | 1.31E-10 | 2.62E-10 | 3.93E-10 |
| CA | 43 | 0.00E+00 | 8.06E-13 | 2.42E-12 | 4.92E-12 | 7.38E-12 | 9.81E-12 | 1.97E-11 | 4.92E-11 | 9.81E-11 | 1.96E-10 | 2.95E-10 |
| CA | 44 | 0.00E+00 | 1.08E-12 | 3.23E-12 | 6.57E-12 | 9.86E-12 | 1.31E-11 | 2.63E-11 | 6.59E-11 | 1.32E-10 | 2.66E-10 | 4.02E-10 |
| CA | 46 | 0.00E+00 | 1.34E-13 | 4.04E-13 | 8.20E-13 | 1.23E-12 | 1.63E-12 | 3.27E-12 | 8.20E-12 | 1.63E-11 | 3.27E-11 | 4.91E-11 |
| SC | 43 | 0.00E+00 | 2.09E-15 | 2.09E-15 | 2.09E-15 | 2.09E-15 | 2.09E-15 | 2.09E-15 | 2.09E-15 | 2.09E-15 | 2.09E-15 | 2.09E-15 |
| SC | 44 | 0.00E+00 | 4.23E-15 | 4.24E-15 | 4.24E-15 | 4.24E-15 | 4.25E-15 | 4.26E-15 | 4.31E-15 | 4.37E-15 | 4.50E-15 | 4.60E-15 |
| SC | 46 | 0.00E+00 | 1.19E-13 | 2.85E-13 | 4.23E-13 | 4.86E-13 | 5.15E-13 | 5.41E-13 | 5.42E-13 | 5.42E-13 | 5.42E-13 | 5.42E-13 |
| TI | 44 | 0.00E+00 | 1.34E-13 | 4.03E-13 | 8.17E-13 | 1.22E-12 | 1.62E-12 | 3.23E-12 | 7.91E-12 | 1.52E-11 | 2.85E-11 | 3.99E-11 |
| TI | 46 | 0.00E+00 | 1.22E-12 | 3.75E-12 | 7.78E-12 | 1.18E-11 | 1.58E-11 | 3.22E-11 | 8.20E-11 | 1.64E-10 | 3.28E-10 | 4.92E-10 |
| TI | 47 | 0.00E+00 | 1.32E-12 | 3.96E-12 | 8.03E-12 | 1.21E-11 | 1.60E-11 | 3.21E-11 | 8.03E-11 | 1.60E-10 | 3.21E-10 | 4.81E-10 |
| TI | 48 | 0.00E+00 | 1.07E-12 | 5.21E-12 | 1.22E-11 | 1.91E-11 | 2.60E-11 | 5.52E-11 | 1.40E-10 | 2.79E-10 | 5.57E-10 | 8.34E-10 |
| TI | 49 | 0.00E+00 | 5.83E-14 | 5.04E-13 | 1.95E-12 | 4.14E-12 | 6.91E-12 | 2.24E-11 | 8.54E-11 | 1.98E-10 | 4.56E-10 | 7.14E-10 |
| TI | 50 | 0.00E+00 | 1.34E-13 | 4.04E-13 | 8.20E-13 | 1.23E-12 | 1.63E-12 | 3.27E-12 | 8.20E-12 | 1.63E-11 | 3.27E-11 | 4.91E-11 |
| V | 46 | 0.00E+00 | 3.16E-20 | 3.16E-20 | 3.16E-20 | 3.16E-20 | 3.16E-20 | 3.16E-20 | 3.16E-20 | 3.16E-20 | 3.16E-20 | 3.16E-20 |
| V | 47 | 0.00E+00 | 2.93E-16 | 2.93E-16 | 2.93E-16 | 2.93E-16 | 2.93E-16 | 2.93E-16 | 2.93E-16 | 2.93E-16 | 2.93E-16 | 2.93E-16 |
| V | 48 | 0.00E+00 | 1.19E-12 | 1.61E-12 | 1.64E-12 | 1.64E-12 | 1.64E-12 | 1.64E-12 | 1.64E-12 | 1.64E-12 | 1.64E-12 | 1.64E-12 |
| V | 49 | 0.00E+00 | 1.81E-12 | 5.12E-12 | 9.47E-12 | 1.30E-11 | 1.59E-11 | 2.32E-11 | 2.89E-11 | 2.95E-11 | 2.95E-11 | 2.95E-11 |
| V | 50 | 0.00E+00 | 9.41E-13 | 2.83E-12 | 5.74E-12 | 8.61E-12 | 1.14E-11 | 2.29E-11 | 5.74E-11 | 1.14E-10 | 2.29E-10 | 3.44E-10 |
| V | 51 | 0.00E+00 | 2.17E-12 | 1.19E-11 | 3.06E-11 | 4.96E-11 | 6.85E-11 | 1.53E-10 | 3.90E-10 | 7.79E-10 | 1.55E-09 | 2.32E-09 |

| Table A.3. (continued) | | | | | | | | | | | | |
|---|---|---|---|---|---|---|---|---|---|---|---|---|
| Proton beam energy: 1 GeV | | | | | | | Operational line loss assumption: 1 nA/m (continuous) | | | | | |
| Nuclide masses integrated over the material zone volume in the HETC & MCNP calculational model | | | | | | | | | | | | |
| Nuclide concentration | | Time (s) | 7.88E+06 | 1.58E+07 | 2.37E+07 | 3.15E+07 | 6.31E+07 | 1.58E+08 | 3.15E+08 | 4.73E+08 | 6.31E+08 | 9.46E+08 |
| (gram-atoms) | | Initial | 3 months | 6 months | 9 months | 1 year | 2 years | 5 years | 10 years | 15 years | 20 years | 30 years |
| V | 52 | 0.00E+00 | 1.68E-17 | 1.68E-17 | 1.68E-17 | 1.68E-17 | 1.68E-17 | 1.68E-17 | 1.68E-17 | 1.68E-17 | 1.68E-17 | 1.68E-17 |
| CR | 48 | 0.00E+00 | 1.16E-14 | 1.16E-14 | 1.16E-14 | 1.16E-14 | 1.16E-14 | 1.16E-14 | 1.16E-14 | 1.16E-14 | 1.16E-14 | 1.16E-14 |
| CR | 49 | 0.00E+00 | 7.53E-16 | 7.53E-16 | 7.53E-16 | 7.53E-16 | 7.53E-16 | 7.53E-16 | 7.53E-16 | 7.53E-16 | 7.53E-16 | 7.53E-16 |
| CR | 50 | 0.00E+00 | 2.73E-12 | 8.19E-12 | 1.66E-11 | 2.49E-11 | 3.32E-11 | 6.64E-11 | 1.66E-10 | 3.32E-10 | 6.64E-10 | 9.96E-10 |
| CR | 51 | 0.00E+00 | 4.10E-12 | 6.95E-12 | 7.69E-12 | 7.76E-12 | 7.77E-12 | 7.77E-12 | 7.77E-12 | 7.77E-12 | 7.77E-12 | 7.77E-12 |
| CR | 52 | 0.00E+00 | 7.15E-12 | 2.58E-11 | 5.38E-11 | 8.14E-11 | 1.09E-10 | 2.15E-10 | 5.30E-10 | 1.05E-09 | 2.10E-09 | 3.14E-09 |
| CR | 53 | 0.00E+00 | 2.69E-13 | 8.07E-13 | 1.64E-12 | 2.46E-12 | 3.27E-12 | 6.55E-12 | 1.64E-11 | 3.27E-11 | 6.55E-11 | 9.82E-11 |
| CR | 54 | 0.00E+00 | 3.05E-13 | 1.87E-12 | 6.50E-12 | 1.32E-11 | 2.16E-11 | 6.76E-11 | 2.50E-10 | 5.74E-10 | 1.31E-09 | 2.04E-09 |
| CR | 55 | 0.00E+00 | 9.86E-18 | 9.86E-18 | 9.86E-18 | 9.86E-18 | 9.86E-18 | 9.86E-18 | 9.86E-18 | 9.86E-18 | 9.86E-18 | 9.86E-18 |
| MN | 51 | 0.00E+00 | 1.80E-15 | 1.80E-15 | 1.80E-15 | 1.80E-15 | 1.80E-15 | 1.80E-15 | 1.80E-15 | 1.80E-15 | 1.80E-15 | 1.80E-15 |
| MN | 52 | 0.00E+00 | 1.42E-12 | 1.46E-12 | 1.46E-12 | 1.46E-12 | 1.46E-12 | 1.46E-12 | 1.46E-12 | 1.46E-12 | 1.46E-12 | 1.46E-12 |
| MN | 53 | 0.00E+00 | 9.47E-12 | 2.84E-11 | 5.78E-11 | 8.66E-11 | 1.15E-10 | 2.31E-10 | 5.78E-10 | 1.15E-09 | 2.31E-09 | 3.46E-09 |
| MN | 54 | 0.00E+00 | 5.06E-12 | 1.42E-11 | 2.62E-11 | 3.58E-11 | 4.36E-11 | 6.30E-11 | 7.72E-11 | 7.85E-11 | 7.86E-11 | 7.86E-11 |
| MN | 55 | 0.00E+00 | 1.70E-12 | 5.90E-12 | 1.44E-11 | 2.51E-11 | 3.77E-11 | 1.07E-10 | 4.42E-10 | 1.20E-09 | 2.92E-09 | 4.68E-09 |
| MN | 56 | 0.00E+00 | 6.95E-16 | 6.95E-16 | 6.95E-16 | 6.95E-16 | 6.95E-16 | 6.95E-16 | 6.95E-16 | 6.95E-16 | 6.95E-16 | 6.95E-16 |
| FE | 53 | 0.00E+00 | 1.53E-16 | 1.53E-16 | 1.53E-16 | 1.53E-16 | 1.53E-16 | 1.53E-16 | 1.53E-16 | 1.53E-16 | 1.53E-16 | 1.53E-16 |
| FE | 54 | 0.00E+00 | 9.18E-12 | 2.76E-11 | 5.60E-11 | 8.40E-11 | 1.12E-10 | 2.24E-10 | 5.60E-10 | 1.12E-09 | 2.24E-09 | 3.35E-09 |
| FE | 55 | 0.00E+00 | 1.28E-11 | 3.77E-11 | 7.41E-11 | 1.08E-10 | 1.39E-10 | 2.46E-10 | 4.43E-10 | 5.64E-10 | 6.07E-10 | 6.10E-10 |
| FE | 56 | 0.00E+00 | 8.39E-12 | 3.26E-11 | 8.18E-11 | 1.37E-10 | 1.95E-10 | 4.36E-10 | 1.22E-09 | 2.47E-09 | 4.95E-09 | 7.43E-09 |
| FE | 57 | 0.00E+00 | 3.21E-12 | 1.36E-11 | 3.84E-11 | 7.14E-11 | 1.11E-10 | 3.12E-10 | 1.06E-09 | 2.35E-09 | 5.19E-09 | 8.03E-09 |
| FE | 58 | 0.00E+00 | 4.34E-12 | 2.51E-11 | 7.52E-11 | 1.34E-10 | 1.97E-10 | 4.58E-10 | 1.32E-09 | 2.70E-09 | 5.40E-09 | 8.09E-09 |
| FE | 59 | 0.00E+00 | 4.30E-13 | 8.69E-13 | 1.09E-12 | 1.14E-12 | 1.15E-12 | 1.15E-12 | 1.15E-12 | 1.15E-12 | 1.15E-12 | 1.15E-12 |
| FE | 60 | 0.00E+00 | 2.69E-13 | 8.07E-13 | 1.64E-12 | 2.46E-12 | 3.27E-12 | 6.55E-12 | 1.64E-11 | 3.27E-11 | 6.55E-11 | 9.82E-11 |
| FE | 61 | 0.00E+00 | 2.69E-17 | 2.69E-17 | 2.69E-17 | 2.69E-17 | 2.69E-17 | 2.69E-17 | 2.69E-17 | 2.69E-17 | 2.69E-17 | 2.69E-17 |
| FE | 62 | 0.00E+00 | 5.09E-18 | 5.09E-18 | 5.09E-18 | 5.09E-18 | 5.09E-18 | 5.09E-18 | 5.09E-18 | 5.09E-18 | 5.09E-18 | 5.09E-18 |
| CO | 55 | 0.00E+00 | 5.60E-14 | 5.60E-14 | 5.60E-14 | 5.60E-14 | 5.60E-14 | 5.60E-14 | 5.60E-14 | 5.60E-14 | 5.60E-14 | 5.60E-14 |
| CO | 56 | 0.00E+00 | 1.14E-11 | 2.71E-11 | 3.98E-11 | 4.53E-11 | 4.77E-11 | 4.96E-11 | 4.97E-11 | 4.97E-11 | 4.97E-11 | 4.97E-11 |
| CO | 57 | 0.00E+00 | 1.81E-11 | 5.05E-11 | 9.18E-11 | 1.24E-10 | 1.49E-10 | 2.08E-10 | 2.43E-10 | 2.46E-10 | 2.46E-10 | 2.46E-10 |
| CO | 58 | 0.00E+00 | 1.73E-11 | 3.98E-11 | 5.65E-11 | 6.32E-11 | 6.60E-11 | 6.78E-11 | 6.79E-11 | 6.79E-11 | 6.79E-11 | 6.79E-11 |
| CO | 59 | 0.00E+00 | 1.83E-11 | 5.53E-11 | 1.13E-10 | 1.70E-10 | 2.26E-10 | 4.54E-10 | 1.14E-09 | 2.27E-09 | 4.56E-09 | 6.83E-09 |
| CO | 60 | 0.00E+00 | 1.09E-11 | 3.23E-11 | 6.46E-11 | 9.53E-11 | 1.25E-10 | 2.34E-10 | 4.89E-10 | 7.41E-10 | 9.41E-10 | 9.94E-10 |
| CO | 61 | 0.00E+00 | 1.64E-14 | 1.64E-14 | 1.64E-14 | 1.64E-14 | 1.64E-14 | 1.64E-14 | 1.64E-14 | 1.64E-14 | 1.64E-14 | 1.64E-14 |
| CO | 62 | 0.00E+00 | 1.43E-16 | 1.43E-16 | 1.43E-16 | 1.43E-16 | 1.43E-16 | 1.43E-16 | 1.43E-16 | 1.43E-16 | 1.43E-16 | 1.43E-16 |
| CO | 63 | 0.00E+00 | 1.86E-17 | 1.86E-17 | 1.86E-17 | 1.86E-17 | 1.86E-17 | 1.86E-17 | 1.86E-17 | 1.86E-17 | 1.86E-17 | 1.86E-17 |

| Table A.3. (continued) | | | | | | | | | | | | |
|---|---|---|---|---|---|---|---|---|---|---|---|---|
| Proton beam energy: 1 GeV | | | | | | | Operational line loss assumption: 1 nA/m (continuous) | | | | | |
| Nuclide masses integrated over the material zone volume in the HETC & MCNP calculational model | | | | | | | | | | | | |
| Nuclide concentration | | Time (s) | 7.88E+06 | 1.58E+07 | 2.37E+07 | 3.15E+07 | 6.31E+07 | 1.58E+08 | 3.15E+08 | 4.73E+08 | 6.31E+08 | 9.46E+08 |
| (gram-atoms) | | Initial | 3 months | 6 months | 9 months | 1 year | 2 years | 5 years | 10 years | 15 years | 20 years | 30 years |
| NI | 56 | 0.00E+00 | 1.14E-13 | 1.18E-13 | 1.18E-13 | 1.18E-13 | 1.18E-13 | 1.18E-13 | 1.18E-13 | 1.18E-13 | 1.18E-13 | 1.18E-13 |
| NI | 57 | 0.00E+00 | 1.16E-13 | 1.16E-13 | 1.16E-13 | 1.16E-13 | 1.16E-13 | 1.16E-13 | 1.16E-13 | 1.16E-13 | 1.16E-13 | 1.16E-13 |
| NI | 58 | 0.00E+00 | 1.72E-11 | 5.16E-11 | 1.05E-10 | 1.57E-10 | 2.09E-10 | 4.18E-10 | 1.05E-09 | 2.09E-09 | 4.18E-09 | 6.27E-09 |
| NI | 59 | 0.00E+00 | 4.61E-11 | 1.38E-10 | 2.81E-10 | 4.21E-10 | 5.60E-10 | 1.12E-09 | 2.81E-09 | 5.60E-09 | 1.12E-08 | 1.68E-08 |
| NI | 60 | 0.00E+00 | 7.78E-11 | 2.34E-10 | 4.77E-10 | 7.16E-10 | 9.54E-10 | 1.93E-09 | 4.92E-09 | 1.00E-08 | 2.07E-08 | 3.14E-08 |
| NI | 61 | 0.00E+00 | 1.34E-10 | 4.01E-10 | 8.15E-10 | 1.22E-09 | 1.63E-09 | 3.26E-09 | 8.15E-09 | 1.62E-08 | 3.25E-08 | 4.88E-08 |
| NI | 62 | 0.00E+00 | 3.44E-10 | 1.03E-09 | 2.10E-09 | 3.15E-09 | 4.18E-09 | 8.38E-09 | 2.10E-08 | 4.18E-08 | 8.38E-08 | 1.26E-07 |
| NI | 63 | 0.00E+00 | 1.19E-10 | 3.56E-10 | 7.22E-10 | 1.08E-09 | 1.44E-09 | 2.87E-09 | 7.11E-09 | 1.39E-08 | 2.70E-08 | 3.91E-08 |
| NI | 64 | 0.00E+00 | 3.21E-10 | 9.73E-10 | 1.98E-09 | 2.96E-09 | 3.94E-09 | 7.87E-09 | 1.96E-08 | 3.91E-08 | 7.84E-08 | 1.17E-07 |
| NI | 65 | 0.00E+00 | 3.67E-14 | 3.67E-14 | 3.67E-14 | 3.67E-14 | 3.67E-14 | 3.67E-14 | 3.67E-14 | 3.67E-14 | 3.67E-14 | 3.67E-14 |
| CU | 59 | 0.00E+00 | 3.05E-17 | 3.05E-17 | 3.05E-17 | 3.05E-17 | 3.05E-17 | 3.05E-17 | 3.05E-17 | 3.05E-17 | 3.05E-17 | 3.05E-17 |
| CU | 60 | 0.00E+00 | 6.81E-15 | 6.81E-15 | 6.81E-15 | 6.81E-15 | 6.81E-15 | 6.81E-15 | 6.81E-15 | 6.81E-15 | 6.81E-15 | 6.81E-15 |
| CU | 61 | 0.00E+00 | 3.92E-13 | 3.92E-13 | 3.92E-13 | 3.92E-13 | 3.92E-13 | 3.92E-13 | 3.92E-13 | 3.92E-13 | 3.92E-13 | 3.92E-13 |
| CU | 62 | 0.00E+00 | 7.15E-14 | 7.15E-14 | 7.15E-14 | 7.15E-14 | 7.15E-14 | 7.15E-14 | 7.15E-14 | 7.15E-14 | 7.15E-14 | 7.15E-14 |
| CU | 63 | 0.00E+00 | 7.57E-11 | 2.27E-10 | 4.63E-10 | 6.95E-10 | 9.25E-10 | 1.86E-09 | 4.74E-09 | 9.68E-09 | 2.03E-08 | 3.18E-08 |
| CU | 64 | 0.00E+00 | 1.24E-11 | 1.24E-11 | 1.24E-11 | 1.24E-11 | 1.24E-11 | 1.24E-11 | 1.24E-11 | 1.24E-11 | 1.24E-11 | 1.24E-11 |
| CU | 65 | 0.00E+00 | 2.35E-11 | 7.07E-11 | 1.44E-10 | 2.17E-10 | 2.88E-10 | 5.81E-10 | 1.46E-09 | 2.93E-09 | 5.88E-09 | 8.82E-09 |
| CU | 66 | 0.00E+00 | 1.77E-14 | 1.77E-14 | 1.77E-14 | 1.77E-14 | 1.77E-14 | 1.77E-14 | 1.77E-14 | 1.77E-14 | 1.77E-14 | 1.77E-14 |
| ZN | 62 | 0.00E+00 | 4.92E-15 | 4.92E-15 | 4.92E-15 | 4.92E-15 | 4.92E-15 | 4.92E-15 | 4.92E-15 | 4.92E-15 | 4.92E-15 | 4.92E-15 |
| ZN | 63 | 0.00E+00 | 2.51E-15 | 2.51E-15 | 2.51E-15 | 2.51E-15 | 2.51E-15 | 2.51E-15 | 2.51E-15 | 2.51E-15 | 2.51E-15 | 2.51E-15 |
| ZN | 64 | 0.00E+00 | 1.95E-10 | 5.90E-10 | 1.20E-09 | 1.80E-09 | 2.39E-09 | 4.77E-09 | 1.19E-08 | 2.37E-08 | 4.75E-08 | 7.12E-08 |
| ZN | 65 | 0.00E+00 | 6.44E-13 | 1.78E-12 | 3.20E-12 | 4.27E-12 | 5.09E-12 | 6.90E-12 | 7.85E-12 | 7.89E-12 | 7.89E-12 | 7.89E-12 |
| ZN | 66 | 0.00E+00 | 1.04E-10 | 3.13E-10 | 6.36E-10 | 9.53E-10 | 1.27E-09 | 2.54E-09 | 6.35E-09 | 1.27E-08 | 2.54E-08 | 3.80E-08 |
| Total | | 0.00E+00 | 5.10E-09 | 1.53E-08 | 3.11E-08 | 4.66E-08 | 6.19E-08 | 1.24E-07 | 3.11E-07 | 6.20E-07 | 1.24E-06 | 1.86E-06 |

| Table A.4. SNS nuclide production during normal proton beam operation: tunnel concrete wall | | | | | | | | | | | | |
|---|---|---|---|---|---|---|---|---|---|---|---|---|
| Proton beam energy: 1 GeV | | | | | | | Operational line loss assumption: 1 nA/m (continuous) | | | | | |
| Nuclide masses integrated over the material zone volume in the HETC & MCNP calculational model | | | | | | | | | | | | |
| Nuclide concentration | | Time (s) | 7.88E+06 | 1.58E+07 | 2.37E+07 | 3.15E+07 | 6.31E+07 | 1.58E+08 | 3.15E+08 | 4.73E+08 | 6.31E+08 | 9.46E+08 |
| (gram-atoms) | | Initial | 3 months | 6 months | 9 months | 1 year | 2 years | 5 years | 10 years | 15 years | 20 years | 30 years |
| H | 1 | 0.00E+00 | 2.06E-07 | 4.18E-07 | 6.27E-07 | 8.33E-07 | 1.67E-06 | 4.18E-06 | 8.33E-06 | 1.25E-05 | 1.67E-05 | 2.50E-05 |
| H | 2 | 0.00E+00 | 8.30E-09 | 1.69E-08 | 2.53E-08 | 3.36E-08 | 6.73E-08 | 1.69E-07 | 3.36E-07 | 5.05E-07 | 6.73E-07 | 1.01E-06 |
| **H** | **3** | **0.00E+00** | **5.75E-09** | **1.16E-08** | **1.73E-08** | **2.28E-08** | **4.44E-08** | **1.03E-07** | **1.79E-07** | **2.38E-07** | **2.82E-07** | **3.40E-07** |
| H | 4 | 0.00E+00 | 4.04E-13 | 8.20E-13 | 1.23E-12 | 1.63E-12 | 3.27E-12 | 8.20E-12 | 1.63E-11 | 2.45E-11 | 3.27E-11 | 4.91E-11 |
| HE | 3 | 0.00E+00 | 1.27E-09 | 2.65E-09 | 4.10E-09 | 5.61E-09 | 1.25E-08 | 4.00E-08 | 1.05E-07 | 1.89E-07 | 2.87E-07 | 5.13E-07 |
| HE | 4 | 0.00E+00 | 6.45E-08 | 1.31E-07 | 1.96E-07 | 2.61E-07 | 5.23E-07 | 1.31E-06 | 2.61E-06 | 3.92E-06 | 5.23E-06 | 7.84E-06 |
| HE | 6 | 0.00E+00 | 6.06E-20 | 6.06E-20 | 6.06E-20 | 6.06E-20 | 6.06E-20 | 6.06E-20 | 6.06E-20 | 6.06E-20 | 6.06E-20 | 6.06E-20 |
| LI | 6 | 0.00E+00 | 7.46E-10 | 1.52E-09 | 2.27E-09 | 3.02E-09 | 6.05E-09 | 1.52E-08 | 3.02E-08 | 4.54E-08 | 6.05E-08 | 9.08E-08 |
| LI | 7 | 0.00E+00 | 5.95E-11 | 1.30E-10 | 2.02E-10 | 2.74E-10 | 5.67E-10 | 1.46E-09 | 2.94E-09 | 4.42E-09 | 5.90E-09 | 8.84E-09 |
| LI | 8 | 0.00E+00 | 1.24E-18 | 1.24E-18 | 1.24E-18 | 1.24E-18 | 1.24E-18 | 1.24E-18 | 1.24E-18 | 1.24E-18 | 1.24E-18 | 1.24E-18 |
| BE | 7 | 0.00E+00 | 1.26E-11 | 1.66E-11 | 1.78E-11 | 1.82E-11 | 1.83E-11 | 1.83E-11 | 1.83E-11 | 1.83E-11 | 1.83E-11 | 1.83E-11 |
| BE | 9 | 0.00E+00 | 1.55E-10 | 3.15E-10 | 4.72E-10 | 6.27E-10 | 1.26E-09 | 3.15E-09 | 6.27E-09 | 9.42E-09 | 1.26E-08 | 1.88E-08 |
| **BE** | **10** | **0.00E+00** | **2.21E-11** | **4.48E-11** | **6.73E-11** | **8.94E-11** | **1.79E-10** | **4.48E-10** | **8.94E-10** | **1.34E-09** | **1.79E-09** | **2.68E-09** |
| BE | 11 | 0.00E+00 | 1.22E-17 | 1.22E-17 | 1.22E-17 | 1.22E-17 | 1.22E-17 | 1.22E-17 | 1.22E-17 | 1.22E-17 | 1.22E-17 | 1.22E-17 |
| B | 10 | 0.00E+00 | 1.20E-09 | 2.43E-09 | 3.65E-09 | 4.85E-09 | 9.71E-09 | 2.43E-08 | 4.85E-08 | 7.28E-08 | 9.71E-08 | 1.46E-07 |
| B | 11 | 0.00E+00 | 1.22E-09 | 2.48E-09 | 3.72E-09 | 4.94E-09 | 9.90E-09 | 2.48E-08 | 4.94E-08 | 7.42E-08 | 9.89E-08 | 1.48E-07 |
| B | 12 | 0.00E+00 | 6.31E-19 | 6.31E-19 | 6.31E-19 | 6.31E-19 | 6.31E-19 | 6.31E-19 | 6.31E-19 | 6.31E-19 | 6.31E-19 | 6.31E-19 |
| B | 13 | 0.00E+00 | 8.58E-20 | 8.58E-20 | 8.58E-20 | 8.58E-20 | 8.58E-20 | 8.58E-20 | 8.58E-20 | 8.58E-20 | 8.58E-20 | 8.58E-20 |
| C | 10 | 0.00E+00 | 1.00E-17 | 1.00E-17 | 1.00E-17 | 1.00E-17 | 1.00E-17 | 1.00E-17 | 1.00E-17 | 1.00E-17 | 1.00E-17 | 1.00E-17 |
| C | 11 | 0.00E+00 | 7.52E-14 | 7.52E-14 | 7.52E-14 | 7.52E-14 | 7.52E-14 | 7.52E-14 | 7.52E-14 | 7.52E-14 | 7.52E-14 | 7.52E-14 |
| C | 12 | 0.00E+00 | 2.50E-08 | 5.08E-08 | 7.63E-08 | 1.01E-07 | 2.03E-07 | 5.08E-07 | 1.01E-06 | 1.52E-06 | 2.03E-06 | 3.04E-06 |
| C | 13 | 0.00E+00 | 2.24E-08 | 4.55E-08 | 6.82E-08 | 9.06E-08 | 1.82E-07 | 4.55E-07 | 9.06E-07 | 1.36E-06 | 1.82E-06 | 2.72E-06 |
| **C** | **14** | **0.00E+00** | **1.98E-09** | **4.02E-09** | **6.03E-09** | **8.01E-09** | **1.60E-08** | **4.02E-08** | **8.01E-08** | **1.20E-07** | **1.60E-07** | **2.40E-07** |
| N | 12 | 0.00E+00 | 6.15E-20 | 6.15E-20 | 6.15E-20 | 6.15E-20 | 6.15E-20 | 6.15E-20 | 6.15E-20 | 6.15E-20 | 6.15E-20 | 6.15E-20 |
| N | 13 | 0.00E+00 | 1.77E-13 | 1.77E-13 | 1.77E-13 | 1.77E-13 | 1.77E-13 | 1.77E-13 | 1.77E-13 | 1.77E-13 | 1.77E-13 | 1.77E-13 |
| N | 14 | 0.00E+00 | 2.07E-08 | 4.21E-08 | 6.31E-08 | 8.38E-08 | 1.68E-07 | 4.21E-07 | 8.38E-07 | 1.26E-06 | 1.68E-06 | 2.52E-06 |
| N | 15 | 0.00E+00 | 2.98E-08 | 6.04E-08 | 9.07E-08 | 1.20E-07 | 2.41E-07 | 6.04E-07 | 1.20E-06 | 1.81E-06 | 2.41E-06 | 3.62E-06 |
| N | 16 | 0.00E+00 | 2.89E-15 | 2.89E-15 | 2.89E-15 | 2.89E-15 | 2.89E-15 | 2.89E-15 | 2.89E-15 | 2.89E-15 | 2.89E-15 | 2.89E-15 |
| N | 17 | 0.00E+00 | 2.28E-18 | 2.28E-18 | 2.28E-18 | 2.28E-18 | 2.28E-18 | 2.28E-18 | 2.28E-18 | 2.28E-18 | 2.28E-18 | 2.28E-18 |
| N | 18 | 0.00E+00 | 1.41E-19 | 1.41E-19 | 1.41E-19 | 1.41E-19 | 1.41E-19 | 1.41E-19 | 1.41E-19 | 1.41E-19 | 1.41E-19 | 1.41E-19 |
| O | 14 | 0.00E+00 | 3.11E-15 | 3.11E-15 | 3.11E-15 | 3.11E-15 | 3.11E-15 | 3.11E-15 | 3.11E-15 | 3.11E-15 | 3.11E-15 | 3.11E-15 |
| O | 15 | 0.00E+00 | 1.55E-13 | 1.55E-13 | 1.55E-13 | 1.55E-13 | 1.55E-13 | 1.55E-13 | 1.55E-13 | 1.55E-13 | 1.55E-13 | 1.55E-13 |
| O | 16 | 0.00E+00 | 1.04E-08 | 2.12E-08 | 3.18E-08 | 4.22E-08 | 8.46E-08 | 2.12E-07 | 4.22E-07 | 6.34E-07 | 8.46E-07 | 1.27E-06 |

| Table A.4. (continued) | | | | | | | | | | | | |
|---|---|---|---|---|---|---|---|---|---|---|---|---|
| Proton beam energy: 1 GeV | | | | | | | Operational line loss assumption: 1 nA/m (continuous) | | | | | |
| Nuclide masses integrated over the material zone volume in the HETC & MCNP calculational model | | | | | | | | | | | | |
| Nuclide concentration | | Time (s) | 7.88E+06 | 1.58E+07 | 2.37E+07 | 3.15E+07 | 6.31E+07 | 1.58E+08 | 3.15E+08 | 4.73E+08 | 6.31E+08 | 9.46E+08 |
| (gram-atoms) | | Initial | 3 months | 6 months | 9 months | 1 year | 2 years | 5 years | 10 years | 15 years | 20 years | 30 years |
| O | 17 | 0.00E+00 | 4.32E-09 | 8.76E-09 | 1.31E-08 | 1.75E-08 | 3.50E-08 | 8.76E-08 | 1.75E-07 | 2.62E-07 | 3.50E-07 | 5.25E-07 |
| O | 18 | 0.00E+00 | 4.94E-10 | 1.00E-09 | 1.51E-09 | 2.00E-09 | 4.01E-09 | 1.00E-08 | 2.00E-08 | 3.01E-08 | 4.01E-08 | 6.01E-08 |
| O | 19 | 0.00E+00 | 4.24E-17 | 4.24E-17 | 4.24E-17 | 4.24E-17 | 4.24E-17 | 4.24E-17 | 4.24E-17 | 4.24E-17 | 4.24E-17 | 4.24E-17 |
| F | 17 | 0.00E+00 | 1.53E-16 | 1.53E-16 | 1.53E-16 | 1.53E-16 | 1.53E-16 | 1.53E-16 | 1.53E-16 | 1.53E-16 | 1.53E-16 | 1.53E-16 |
| F | 18 | 0.00E+00 | 5.34E-13 | 5.34E-13 | 5.34E-13 | 5.34E-13 | 5.34E-13 | 5.34E-13 | 5.34E-13 | 5.34E-13 | 5.34E-13 | 5.34E-13 |
| F | 19 | 0.00E+00 | 5.69E-10 | 1.16E-09 | 1.73E-09 | 2.31E-09 | 4.62E-09 | 1.16E-08 | 2.31E-08 | 3.46E-08 | 4.62E-08 | 6.92E-08 |
| F | 20 | 0.00E+00 | 5.83E-16 | 5.83E-16 | 5.83E-16 | 5.83E-16 | 5.83E-16 | 5.83E-16 | 5.83E-16 | 5.83E-16 | 5.83E-16 | 5.83E-16 |
| F | 21 | 0.00E+00 | 3.30E-17 | 3.30E-17 | 3.30E-17 | 3.30E-17 | 3.30E-17 | 3.30E-17 | 3.30E-17 | 3.30E-17 | 3.30E-17 | 3.30E-17 |
| F | 22 | 0.00E+00 | 3.48E-18 | 3.48E-18 | 3.48E-18 | 3.48E-18 | 3.48E-18 | 3.48E-18 | 3.48E-18 | 3.48E-18 | 3.48E-18 | 3.48E-18 |
| NE | 19 | 0.00E+00 | 1.29E-16 | 1.29E-16 | 1.29E-16 | 1.29E-16 | 1.29E-16 | 1.29E-16 | 1.29E-16 | 1.29E-16 | 1.29E-16 | 1.29E-16 |
| NE | 20 | 0.00E+00 | 1.36E-09 | 2.76E-09 | 4.14E-09 | 5.50E-09 | 1.10E-08 | 2.76E-08 | 5.50E-08 | 8.26E-08 | 1.10E-07 | 1.65E-07 |
| NE | 21 | 0.00E+00 | 8.97E-10 | 1.82E-09 | 2.73E-09 | 3.63E-09 | 7.28E-09 | 1.82E-08 | 3.63E-08 | 5.45E-08 | 7.28E-08 | 1.09E-07 |
| NE | 22 | 0.00E+00 | 1.67E-09 | 3.47E-09 | 5.33E-09 | 7.23E-09 | 1.56E-08 | 4.52E-08 | 1.01E-07 | 1.60E-07 | 2.21E-07 | 3.41E-07 |
| NE | 23 | 0.00E+00 | 1.66E-15 | 1.66E-15 | 1.66E-15 | 1.66E-15 | 1.66E-15 | 1.66E-15 | 1.66E-15 | 1.66E-15 | 1.66E-15 | 1.66E-15 |
| NE | 24 | 0.00E+00 | 2.47E-16 | 2.47E-16 | 2.47E-16 | 2.47E-16 | 2.47E-16 | 2.47E-16 | 2.47E-16 | 2.47E-16 | 2.47E-16 | 2.47E-16 |
| NA | 21 | 0.00E+00 | 1.24E-16 | 1.24E-16 | 1.24E-16 | 1.24E-16 | 1.24E-16 | 1.24E-16 | 1.24E-16 | 1.24E-16 | 1.24E-16 | 1.24E-16 |
| **NA** | **22** | **0.00E+00** | **1.31E-09** | **2.57E-09** | **3.73E-09** | **4.80E-09** | **8.50E-09** | **1.52E-08** | **1.92E-08** | **2.03E-08** | **2.06E-08** | **2.07E-08** |
| NA | 23 | 0.00E+00 | 3.77E-09 | 7.65E-09 | 1.15E-08 | 1.52E-08 | 3.05E-08 | 7.65E-08 | 1.52E-07 | 2.29E-07 | 3.05E-07 | 4.58E-07 |
| NA | 24 | 0.00E+00 | 7.50E-12 | 7.50E-12 | 7.50E-12 | 7.50E-12 | 7.50E-12 | 7.50E-12 | 7.50E-12 | 7.50E-12 | 7.50E-12 | 7.50E-12 |
| NA | 25 | 0.00E+00 | 1.48E-15 | 1.48E-15 | 1.48E-15 | 1.48E-15 | 1.48E-15 | 1.48E-15 | 1.48E-15 | 1.48E-15 | 1.48E-15 | 1.48E-15 |
| NA | 26 | 0.00E+00 | 4.44E-18 | 4.44E-18 | 4.44E-18 | 4.44E-18 | 4.44E-18 | 4.44E-18 | 4.44E-18 | 4.44E-18 | 4.44E-18 | 4.44E-18 |
| MG | 23 | 0.00E+00 | 2.33E-16 | 2.33E-16 | 2.33E-16 | 2.33E-16 | 2.33E-16 | 2.33E-16 | 2.33E-16 | 2.33E-16 | 2.33E-16 | 2.33E-16 |
| MG | 24 | 0.00E+00 | 1.69E-08 | 3.43E-08 | 5.15E-08 | 6.84E-08 | 1.37E-07 | 3.43E-07 | 6.84E-07 | 1.03E-06 | 1.37E-06 | 2.05E-06 |
| MG | 25 | 0.00E+00 | 6.89E-09 | 1.40E-08 | 2.10E-08 | 2.79E-08 | 5.58E-08 | 1.40E-07 | 2.79E-07 | 4.19E-07 | 5.58E-07 | 8.37E-07 |
| MG | 26 | 0.00E+00 | 4.91E-09 | 9.97E-09 | 1.50E-08 | 1.99E-08 | 3.98E-08 | 9.97E-08 | 1.99E-07 | 2.98E-07 | 3.98E-07 | 5.97E-07 |
| MG | 27 | 0.00E+00 | 1.30E-13 | 1.30E-13 | 1.30E-13 | 1.30E-13 | 1.30E-13 | 1.30E-13 | 1.30E-13 | 1.30E-13 | 1.30E-13 | 1.30E-13 |
| AL | 24 | 0.00E+00 | 3.60E-18 | 3.60E-18 | 3.60E-18 | 3.60E-18 | 3.60E-18 | 3.60E-18 | 3.60E-18 | 3.60E-18 | 3.60E-18 | 3.60E-18 |
| AL | 25 | 0.00E+00 | 3.54E-16 | 3.54E-16 | 3.54E-16 | 3.54E-16 | 3.54E-16 | 3.54E-16 | 3.54E-16 | 3.54E-16 | 3.54E-16 | 3.54E-16 |
| **AL** | **26** | **0.00E+00** | **7.16E-09** | **1.45E-08** | **2.18E-08** | **2.90E-08** | **5.81E-08** | **1.45E-07** | **2.90E-07** | **4.35E-07** | **5.81E-07** | **8.70E-07** |
| AL | 27 | 0.00E+00 | 2.70E-08 | 5.49E-08 | 8.24E-08 | 1.09E-07 | 2.19E-07 | 5.49E-07 | 1.09E-06 | 1.64E-06 | 2.19E-06 | 3.29E-06 |
| AL | 28 | 0.00E+00 | 2.32E-13 | 2.32E-13 | 2.32E-13 | 2.32E-13 | 2.32E-13 | 2.32E-13 | 2.32E-13 | 2.32E-13 | 2.32E-13 | 2.32E-13 |
| AL | 29 | 0.00E+00 | 3.54E-14 | 3.54E-14 | 3.54E-14 | 3.54E-14 | 3.54E-14 | 3.54E-14 | 3.54E-14 | 3.54E-14 | 3.54E-14 | 3.54E-14 |
| AL | 30 | 0.00E+00 | 4.54E-17 | 4.54E-17 | 4.54E-17 | 4.54E-17 | 4.54E-17 | 4.54E-17 | 4.54E-17 | 4.54E-17 | 4.54E-17 | 4.54E-17 |
| SI | 26 | 0.00E+00 | 3.95E-17 | 3.95E-17 | 3.95E-17 | 3.95E-17 | 3.95E-17 | 3.95E-17 | 3.95E-17 | 3.95E-17 | 3.95E-17 | 3.95E-17 |

| Table A.4. (continued) | | | | | | | | | | | | |
|---|---|---|---|---|---|---|---|---|---|---|---|---|
| Proton beam energy: 1 GeV | | | | | | | Operational line loss assumption: 1 nA/m (continuous) | | | | | |
| Nuclide masses integrated over the material zone volume in the HETC & MCNP calculational model | | | | | | | | | | | | |
| Nuclide concentration | | Time (s) | 7.88E+06 | 1.58E+07 | 2.37E+07 | 3.15E+07 | 6.31E+07 | 1.58E+08 | 3.15E+08 | 4.73E+08 | 6.31E+08 | 9.46E+08 |
| (gram-atoms) | | Initial | 3 months | 6 months | 9 months | 1 year | 2 years | 5 years | 10 years | 15 years | 20 years | 30 years |
| SI | 27 | 0.00E+00 | 1.96E-15 | 1.96E-15 | 1.96E-15 | 1.96E-15 | 1.96E-15 | 1.96E-15 | 1.96E-15 | 1.96E-15 | 1.96E-15 | 1.96E-15 |
| SI | 28 | 0.00E+00 | 1.41E-08 | 2.86E-08 | 4.29E-08 | 5.70E-08 | 1.14E-07 | 2.86E-07 | 5.70E-07 | 8.56E-07 | 1.14E-06 | 1.71E-06 |
| SI | 29 | 0.00E+00 | 4.47E-09 | 9.08E-09 | 1.36E-08 | 1.81E-08 | 3.63E-08 | 9.08E-08 | 1.81E-07 | 2.72E-07 | 3.63E-07 | 5.44E-07 |
| SI | 30 | 0.00E+00 | 7.08E-10 | 1.44E-09 | 2.16E-09 | 2.87E-09 | 5.74E-09 | 1.44E-08 | 2.87E-08 | 4.30E-08 | 5.74E-08 | 8.61E-08 |
| SI | 31 | 0.00E+00 | 3.13E-13 | 3.13E-13 | 3.13E-13 | 3.13E-13 | 3.13E-13 | 3.13E-13 | 3.13E-13 | 3.13E-13 | 3.13E-13 | 3.13E-13 |
| SI | 32 | 0.00E+00 | 4.04E-13 | 8.20E-13 | 1.23E-12 | 1.63E-12 | 3.27E-12 | 8.18E-12 | 1.63E-11 | 2.43E-11 | 3.24E-11 | 4.83E-11 |
| P | 31 | 0.00E+00 | 3.70E-10 | 7.51E-10 | 1.13E-09 | 1.50E-09 | 3.00E-09 | 7.51E-09 | 1.50E-08 | 2.25E-08 | 3.00E-08 | 4.50E-08 |
| P | 32 | 0.00E+00 | 2.37E-11 | 2.41E-11 | 2.41E-11 | 2.41E-11 | 2.41E-11 | 2.41E-11 | 2.41E-11 | 2.41E-11 | 2.41E-11 | 2.41E-11 |
| P | 33 | 0.00E+00 | 6.49E-12 | 7.02E-12 | 7.06E-12 | 7.07E-12 | 7.07E-12 | 7.07E-12 | 7.07E-12 | 7.07E-12 | 7.07E-12 | 7.07E-12 |
| P | 34 | 0.00E+00 | 4.64E-18 | 4.64E-18 | 4.64E-18 | 4.64E-18 | 4.64E-18 | 4.64E-18 | 4.64E-18 | 4.64E-18 | 4.64E-18 | 4.64E-18 |
| S | 31 | 0.00E+00 | 1.56E-18 | 1.56E-18 | 1.56E-18 | 1.56E-18 | 1.56E-18 | 1.56E-18 | 1.56E-18 | 1.56E-18 | 1.56E-18 | 1.56E-18 |
| S | 32 | 0.00E+00 | 1.52E-10 | 3.33E-10 | 5.12E-10 | 6.88E-10 | 1.43E-09 | 3.60E-09 | 7.17E-09 | 1.08E-08 | 1.44E-08 | 2.15E-08 |
| S | 33 | 0.00E+00 | 2.18E-10 | 4.48E-10 | 6.76E-10 | 9.00E-10 | 1.82E-09 | 4.56E-09 | 9.09E-09 | 1.36E-08 | 1.82E-08 | 2.73E-08 |
| S | 34 | 0.00E+00 | 2.06E-10 | 4.19E-10 | 6.28E-10 | 8.35E-10 | 1.67E-09 | 4.19E-09 | 8.35E-09 | 1.25E-08 | 1.67E-08 | 2.51E-08 |
| S | 35 | 0.00E+00 | 3.94E-11 | 5.93E-11 | 6.87E-11 | 7.32E-11 | 7.74E-11 | 7.77E-11 | 7.76E-11 | 7.76E-11 | 7.76E-11 | 7.76E-11 |
| S | 36 | 0.00E+00 | 5.25E-12 | 1.07E-11 | 1.60E-11 | 2.12E-11 | 4.26E-11 | 1.07E-10 | 2.12E-10 | 3.19E-10 | 4.26E-10 | 6.38E-10 |
| S | 38 | 0.00E+00 | 7.60E-16 | 7.60E-16 | 7.60E-16 | 7.60E-16 | 7.60E-16 | 7.60E-16 | 7.60E-16 | 7.60E-16 | 7.60E-16 | 7.60E-16 |
| CL | 35 | 0.00E+00 | 5.73E-10 | 1.18E-09 | 1.80E-09 | 2.40E-09 | 4.89E-09 | 1.24E-08 | 2.49E-08 | 3.74E-08 | 4.99E-08 | 7.47E-08 |
| **CL** | **36** | **0.00E+00** | **9.12E-10** | **1.85E-09** | **2.78E-09** | **3.69E-09** | **7.39E-09** | **1.85E-08** | **3.69E-08** | **5.54E-08** | **7.39E-08** | **1.11E-07** |
| CL | 37 | 0.00E+00 | 2.86E-09 | 7.84E-09 | 1.31E-08 | 1.83E-08 | 4.24E-08 | 1.09E-07 | 2.17E-07 | 3.27E-07 | 4.36E-07 | 6.50E-07 |
| CL | 38 | 0.00E+00 | 5.52E-15 | 5.52E-15 | 5.52E-15 | 5.52E-15 | 5.52E-15 | 5.52E-15 | 5.52E-15 | 5.52E-15 | 5.52E-15 | 5.52E-15 |
| CL | 39 | 0.00E+00 | 4.35E-16 | 4.35E-16 | 4.35E-16 | 4.35E-16 | 4.35E-16 | 4.35E-16 | 4.35E-16 | 4.35E-16 | 4.35E-16 | 4.35E-16 |
| CL | 40 | 0.00E+00 | 1.32E-17 | 1.32E-17 | 1.32E-17 | 1.32E-17 | 1.32E-17 | 1.32E-17 | 1.32E-17 | 1.32E-17 | 1.32E-17 | 1.32E-17 |
| AR | 36 | 0.00E+00 | 4.40E-10 | 8.94E-10 | 1.34E-09 | 1.78E-09 | 3.57E-09 | 8.94E-09 | 1.78E-08 | 2.68E-08 | 3.57E-08 | 5.35E-08 |
| AR | 37 | 0.00E+00 | 2.37E-09 | 2.78E-09 | 2.84E-09 | 2.85E-09 | 2.86E-09 | 2.85E-09 | 2.85E-09 | 2.85E-09 | 2.85E-09 | 2.85E-09 |
| AR | 38 | 0.00E+00 | 2.99E-09 | 6.06E-09 | 9.09E-09 | 1.21E-08 | 2.42E-08 | 6.06E-08 | 1.21E-07 | 1.81E-07 | 2.42E-07 | 3.63E-07 |
| **AR** | **39** | **0.00E+00** | **1.86E-09** | **3.78E-09** | **5.67E-09** | **7.54E-09** | **1.51E-08** | **3.76E-08** | **7.45E-08** | **1.11E-07** | **1.47E-07** | **2.18E-07** |
| AR | 40 | 0.00E+00 | 3.17E-11 | 6.43E-11 | 9.65E-11 | 1.28E-10 | 2.57E-10 | 6.43E-10 | 1.28E-09 | 1.93E-09 | 2.57E-09 | 3.85E-09 |
| AR | 41 | 0.00E+00 | 1.53E-14 | 1.53E-14 | 1.53E-14 | 1.53E-14 | 1.53E-14 | 1.53E-14 | 1.53E-14 | 1.53E-14 | 1.53E-14 | 1.53E-14 |
| AR | 42 | 0.00E+00 | 2.04E-12 | 4.13E-12 | 6.18E-12 | 8.20E-12 | 1.62E-11 | 3.94E-11 | 7.47E-11 | 1.07E-10 | 1.35E-10 | 1.84E-10 |
| AR | 43 | 0.00E+00 | 2.67E-17 | 2.67E-17 | 2.67E-17 | 2.67E-17 | 2.67E-17 | 2.67E-17 | 2.67E-17 | 2.67E-17 | 2.67E-17 | 2.67E-17 |
| AR | 44 | 0.00E+00 | 2.90E-19 | 2.90E-19 | 2.90E-19 | 2.90E-19 | 2.90E-19 | 2.90E-19 | 2.90E-19 | 2.90E-19 | 2.90E-19 | 2.90E-19 |
| K | 38 | 0.00E+00 | 6.68E-14 | 6.68E-14 | 6.68E-14 | 6.68E-14 | 6.68E-14 | 6.68E-14 | 6.68E-14 | 6.68E-14 | 6.68E-14 | 6.68E-14 |
| K | 39 | 0.00E+00 | 5.35E-09 | 1.09E-08 | 1.63E-08 | 2.17E-08 | 4.34E-08 | 1.09E-07 | 2.18E-07 | 3.28E-07 | 4.38E-07 | 6.59E-07 |

**Table A.4. (continued)**

| Proton beam energy: 1 GeV | | | | | | | Operational line loss assumption: 1 nA/m (continuous) | | | | | |
|---|---|---|---|---|---|---|---|---|---|---|---|---|
| Nuclide masses integrated over the material zone volume in the HETC & MCNP calculational model | | | | | | | | | | | | |
| Nuclide concentration | | Time (s) | 7.88E+06 | 1.58E+07 | 2.37E+07 | 3.15E+07 | 6.31E+07 | 1.58E+08 | 3.15E+08 | 4.73E+08 | 6.31E+08 | 9.46E+08 |
| (gram-atoms) | | Initial | 3 months | 6 months | 9 months | 1 year | 2 years | 5 years | 10 years | 15 years | 20 years | 30 years |
| **K** | **40** | **0.00E+00** | **1.09E-08** | **2.22E-08** | **3.33E-08** | **4.42E-08** | **8.86E-08** | **2.22E-07** | **4.42E-07** | **6.64E-07** | **8.86E-07** | **1.33E-06** |
| K | 41 | 0.00E+00 | 5.22E-11 | 1.06E-10 | 1.59E-10 | 2.11E-10 | 4.24E-10 | 1.06E-09 | 2.12E-09 | 3.18E-09 | 4.24E-09 | 6.36E-09 |
| K | 42 | 0.00E+00 | 7.70E-13 | 7.70E-13 | 7.70E-13 | 7.70E-13 | 7.71E-13 | 7.72E-13 | 7.73E-13 | 7.74E-13 | 7.76E-13 | 7.78E-13 |
| K | 43 | 0.00E+00 | 3.94E-13 | 3.94E-13 | 3.94E-13 | 3.94E-13 | 3.94E-13 | 3.94E-13 | 3.94E-13 | 3.94E-13 | 3.94E-13 | 3.94E-13 |
| K | 44 | 0.00E+00 | 2.50E-15 | 2.50E-15 | 2.50E-15 | 2.50E-15 | 2.50E-15 | 2.50E-15 | 2.50E-15 | 2.50E-15 | 2.50E-15 | 2.50E-15 |
| K | 45 | 0.00E+00 | 1.80E-16 | 1.80E-16 | 1.80E-16 | 1.80E-16 | 1.80E-16 | 1.80E-16 | 1.80E-16 | 1.80E-16 | 1.80E-16 | 1.80E-16 |
| K | 46 | 0.00E+00 | 2.64E-17 | 2.64E-17 | 2.64E-17 | 2.64E-17 | 2.64E-17 | 2.64E-17 | 2.64E-17 | 2.64E-17 | 2.64E-17 | 2.64E-17 |
| K | 47 | 0.00E+00 | 4.09E-18 | 4.09E-18 | 4.09E-18 | 4.09E-18 | 4.09E-18 | 4.09E-18 | 4.09E-18 | 4.09E-18 | 4.09E-18 | 4.09E-18 |
| K | 48 | 0.00E+00 | 1.36E-20 | 1.36E-20 | 1.36E-20 | 1.36E-20 | 1.36E-20 | 1.36E-20 | 1.36E-20 | 1.36E-20 | 1.36E-20 | 1.36E-20 |
| CA | 40 | 0.00E+00 | 6.70E-10 | 1.36E-09 | 2.04E-09 | 2.71E-09 | 5.44E-09 | 1.36E-08 | 2.71E-08 | 4.07E-08 | 5.44E-08 | 8.15E-08 |
| **CA** | **41** | **0.00E+00** | **9.73E-10** | **1.98E-09** | **2.97E-09** | **3.94E-09** | **7.89E-09** | **1.98E-08** | **3.94E-08** | **5.92E-08** | **7.89E-08** | **1.18E-07** |
| CA | 42 | 0.00E+00 | 1.35E-10 | 2.75E-10 | 4.13E-10 | 5.49E-10 | 1.10E-09 | 2.75E-09 | 5.47E-09 | 8.22E-09 | 1.10E-08 | 1.65E-08 |
| CA | 43 | 0.00E+00 | 1.29E-10 | 2.62E-10 | 3.94E-10 | 5.23E-10 | 1.05E-09 | 2.62E-09 | 5.22E-09 | 7.84E-09 | 1.05E-08 | 1.57E-08 |
| CA | 44 | 0.00E+00 | 4.45E-11 | 9.04E-11 | 1.36E-10 | 1.80E-10 | 3.61E-10 | 9.04E-10 | 1.80E-09 | 2.71E-09 | 3.61E-09 | 5.42E-09 |
| CA | 45 | 0.00E+00 | 3.21E-11 | 5.47E-11 | 6.98E-11 | 8.00E-11 | 9.73E-11 | 1.02E-10 | 1.02E-10 | 1.02E-10 | 1.02E-10 | 1.02E-10 |
| CA | 46 | 0.00E+00 | 4.96E-12 | 1.01E-11 | 1.51E-11 | 2.01E-11 | 4.03E-11 | 1.01E-10 | 2.01E-10 | 3.02E-10 | 4.03E-10 | 6.04E-10 |
| CA | 47 | 0.00E+00 | 7.50E-13 | 7.50E-13 | 7.50E-13 | 7.50E-13 | 7.50E-13 | 7.50E-13 | 7.50E-13 | 7.50E-13 | 7.50E-13 | 7.50E-13 |
| CA | 48 | 0.00E+00 | 1.08E-14 | 2.19E-14 | 3.28E-14 | 4.36E-14 | 8.74E-14 | 2.19E-13 | 4.36E-13 | 6.55E-13 | 8.74E-13 | 1.31E-12 |
| CA | 49 | 0.00E+00 | 5.11E-18 | 5.11E-18 | 5.11E-18 | 5.11E-18 | 5.11E-18 | 5.11E-18 | 5.11E-18 | 5.11E-18 | 5.11E-18 | 5.11E-18 |
| SC | 40 | 0.00E+00 | 5.47E-20 | 5.47E-20 | 5.47E-20 | 5.47E-20 | 5.47E-20 | 5.47E-20 | 5.47E-20 | 5.47E-20 | 5.47E-20 | 5.47E-20 |
| SC | 42 | 0.00E+00 | 5.10E-20 | 5.10E-20 | 5.10E-20 | 5.10E-20 | 5.10E-20 | 5.10E-20 | 5.10E-20 | 5.10E-20 | 5.10E-20 | 5.10E-20 |
| SC | 43 | 0.00E+00 | 3.14E-15 | 3.14E-15 | 3.14E-15 | 3.14E-15 | 3.14E-15 | 3.14E-15 | 3.14E-15 | 3.14E-15 | 3.14E-15 | 3.14E-15 |
| SC | 44 | 0.00E+00 | 1.34E-14 | 1.34E-14 | 1.34E-14 | 1.34E-14 | 1.34E-14 | 1.34E-14 | 1.35E-14 | 1.36E-14 | 1.36E-14 | 1.37E-14 |
| SC | 45 | 0.00E+00 | 1.25E-11 | 3.60E-11 | 6.62E-11 | 1.01E-10 | 2.65E-10 | 8.05E-10 | 1.81E-09 | 2.82E-09 | 3.83E-09 | 5.74E-09 |
| SC | 46 | 0.00E+00 | 1.99E-12 | 2.96E-12 | 3.40E-12 | 3.61E-12 | 3.78E-12 | 3.79E-12 | 3.79E-12 | 3.79E-12 | 3.79E-12 | 3.79E-12 |
| SC | 47 | 0.00E+00 | 6.32E-13 | 6.32E-13 | 6.32E-13 | 6.32E-13 | 6.32E-13 | 6.32E-13 | 6.32E-13 | 6.32E-13 | 6.32E-13 | 6.32E-13 |
| SC | 48 | 0.00E+00 | 8.99E-15 | 8.99E-15 | 8.99E-15 | 8.99E-15 | 8.99E-15 | 8.99E-15 | 8.99E-15 | 8.99E-15 | 8.99E-15 | 8.99E-15 |
| SC | 49 | 0.00E+00 | 3.34E-17 | 3.34E-17 | 3.34E-17 | 3.34E-17 | 3.34E-17 | 3.34E-17 | 3.34E-17 | 3.34E-17 | 3.34E-17 | 3.34E-17 |
| TI | 44 | 0.00E+00 | 4.03E-13 | 8.17E-13 | 1.22E-12 | 1.62E-12 | 3.23E-12 | 7.91E-12 | 1.52E-11 | 2.21E-11 | 2.85E-11 | 3.99E-11 |
| TI | 45 | 0.00E+00 | 4.15E-15 | 4.15E-15 | 4.15E-15 | 4.15E-15 | 4.15E-15 | 4.15E-15 | 4.15E-15 | 4.15E-15 | 4.15E-15 | 4.15E-15 |
| TI | 46 | 0.00E+00 | 9.64E-12 | 2.07E-11 | 3.20E-11 | 4.35E-11 | 9.06E-11 | 2.36E-10 | 4.75E-10 | 7.15E-10 | 9.55E-10 | 1.43E-09 |
| TI | 47 | 0.00E+00 | 2.51E-11 | 5.25E-11 | 7.94E-11 | 1.06E-10 | 2.12E-10 | 5.28E-10 | 1.05E-09 | 1.58E-09 | 2.10E-09 | 3.15E-09 |
| TI | 48 | 0.00E+00 | 2.24E-11 | 5.11E-11 | 7.94E-11 | 1.07E-10 | 2.27E-10 | 5.73E-10 | 1.14E-09 | 1.71E-09 | 2.29E-09 | 3.42E-09 |
| TI | 49 | 0.00E+00 | 4.95E-12 | 1.41E-11 | 2.65E-11 | 4.14E-11 | 1.20E-10 | 4.30E-10 | 9.80E-10 | 1.54E-09 | 2.09E-09 | 3.33E-09 |

**Table A.4. (continued)**

| Proton beam energy: 1 GeV | | | | | | | Operational line loss assumption: 1 nA/m (continuous) | | | | | |
|---|---|---|---|---|---|---|---|---|---|---|---|---|
| Nuclide masses integrated over the material zone volume in the HETC & MCNP calculational model | | | | | | | | | | | | |
| Nuclide concentration | | Time (s) | 7.88E+06 | 1.58E+07 | 2.37E+07 | 3.15E+07 | 6.31E+07 | 1.58E+08 | 3.15E+08 | 4.73E+08 | 6.31E+08 | 9.46E+08 |
| (gram-atoms) | | Initial | 3 months | 6 months | 9 months | 1 year | 2 years | 5 years | 10 years | 15 years | 20 years | 30 years |
| TI | 50 | 0.00E+00 | 8.07E-13 | 1.64E-12 | 2.46E-12 | 3.27E-12 | 6.55E-12 | 1.64E-11 | 3.27E-11 | 4.91E-11 | 6.55E-11 | 9.82E-11 |
| V | 47 | 0.00E+00 | 7.32E-16 | 7.32E-16 | 7.32E-16 | 7.32E-16 | 7.32E-16 | 7.32E-16 | 7.32E-16 | 7.32E-16 | 7.32E-16 | 7.32E-16 |
| V | 48 | 0.00E+00 | 5.54E-12 | 5.66E-12 | 5.66E-12 | 5.66E-12 | 5.66E-12 | 5.66E-12 | 5.66E-12 | 5.66E-12 | 5.66E-12 | 5.66E-12 |
| V | 49 | 0.00E+00 | 2.24E-11 | 4.15E-11 | 5.69E-11 | 6.95E-11 | 1.02E-10 | 1.26E-10 | 1.29E-10 | 1.29E-10 | 1.29E-10 | 1.29E-10 |
| V | 50 | 0.00E+00 | 1.45E-11 | 2.94E-11 | 4.41E-11 | 5.86E-11 | 1.17E-10 | 2.94E-10 | 5.86E-10 | 8.80E-10 | 1.17E-09 | 1.76E-09 |
| V | 51 | 0.00E+00 | 4.09E-11 | 1.06E-10 | 1.73E-10 | 2.38E-10 | 5.33E-10 | 1.36E-09 | 2.72E-09 | 4.08E-09 | 5.44E-09 | 8.13E-09 |
| CR | 49 | 0.00E+00 | 3.51E-15 | 3.51E-15 | 3.51E-15 | 3.51E-15 | 3.51E-15 | 3.51E-15 | 3.51E-15 | 3.51E-15 | 3.51E-15 | 3.51E-15 |
| CR | 50 | 0.00E+00 | 2.65E-11 | 5.38E-11 | 8.07E-11 | 1.07E-10 | 2.15E-10 | 5.38E-10 | 1.07E-09 | 1.61E-09 | 2.15E-09 | 3.22E-09 |
| CR | 51 | 0.00E+00 | 2.48E-11 | 2.75E-11 | 2.77E-11 | 2.77E-11 | 2.77E-11 | 2.77E-11 | 2.77E-11 | 2.77E-11 | 2.77E-11 | 2.77E-11 |
| CR | 52 | 0.00E+00 | 1.14E-10 | 2.38E-10 | 3.60E-10 | 4.81E-10 | 9.52E-10 | 2.35E-09 | 4.67E-09 | 7.00E-09 | 9.33E-09 | 1.40E-08 |
| CR | 53 | 0.00E+00 | 2.97E-11 | 6.03E-11 | 9.05E-11 | 1.20E-10 | 2.41E-10 | 6.03E-10 | 1.20E-09 | 1.81E-09 | 2.41E-09 | 3.61E-09 |
| CR | 54 | 0.00E+00 | 2.52E-11 | 8.16E-11 | 1.62E-10 | 2.61E-10 | 7.98E-10 | 2.91E-09 | 6.66E-09 | 1.04E-08 | 1.42E-08 | 2.27E-08 |
| CR | 55 | 0.00E+00 | 4.85E-17 | 4.85E-17 | 4.85E-17 | 4.85E-17 | 4.85E-17 | 4.85E-17 | 4.85E-17 | 4.85E-17 | 4.85E-17 | 4.85E-17 |
| CR | 56 | 0.00E+00 | 1.05E-18 | 1.05E-18 | 1.05E-18 | 1.05E-18 | 1.05E-18 | 1.05E-18 | 1.05E-18 | 1.05E-18 | 1.05E-18 | 1.05E-18 |
| MN | 50 | 0.00E+00 | 2.12E-20 | 2.12E-20 | 2.12E-20 | 2.12E-20 | 2.12E-20 | 2.12E-20 | 2.12E-20 | 2.12E-20 | 2.12E-20 | 2.12E-20 |
| MN | 51 | 0.00E+00 | 6.31E-15 | 6.31E-15 | 6.31E-15 | 6.31E-15 | 6.31E-15 | 6.31E-15 | 6.31E-15 | 6.31E-15 | 6.31E-15 | 6.31E-15 |
| MN | 52 | 0.00E+00 | 5.90E-12 | 5.90E-12 | 5.90E-12 | 5.90E-12 | 5.90E-12 | 5.90E-12 | 5.90E-12 | 5.90E-12 | 5.90E-12 | 5.90E-12 |
| **MN** | **53** | **0.00E+00** | **1.68E-10** | **3.41E-10** | **5.12E-10** | **6.80E-10** | **1.36E-09** | **3.41E-09** | **6.80E-09** | **1.02E-08** | **1.36E-08** | **2.04E-08** |
| MN | 54 | 0.00E+00 | 1.61E-10 | 2.97E-10 | 4.06E-10 | 4.94E-10 | 7.14E-10 | 8.74E-10 | 8.90E-10 | 8.90E-10 | 8.90E-10 | 8.90E-10 |
| MN | 55 | 0.00E+00 | 2.03E-10 | 4.39E-10 | 6.96E-10 | 9.72E-10 | 2.29E-09 | 7.62E-09 | 1.87E-08 | 3.07E-08 | 4.31E-08 | 6.79E-08 |
| MN | 56 | 0.00E+00 | 1.16E-13 | 1.16E-13 | 1.16E-13 | 1.16E-13 | 1.16E-13 | 1.16E-13 | 1.16E-13 | 1.16E-13 | 1.16E-13 | 1.16E-13 |
| MN | 57 | 0.00E+00 | 2.44E-17 | 2.44E-17 | 2.44E-17 | 2.44E-17 | 2.44E-17 | 2.44E-17 | 2.44E-17 | 2.44E-17 | 2.44E-17 | 2.44E-17 |
| MN | 58 | 0.00E+00 | 8.23E-20 | 8.23E-20 | 8.23E-20 | 8.23E-20 | 8.23E-20 | 8.23E-20 | 8.23E-20 | 8.23E-20 | 8.23E-20 | 8.23E-20 |
| FE | 52 | 0.00E+00 | 1.11E-14 | 1.11E-14 | 1.11E-14 | 1.11E-14 | 1.11E-14 | 1.11E-14 | 1.11E-14 | 1.11E-14 | 1.11E-14 | 1.11E-14 |
| FE | 53 | 0.00E+00 | 1.21E-15 | 1.21E-15 | 1.21E-15 | 1.21E-15 | 1.21E-15 | 1.21E-15 | 1.21E-15 | 1.21E-15 | 1.21E-15 | 1.21E-15 |
| FE | 54 | 0.00E+00 | 1.07E-10 | 2.17E-10 | 3.26E-10 | 4.33E-10 | 8.68E-10 | 2.17E-09 | 4.33E-09 | 6.50E-09 | 8.68E-09 | 1.30E-08 |
| **FE** | **55** | **0.00E+00** | **4.09E-10** | **8.05E-10** | **1.17E-09** | **1.51E-09** | **2.68E-09** | **4.82E-09** | **6.14E-09** | **6.50E-09** | **6.60E-09** | **6.64E-09** |
| FE | 56 | 0.00E+00 | 1.47E-10 | 3.01E-10 | 4.53E-10 | 6.03E-10 | 1.21E-09 | 3.05E-09 | 6.09E-09 | 9.15E-09 | 1.22E-08 | 1.83E-08 |
| FE | 57 | 0.00E+00 | 3.85E-10 | 7.82E-10 | 1.17E-09 | 1.56E-09 | 3.12E-09 | 7.82E-09 | 1.56E-08 | 2.34E-08 | 3.12E-08 | 4.68E-08 |
| FE | 58 | 0.00E+00 | 8.97E-12 | 1.82E-11 | 2.73E-11 | 3.63E-11 | 7.28E-11 | 1.82E-10 | 3.63E-10 | 5.45E-10 | 7.28E-10 | 1.09E-09 |
| FE | 59 | 0.00E+00 | 9.65E-13 | 1.21E-12 | 1.26E-12 | 1.28E-12 | 1.28E-12 | 1.28E-12 | 1.28E-12 | 1.28E-12 | 1.28E-12 | 1.28E-12 |
| CO | 54 | 0.00E+00 | 1.44E-20 | 1.44E-20 | 1.44E-20 | 1.44E-20 | 1.44E-20 | 1.44E-20 | 1.44E-20 | 1.44E-20 | 1.44E-20 | 1.44E-20 |
| CO | 55 | 0.00E+00 | 1.89E-14 | 1.89E-14 | 1.89E-14 | 1.89E-14 | 1.89E-14 | 1.89E-14 | 1.89E-14 | 1.89E-14 | 1.89E-14 | 1.89E-14 |
| CO | 56 | 0.00E+00 | 3.06E-12 | 4.47E-12 | 5.09E-12 | 5.37E-12 | 5.58E-12 | 5.59E-12 | 5.59E-12 | 5.59E-12 | 5.59E-12 | 5.59E-12 |

| Table A.4. (continued) | | | | | | | | | | | | |
|---|---|---|---|---|---|---|---|---|---|---|---|---|
| Proton beam energy: 1 GeV | | | | | | | Operational line loss assumption: 1 nA/m (continuous) | | | | | |
| Nuclide masses integrated over the material zone volume in the HETC & MCNP calculational model | | | | | | | | | | | | |
| Nuclide concentration | | Time (s) | 7.88E+06 | 1.58E+07 | 2.37E+07 | 3.15E+07 | 6.31E+07 | 1.58E+08 | 3.15E+08 | 4.73E+08 | 6.31E+08 | 9.46E+08 |
| (gram-atoms) | | Initial | 3 months | 6 months | 9 months | 1 year | 2 years | 5 years | 10 years | 15 years | 20 years | 30 years |
| CO | 59 | 0.00E+00 | 8.28E-13 | 2.44E-12 | 4.20E-12 | 5.98E-12 | 1.33E-11 | 3.64E-11 | 7.39E-11 | 1.12E-10 | 1.49E-10 | 2.23E-10 |
| Total | | 0.00E+00 | 5.29E-07 | 1.07E-06 | 1.61E-06 | 2.14E-06 | 4.29E-06 | 1.08E-05 | 2.14E-05 | 3.22E-05 | 4.29E-05 | 6.44E-05 |

| Table A.5. SNS nuclide production during normal proton beam operation: earth berm Zone 1 | | | | | | | | | | | | |
|---|---|---|---|---|---|---|---|---|---|---|---|---|
| Proton beam energy: 1 GeV | | | | | | | Operational line loss assumption: 1 nA/m (continuous) | | | | | |
| Nuclide masses integrated over the material zone volume in the HETC & MCNP calculational model | | | | | | | | | | | | |
| Nuclide concentration | | Time (s) | 7.88E+06 | 1.58E+07 | 2.37E+07 | 3.15E+07 | 6.31E+07 | 1.58E+08 | 3.15E+08 | 4.73E+08 | 6.31E+08 | 9.46E+08 |
| (gram-atoms) | | Initial | 3 months | 6 months | 9 months | 1 year | 2 years | 5 years | 10 years | 15 years | 20 years | 30 years |
| H | 1 | 0.00E+00 | 4.69E-08 | 9.52E-08 | 1.43E-07 | 1.90E-07 | 3.80E-07 | 9.52E-07 | 1.90E-06 | 2.85E-06 | 3.80E-06 | 5.70E-06 |
| H | 2 | 0.00E+00 | 1.39E-09 | 2.82E-09 | 4.23E-09 | 5.62E-09 | 1.13E-08 | 2.82E-08 | 5.62E-08 | 8.45E-08 | 1.13E-07 | 1.69E-07 |
| **H** | **3** | **0.00E+00** | **1.09E-09** | **2.20E-09** | **3.27E-09** | **4.32E-09** | **8.41E-09** | **1.94E-08** | **3.39E-08** | **4.50E-08** | **5.33E-08** | **6.43E-08** |
| HE | 3 | 0.00E+00 | 2.13E-10 | 4.49E-10 | 6.97E-10 | 9.56E-10 | 2.15E-09 | 7.05E-09 | 1.88E-08 | 3.42E-08 | 5.23E-08 | 9.40E-08 |
| HE | 4 | 0.00E+00 | 1.07E-08 | 2.18E-08 | 3.27E-08 | 4.34E-08 | 8.70E-08 | 2.18E-07 | 4.34E-07 | 6.52E-07 | 8.70E-07 | 1.30E-06 |
| LI | 6 | 0.00E+00 | 2.00E-10 | 4.06E-10 | 6.10E-10 | 8.10E-10 | 1.62E-09 | 4.06E-09 | 8.10E-09 | 1.22E-08 | 1.62E-08 | 2.43E-08 |
| LI | 7 | 0.00E+00 | 1.52E-11 | 3.33E-11 | 5.19E-11 | 7.04E-11 | 1.46E-10 | 3.77E-10 | 7.57E-10 | 1.14E-09 | 1.52E-09 | 2.28E-09 |
| LI | 8 | 0.00E+00 | 3.14E-19 | 3.14E-19 | 3.14E-19 | 3.14E-19 | 3.14E-19 | 3.14E-19 | 3.14E-19 | 3.14E-19 | 3.14E-19 | 3.14E-19 |
| BE | 7 | 0.00E+00 | 3.33E-12 | 4.38E-12 | 4.69E-12 | 4.78E-12 | 4.82E-12 | 4.82E-12 | 4.82E-12 | 4.82E-12 | 4.82E-12 | 4.82E-12 |
| BE | 9 | 0.00E+00 | 4.36E-11 | 8.85E-11 | 1.33E-10 | 1.76E-10 | 3.53E-10 | 8.85E-10 | 1.76E-09 | 2.65E-09 | 3.53E-09 | 5.30E-09 |
| **BE** | **10** | **0.00E+00** | **6.09E-12** | **1.24E-11** | **1.86E-11** | **2.47E-11** | **4.94E-11** | **1.24E-10** | **2.47E-10** | **3.71E-10** | **4.94E-10** | **7.41E-10** |
| BE | 11 | 0.00E+00 | 4.07E-18 | 4.07E-18 | 4.07E-18 | 4.07E-18 | 4.07E-18 | 4.07E-18 | 4.07E-18 | 4.07E-18 | 4.07E-18 | 4.07E-18 |
| B | 10 | 0.00E+00 | 3.30E-10 | 6.70E-10 | 1.00E-09 | 1.34E-09 | 2.67E-09 | 6.70E-09 | 1.34E-08 | 2.00E-08 | 2.67E-08 | 4.01E-08 |
| B | 11 | 0.00E+00 | 4.16E-10 | 8.46E-10 | 1.27E-09 | 1.69E-09 | 3.38E-09 | 8.46E-09 | 1.69E-08 | 2.53E-08 | 3.38E-08 | 5.06E-08 |
| B | 12 | 0.00E+00 | 2.00E-19 | 2.00E-19 | 2.00E-19 | 2.00E-19 | 2.00E-19 | 2.00E-19 | 2.00E-19 | 2.00E-19 | 2.00E-19 | 2.00E-19 |
| B | 13 | 0.00E+00 | 3.00E-20 | 3.00E-20 | 3.00E-20 | 3.00E-20 | 3.00E-20 | 3.00E-20 | 3.00E-20 | 3.00E-20 | 3.00E-20 | 3.00E-20 |
| C | 10 | 0.00E+00 | 8.60E-18 | 8.60E-18 | 8.60E-18 | 8.60E-18 | 8.60E-18 | 8.60E-18 | 8.60E-18 | 8.60E-18 | 8.60E-18 | 8.60E-18 |
| C | 11 | 0.00E+00 | 2.74E-14 | 2.74E-14 | 2.74E-14 | 2.74E-14 | 2.74E-14 | 2.74E-14 | 2.74E-14 | 2.74E-14 | 2.74E-14 | 2.74E-14 |
| C | 12 | 0.00E+00 | 5.84E-09 | 1.19E-08 | 1.78E-08 | 2.36E-08 | 4.73E-08 | 1.19E-07 | 2.36E-07 | 3.55E-07 | 4.73E-07 | 7.10E-07 |
| C | 13 | 0.00E+00 | 4.48E-09 | 9.10E-09 | 1.37E-08 | 1.82E-08 | 3.64E-08 | 9.10E-08 | 1.82E-07 | 2.73E-07 | 3.64E-07 | 5.45E-07 |
| **C** | **14** | **0.00E+00** | **5.86E-10** | **1.19E-09** | **1.79E-09** | **2.37E-09** | **4.75E-09** | **1.19E-08** | **2.37E-08** | **3.56E-08** | **4.75E-08** | **7.11E-08** |
| N | 13 | 0.00E+00 | 5.21E-14 | 5.21E-14 | 5.21E-14 | 5.21E-14 | 5.21E-14 | 5.21E-14 | 5.21E-14 | 5.21E-14 | 5.21E-14 | 5.21E-14 |
| N | 14 | 0.00E+00 | 5.77E-09 | 1.17E-08 | 1.76E-08 | 2.34E-08 | 4.68E-08 | 1.17E-07 | 2.34E-07 | 3.51E-07 | 4.68E-07 | 7.02E-07 |
| N | 15 | 0.00E+00 | 8.58E-09 | 1.74E-08 | 2.61E-08 | 3.47E-08 | 6.96E-08 | 1.74E-07 | 3.47E-07 | 5.22E-07 | 6.96E-07 | 1.04E-06 |
| N | 16 | 0.00E+00 | 6.26E-16 | 6.26E-16 | 6.26E-16 | 6.26E-16 | 6.26E-16 | 6.26E-16 | 6.26E-16 | 6.26E-16 | 6.26E-16 | 6.26E-16 |
| N | 17 | 0.00E+00 | 9.17E-18 | 9.17E-18 | 9.17E-18 | 9.17E-18 | 9.17E-18 | 9.17E-18 | 9.17E-18 | 9.17E-18 | 9.17E-18 | 9.17E-18 |
| N | 18 | 0.00E+00 | 1.02E-19 | 1.02E-19 | 1.02E-19 | 1.02E-19 | 1.02E-19 | 1.02E-19 | 1.02E-19 | 1.02E-19 | 1.02E-19 | 1.02E-19 |
| O | 14 | 0.00E+00 | 7.38E-16 | 7.38E-16 | 7.38E-16 | 7.38E-16 | 7.38E-16 | 7.38E-16 | 7.38E-16 | 7.38E-16 | 7.38E-16 | 7.38E-16 |
| O | 15 | 0.00E+00 | 4.31E-14 | 4.31E-14 | 4.31E-14 | 4.31E-14 | 4.31E-14 | 4.31E-14 | 4.31E-14 | 4.31E-14 | 4.31E-14 | 4.31E-14 |
| O | 16 | 0.00E+00 | 2.73E-09 | 5.55E-09 | 8.32E-09 | 1.11E-08 | 2.21E-08 | 5.55E-08 | 1.11E-07 | 1.66E-07 | 2.21E-07 | 3.32E-07 |
| O | 17 | 0.00E+00 | 3.12E-10 | 6.33E-10 | 9.49E-10 | 1.26E-09 | 2.53E-09 | 6.33E-09 | 1.26E-08 | 1.89E-08 | 2.53E-08 | 3.79E-08 |
| O | 18 | 0.00E+00 | 8.67E-11 | 1.76E-10 | 2.64E-10 | 3.51E-10 | 7.04E-10 | 1.76E-09 | 3.51E-09 | 5.27E-09 | 7.04E-09 | 1.05E-08 |
| O | 19 | 0.00E+00 | 1.40E-17 | 1.40E-17 | 1.40E-17 | 1.40E-17 | 1.40E-17 | 1.40E-17 | 1.40E-17 | 1.40E-17 | 1.40E-17 | 1.40E-17 |

**Table A.5. (continued)**

| Proton beam energy: 1 GeV | | | | | | | Operational line loss assumption: 1 nA/m (continuous) | | | | | |
|---|---|---|---|---|---|---|---|---|---|---|---|---|
| Nuclide masses integrated over the material zone volume in the HETC & MCNP calculational model | | | | | | | | | | | | |
| Nuclide concentration | | Time (s) | 7.88E+06 | 1.58E+07 | 2.37E+07 | 3.15E+07 | 6.31E+07 | 1.58E+08 | 3.15E+08 | 4.73E+08 | 6.31E+08 | 9.46E+08 |
| (gram-atoms) | | Initial | 3 months | 6 months | 9 months | 1 year | 2 years | 5 years | 10 years | 15 years | 20 years | 30 years |
| F | 17 | 0.00E+00 | 1.93E-17 | 1.93E-17 | 1.93E-17 | 1.93E-17 | 1.93E-17 | 1.93E-17 | 1.93E-17 | 1.93E-17 | 1.93E-17 | 1.93E-17 |
| F | 18 | 0.00E+00 | 9.20E-14 | 9.20E-14 | 9.20E-14 | 9.20E-14 | 9.20E-14 | 9.20E-14 | 9.20E-14 | 9.20E-14 | 9.20E-14 | 9.20E-14 |
| F | 19 | 0.00E+00 | 8.09E-11 | 1.64E-10 | 2.47E-10 | 3.28E-10 | 6.56E-10 | 1.64E-09 | 3.28E-09 | 4.92E-09 | 6.56E-09 | 9.84E-09 |
| F | 20 | 0.00E+00 | 1.60E-17 | 1.60E-17 | 1.60E-17 | 1.60E-17 | 1.60E-17 | 1.60E-17 | 1.60E-17 | 1.60E-17 | 1.60E-17 | 1.60E-17 |
| F | 21 | 0.00E+00 | 6.53E-19 | 6.53E-19 | 6.53E-19 | 6.53E-19 | 6.53E-19 | 6.53E-19 | 6.53E-19 | 6.53E-19 | 6.53E-19 | 6.53E-19 |
| NE | 19 | 0.00E+00 | 2.58E-17 | 2.58E-17 | 2.58E-17 | 2.58E-17 | 2.58E-17 | 2.58E-17 | 2.58E-17 | 2.58E-17 | 2.58E-17 | 2.58E-17 |
| NE | 20 | 0.00E+00 | 1.93E-10 | 3.91E-10 | 5.87E-10 | 7.80E-10 | 1.56E-09 | 3.91E-09 | 7.80E-09 | 1.17E-08 | 1.56E-08 | 2.34E-08 |
| NE | 21 | 0.00E+00 | 6.95E-11 | 1.41E-10 | 2.12E-10 | 2.81E-10 | 5.64E-10 | 1.41E-09 | 2.81E-09 | 4.23E-09 | 5.64E-09 | 8.45E-09 |
| NE | 22 | 0.00E+00 | 4.64E-11 | 1.06E-10 | 1.75E-10 | 2.53E-10 | 6.56E-10 | 2.45E-09 | 6.37E-09 | 1.07E-08 | 1.51E-08 | 2.41E-08 |
| NE | 23 | 0.00E+00 | 4.54E-17 | 4.54E-17 | 4.54E-17 | 4.54E-17 | 4.54E-17 | 4.54E-17 | 4.54E-17 | 4.54E-17 | 4.54E-17 | 4.54E-17 |
| NE | 24 | 0.00E+00 | 4.66E-17 | 4.66E-17 | 4.66E-17 | 4.66E-17 | 4.66E-17 | 4.66E-17 | 4.66E-17 | 4.66E-17 | 4.66E-17 | 4.66E-17 |
| NE | 25 | 0.00E+00 | 4.51E-20 | 4.51E-20 | 4.51E-20 | 4.51E-20 | 4.51E-20 | 4.51E-20 | 4.51E-20 | 4.51E-20 | 4.51E-20 | 4.51E-20 |
| NA | 21 | 0.00E+00 | 1.35E-17 | 1.35E-17 | 1.35E-17 | 1.35E-17 | 1.35E-17 | 1.35E-17 | 1.35E-17 | 1.35E-17 | 1.35E-17 | 1.35E-17 |
| **NA** | **22** | **0.00E+00** | **1.74E-10** | **3.42E-10** | **4.97E-10** | **6.40E-10** | **1.13E-09** | **2.03E-09** | **2.56E-09** | **2.71E-09** | **2.75E-09** | **2.76E-09** |
| NA | 23 | 0.00E+00 | 8.21E-10 | 1.67E-09 | 2.50E-09 | 3.32E-09 | 6.66E-09 | 1.67E-08 | 3.32E-08 | 4.99E-08 | 6.66E-08 | 9.98E-08 |
| NA | 24 | 0.00E+00 | 1.66E-12 | 1.66E-12 | 1.66E-12 | 1.66E-12 | 1.66E-12 | 1.66E-12 | 1.66E-12 | 1.66E-12 | 1.66E-12 | 1.66E-12 |
| NA | 25 | 0.00E+00 | 5.06E-16 | 5.06E-16 | 5.06E-16 | 5.06E-16 | 5.06E-16 | 5.06E-16 | 5.06E-16 | 5.06E-16 | 5.06E-16 | 5.06E-16 |
| NA | 26 | 0.00E+00 | 1.68E-18 | 1.68E-18 | 1.68E-18 | 1.68E-18 | 1.68E-18 | 1.68E-18 | 1.68E-18 | 1.68E-18 | 1.68E-18 | 1.68E-18 |
| MG | 23 | 0.00E+00 | 3.85E-17 | 3.85E-17 | 3.85E-17 | 3.85E-17 | 3.85E-17 | 3.85E-17 | 3.85E-17 | 3.85E-17 | 3.85E-17 | 3.85E-17 |
| MG | 24 | 0.00E+00 | 2.58E-09 | 5.25E-09 | 7.87E-09 | 1.05E-08 | 2.09E-08 | 5.24E-08 | 1.05E-07 | 1.57E-07 | 2.09E-07 | 3.14E-07 |
| MG | 25 | 0.00E+00 | 1.47E-09 | 2.99E-09 | 4.48E-09 | 5.95E-09 | 1.19E-08 | 2.99E-08 | 5.95E-08 | 8.94E-08 | 1.19E-07 | 1.79E-07 |
| MG | 26 | 0.00E+00 | 1.35E-09 | 2.74E-09 | 4.11E-09 | 5.46E-09 | 1.09E-08 | 2.74E-08 | 5.46E-08 | 8.20E-08 | 1.09E-07 | 1.64E-07 |
| MG | 27 | 0.00E+00 | 2.66E-14 | 2.66E-14 | 2.66E-14 | 2.66E-14 | 2.66E-14 | 2.66E-14 | 2.66E-14 | 2.66E-14 | 2.66E-14 | 2.66E-14 |
| AL | 24 | 0.00E+00 | 3.03E-19 | 3.03E-19 | 3.03E-19 | 3.03E-19 | 3.03E-19 | 3.03E-19 | 3.03E-19 | 3.03E-19 | 3.03E-19 | 3.03E-19 |
| AL | 25 | 0.00E+00 | 6.50E-17 | 6.50E-17 | 6.50E-17 | 6.50E-17 | 6.50E-17 | 6.50E-17 | 6.50E-17 | 6.50E-17 | 6.50E-17 | 6.50E-17 |
| **AL** | **26** | **0.00E+00** | **1.62E-09** | **3.30E-09** | **4.95E-09** | **6.58E-09** | **1.32E-08** | **3.30E-08** | **6.58E-08** | **9.88E-08** | **1.32E-07** | **1.98E-07** |
| AL | 27 | 0.00E+00 | 4.63E-09 | 9.40E-09 | 1.41E-08 | 1.87E-08 | 3.75E-08 | 9.40E-08 | 1.87E-07 | 2.81E-07 | 3.75E-07 | 5.63E-07 |
| AL | 28 | 0.00E+00 | 2.83E-14 | 2.83E-14 | 2.83E-14 | 2.83E-14 | 2.83E-14 | 2.83E-14 | 2.83E-14 | 2.83E-14 | 2.83E-14 | 2.83E-14 |
| AL | 29 | 0.00E+00 | 5.50E-15 | 5.50E-15 | 5.50E-15 | 5.50E-15 | 5.50E-15 | 5.50E-15 | 5.50E-15 | 5.50E-15 | 5.50E-15 | 5.50E-15 |
| AL | 30 | 0.00E+00 | 6.20E-18 | 6.20E-18 | 6.20E-18 | 6.20E-18 | 6.20E-18 | 6.20E-18 | 6.20E-18 | 6.20E-18 | 6.20E-18 | 6.20E-18 |
| SI | 26 | 0.00E+00 | 4.96E-18 | 4.96E-18 | 4.96E-18 | 4.96E-18 | 4.96E-18 | 4.96E-18 | 4.96E-18 | 4.96E-18 | 4.96E-18 | 4.96E-18 |
| SI | 27 | 0.00E+00 | 3.75E-16 | 3.75E-16 | 3.75E-16 | 3.75E-16 | 3.75E-16 | 3.75E-16 | 3.75E-16 | 3.75E-16 | 3.75E-16 | 3.75E-16 |
| SI | 28 | 0.00E+00 | 2.01E-09 | 4.09E-09 | 6.13E-09 | 8.15E-09 | 1.63E-08 | 4.09E-08 | 8.15E-08 | 1.22E-07 | 1.63E-07 | 2.45E-07 |
| SI | 29 | 0.00E+00 | 3.19E-10 | 6.47E-10 | 9.71E-10 | 1.29E-09 | 2.59E-09 | 6.47E-09 | 1.29E-08 | 1.94E-08 | 2.59E-08 | 3.88E-08 |

**Table A.5. (continued)**

| Proton beam energy: 1 GeV | | | | | | | Operational line loss assumption: 1 nA/m (continuous) | | | | | |
|---|---|---|---|---|---|---|---|---|---|---|---|---|
| Nuclide masses integrated over the material zone volume in the HETC & MCNP calculational model | | | | | | | | | | | | |
| Nuclide concentration | | Time (s) | 7.88E+06 | 1.58E+07 | 2.37E+07 | 3.15E+07 | 6.31E+07 | 1.58E+08 | 3.15E+08 | 4.73E+08 | 6.31E+08 | 9.46E+08 |
| (gram-atoms) | | Initial | 3 months | 6 months | 9 months | 1 year | 2 years | 5 years | 10 years | 15 years | 20 years | 30 years |
| SI | 30 | 0.00E+00 | 5.77E-11 | 1.17E-10 | 1.76E-10 | 2.33E-10 | 4.68E-10 | 1.17E-09 | 2.33E-09 | 3.51E-09 | 4.68E-09 | 7.01E-09 |
| SI | 31 | 0.00E+00 | 1.51E-14 | 1.51E-14 | 1.51E-14 | 1.51E-14 | 1.51E-14 | 1.51E-14 | 1.51E-14 | 1.51E-14 | 1.51E-14 | 1.51E-14 |
| P | 31 | 0.00E+00 | 1.43E-11 | 2.90E-11 | 4.36E-11 | 5.79E-11 | 1.16E-10 | 2.90E-10 | 5.79E-10 | 8.69E-10 | 1.16E-09 | 1.74E-09 |
| P | 32 | 0.00E+00 | 7.38E-13 | 7.47E-13 | 7.47E-13 | 7.47E-13 | 7.47E-13 | 7.47E-13 | 7.47E-13 | 7.47E-13 | 7.47E-13 | 7.47E-13 |
| P | 33 | 0.00E+00 | 1.48E-13 | 1.61E-13 | 1.62E-13 | 1.62E-13 | 1.62E-13 | 1.62E-13 | 1.62E-13 | 1.62E-13 | 1.62E-13 | 1.62E-13 |
| S | 32 | 0.00E+00 | 2.93E-12 | 6.70E-12 | 1.04E-11 | 1.41E-11 | 2.97E-11 | 7.52E-11 | 1.50E-10 | 2.25E-10 | 3.00E-10 | 4.50E-10 |
| S | 33 | 0.00E+00 | 3.89E-12 | 8.04E-12 | 1.21E-11 | 1.62E-11 | 3.27E-11 | 8.21E-11 | 1.64E-10 | 2.46E-10 | 3.28E-10 | 4.92E-10 |
| S | 34 | 0.00E+00 | 5.25E-12 | 1.07E-11 | 1.60E-11 | 2.12E-11 | 4.26E-11 | 1.07E-10 | 2.12E-10 | 3.19E-10 | 4.26E-10 | 6.38E-10 |
| S | 35 | 0.00E+00 | 1.16E-12 | 1.74E-12 | 2.01E-12 | 2.15E-12 | 2.27E-12 | 2.28E-12 | 2.28E-12 | 2.28E-12 | 2.28E-12 | 2.28E-12 |
| S | 36 | 0.00E+00 | 4.04E-13 | 8.20E-13 | 1.23E-12 | 1.63E-12 | 3.27E-12 | 8.20E-12 | 1.63E-11 | 2.45E-11 | 3.27E-11 | 4.91E-11 |
| CL | 35 | 0.00E+00 | 1.74E-11 | 3.59E-11 | 5.44E-11 | 7.28E-11 | 1.48E-10 | 3.76E-10 | 7.52E-10 | 1.13E-09 | 1.51E-09 | 2.26E-09 |
| **CL** | **36** | **0.00E+00** | **2.59E-11** | **5.26E-11** | **7.89E-11** | **1.05E-10** | **2.10E-10** | **5.26E-10** | **1.05E-09** | **1.57E-09** | **2.10E-09** | **3.15E-09** |
| CL | 37 | 0.00E+00 | 2.39E-11 | 6.23E-11 | 1.02E-10 | 1.42E-10 | 3.23E-10 | 8.29E-10 | 1.65E-09 | 2.48E-09 | 3.31E-09 | 4.94E-09 |
| CL | 38 | 0.00E+00 | 2.76E-16 | 2.76E-16 | 2.76E-16 | 2.76E-16 | 2.76E-16 | 2.76E-16 | 2.76E-16 | 2.76E-16 | 2.76E-16 | 2.76E-16 |
| CL | 39 | 0.00E+00 | 9.94E-18 | 9.94E-18 | 9.94E-18 | 9.94E-18 | 9.94E-18 | 9.94E-18 | 9.94E-18 | 9.94E-18 | 9.94E-18 | 9.94E-18 |
| CL | 40 | 0.00E+00 | 7.37E-20 | 7.37E-20 | 7.37E-20 | 7.37E-20 | 7.37E-20 | 7.37E-20 | 7.37E-20 | 7.37E-20 | 7.37E-20 | 7.37E-20 |
| AR | 36 | 0.00E+00 | 3.71E-12 | 7.53E-12 | 1.13E-11 | 1.50E-11 | 3.01E-11 | 7.53E-11 | 1.50E-10 | 2.25E-10 | 3.01E-10 | 4.51E-10 |
| AR | 37 | 0.00E+00 | 1.59E-11 | 1.87E-11 | 1.91E-11 | 1.92E-11 | 1.92E-11 | 1.92E-11 | 1.92E-11 | 1.92E-11 | 1.92E-11 | 1.92E-11 |
| AR | 38 | 0.00E+00 | 8.54E-11 | 1.73E-10 | 2.60E-10 | 3.46E-10 | 6.92E-10 | 1.73E-09 | 3.46E-09 | 5.19E-09 | 6.92E-09 | 1.04E-08 |
| **AR** | **39** | **0.00E+00** | **4.67E-11** | **9.47E-11** | **1.42E-10** | **1.89E-10** | **3.78E-10** | **9.42E-10** | **1.87E-09** | **2.78E-09** | **3.69E-09** | **5.46E-09** |
| AR | 40 | 0.00E+00 | 2.51E-12 | 5.09E-12 | 7.63E-12 | 1.01E-11 | 2.03E-11 | 5.09E-11 | 1.01E-10 | 1.52E-10 | 2.03E-10 | 3.05E-10 |
| AR | 41 | 0.00E+00 | 7.66E-16 | 7.66E-16 | 7.66E-16 | 7.66E-16 | 7.66E-16 | 7.66E-16 | 7.66E-16 | 7.66E-16 | 7.66E-16 | 7.66E-16 |
| AR | 42 | 0.00E+00 | 7.44E-18 | 1.51E-17 | 2.26E-17 | 2.99E-17 | 5.93E-17 | 1.44E-16 | 2.72E-16 | 3.89E-16 | 4.94E-16 | 6.73E-16 |
| K | 38 | 0.00E+00 | 1.61E-15 | 1.61E-15 | 1.61E-15 | 1.61E-15 | 1.61E-15 | 1.61E-15 | 1.61E-15 | 1.61E-15 | 1.61E-15 | 1.61E-15 |
| K | 39 | 0.00E+00 | 1.44E-11 | 2.93E-11 | 4.40E-11 | 5.86E-11 | 1.18E-10 | 2.99E-10 | 6.07E-10 | 9.30E-10 | 1.26E-09 | 1.97E-09 |
| **K** | **40** | **0.00E+00** | **2.21E-11** | **4.50E-11** | **6.74E-11** | **8.96E-11** | **1.80E-10** | **4.50E-10** | **8.96E-10** | **1.35E-09** | **1.80E-09** | **2.69E-09** |
| K | 41 | 0.00E+00 | 1.84E-12 | 3.74E-12 | 5.61E-12 | 7.46E-12 | 1.49E-11 | 3.74E-11 | 7.46E-11 | 1.12E-10 | 1.49E-10 | 2.24E-10 |
| K | 42 | 0.00E+00 | 1.53E-14 | 1.53E-14 | 1.53E-14 | 1.53E-14 | 1.53E-14 | 1.53E-14 | 1.53E-14 | 1.53E-14 | 1.53E-14 | 1.53E-14 |
| K | 43 | 0.00E+00 | 7.70E-18 | 7.70E-18 | 7.70E-18 | 7.70E-18 | 7.70E-18 | 7.70E-18 | 7.70E-18 | 7.70E-18 | 7.70E-18 | 7.70E-18 |
| K | 44 | 0.00E+00 | 2.52E-19 | 2.52E-19 | 2.52E-19 | 2.52E-19 | 2.52E-19 | 2.52E-19 | 2.52E-19 | 2.52E-19 | 2.52E-19 | 2.52E-19 |
| CA | 40 | 0.00E+00 | 1.21E-12 | 2.46E-12 | 3.69E-12 | 4.90E-12 | 9.82E-12 | 2.46E-11 | 4.90E-11 | 7.36E-11 | 9.82E-11 | 1.47E-10 |
| **CA** | **41** | **0.00E+00** | **3.32E-12** | **6.74E-12** | **1.01E-11** | **1.34E-11** | **2.69E-11** | **6.74E-11** | **1.34E-10** | **2.02E-10** | **2.69E-10** | **4.04E-10** |
| CA | 42 | 0.00E+00 | 1.12E-11 | 2.27E-11 | 3.40E-11 | 4.52E-11 | 9.06E-11 | 2.27E-10 | 4.52E-10 | 6.78E-10 | 9.05E-10 | 1.36E-09 |
| CA | 43 | 0.00E+00 | 8.19E-12 | 1.66E-11 | 2.50E-11 | 3.32E-11 | 6.65E-11 | 1.66E-10 | 3.32E-10 | 4.98E-10 | 6.65E-10 | 9.96E-10 |

**Table A.5. (continued)**

| Proton beam energy: 1 GeV | | | | | | | Operational line loss assumption: 1 nA/m (continuous) | | | | | |
|---|---|---|---|---|---|---|---|---|---|---|---|---|
| Nuclide masses integrated over the material zone volume in the HETC & MCNP calculational model | | | | | | | | | | | | |
| Nuclide concentration | | Time (s) | 7.88E+06 | 1.58E+07 | 2.37E+07 | 3.15E+07 | 6.31E+07 | 1.58E+08 | 3.15E+08 | 4.73E+08 | 6.31E+08 | 9.46E+08 |
| (gram-atoms) | | Initial | 3 months | 6 months | 9 months | 1 year | 2 years | 5 years | 10 years | 15 years | 20 years | 30 years |
| CA | 44 | 0.00E+00 | 1.98E-11 | 4.02E-11 | 6.03E-11 | 8.01E-11 | 1.60E-10 | 4.02E-10 | 8.01E-10 | 1.20E-09 | 1.61E-09 | 2.41E-09 |
| CA | 45 | 0.00E+00 | 1.29E-12 | 2.19E-12 | 2.79E-12 | 3.20E-12 | 3.89E-12 | 4.08E-12 | 4.09E-12 | 4.09E-12 | 4.09E-12 | 4.09E-12 |
| CA | 46 | 0.00E+00 | 1.64E-12 | 3.32E-12 | 4.98E-12 | 6.62E-12 | 1.33E-11 | 3.32E-11 | 6.62E-11 | 9.95E-11 | 1.33E-10 | 1.99E-10 |
| CA | 47 | 0.00E+00 | 2.68E-15 | 2.68E-15 | 2.68E-15 | 2.68E-15 | 2.68E-15 | 2.68E-15 | 2.68E-15 | 2.68E-15 | 2.68E-15 | 2.68E-15 |
| CA | 48 | 0.00E+00 | 1.56E-15 | 3.16E-15 | 4.74E-15 | 6.30E-15 | 1.26E-14 | 3.16E-14 | 6.30E-14 | 9.45E-14 | 1.26E-13 | 1.89E-13 |
| CA | 49 | 0.00E+00 | 1.44E-20 | 1.44E-20 | 1.44E-20 | 1.44E-20 | 1.44E-20 | 1.44E-20 | 1.44E-20 | 1.44E-20 | 1.44E-20 | 1.44E-20 |
| SC | 42 | 0.00E+00 | 1.02E-19 | 1.02E-19 | 1.02E-19 | 1.02E-19 | 1.02E-19 | 1.02E-19 | 1.02E-19 | 1.02E-19 | 1.02E-19 | 1.02E-19 |
| SC | 43 | 0.00E+00 | 6.28E-15 | 6.28E-15 | 6.28E-15 | 6.28E-15 | 6.28E-15 | 6.28E-15 | 6.28E-15 | 6.28E-15 | 6.28E-15 | 6.28E-15 |
| SC | 44 | 0.00E+00 | 4.20E-14 | 4.20E-14 | 4.20E-14 | 4.21E-14 | 4.21E-14 | 4.21E-14 | 4.22E-14 | 4.22E-14 | 4.23E-14 | 4.24E-14 |
| SC | 45 | 0.00E+00 | 1.30E-11 | 2.68E-11 | 4.06E-11 | 5.45E-11 | 1.12E-10 | 2.85E-10 | 5.77E-10 | 8.70E-10 | 1.16E-09 | 1.74E-09 |
| SC | 46 | 0.00E+00 | 6.32E-12 | 9.38E-12 | 1.08E-11 | 1.14E-11 | 1.20E-11 | 1.20E-11 | 1.20E-11 | 1.20E-11 | 1.20E-11 | 1.20E-11 |
| SC | 47 | 0.00E+00 | 3.00E-13 | 3.00E-13 | 3.00E-13 | 3.00E-13 | 3.00E-13 | 3.00E-13 | 3.00E-13 | 3.00E-13 | 3.00E-13 | 3.00E-13 |
| SC | 48 | 0.00E+00 | 8.05E-14 | 8.05E-14 | 8.05E-14 | 8.05E-14 | 8.05E-14 | 8.05E-14 | 8.05E-14 | 8.05E-14 | 8.05E-14 | 8.05E-14 |
| SC | 49 | 0.00E+00 | 2.76E-16 | 2.76E-16 | 2.76E-16 | 2.76E-16 | 2.76E-16 | 2.76E-16 | 2.76E-16 | 2.76E-16 | 2.76E-16 | 2.76E-16 |
| SC | 50 | 0.00E+00 | 9.17E-20 | 9.17E-20 | 9.17E-20 | 9.17E-20 | 9.17E-20 | 9.17E-20 | 9.17E-20 | 9.17E-20 | 9.17E-20 | 9.17E-20 |
| TI | 44 | 0.00E+00 | 4.03E-13 | 8.17E-13 | 1.22E-12 | 1.62E-12 | 3.23E-12 | 7.91E-12 | 1.52E-11 | 2.21E-11 | 2.85E-11 | 3.99E-11 |
| TI | 45 | 0.00E+00 | 4.45E-15 | 4.45E-15 | 4.45E-15 | 4.45E-15 | 4.45E-15 | 4.45E-15 | 4.45E-15 | 4.45E-15 | 4.45E-15 | 4.45E-15 |
| TI | 46 | 0.00E+00 | 1.67E-11 | 3.73E-11 | 5.93E-11 | 8.17E-11 | 1.75E-10 | 4.67E-10 | 9.43E-10 | 1.42E-09 | 1.90E-09 | 2.85E-09 |
| TI | 47 | 0.00E+00 | 2.71E-11 | 5.54E-11 | 8.33E-11 | 1.11E-10 | 2.21E-10 | 5.53E-10 | 1.10E-09 | 1.65E-09 | 2.20E-09 | 3.30E-09 |
| TI | 48 | 0.00E+00 | 2.09E-11 | 4.57E-11 | 7.02E-11 | 9.45E-11 | 1.96E-10 | 4.93E-10 | 9.82E-10 | 1.47E-09 | 1.97E-09 | 2.95E-09 |
| TI | 49 | 0.00E+00 | 9.43E-12 | 2.22E-11 | 3.71E-11 | 5.39E-11 | 1.36E-10 | 4.34E-10 | 9.56E-10 | 1.48E-09 | 2.01E-09 | 3.16E-09 |
| TI | 50 | 0.00E+00 | 1.15E-12 | 2.33E-12 | 3.49E-12 | 4.64E-12 | 9.29E-12 | 2.33E-11 | 4.64E-11 | 6.96E-11 | 9.29E-11 | 1.39E-10 |
| TI | 51 | 0.00E+00 | 3.26E-18 | 3.26E-18 | 3.26E-18 | 3.26E-18 | 3.26E-18 | 3.26E-18 | 3.26E-18 | 3.26E-18 | 3.26E-18 | 3.26E-18 |
| V | 47 | 0.00E+00 | 7.32E-16 | 7.32E-16 | 7.32E-16 | 7.32E-16 | 7.32E-16 | 7.32E-16 | 7.32E-16 | 7.32E-16 | 7.32E-16 | 7.32E-16 |
| V | 48 | 0.00E+00 | 3.22E-12 | 3.29E-12 | 3.29E-12 | 3.29E-12 | 3.29E-12 | 3.29E-12 | 3.29E-12 | 3.29E-12 | 3.29E-12 | 3.29E-12 |
| V | 49 | 0.00E+00 | 1.65E-11 | 3.06E-11 | 4.20E-11 | 5.12E-11 | 7.49E-11 | 9.32E-11 | 9.51E-11 | 9.52E-11 | 9.52E-11 | 9.52E-11 |
| V | 50 | 0.00E+00 | 1.03E-11 | 2.10E-11 | 3.15E-11 | 4.18E-11 | 8.38E-11 | 2.10E-10 | 4.18E-10 | 6.28E-10 | 8.38E-10 | 1.26E-09 |
| V | 51 | 0.00E+00 | 3.54E-11 | 9.10E-11 | 1.48E-10 | 2.04E-10 | 4.54E-10 | 1.16E-09 | 2.31E-09 | 3.47E-09 | 4.64E-09 | 6.93E-09 |
| V | 52 | 0.00E+00 | 4.83E-17 | 4.83E-17 | 4.83E-17 | 4.83E-17 | 4.83E-17 | 4.83E-17 | 4.83E-17 | 4.83E-17 | 4.83E-17 | 4.83E-17 |
| CR | 49 | 0.00E+00 | 2.26E-15 | 2.26E-15 | 2.26E-15 | 2.26E-15 | 2.26E-15 | 2.26E-15 | 2.26E-15 | 2.26E-15 | 2.26E-15 | 2.26E-15 |
| CR | 50 | 0.00E+00 | 2.49E-11 | 5.05E-11 | 7.57E-11 | 1.01E-10 | 2.02E-10 | 5.05E-10 | 1.01E-09 | 1.51E-09 | 2.02E-09 | 3.02E-09 |
| CR | 51 | 0.00E+00 | 2.06E-11 | 2.28E-11 | 2.30E-11 | 2.30E-11 | 2.30E-11 | 2.30E-11 | 2.30E-11 | 2.30E-11 | 2.30E-11 | 2.30E-11 |
| CR | 52 | 0.00E+00 | 8.67E-11 | 1.81E-10 | 2.73E-10 | 3.64E-10 | 7.21E-10 | 1.78E-09 | 3.54E-09 | 5.30E-09 | 7.07E-09 | 1.06E-08 |
| CR | 53 | 0.00E+00 | 2.34E-11 | 4.75E-11 | 7.12E-11 | 9.47E-11 | 1.90E-10 | 4.75E-10 | 9.47E-10 | 1.42E-09 | 1.90E-09 | 2.84E-09 |

**Table A.5. (continued)**

| Proton beam energy: 1 GeV | | | | | | | Operational line loss assumption: 1 nA/m (continuous) | | | | | |
|---|---|---|---|---|---|---|---|---|---|---|---|---|
| Nuclide masses integrated over the material zone volume in the HETC & MCNP calculational model | | | | | | | | | | | | |
| Nuclide concentration | | Time (s) | 7.88E+06 | 1.58E+07 | 2.37E+07 | 3.15E+07 | 6.31E+07 | 1.58E+08 | 3.15E+08 | 4.73E+08 | 6.31E+08 | 9.46E+08 |
| (gram-atoms) | | Initial | 3 months | 6 months | 9 months | 1 year | 2 years | 5 years | 10 years | 15 years | 20 years | 30 years |
| CR | 54 | 0.00E+00 | 1.93E-11 | 6.11E-11 | 1.20E-10 | 1.92E-10 | 5.81E-10 | 2.11E-09 | 4.81E-09 | 7.54E-09 | 1.03E-08 | 1.63E-08 |
| CR | 55 | 0.00E+00 | 1.59E-18 | 1.59E-18 | 1.59E-18 | 1.59E-18 | 1.59E-18 | 1.59E-18 | 1.59E-18 | 1.59E-18 | 1.59E-18 | 1.59E-18 |
| CR | 56 | 0.00E+00 | 5.09E-19 | 5.09E-19 | 5.09E-19 | 5.09E-19 | 5.09E-19 | 5.09E-19 | 5.09E-19 | 5.09E-19 | 5.09E-19 | 5.09E-19 |
| MN | 50 | 0.00E+00 | 2.12E-20 | 2.12E-20 | 2.12E-20 | 2.12E-20 | 2.12E-20 | 2.12E-20 | 2.12E-20 | 2.12E-20 | 2.12E-20 | 2.12E-20 |
| MN | 51 | 0.00E+00 | 5.19E-15 | 5.19E-15 | 5.19E-15 | 5.19E-15 | 5.19E-15 | 5.19E-15 | 5.19E-15 | 5.19E-15 | 5.19E-15 | 5.19E-15 |
| MN | 52 | 0.00E+00 | 4.40E-12 | 4.40E-12 | 4.40E-12 | 4.40E-12 | 4.40E-12 | 4.40E-12 | 4.40E-12 | 4.40E-12 | 4.40E-12 | 4.40E-12 |
| **MN** | **53** | **0.00E+00** | **1.33E-10** | **2.70E-10** | **4.05E-10** | **5.39E-10** | **1.08E-09** | **2.70E-09** | **5.39E-09** | **8.09E-09** | **1.08E-08** | **1.62E-08** |
| MN | 54 | 0.00E+00 | 1.15E-10 | 2.12E-10 | 2.90E-10 | 3.53E-10 | 5.10E-10 | 6.24E-10 | 6.35E-10 | 6.35E-10 | 6.35E-10 | 6.36E-10 |
| MN | 55 | 0.00E+00 | 1.36E-10 | 2.92E-10 | 4.63E-10 | 6.45E-10 | 1.51E-09 | 5.00E-09 | 1.22E-08 | 2.00E-08 | 2.81E-08 | 4.42E-08 |
| MN | 56 | 0.00E+00 | 6.90E-14 | 6.90E-14 | 6.90E-14 | 6.90E-14 | 6.90E-14 | 6.90E-14 | 6.90E-14 | 6.90E-14 | 6.90E-14 | 6.90E-14 |
| MN | 57 | 0.00E+00 | 1.12E-17 | 1.12E-17 | 1.12E-17 | 1.12E-17 | 1.12E-17 | 1.12E-17 | 1.12E-17 | 1.12E-17 | 1.12E-17 | 1.12E-17 |
| MN | 58 | 0.00E+00 | 3.20E-20 | 3.20E-20 | 3.20E-20 | 3.20E-20 | 3.20E-20 | 3.20E-20 | 3.20E-20 | 3.20E-20 | 3.20E-20 | 3.20E-20 |
| FE | 52 | 0.00E+00 | 4.46E-15 | 4.46E-15 | 4.46E-15 | 4.46E-15 | 4.46E-15 | 4.46E-15 | 4.46E-15 | 4.46E-15 | 4.46E-15 | 4.46E-15 |
| FE | 53 | 0.00E+00 | 9.89E-16 | 9.89E-16 | 9.89E-16 | 9.89E-16 | 9.89E-16 | 9.89E-16 | 9.89E-16 | 9.89E-16 | 9.89E-16 | 9.89E-16 |
| FE | 54 | 0.00E+00 | 7.49E-11 | 1.52E-10 | 2.28E-10 | 3.03E-10 | 6.08E-10 | 1.52E-09 | 3.03E-09 | 4.55E-09 | 6.08E-09 | 9.11E-09 |
| **FE** | **55** | **0.00E+00** | **2.63E-10** | **5.16E-10** | **7.50E-10** | **9.67E-10** | **1.72E-09** | **3.09E-09** | **3.93E-09** | **4.17E-09** | **4.23E-09** | **4.26E-09** |
| FE | 56 | 0.00E+00 | 9.96E-11 | 2.03E-10 | 3.06E-10 | 4.07E-10 | 8.19E-10 | 2.06E-09 | 4.10E-09 | 6.16E-09 | 8.22E-09 | 1.23E-08 |
| FE | 57 | 0.00E+00 | 6.77E-11 | 1.38E-10 | 2.06E-10 | 2.75E-10 | 5.51E-10 | 1.38E-09 | 2.75E-09 | 4.14E-09 | 5.52E-09 | 8.28E-09 |
| FE | 58 | 0.00E+00 | 1.93E-12 | 3.91E-12 | 5.87E-12 | 7.80E-12 | 1.56E-11 | 3.91E-11 | 7.80E-11 | 1.17E-10 | 1.56E-10 | 2.34E-10 |
| FE | 59 | 0.00E+00 | 1.44E-13 | 1.80E-13 | 1.89E-13 | 1.91E-13 | 1.92E-13 | 1.92E-13 | 1.92E-13 | 1.92E-13 | 1.92E-13 | 1.92E-13 |
| CO | 55 | 0.00E+00 | 1.42E-14 | 1.42E-14 | 1.42E-14 | 1.42E-14 | 1.42E-14 | 1.42E-14 | 1.42E-14 | 1.42E-14 | 1.42E-14 | 1.42E-14 |
| CO | 56 | 0.00E+00 | 1.67E-12 | 2.44E-12 | 2.78E-12 | 2.93E-12 | 3.05E-12 | 3.06E-12 | 3.06E-12 | 3.06E-12 | 3.06E-12 | 3.06E-12 |
| CO | 57 | 0.00E+00 | 3.61E-13 | 6.55E-13 | 8.84E-13 | 1.06E-12 | 1.48E-12 | 1.74E-12 | 1.76E-12 | 1.76E-12 | 1.76E-12 | 1.76E-12 |
| CO | 59 | 0.00E+00 | 1.24E-13 | 3.64E-13 | 6.28E-13 | 8.95E-13 | 1.98E-12 | 5.45E-12 | 1.11E-11 | 1.67E-11 | 2.23E-11 | 3.34E-11 |
| NI | 60 | 0.00E+00 | 1.59E-14 | 3.22E-14 | 4.83E-14 | 6.42E-14 | 1.29E-13 | 3.22E-13 | 6.42E-13 | 9.64E-13 | 1.29E-12 | 1.93E-12 |
| NI | 61 | 0.00E+00 | 1.01E-14 | 2.06E-14 | 3.09E-14 | 4.10E-14 | 8.22E-14 | 2.06E-13 | 4.10E-13 | 6.16E-13 | 8.22E-13 | 1.23E-12 |
| NI | 62 | 0.00E+00 | 1.49E-15 | 3.04E-15 | 4.55E-15 | 6.05E-15 | 1.21E-14 | 3.04E-14 | 6.05E-14 | 9.09E-14 | 1.21E-13 | 1.82E-13 |
| NI | 63 | 0.00E+00 | 6.38E-15 | 1.29E-14 | 1.94E-14 | 2.58E-14 | 5.14E-14 | 1.27E-13 | 2.50E-13 | 3.69E-13 | 4.83E-13 | 7.01E-13 |
| NI | 64 | 0.00E+00 | 1.49E-13 | 3.04E-13 | 4.57E-13 | 6.08E-13 | 1.21E-12 | 3.04E-12 | 6.05E-12 | 9.08E-12 | 1.21E-11 | 1.81E-11 |
| NI | 65 | 0.00E+00 | 2.31E-18 | 2.31E-18 | 2.31E-18 | 2.31E-18 | 2.31E-18 | 2.31E-18 | 2.31E-18 | 2.31E-18 | 2.31E-18 | 2.31E-18 |
| NI | 66 | 0.00E+00 | 1.29E-18 | 1.29E-18 | 1.29E-18 | 1.29E-18 | 1.29E-18 | 1.29E-18 | 1.29E-18 | 1.29E-18 | 1.29E-18 | 1.29E-18 |
| CU | 61 | 0.00E+00 | 1.10E-19 | 1.10E-19 | 1.10E-19 | 1.10E-19 | 1.10E-19 | 1.10E-19 | 1.10E-19 | 1.10E-19 | 1.10E-19 | 1.10E-19 |
| CU | 62 | 0.00E+00 | 6.86E-20 | 6.86E-20 | 6.86E-20 | 6.86E-20 | 6.86E-20 | 6.86E-20 | 6.86E-20 | 6.86E-20 | 6.86E-20 | 6.86E-20 |
| CU | 63 | 0.00E+00 | 2.62E-13 | 5.32E-13 | 7.99E-13 | 1.06E-12 | 2.13E-12 | 5.33E-12 | 1.06E-11 | 1.60E-11 | 2.13E-11 | 3.19E-11 |

**Table A.5. (continued)**

| Proton beam energy: 1 GeV | | | | | | | Operational line loss assumption: 1 nA/m (continuous) | | | | | |
|---|---|---|---|---|---|---|---|---|---|---|---|---|
| Nuclide masses integrated over the material zone volume in the HETC & MCNP calculational model | | | | | | | | | | | | |
| Nuclide concentration | | Time (s) | 7.88E+06 | 1.58E+07 | 2.37E+07 | 3.15E+07 | 6.31E+07 | 1.58E+08 | 3.15E+08 | 4.73E+08 | 6.31E+08 | 9.46E+08 |
| (gram-atoms) | | Initial | 3 months | 6 months | 9 months | 1 year | 2 years | 5 years | 10 years | 15 years | 20 years | 30 years |
| CU | 64 | 0.00E+00 | 2.07E-15 | 2.07E-15 | 2.07E-15 | 2.07E-15 | 2.07E-15 | 2.07E-15 | 2.07E-15 | 2.07E-15 | 2.07E-15 | 2.07E-15 |
| CU | 65 | 0.00E+00 | 1.41E-12 | 3.19E-12 | 5.19E-12 | 7.34E-12 | 1.72E-11 | 5.04E-11 | 1.06E-10 | 1.63E-10 | 2.19E-10 | 3.38E-10 |
| CU | 66 | 0.00E+00 | 1.12E-18 | 1.12E-18 | 1.12E-18 | 1.12E-18 | 1.12E-18 | 1.12E-18 | 1.12E-18 | 1.12E-18 | 1.12E-18 | 1.12E-18 |
| CU | 67 | 0.00E+00 | 1.68E-14 | 1.68E-14 | 1.68E-14 | 1.68E-14 | 1.68E-14 | 1.68E-14 | 1.68E-14 | 1.68E-14 | 1.68E-14 | 1.68E-14 |
| ZN | 63 | 0.00E+00 | 4.63E-17 | 4.63E-17 | 4.63E-17 | 4.63E-17 | 4.63E-17 | 4.63E-17 | 4.63E-17 | 4.63E-17 | 4.63E-17 | 4.63E-17 |
| ZN | 64 | 0.00E+00 | 9.69E-14 | 1.98E-13 | 2.97E-13 | 3.95E-13 | 7.89E-13 | 1.97E-12 | 3.93E-12 | 5.90E-12 | 7.86E-12 | 1.18E-11 |
| ZN | 65 | 0.00E+00 | 1.37E-12 | 2.45E-12 | 3.27E-12 | 3.90E-12 | 5.29E-12 | 6.02E-12 | 6.05E-12 | 6.05E-12 | 6.05E-12 | 6.05E-12 |
| ZN | 66 | 0.00E+00 | 4.54E-13 | 9.21E-13 | 1.38E-12 | 1.84E-12 | 3.68E-12 | 9.21E-12 | 1.84E-11 | 2.76E-11 | 3.68E-11 | 5.52E-11 |
| ZN | 67 | 0.00E+00 | 1.49E-12 | 3.03E-12 | 4.56E-12 | 6.07E-12 | 1.21E-11 | 3.03E-11 | 6.03E-11 | 9.05E-11 | 1.21E-10 | 1.81E-10 |
| ZN | 68 | 0.00E+00 | 1.21E-13 | 2.46E-13 | 3.69E-13 | 4.91E-13 | 9.83E-13 | 2.46E-12 | 4.91E-12 | 7.37E-12 | 9.83E-12 | 1.47E-11 |
| ZN | 69 | 0.00E+00 | 3.34E-17 | 3.34E-17 | 3.34E-17 | 3.34E-17 | 3.34E-17 | 3.34E-17 | 3.34E-17 | 3.34E-17 | 3.34E-17 | 3.34E-17 |
| ZN | 70 | 0.00E+00 | 1.33E-17 | 2.70E-17 | 4.06E-17 | 5.39E-17 | 1.08E-16 | 2.70E-16 | 5.39E-16 | 8.10E-16 | 1.08E-15 | 1.62E-15 |
| ZN | 71 | 0.00E+00 | 4.10E-20 | 4.10E-20 | 4.10E-20 | 4.10E-20 | 4.10E-20 | 4.10E-20 | 4.10E-20 | 4.10E-20 | 4.10E-20 | 4.10E-20 |
| GA | 69 | 0.00E+00 | 5.39E-14 | 1.10E-13 | 1.64E-13 | 2.19E-13 | 4.38E-13 | 1.10E-12 | 2.18E-12 | 3.28E-12 | 4.38E-12 | 6.56E-12 |
| GA | 71 | 0.00E+00 | 1.50E-15 | 3.05E-15 | 4.58E-15 | 6.08E-15 | 1.22E-14 | 3.05E-14 | 6.08E-14 | 9.14E-14 | 1.22E-13 | 1.83E-13 |
| SE | 77 | 0.00E+00 | 4.04E-13 | 8.35E-13 | 1.26E-12 | 1.68E-12 | 3.34E-12 | 8.27E-12 | 1.64E-11 | 2.46E-11 | 3.29E-11 | 4.92E-11 |
| BR | 77 | 0.00E+00 | 1.54E-14 | 1.54E-14 | 1.54E-14 | 1.54E-14 | 1.54E-14 | 1.54E-14 | 1.54E-14 | 1.54E-14 | 1.54E-14 | 1.54E-14 |
| BR | 81 | 0.00E+00 | 1.19E-15 | 2.42E-15 | 3.63E-15 | 4.82E-15 | 9.68E-15 | 2.44E-14 | 4.90E-14 | 7.41E-14 | 9.97E-14 | 1.52E-13 |
| BR | 82 | 0.00E+00 | 8.55E-17 | 8.55E-17 | 8.55E-17 | 8.55E-17 | 8.55E-17 | 8.55E-17 | 8.55E-17 | 8.55E-17 | 8.55E-17 | 8.55E-17 |
| BR | 83 | 0.00E+00 | 7.13E-19 | 7.13E-19 | 7.13E-19 | 7.13E-19 | 7.13E-19 | 7.13E-19 | 7.13E-19 | 7.13E-19 | 7.13E-19 | 7.13E-19 |
| BR | 84 | 0.00E+00 | 3.56E-19 | 3.56E-19 | 3.56E-19 | 3.56E-19 | 3.56E-19 | 3.56E-19 | 3.56E-19 | 3.56E-19 | 3.56E-19 | 3.56E-19 |
| KR | 80 | 0.00E+00 | 1.61E-12 | 3.28E-12 | 4.92E-12 | 6.54E-12 | 1.31E-11 | 3.28E-11 | 6.54E-11 | 9.82E-11 | 1.31E-10 | 1.96E-10 |
| KR | 81 | 0.00E+00 | 1.21E-12 | 2.46E-12 | 3.69E-12 | 4.91E-12 | 9.83E-12 | 2.46E-11 | 4.90E-11 | 7.36E-11 | 9.82E-11 | 1.47E-10 |
| KR | 82 | 0.00E+00 | 2.02E-12 | 4.11E-12 | 6.16E-12 | 8.19E-12 | 1.64E-11 | 4.11E-11 | 8.19E-11 | 1.23E-10 | 1.64E-10 | 2.46E-10 |
| KR | 83 | 0.00E+00 | 1.28E-12 | 3.21E-12 | 5.41E-12 | 7.72E-12 | 1.75E-11 | 4.93E-11 | 1.01E-10 | 1.52E-10 | 2.04E-10 | 3.04E-10 |
| KR | 83M | 0.00E+00 | 5.53E-19 | 5.53E-19 | 5.53E-19 | 5.53E-19 | 5.53E-19 | 5.53E-19 | 5.53E-19 | 5.53E-19 | 5.53E-19 | 5.53E-19 |
| KR | 84 | 0.00E+00 | 2.22E-12 | 5.50E-12 | 8.87E-12 | 1.22E-11 | 2.71E-11 | 6.93E-11 | 1.38E-10 | 2.07E-10 | 2.77E-10 | 4.13E-10 |
| KR | 85 | 0.00E+00 | 4.37E-13 | 8.81E-13 | 1.31E-12 | 1.73E-12 | 3.35E-12 | 7.65E-12 | 1.32E-11 | 1.72E-11 | 2.01E-11 | 2.37E-11 |
| KR | 85M | 0.00E+00 | 3.28E-20 | 3.28E-20 | 3.28E-20 | 3.28E-20 | 3.28E-20 | 3.28E-20 | 3.28E-20 | 3.28E-20 | 3.28E-20 | 3.28E-20 |
| KR | 86 | 0.00E+00 | 8.09E-13 | 1.64E-12 | 2.46E-12 | 3.28E-12 | 6.56E-12 | 1.64E-11 | 3.28E-11 | 4.92E-11 | 6.56E-11 | 9.84E-11 |
| KR | 87 | 0.00E+00 | 3.40E-18 | 3.40E-18 | 3.40E-18 | 3.40E-18 | 3.40E-18 | 3.40E-18 | 3.40E-18 | 3.40E-18 | 3.40E-18 | 3.40E-18 |
| RB | 80 | 0.00E+00 | 2.55E-18 | 2.55E-18 | 2.55E-18 | 2.55E-18 | 2.55E-18 | 2.55E-18 | 2.55E-18 | 2.55E-18 | 2.55E-18 | 2.55E-18 |
| RB | 81 | 0.00E+00 | 2.47E-15 | 2.47E-15 | 2.47E-15 | 2.47E-15 | 2.47E-15 | 2.47E-15 | 2.47E-15 | 2.47E-15 | 2.47E-15 | 2.47E-15 |
| RB | 82 | 0.00E+00 | 2.81E-17 | 2.81E-17 | 2.81E-17 | 2.81E-17 | 2.81E-17 | 2.81E-17 | 2.81E-17 | 2.81E-17 | 2.81E-17 | 2.81E-17 |

**Table A.5. (continued)**

| Proton beam energy: 1 GeV | | | | | | | Operational line loss assumption: 1 nA/m (continuous) | | | | | |
|---|---|---|---|---|---|---|---|---|---|---|---|---|
| Nuclide masses integrated over the material zone volume in the HETC & MCNP calculational model | | | | | | | | | | | | |
| Nuclide concentration | | Time (s) | 7.88E+06 | 1.58E+07 | 2.37E+07 | 3.15E+07 | 6.31E+07 | 1.58E+08 | 3.15E+08 | 4.73E+08 | 6.31E+08 | 9.46E+08 |
| (gram-atoms) | | Initial | 3 months | 6 months | 9 months | 1 year | 2 years | 5 years | 10 years | 15 years | 20 years | 30 years |
| RB | 83 | 0.00E+00 | 1.15E-12 | 1.72E-12 | 1.98E-12 | 2.11E-12 | 2.22E-12 | 2.23E-12 | 2.23E-12 | 2.23E-12 | 2.23E-12 | 2.23E-12 |
| RB | 84 | 0.00E+00 | 1.16E-12 | 1.34E-12 | 1.36E-12 | 1.37E-12 | 1.37E-12 | 1.37E-12 | 1.37E-12 | 1.37E-12 | 1.37E-12 | 1.37E-12 |
| RB | 85 | 0.00E+00 | 4.08E-13 | 8.36E-13 | 1.26E-12 | 1.69E-12 | 3.50E-12 | 9.52E-12 | 2.11E-11 | 3.42E-11 | 4.85E-11 | 7.91E-11 |
| RB | 86 | 0.00E+00 | 1.45E-12 | 1.51E-12 | 1.51E-12 | 1.51E-12 | 1.51E-12 | 1.51E-12 | 1.51E-12 | 1.51E-12 | 1.51E-12 | 1.51E-12 |
| RB | 87 | 0.00E+00 | 4.02E-15 | 8.16E-15 | 1.22E-14 | 1.63E-14 | 3.26E-14 | 8.16E-14 | 1.63E-13 | 2.44E-13 | 3.26E-13 | 4.89E-13 |
| RB | 88 | 0.00E+00 | 4.77E-17 | 4.77E-17 | 4.77E-17 | 4.77E-17 | 4.77E-17 | 4.77E-17 | 4.77E-17 | 4.77E-17 | 4.77E-17 | 4.77E-17 |
| SR | 84 | 0.00E+00 | 4.32E-14 | 1.18E-13 | 1.97E-13 | 2.75E-13 | 6.33E-13 | 1.63E-12 | 3.24E-12 | 4.87E-12 | 6.50E-12 | 9.70E-12 |
| SR | 86 | 0.00E+00 | 3.59E-12 | 8.74E-12 | 1.39E-11 | 1.89E-11 | 4.09E-11 | 1.04E-10 | 2.07E-10 | 3.11E-10 | 4.15E-10 | 6.21E-10 |
| SR | 88 | 0.00E+00 | 2.42E-13 | 4.92E-13 | 7.39E-13 | 9.82E-13 | 1.97E-12 | 4.92E-12 | 9.82E-12 | 1.47E-11 | 1.97E-11 | 2.95E-11 |
| I | 127 | 0.00E+00 | 5.03E-19 | 1.41E-18 | 2.38E-18 | 3.34E-18 | 7.82E-18 | 2.01E-17 | 4.02E-17 | 6.03E-17 | 8.05E-17 | 1.20E-16 |
| XE | 124 | 0.00E+00 | 4.04E-13 | 8.20E-13 | 1.23E-12 | 1.63E-12 | 3.27E-12 | 8.20E-12 | 1.63E-11 | 2.45E-11 | 3.27E-11 | 4.91E-11 |
| XE | 126 | 0.00E+00 | 3.97E-19 | 8.06E-19 | 1.21E-18 | 1.61E-18 | 3.22E-18 | 8.06E-18 | 1.61E-17 | 2.41E-17 | 3.22E-17 | 4.83E-17 |
| XE | 127 | 0.00E+00 | 4.61E-19 | 5.45E-19 | 5.59E-19 | 5.62E-19 | 5.63E-19 | 5.62E-19 | 5.62E-19 | 5.62E-19 | 5.62E-19 | 5.62E-19 |
| XE | 128 | 0.00E+00 | 9.20E-18 | 1.90E-17 | 2.87E-17 | 3.82E-17 | 7.68E-17 | 1.93E-16 | 3.85E-16 | 5.78E-16 | 7.71E-16 | 1.16E-15 |
| XE | 129 | 0.00E+00 | 1.40E-16 | 2.88E-16 | 4.34E-16 | 5.78E-16 | 1.15E-15 | 2.87E-15 | 5.71E-15 | 8.57E-15 | 1.14E-14 | 1.71E-14 |
| XE | 130 | 0.00E+00 | 9.98E-18 | 2.03E-17 | 3.04E-17 | 4.04E-17 | 8.10E-17 | 2.03E-16 | 4.04E-16 | 6.07E-16 | 8.10E-16 | 1.21E-15 |
| XE | 131 | 0.00E+00 | 1.35E-15 | 3.44E-15 | 5.51E-15 | 7.56E-15 | 1.62E-14 | 4.14E-14 | 8.29E-14 | 1.25E-13 | 1.66E-13 | 2.49E-13 |
| XE | 132 | 0.00E+00 | 6.35E-17 | 1.31E-16 | 1.97E-16 | 2.63E-16 | 5.23E-16 | 1.30E-15 | 2.58E-15 | 3.87E-15 | 5.17E-15 | 7.74E-15 |
| XE | 133 | 0.00E+00 | 2.48E-18 | 2.48E-18 | 2.48E-18 | 2.48E-18 | 2.48E-18 | 2.48E-18 | 2.48E-18 | 2.48E-18 | 2.48E-18 | 2.48E-18 |
| XE | 134 | 0.00E+00 | 7.12E-17 | 1.45E-16 | 2.17E-16 | 2.88E-16 | 5.78E-16 | 1.45E-15 | 2.88E-15 | 4.33E-15 | 5.78E-15 | 8.66E-15 |
| XE | 135 | 0.00E+00 | 2.02E-18 | 2.02E-18 | 2.02E-18 | 2.02E-18 | 2.02E-18 | 2.02E-18 | 2.02E-18 | 2.02E-18 | 2.02E-18 | 2.02E-18 |
| XE | 136 | 0.00E+00 | 6.75E-18 | 1.37E-17 | 2.06E-17 | 2.73E-17 | 5.47E-17 | 1.37E-16 | 2.73E-16 | 4.10E-16 | 5.47E-16 | 8.20E-16 |
| CS | 124 | 0.00E+00 | 2.31E-18 | 2.31E-18 | 2.31E-18 | 2.31E-18 | 2.31E-18 | 2.31E-18 | 2.31E-18 | 2.31E-18 | 2.31E-18 | 2.31E-18 |
| CS | 129 | 0.00E+00 | 3.02E-18 | 3.02E-18 | 3.02E-18 | 3.02E-18 | 3.02E-18 | 3.02E-18 | 3.02E-18 | 3.02E-18 | 3.02E-18 | 3.02E-18 |
| CS | 131 | 0.00E+00 | 3.08E-16 | 3.14E-16 | 3.14E-16 | 3.14E-16 | 3.14E-16 | 3.14E-16 | 3.14E-16 | 3.14E-16 | 3.14E-16 | 3.14E-16 |
| CS | 132 | 0.00E+00 | 2.01E-18 | 2.01E-18 | 2.01E-18 | 2.01E-18 | 2.01E-18 | 2.01E-18 | 2.01E-18 | 2.01E-18 | 2.01E-18 | 2.01E-18 |
| CS | 133 | 0.00E+00 | 1.47E-16 | 4.23E-16 | 8.15E-16 | 1.32E-15 | 4.46E-15 | 2.38E-14 | 8.28E-14 | 1.68E-13 | 2.71E-13 | 5.15E-13 |
| CS | 134 | 0.00E+00 | 1.34E-16 | 2.61E-16 | 3.76E-16 | 4.81E-16 | 8.26E-16 | 1.37E-15 | 1.63E-15 | 1.67E-15 | 1.68E-15 | 1.69E-15 |
| CS | 135 | 0.00E+00 | 4.04E-13 | 8.21E-13 | 1.23E-12 | 1.64E-12 | 3.28E-12 | 8.21E-12 | 1.64E-11 | 2.46E-11 | 3.28E-11 | 4.91E-11 |
| CS | 136 | 0.00E+00 | 5.00E-17 | 5.04E-17 | 5.04E-17 | 5.04E-17 | 5.04E-17 | 5.04E-17 | 5.04E-17 | 5.04E-17 | 5.04E-17 | 5.04E-17 |
| CS | 137 | 0.00E+00 | 9.08E-16 | 1.84E-15 | 2.75E-15 | 3.65E-15 | 7.22E-15 | 1.75E-14 | 3.30E-14 | 4.68E-14 | 5.92E-14 | 8.00E-14 |
| CS | 138 | 0.00E+00 | 3.65E-19 | 3.65E-19 | 3.65E-19 | 3.65E-19 | 3.65E-19 | 3.65E-19 | 3.65E-19 | 3.65E-19 | 3.65E-19 | 3.65E-19 |
| BA | 128 | 0.00E+00 | 3.04E-19 | 3.04E-19 | 3.04E-19 | 3.04E-19 | 3.04E-19 | 3.04E-19 | 3.04E-19 | 3.04E-19 | 3.04E-19 | 3.04E-19 |
| BA | 129 | 0.00E+00 | 1.98E-19 | 1.98E-19 | 1.98E-19 | 1.98E-19 | 1.98E-19 | 1.98E-19 | 1.98E-19 | 1.98E-19 | 1.98E-19 | 1.98E-19 |

| Table A.5. (continued) | | | | | | | | | | | | |
|---|---|---|---|---|---|---|---|---|---|---|---|---|
| Proton beam energy: 1 GeV | | | | | | | Operational line loss assumption: 1 nA/m (continuous) | | | | | |
| Nuclide masses integrated over the material zone volume in the HETC & MCNP calculational model | | | | | | | | | | | | |
| Nuclide concentration | | Time (s) | 7.88E+06 | 1.58E+07 | 2.37E+07 | 3.15E+07 | 6.31E+07 | 1.58E+08 | 3.15E+08 | 4.73E+08 | 6.31E+08 | 9.46E+08 |
| (gram-atoms) | | Initial | 3 months | 6 months | 9 months | 1 year | 2 years | 5 years | 10 years | 15 years | 20 years | 30 years |
| BA | 130 | 0.00E+00 | 2.35E-17 | 4.76E-17 | 7.15E-17 | 9.50E-17 | 1.90E-16 | 4.76E-16 | 9.50E-16 | 1.43E-15 | 1.90E-15 | 2.85E-15 |
| BA | 131 | 0.00E+00 | 3.87E-16 | 3.89E-16 | 3.89E-16 | 3.89E-16 | 3.89E-16 | 3.89E-16 | 3.89E-16 | 3.89E-16 | 3.89E-16 | 3.89E-16 |
| BA | 132 | 0.00E+00 | 1.08E-15 | 2.19E-15 | 3.29E-15 | 4.37E-15 | 8.75E-15 | 2.19E-14 | 4.37E-14 | 6.56E-14 | 8.75E-14 | 1.31E-13 |
| BA | 133 | 0.00E+00 | 7.34E-15 | 1.48E-14 | 2.20E-14 | 2.90E-14 | 5.63E-14 | 1.28E-13 | 2.20E-13 | 2.87E-13 | 3.36E-13 | 3.96E-13 |
| BA | 134 | 0.00E+00 | 4.36E-13 | 8.85E-13 | 1.33E-12 | 1.76E-12 | 3.53E-12 | 8.85E-12 | 1.76E-11 | 2.65E-11 | 3.53E-11 | 5.30E-11 |
| BA | 135 | 0.00E+00 | 2.10E-14 | 4.27E-14 | 6.41E-14 | 8.52E-14 | 1.71E-13 | 4.27E-13 | 8.52E-13 | 1.28E-12 | 1.71E-12 | 2.56E-12 |
| BA | 136 | 0.00E+00 | 1.66E-13 | 3.37E-13 | 5.06E-13 | 6.72E-13 | 1.35E-12 | 3.37E-12 | 6.72E-12 | 1.01E-11 | 1.35E-11 | 2.02E-11 |
| BA | 137 | 0.00E+00 | 1.16E-13 | 2.36E-13 | 3.54E-13 | 4.70E-13 | 9.42E-13 | 2.36E-12 | 4.71E-12 | 7.07E-12 | 9.43E-12 | 1.42E-11 |
| BA | 138 | 0.00E+00 | 3.55E-14 | 7.22E-14 | 1.08E-13 | 1.44E-13 | 2.88E-13 | 7.22E-13 | 1.44E-12 | 2.16E-12 | 2.88E-12 | 4.32E-12 |
| BA | 139 | 0.00E+00 | 3.57E-17 | 3.57E-17 | 3.57E-17 | 3.57E-17 | 3.57E-17 | 3.57E-17 | 3.57E-17 | 3.57E-17 | 3.57E-17 | 3.57E-17 |
| LA | 139 | 0.00E+00 | 3.85E-14 | 7.82E-14 | 1.17E-13 | 1.56E-13 | 3.12E-13 | 7.82E-13 | 1.56E-12 | 2.34E-12 | 3.12E-12 | 4.68E-12 |
| EU | 155 | 0.00E+00 | 2.38E-19 | 4.75E-19 | 7.00E-19 | 9.14E-19 | 1.71E-18 | 3.51E-18 | 5.20E-18 | 6.03E-18 | 6.43E-18 | 6.72E-18 |
| EU | 156 | 0.00E+00 | 4.34E-19 | 4.41E-19 | 4.41E-19 | 4.41E-19 | 4.41E-19 | 4.41E-19 | 4.41E-19 | 4.41E-19 | 4.41E-19 | 4.41E-19 |
| GD | 156 | 0.00E+00 | 1.40E-18 | 3.27E-18 | 5.13E-18 | 6.97E-18 | 1.48E-17 | 3.76E-17 | 7.50E-17 | 1.13E-16 | 1.50E-16 | 2.25E-16 |
| GD | 157 | 0.00E+00 | 5.03E-19 | 1.33E-18 | 2.46E-18 | 3.86E-18 | 1.26E-17 | 6.78E-17 | 2.53E-16 | 5.57E-16 | 9.74E-16 | 2.14E-15 |
| GD | 158 | 0.00E+00 | 2.93E-18 | 6.40E-18 | 1.02E-17 | 1.45E-17 | 3.59E-17 | 1.41E-16 | 4.50E-16 | 9.25E-16 | 1.56E-15 | 3.30E-15 |
| GD | 159 | 0.00E+00 | 3.26E-20 | 3.26E-20 | 3.26E-20 | 3.26E-20 | 3.26E-20 | 3.26E-20 | 3.26E-20 | 3.26E-20 | 3.26E-20 | 3.26E-20 |
| TB | 157 | 0.00E+00 | 2.60E-16 | 5.27E-16 | 7.91E-16 | 1.05E-15 | 2.10E-15 | 5.22E-15 | 1.03E-14 | 1.53E-14 | 2.01E-14 | 2.95E-14 |
| TB | 158 | 0.00E+00 | 4.50E-16 | 9.13E-16 | 1.37E-15 | 1.82E-15 | 3.63E-15 | 9.03E-15 | 1.78E-14 | 2.64E-14 | 3.49E-14 | 5.11E-14 |
| TB | 159 | 0.00E+00 | 2.63E-18 | 5.37E-18 | 8.07E-18 | 1.07E-17 | 2.15E-17 | 5.35E-17 | 1.07E-16 | 1.60E-16 | 2.13E-16 | 3.20E-16 |
| TB | 160 | 0.00E+00 | 1.40E-14 | 2.00E-14 | 2.25E-14 | 2.35E-14 | 2.42E-14 | 2.42E-14 | 2.42E-14 | 2.42E-14 | 2.42E-14 | 2.42E-14 |
| DY | 158 | 0.00E+00 | 4.61E-20 | 1.90E-19 | 4.28E-19 | 7.55E-19 | 3.03E-18 | 1.89E-17 | 7.45E-17 | 1.67E-16 | 2.94E-16 | 6.52E-16 |
| DY | 160 | 0.00E+00 | 6.90E-15 | 2.24E-14 | 4.12E-14 | 6.11E-14 | 1.45E-13 | 4.24E-13 | 8.70E-13 | 1.32E-12 | 1.77E-12 | 2.64E-12 |
| Total | | 0.00E+00 | 1.07E-07 | 2.17E-07 | 3.25E-07 | 4.32E-07 | 8.66E-07 | 2.17E-06 | 4.32E-06 | 6.49E-06 | 8.65E-06 | 1.30E-05 |

| Table A.6. SNS nuclide production during normal proton beam operation: earth berm Zone 2 | | | | | | | | | | | | |
|---|---|---|---|---|---|---|---|---|---|---|---|---|
| Proton beam energy: 1 GeV | | | | | | | Operational line loss assumption: 1 nA/m (continuous) | | | | | |
| Nuclide masses integrated over the material zone volume in the HETC & MCNP calculational model | | | | | | | | | | | | |
| Nuclide concentration | | Time (s) | 7.88E+06 | 1.58E+07 | 2.37E+07 | 3.15E+07 | 6.31E+07 | 1.58E+08 | 3.15E+08 | 4.73E+08 | 6.31E+08 | 9.46E+08 |
| (gram-atoms) | | Initial | 3 months | 6 months | 9 months | 1 year | 2 years | 5 years | 10 years | 15 years | 20 years | 30 years |
| H | 1 | 0.00E+00 | 1.93E-08 | 3.92E-08 | 5.89E-08 | 7.82E-08 | 1.57E-07 | 3.92E-07 | 7.82E-07 | 1.17E-06 | 1.57E-06 | 2.35E-06 |
| H | 2 | 0.00E+00 | 5.58E-10 | 1.13E-09 | 1.70E-09 | 2.26E-09 | 4.53E-09 | 1.13E-08 | 2.26E-08 | 3.39E-08 | 4.53E-08 | 6.79E-08 |
| **H** | **3** | **0.00E+00** | **4.20E-10** | **8.46E-10** | **1.26E-09** | **1.66E-09** | **3.24E-09** | **7.47E-09** | **1.31E-08** | **1.73E-08** | **2.06E-08** | **2.48E-08** |
| HE | 3 | 0.00E+00 | 8.27E-11 | 1.74E-10 | 2.70E-10 | 3.70E-10 | 8.33E-10 | 2.72E-09 | 7.25E-09 | 1.32E-08 | 2.02E-08 | 3.63E-08 |
| HE | 4 | 0.00E+00 | 4.14E-09 | 8.40E-09 | 1.26E-08 | 1.68E-08 | 3.36E-08 | 8.40E-08 | 1.68E-07 | 2.52E-07 | 3.36E-07 | 5.03E-07 |
| LI | 6 | 0.00E+00 | 7.59E-11 | 1.54E-10 | 2.31E-10 | 3.07E-10 | 6.15E-10 | 1.54E-09 | 3.07E-09 | 4.61E-09 | 6.15E-09 | 9.23E-09 |
| LI | 7 | 0.00E+00 | 5.18E-12 | 1.09E-11 | 1.65E-11 | 2.22E-11 | 4.51E-11 | 1.15E-10 | 2.29E-10 | 3.45E-10 | 4.60E-10 | 6.90E-10 |
| LI | 8 | 0.00E+00 | 6.29E-20 | 6.29E-20 | 6.29E-20 | 6.29E-20 | 6.29E-20 | 6.29E-20 | 6.29E-20 | 6.29E-20 | 6.29E-20 | 6.29E-20 |
| BE | 7 | 0.00E+00 | 4.76E-13 | 6.25E-13 | 6.70E-13 | 6.83E-13 | 6.89E-13 | 6.89E-13 | 6.89E-13 | 6.89E-13 | 6.89E-13 | 6.89E-13 |
| BE | 9 | 0.00E+00 | 1.90E-11 | 3.85E-11 | 5.78E-11 | 7.69E-11 | 1.54E-10 | 3.85E-10 | 7.69E-10 | 1.15E-09 | 1.54E-09 | 2.31E-09 |
| **BE** | **10** | **0.00E+00** | **2.84E-12** | **5.77E-12** | **8.65E-12** | **1.15E-11** | **2.30E-11** | **5.77E-11** | **1.15E-10** | **1.73E-10** | **2.30E-10** | **3.45E-10** |
| BE | 11 | 0.00E+00 | 2.04E-18 | 2.04E-18 | 2.04E-18 | 2.04E-18 | 2.04E-18 | 2.04E-18 | 2.04E-18 | 2.04E-18 | 2.04E-18 | 2.04E-18 |
| B | 10 | 0.00E+00 | 1.35E-10 | 2.74E-10 | 4.11E-10 | 5.46E-10 | 1.09E-09 | 2.74E-09 | 5.46E-09 | 8.19E-09 | 1.09E-08 | 1.64E-08 |
| B | 11 | 0.00E+00 | 1.72E-10 | 3.49E-10 | 5.24E-10 | 6.96E-10 | 1.39E-09 | 3.49E-09 | 6.96E-09 | 1.04E-08 | 1.39E-08 | 2.09E-08 |
| B | 12 | 0.00E+00 | 6.93E-20 | 6.93E-20 | 6.93E-20 | 6.93E-20 | 6.93E-20 | 6.93E-20 | 6.93E-20 | 6.93E-20 | 6.93E-20 | 6.93E-20 |
| B | 13 | 0.00E+00 | 1.30E-20 | 1.30E-20 | 1.30E-20 | 1.30E-20 | 1.30E-20 | 1.30E-20 | 1.30E-20 | 1.30E-20 | 1.30E-20 | 1.30E-20 |
| C | 10 | 0.00E+00 | 1.43E-18 | 1.43E-18 | 1.43E-18 | 1.43E-18 | 1.43E-18 | 1.43E-18 | 1.43E-18 | 1.43E-18 | 1.43E-18 | 1.43E-18 |
| C | 11 | 0.00E+00 | 1.22E-14 | 1.22E-14 | 1.22E-14 | 1.22E-14 | 1.22E-14 | 1.22E-14 | 1.22E-14 | 1.22E-14 | 1.22E-14 | 1.22E-14 |
| C | 12 | 0.00E+00 | 2.30E-09 | 4.67E-09 | 7.00E-09 | 9.31E-09 | 1.86E-08 | 4.67E-08 | 9.31E-08 | 1.40E-07 | 1.86E-07 | 2.79E-07 |
| C | 13 | 0.00E+00 | 1.77E-09 | 3.60E-09 | 5.41E-09 | 7.19E-09 | 1.44E-08 | 3.60E-08 | 7.19E-08 | 1.08E-07 | 1.44E-07 | 2.16E-07 |
| **C** | **14** | **0.00E+00** | **2.37E-10** | **4.81E-10** | **7.21E-10** | **9.59E-10** | **1.92E-09** | **4.81E-09** | **9.58E-09** | **1.44E-08** | **1.92E-08** | **2.87E-08** |
| N | 13 | 0.00E+00 | 2.32E-14 | 2.32E-14 | 2.32E-14 | 2.32E-14 | 2.32E-14 | 2.32E-14 | 2.32E-14 | 2.32E-14 | 2.32E-14 | 2.32E-14 |
| N | 14 | 0.00E+00 | 2.33E-09 | 4.73E-09 | 7.09E-09 | 9.42E-09 | 1.89E-08 | 4.73E-08 | 9.42E-08 | 1.42E-07 | 1.89E-07 | 2.83E-07 |
| N | 15 | 0.00E+00 | 3.53E-09 | 7.18E-09 | 1.08E-08 | 1.43E-08 | 2.87E-08 | 7.18E-08 | 1.43E-07 | 2.15E-07 | 2.87E-07 | 4.30E-07 |
| N | 16 | 0.00E+00 | 2.33E-16 | 2.33E-16 | 2.33E-16 | 2.33E-16 | 2.33E-16 | 2.33E-16 | 2.33E-16 | 2.33E-16 | 2.33E-16 | 2.33E-16 |
| N | 17 | 0.00E+00 | 3.41E-18 | 3.41E-18 | 3.41E-18 | 3.41E-18 | 3.41E-18 | 3.41E-18 | 3.41E-18 | 3.41E-18 | 3.41E-18 | 3.41E-18 |
| N | 18 | 0.00E+00 | 9.71E-20 | 9.71E-20 | 9.71E-20 | 9.71E-20 | 9.71E-20 | 9.71E-20 | 9.71E-20 | 9.71E-20 | 9.71E-20 | 9.71E-20 |
| O | 14 | 0.00E+00 | 3.12E-16 | 3.12E-16 | 3.12E-16 | 3.12E-16 | 3.12E-16 | 3.12E-16 | 3.12E-16 | 3.12E-16 | 3.12E-16 | 3.12E-16 |
| O | 15 | 0.00E+00 | 1.88E-14 | 1.88E-14 | 1.88E-14 | 1.88E-14 | 1.88E-14 | 1.88E-14 | 1.88E-14 | 1.88E-14 | 1.88E-14 | 1.88E-14 |
| O | 16 | 0.00E+00 | 1.13E-09 | 2.30E-09 | 3.45E-09 | 4.58E-09 | 9.17E-09 | 2.30E-08 | 4.58E-08 | 6.88E-08 | 9.17E-08 | 1.38E-07 |

**Table A.6. (continued)**

| Proton beam energy: 1 GeV | | | | | | | Operational line loss assumption: 1 nA/m (continuous) | | | | | |
|---|---|---|---|---|---|---|---|---|---|---|---|---|
| Nuclide masses integrated over the material zone volume in the HETC & MCNP calculational model | | | | | | | | | | | | |
| Nuclide concentration | | Time (s) | 7.88E+06 | 1.58E+07 | 2.37E+07 | 3.15E+07 | 6.31E+07 | 1.58E+08 | 3.15E+08 | 4.73E+08 | 6.31E+08 | 9.46E+08 |
| (gram-atoms) | | Initial | 3 months | 6 months | 9 months | 1 year | 2 years | 5 years | 10 years | 15 years | 20 years | 30 years |
| O | 17 | 0.00E+00 | 8.56E-11 | 1.74E-10 | 2.61E-10 | 3.47E-10 | 6.95E-10 | 1.74E-09 | 3.47E-09 | 5.21E-09 | 6.95E-09 | 1.04E-08 |
| O | 18 | 0.00E+00 | 3.47E-11 | 7.06E-11 | 1.06E-10 | 1.41E-10 | 2.82E-10 | 7.06E-10 | 1.41E-09 | 2.11E-09 | 2.82E-09 | 4.22E-09 |
| O | 19 | 0.00E+00 | 2.90E-18 | 2.90E-18 | 2.90E-18 | 2.90E-18 | 2.90E-18 | 2.90E-18 | 2.90E-18 | 2.90E-18 | 2.90E-18 | 2.90E-18 |
| F | 17 | 0.00E+00 | 1.93E-17 | 1.93E-17 | 1.93E-17 | 1.93E-17 | 1.93E-17 | 1.93E-17 | 1.93E-17 | 1.93E-17 | 1.93E-17 | 1.93E-17 |
| F | 18 | 0.00E+00 | 3.65E-14 | 3.65E-14 | 3.65E-14 | 3.65E-14 | 3.65E-14 | 3.65E-14 | 3.65E-14 | 3.65E-14 | 3.65E-14 | 3.65E-14 |
| F | 19 | 0.00E+00 | 3.65E-11 | 7.41E-11 | 1.11E-10 | 1.48E-10 | 2.96E-10 | 7.41E-10 | 1.48E-09 | 2.22E-09 | 2.96E-09 | 4.44E-09 |
| F | 20 | 0.00E+00 | 9.19E-18 | 9.19E-18 | 9.19E-18 | 9.19E-18 | 9.19E-18 | 9.19E-18 | 9.19E-18 | 9.19E-18 | 9.19E-18 | 9.19E-18 |
| F | 21 | 0.00E+00 | 3.26E-19 | 3.26E-19 | 3.26E-19 | 3.26E-19 | 3.26E-19 | 3.26E-19 | 3.26E-19 | 3.26E-19 | 3.26E-19 | 3.26E-19 |
| F | 22 | 0.00E+00 | 6.33E-19 | 6.33E-19 | 6.33E-19 | 6.33E-19 | 6.33E-19 | 6.33E-19 | 6.33E-19 | 6.33E-19 | 6.33E-19 | 6.33E-19 |
| NE | 19 | 0.00E+00 | 9.02E-18 | 9.02E-18 | 9.02E-18 | 9.02E-18 | 9.02E-18 | 9.02E-18 | 9.02E-18 | 9.02E-18 | 9.02E-18 | 9.02E-18 |
| NE | 20 | 0.00E+00 | 8.56E-11 | 1.74E-10 | 2.61E-10 | 3.46E-10 | 6.94E-10 | 1.74E-09 | 3.46E-09 | 5.20E-09 | 6.94E-09 | 1.04E-08 |
| NE | 21 | 0.00E+00 | 2.88E-11 | 5.85E-11 | 8.78E-11 | 1.17E-10 | 2.34E-10 | 5.85E-10 | 1.17E-09 | 1.75E-09 | 2.34E-09 | 3.50E-09 |
| NE | 22 | 0.00E+00 | 2.16E-11 | 4.87E-11 | 7.99E-11 | 1.15E-10 | 2.94E-10 | 1.08E-09 | 2.78E-09 | 4.66E-09 | 6.58E-09 | 1.04E-08 |
| NE | 23 | 0.00E+00 | 2.20E-17 | 2.20E-17 | 2.20E-17 | 2.20E-17 | 2.20E-17 | 2.20E-17 | 2.20E-17 | 2.20E-17 | 2.20E-17 | 2.20E-17 |
| NE | 24 | 0.00E+00 | 1.56E-17 | 1.56E-17 | 1.56E-17 | 1.56E-17 | 1.56E-17 | 1.56E-17 | 1.56E-17 | 1.56E-17 | 1.56E-17 | 1.56E-17 |
| NA | 21 | 0.00E+00 | 8.41E-18 | 8.41E-18 | 8.41E-18 | 8.41E-18 | 8.41E-18 | 8.41E-18 | 8.41E-18 | 8.41E-18 | 8.41E-18 | 8.41E-18 |
| **NA** | **22** | **0.00E+00** | **7.40E-11** | **1.45E-10** | **2.11E-10** | **2.72E-10** | **4.81E-10** | **8.60E-10** | **1.09E-09** | **1.15E-09** | **1.17E-09** | **1.17E-09** |
| NA | 23 | 0.00E+00 | 3.47E-10 | 7.04E-10 | 1.06E-09 | 1.40E-09 | 2.81E-09 | 7.04E-09 | 1.40E-08 | 2.11E-08 | 2.81E-08 | 4.22E-08 |
| NA | 24 | 0.00E+00 | 7.02E-13 | 7.02E-13 | 7.02E-13 | 7.02E-13 | 7.02E-13 | 7.02E-13 | 7.02E-13 | 7.02E-13 | 7.02E-13 | 7.02E-13 |
| NA | 25 | 0.00E+00 | 1.56E-16 | 1.56E-16 | 1.56E-16 | 1.56E-16 | 1.56E-16 | 1.56E-16 | 1.56E-16 | 1.56E-16 | 1.56E-16 | 1.56E-16 |
| NA | 26 | 0.00E+00 | 9.84E-19 | 9.84E-19 | 9.84E-19 | 9.84E-19 | 9.84E-19 | 9.84E-19 | 9.84E-19 | 9.84E-19 | 9.84E-19 | 9.84E-19 |
| MG | 23 | 0.00E+00 | 2.59E-17 | 2.59E-17 | 2.59E-17 | 2.59E-17 | 2.59E-17 | 2.59E-17 | 2.59E-17 | 2.59E-17 | 2.59E-17 | 2.59E-17 |
| MG | 24 | 0.00E+00 | 1.06E-09 | 2.14E-09 | 3.22E-09 | 4.28E-09 | 8.56E-09 | 2.14E-08 | 4.27E-08 | 6.42E-08 | 8.56E-08 | 1.28E-07 |
| MG | 25 | 0.00E+00 | 6.26E-10 | 1.27E-09 | 1.91E-09 | 2.53E-09 | 5.08E-09 | 1.27E-08 | 2.53E-08 | 3.80E-08 | 5.08E-08 | 7.61E-08 |
| MG | 26 | 0.00E+00 | 5.54E-10 | 1.13E-09 | 1.69E-09 | 2.24E-09 | 4.49E-09 | 1.13E-08 | 2.24E-08 | 3.37E-08 | 4.49E-08 | 6.74E-08 |
| MG | 27 | 0.00E+00 | 1.09E-14 | 1.09E-14 | 1.09E-14 | 1.09E-14 | 1.09E-14 | 1.09E-14 | 1.09E-14 | 1.09E-14 | 1.09E-14 | 1.09E-14 |
| AL | 24 | 0.00E+00 | 1.54E-19 | 1.54E-19 | 1.54E-19 | 1.54E-19 | 1.54E-19 | 1.54E-19 | 1.54E-19 | 1.54E-19 | 1.54E-19 | 1.54E-19 |
| AL | 25 | 0.00E+00 | 2.47E-17 | 2.47E-17 | 2.47E-17 | 2.47E-17 | 2.47E-17 | 2.47E-17 | 2.47E-17 | 2.47E-17 | 2.47E-17 | 2.47E-17 |
| **AL** | **26** | **0.00E+00** | **6.56E-10** | **1.33E-09** | **2.00E-09** | **2.66E-09** | **5.32E-09** | **1.33E-08** | **2.66E-08** | **3.99E-08** | **5.32E-08** | **7.98E-08** |
| AL | 27 | 0.00E+00 | 1.82E-09 | 3.70E-09 | 5.54E-09 | 7.37E-09 | 1.48E-08 | 3.70E-08 | 7.37E-08 | 1.11E-07 | 1.48E-07 | 2.21E-07 |
| AL | 28 | 0.00E+00 | 9.92E-15 | 9.92E-15 | 9.92E-15 | 9.92E-15 | 9.92E-15 | 9.92E-15 | 9.92E-15 | 9.92E-15 | 9.92E-15 | 9.92E-15 |

**Table A.6. (continued)**

| Proton beam energy: 1 GeV | | | | | | | Operational line loss assumption: 1 nA/m (continuous) | | | | | |
|---|---|---|---|---|---|---|---|---|---|---|---|---|
| Nuclide masses integrated over the material zone volume in the HETC & MCNP calculational model | | | | | | | | | | | | |
| Nuclide concentration | | Time (s) | 7.88E+06 | 1.58E+07 | 2.37E+07 | 3.15E+07 | 6.31E+07 | 1.58E+08 | 3.15E+08 | 4.73E+08 | 6.31E+08 | 9.46E+08 |
| (gram-atoms) | | Initial | 3 months | 6 months | 9 months | 1 year | 2 years | 5 years | 10 years | 15 years | 20 years | 30 years |
| AL | 29 | 0.00E+00 | 2.50E-15 | 2.50E-15 | 2.50E-15 | 2.50E-15 | 2.50E-15 | 2.50E-15 | 2.50E-15 | 2.50E-15 | 2.50E-15 | 2.50E-15 |
| AL | 30 | 0.00E+00 | 2.57E-18 | 2.57E-18 | 2.57E-18 | 2.57E-18 | 2.57E-18 | 2.57E-18 | 2.57E-18 | 2.57E-18 | 2.57E-18 | 2.57E-18 |
| SI | 26 | 0.00E+00 | 2.81E-18 | 2.81E-18 | 2.81E-18 | 2.81E-18 | 2.81E-18 | 2.81E-18 | 2.81E-18 | 2.81E-18 | 2.81E-18 | 2.81E-18 |
| SI | 27 | 0.00E+00 | 1.49E-16 | 1.49E-16 | 1.49E-16 | 1.49E-16 | 1.49E-16 | 1.49E-16 | 1.49E-16 | 1.49E-16 | 1.49E-16 | 1.49E-16 |
| SI | 28 | 0.00E+00 | 7.69E-10 | 1.56E-09 | 2.34E-09 | 3.11E-09 | 6.23E-09 | 1.56E-08 | 3.11E-08 | 4.67E-08 | 6.23E-08 | 9.35E-08 |
| SI | 29 | 0.00E+00 | 1.05E-10 | 2.14E-10 | 3.21E-10 | 4.26E-10 | 8.53E-10 | 2.14E-09 | 4.26E-09 | 6.40E-09 | 8.53E-09 | 1.28E-08 |
| SI | 30 | 0.00E+00 | 1.75E-11 | 3.55E-11 | 5.33E-11 | 7.09E-11 | 1.42E-10 | 3.55E-10 | 7.09E-10 | 1.06E-09 | 1.42E-09 | 2.13E-09 |
| SI | 31 | 0.00E+00 | 3.10E-15 | 3.10E-15 | 3.10E-15 | 3.10E-15 | 3.10E-15 | 3.10E-15 | 3.10E-15 | 3.10E-15 | 3.10E-15 | 3.10E-15 |
| P | 31 | 0.00E+00 | 2.99E-12 | 6.07E-12 | 9.10E-12 | 1.21E-11 | 2.42E-11 | 6.07E-11 | 1.21E-10 | 1.82E-10 | 2.42E-10 | 3.63E-10 |
| P | 32 | 0.00E+00 | 4.58E-13 | 4.64E-13 | 4.64E-13 | 4.64E-13 | 4.64E-13 | 4.64E-13 | 4.64E-13 | 4.64E-13 | 4.64E-13 | 4.64E-13 |
| P | 35 | 0.00E+00 | 3.52E-18 | 3.52E-18 | 3.52E-18 | 3.52E-18 | 3.52E-18 | 3.52E-18 | 3.52E-18 | 3.52E-18 | 3.52E-18 | 3.52E-18 |
| S | 32 | 0.00E+00 | 1.97E-12 | 4.47E-12 | 6.94E-12 | 9.37E-12 | 1.97E-11 | 4.98E-11 | 9.93E-11 | 1.49E-10 | 1.99E-10 | 2.98E-10 |
| S | 33 | 0.00E+00 | 1.61E-12 | 3.28E-12 | 4.92E-12 | 6.54E-12 | 1.31E-11 | 3.28E-11 | 6.54E-11 | 9.82E-11 | 1.31E-10 | 1.96E-10 |
| S | 34 | 0.00E+00 | 2.02E-12 | 4.10E-12 | 6.15E-12 | 8.17E-12 | 1.64E-11 | 4.10E-11 | 8.17E-11 | 1.23E-10 | 1.64E-10 | 2.45E-10 |
| S | 35 | 0.00E+00 | 8.67E-13 | 1.30E-12 | 1.51E-12 | 1.61E-12 | 1.70E-12 | 1.71E-12 | 1.71E-12 | 1.71E-12 | 1.71E-12 | 1.71E-12 |
| S | 36 | 0.00E+00 | 4.04E-13 | 8.20E-13 | 1.23E-12 | 1.63E-12 | 3.27E-12 | 8.20E-12 | 1.63E-11 | 2.45E-11 | 3.27E-11 | 4.91E-11 |
| CL | 35 | 0.00E+00 | 5.90E-12 | 1.24E-11 | 1.91E-11 | 2.58E-11 | 5.32E-11 | 1.37E-10 | 2.76E-10 | 4.15E-10 | 5.54E-10 | 8.30E-10 |
| **CL** | **36** | **0.00E+00** | **1.34E-11** | **2.72E-11** | **4.08E-11** | **5.43E-11** | **1.09E-10** | **2.72E-10** | **5.43E-10** | **8.15E-10** | **1.09E-09** | **1.63E-09** |
| CL | 37 | 0.00E+00 | 1.02E-11 | 2.74E-11 | 4.55E-11 | 6.35E-11 | 1.46E-10 | 3.75E-10 | 7.48E-10 | 1.12E-09 | 1.50E-09 | 2.24E-09 |
| CL | 38 | 0.00E+00 | 4.07E-17 | 4.07E-17 | 4.07E-17 | 4.07E-17 | 4.07E-17 | 4.07E-17 | 4.07E-17 | 4.07E-17 | 4.07E-17 | 4.07E-17 |
| CL | 39 | 0.00E+00 | 3.81E-18 | 3.81E-18 | 3.81E-18 | 3.81E-18 | 3.81E-18 | 3.81E-18 | 3.81E-18 | 3.81E-18 | 3.81E-18 | 3.81E-18 |
| CL | 40 | 0.00E+00 | 2.82E-20 | 2.82E-20 | 2.82E-20 | 2.82E-20 | 2.82E-20 | 2.82E-20 | 2.82E-20 | 2.82E-20 | 2.82E-20 | 2.82E-20 |
| AR | 36 | 0.00E+00 | 2.05E-12 | 4.16E-12 | 6.23E-12 | 8.29E-12 | 1.66E-11 | 4.16E-11 | 8.29E-11 | 1.24E-10 | 1.66E-10 | 2.49E-10 |
| AR | 37 | 0.00E+00 | 7.83E-12 | 9.16E-12 | 9.37E-12 | 9.41E-12 | 9.42E-12 | 9.41E-12 | 9.41E-12 | 9.41E-12 | 9.41E-12 | 9.41E-12 |
| AR | 38 | 0.00E+00 | 3.59E-11 | 7.30E-11 | 1.10E-10 | 1.46E-10 | 2.92E-10 | 7.30E-10 | 1.46E-09 | 2.19E-09 | 2.92E-09 | 4.37E-09 |
| **AR** | **39** | **0.00E+00** | **1.74E-11** | **3.52E-11** | **5.28E-11** | **7.02E-11** | **1.40E-10** | **3.50E-10** | **6.94E-10** | **1.04E-09** | **1.37E-09** | **2.03E-09** |
| AR | 40 | 0.00E+00 | 1.24E-12 | 2.52E-12 | 3.78E-12 | 5.03E-12 | 1.01E-11 | 2.52E-11 | 5.03E-11 | 7.55E-11 | 1.01E-10 | 1.51E-10 |
| AR | 41 | 0.00E+00 | 9.78E-17 | 9.78E-17 | 9.78E-17 | 9.78E-17 | 9.78E-17 | 9.78E-17 | 9.78E-17 | 9.78E-17 | 9.78E-17 | 9.78E-17 |
| AR | 42 | 0.00E+00 | 2.84E-18 | 5.74E-18 | 8.59E-18 | 1.14E-17 | 2.26E-17 | 5.48E-17 | 1.04E-16 | 1.48E-16 | 1.88E-16 | 2.56E-16 |
| K | 38 | 0.00E+00 | 4.58E-16 | 4.58E-16 | 4.58E-16 | 4.58E-16 | 4.58E-16 | 4.58E-16 | 4.58E-16 | 4.58E-16 | 4.58E-16 | 4.58E-16 |
| K | 39 | 0.00E+00 | 4.70E-12 | 9.56E-12 | 1.44E-11 | 1.91E-11 | 3.85E-11 | 9.76E-11 | 1.99E-10 | 3.06E-10 | 4.17E-10 | 6.51E-10 |

**Table A.6. (continued)**

| Proton beam energy: 1 GeV | | | | | | | Operational line loss assumption: 1 nA/m (continuous) | | | | | |
|---|---|---|---|---|---|---|---|---|---|---|---|---|
| Nuclide masses integrated over the material zone volume in the HETC & MCNP calculational model | | | | | | | | | | | | |
| Nuclide concentration | | Time (s) | 7.88E+06 | 1.58E+07 | 2.37E+07 | 3.15E+07 | 6.31E+07 | 1.58E+08 | 3.15E+08 | 4.73E+08 | 6.31E+08 | 9.46E+08 |
| (gram-atoms) | | Initial | 3 months | 6 months | 9 months | 1 year | 2 years | 5 years | 10 years | 15 years | 20 years | 30 years |
| **K** | **40** | **0.00E+00** | **5.21E-12** | **1.06E-11** | **1.59E-11** | **2.11E-11** | **4.22E-11** | **1.06E-10** | **2.11E-10** | **3.17E-10** | **4.22E-10** | **6.33E-10** |
| K | 41 | 0.00E+00 | 1.29E-12 | 2.62E-12 | 3.94E-12 | 5.23E-12 | 1.05E-11 | 2.62E-11 | 5.23E-11 | 7.85E-11 | 1.05E-10 | 1.57E-10 |
| K | 42 | 0.00E+00 | 5.18E-15 | 5.18E-15 | 5.18E-15 | 5.18E-15 | 5.18E-15 | 5.18E-15 | 5.18E-15 | 5.18E-15 | 5.18E-15 | 5.18E-15 |
| K | 43 | 0.00E+00 | 2.74E-18 | 2.74E-18 | 2.74E-18 | 2.74E-18 | 2.74E-18 | 2.74E-18 | 2.74E-18 | 2.74E-18 | 2.74E-18 | 2.74E-18 |
| K | 44 | 0.00E+00 | 9.30E-20 | 9.30E-20 | 9.30E-20 | 9.30E-20 | 9.30E-20 | 9.30E-20 | 9.30E-20 | 9.30E-20 | 9.30E-20 | 9.30E-20 |
| **CA** | **41** | **0.00E+00** | **1.23E-12** | **2.50E-12** | **3.75E-12** | **4.98E-12** | **9.98E-12** | **2.50E-11** | **4.98E-11** | **7.48E-11** | **9.98E-11** | **1.50E-10** |
| CA | 42 | 0.00E+00 | 1.84E-12 | 3.75E-12 | 5.63E-12 | 7.48E-12 | 1.50E-11 | 3.75E-11 | 7.47E-11 | 1.12E-10 | 1.50E-10 | 2.24E-10 |
| CA | 43 | 0.00E+00 | 8.52E-13 | 1.73E-12 | 2.59E-12 | 3.45E-12 | 6.91E-12 | 1.73E-11 | 3.45E-11 | 5.18E-11 | 6.91E-11 | 1.04E-10 |
| CA | 44 | 0.00E+00 | 6.72E-12 | 1.37E-11 | 2.05E-11 | 2.73E-11 | 5.46E-11 | 1.37E-10 | 2.72E-10 | 4.09E-10 | 5.46E-10 | 8.18E-10 |
| CA | 45 | 0.00E+00 | 1.03E-13 | 1.75E-13 | 2.24E-13 | 2.56E-13 | 3.12E-13 | 3.27E-13 | 3.27E-13 | 3.27E-13 | 3.27E-13 | 3.27E-13 |
| CA | 46 | 0.00E+00 | 8.11E-15 | 1.65E-14 | 2.47E-14 | 3.28E-14 | 6.57E-14 | 1.65E-13 | 3.28E-13 | 4.93E-13 | 6.57E-13 | 9.86E-13 |
| CA | 47 | 0.00E+00 | 1.02E-15 | 1.02E-15 | 1.02E-15 | 1.02E-15 | 1.02E-15 | 1.02E-15 | 1.02E-15 | 1.02E-15 | 1.02E-15 | 1.02E-15 |
| CA | 48 | 0.00E+00 | 5.93E-16 | 1.20E-15 | 1.81E-15 | 2.40E-15 | 4.81E-15 | 1.20E-14 | 2.40E-14 | 3.60E-14 | 4.81E-14 | 7.21E-14 |
| SC | 44 | 0.00E+00 | 1.54E-14 | 1.54E-14 | 1.54E-14 | 1.54E-14 | 1.54E-14 | 1.54E-14 | 1.54E-14 | 1.54E-14 | 1.54E-14 | 1.54E-14 |
| SC | 45 | 0.00E+00 | 8.63E-12 | 1.76E-11 | 2.64E-11 | 3.51E-11 | 7.05E-11 | 1.77E-10 | 3.54E-10 | 5.31E-10 | 7.09E-10 | 1.06E-09 |
| SC | 46 | 0.00E+00 | 2.11E-12 | 3.14E-12 | 3.61E-12 | 3.83E-12 | 4.02E-12 | 4.03E-12 | 4.03E-12 | 4.03E-12 | 4.03E-12 | 4.03E-12 |
| SC | 47 | 0.00E+00 | 1.75E-13 | 1.75E-13 | 1.75E-13 | 1.75E-13 | 1.75E-13 | 1.75E-13 | 1.75E-13 | 1.75E-13 | 1.75E-13 | 1.75E-13 |
| SC | 48 | 0.00E+00 | 3.15E-14 | 3.15E-14 | 3.15E-14 | 3.15E-14 | 3.15E-14 | 3.15E-14 | 3.15E-14 | 3.15E-14 | 3.15E-14 | 3.15E-14 |
| SC | 49 | 0.00E+00 | 7.29E-18 | 7.29E-18 | 7.29E-18 | 7.29E-18 | 7.29E-18 | 7.29E-18 | 7.29E-18 | 7.29E-18 | 7.29E-18 | 7.29E-18 |
| SC | 50 | 0.00E+00 | 3.45E-20 | 3.45E-20 | 3.45E-20 | 3.45E-20 | 3.45E-20 | 3.45E-20 | 3.45E-20 | 3.45E-20 | 3.45E-20 | 3.45E-20 |
| TI | 45 | 0.00E+00 | 5.09E-15 | 5.09E-15 | 5.09E-15 | 5.09E-15 | 5.09E-15 | 5.09E-15 | 5.09E-15 | 5.09E-15 | 5.09E-15 | 5.09E-15 |
| TI | 46 | 0.00E+00 | 3.83E-12 | 8.94E-12 | 1.45E-11 | 2.02E-11 | 4.42E-11 | 1.21E-10 | 2.45E-10 | 3.70E-10 | 4.94E-10 | 7.39E-10 |
| TI | 47 | 0.00E+00 | 1.19E-11 | 2.44E-11 | 3.67E-11 | 4.89E-11 | 9.76E-11 | 2.44E-10 | 4.85E-10 | 7.28E-10 | 9.70E-10 | 1.45E-09 |
| TI | 48 | 0.00E+00 | 7.17E-12 | 1.57E-11 | 2.41E-11 | 3.25E-11 | 6.73E-11 | 1.69E-10 | 3.38E-10 | 5.07E-10 | 6.76E-10 | 1.01E-09 |
| TI | 49 | 0.00E+00 | 2.02E-12 | 5.50E-12 | 1.01E-11 | 1.55E-11 | 4.40E-11 | 1.54E-10 | 3.50E-10 | 5.47E-10 | 7.45E-10 | 1.18E-09 |
| TI | 50 | 0.00E+00 | 8.06E-14 | 1.64E-13 | 2.45E-13 | 3.26E-13 | 6.54E-13 | 1.64E-12 | 3.26E-12 | 4.90E-12 | 6.54E-12 | 9.80E-12 |
| TI | 51 | 0.00E+00 | 9.09E-19 | 9.09E-19 | 9.09E-19 | 9.09E-19 | 9.09E-19 | 9.09E-19 | 9.09E-19 | 9.09E-19 | 9.09E-19 | 9.09E-19 |
| V | 47 | 0.00E+00 | 2.93E-16 | 2.93E-16 | 2.93E-16 | 2.93E-16 | 2.93E-16 | 2.93E-16 | 2.93E-16 | 2.93E-16 | 2.93E-16 | 2.93E-16 |
| V | 48 | 0.00E+00 | 1.11E-12 | 1.14E-12 | 1.14E-12 | 1.14E-12 | 1.14E-12 | 1.14E-12 | 1.14E-12 | 1.14E-12 | 1.14E-12 | 1.14E-12 |
| V | 49 | 0.00E+00 | 7.72E-12 | 1.43E-11 | 1.96E-11 | 2.39E-11 | 3.50E-11 | 4.35E-11 | 4.44E-11 | 4.44E-11 | 4.44E-11 | 4.44E-11 |
| V | 50 | 0.00E+00 | 6.55E-12 | 1.33E-11 | 2.00E-11 | 2.65E-11 | 5.31E-11 | 1.33E-10 | 2.65E-10 | 3.98E-10 | 5.31E-10 | 7.97E-10 |

**Table A.6. (continued)**

| Proton beam energy: 1 GeV | | | | | | | Operational line loss assumption: 1 nA/m (continuous) | | | | | |
|---|---|---|---|---|---|---|---|---|---|---|---|---|
| Nuclide masses integrated over the material zone volume in the HETC & MCNP calculational model | | | | | | | | | | | | |
| Nuclide concentration | | Time (s) | 7.88E+06 | 1.58E+07 | 2.37E+07 | 3.15E+07 | 6.31E+07 | 1.58E+08 | 3.15E+08 | 4.73E+08 | 6.31E+08 | 9.46E+08 |
| (gram-atoms) | | Initial | 3 months | 6 months | 9 months | 1 year | 2 years | 5 years | 10 years | 15 years | 20 years | 30 years |
| V | 51 | 0.00E+00 | 1.96E-11 | 5.08E-11 | 8.27E-11 | 1.14E-10 | 2.55E-10 | 6.53E-10 | 1.30E-09 | 1.95E-09 | 2.61E-09 | 3.90E-09 |
| V | 52 | 0.00E+00 | 3.07E-18 | 3.07E-18 | 3.07E-18 | 3.07E-18 | 3.07E-18 | 3.07E-18 | 3.07E-18 | 3.07E-18 | 3.07E-18 | 3.07E-18 |
| CR | 49 | 0.00E+00 | 9.41E-16 | 9.41E-16 | 9.41E-16 | 9.41E-16 | 9.41E-16 | 9.41E-16 | 9.41E-16 | 9.41E-16 | 9.41E-16 | 9.41E-16 |
| CR | 50 | 0.00E+00 | 1.22E-11 | 2.48E-11 | 3.72E-11 | 4.94E-11 | 9.89E-11 | 2.48E-10 | 4.94E-10 | 7.42E-10 | 9.89E-10 | 1.48E-09 |
| CR | 51 | 0.00E+00 | 1.19E-11 | 1.31E-11 | 1.32E-11 | 1.33E-11 | 1.33E-11 | 1.33E-11 | 1.33E-11 | 1.33E-11 | 1.33E-11 | 1.33E-11 |
| CR | 52 | 0.00E+00 | 4.24E-11 | 8.84E-11 | 1.34E-10 | 1.79E-10 | 3.53E-10 | 8.72E-10 | 1.73E-09 | 2.59E-09 | 3.46E-09 | 5.17E-09 |
| CR | 53 | 0.00E+00 | 1.11E-11 | 2.25E-11 | 3.38E-11 | 4.49E-11 | 8.99E-11 | 2.25E-10 | 4.49E-10 | 6.74E-10 | 8.99E-10 | 1.35E-09 |
| CR | 54 | 0.00E+00 | 8.85E-12 | 2.60E-11 | 4.93E-11 | 7.74E-11 | 2.27E-10 | 8.07E-10 | 1.83E-09 | 2.87E-09 | 3.90E-09 | 6.20E-09 |
| CR | 55 | 0.00E+00 | 3.22E-17 | 3.22E-17 | 3.22E-17 | 3.22E-17 | 3.22E-17 | 3.22E-17 | 3.22E-17 | 3.22E-17 | 3.22E-17 | 3.22E-17 |
| CR | 56 | 0.00E+00 | 1.95E-19 | 1.95E-19 | 1.95E-19 | 1.95E-19 | 1.95E-19 | 1.95E-19 | 1.95E-19 | 1.95E-19 | 1.95E-19 | 1.95E-19 |
| MN | 50 | 0.00E+00 | 2.12E-20 | 2.12E-20 | 2.12E-20 | 2.12E-20 | 2.12E-20 | 2.12E-20 | 2.12E-20 | 2.12E-20 | 2.12E-20 | 2.12E-20 |
| MN | 51 | 0.00E+00 | 3.11E-15 | 3.11E-15 | 3.11E-15 | 3.11E-15 | 3.11E-15 | 3.11E-15 | 3.11E-15 | 3.11E-15 | 3.11E-15 | 3.11E-15 |
| MN | 52 | 0.00E+00 | 2.33E-12 | 2.33E-12 | 2.33E-12 | 2.33E-12 | 2.33E-12 | 2.33E-12 | 2.33E-12 | 2.33E-12 | 2.33E-12 | 2.33E-12 |
| **MN** | **53** | **0.00E+00** | **5.79E-11** | **1.18E-10** | **1.76E-10** | **2.34E-10** | **4.69E-10** | **1.18E-09** | **2.34E-09** | **3.52E-09** | **4.69E-09** | **7.04E-09** |
| MN | 54 | 0.00E+00 | 4.21E-11 | 7.76E-11 | 1.06E-10 | 1.29E-10 | 1.87E-10 | 2.29E-10 | 2.32E-10 | 2.33E-10 | 2.33E-10 | 2.33E-10 |
| MN | 55 | 0.00E+00 | 5.70E-11 | 1.21E-10 | 1.90E-10 | 2.62E-10 | 5.98E-10 | 1.89E-09 | 4.50E-09 | 7.33E-09 | 1.02E-08 | 1.60E-08 |
| MN | 56 | 0.00E+00 | 2.26E-14 | 2.26E-14 | 2.26E-14 | 2.26E-14 | 2.26E-14 | 2.26E-14 | 2.26E-14 | 2.26E-14 | 2.26E-14 | 2.26E-14 |
| MN | 57 | 0.00E+00 | 1.57E-18 | 1.57E-18 | 1.57E-18 | 1.57E-18 | 1.57E-18 | 1.57E-18 | 1.57E-18 | 1.57E-18 | 1.57E-18 | 1.57E-18 |
| MN | 58 | 0.00E+00 | 1.20E-20 | 1.20E-20 | 1.20E-20 | 1.20E-20 | 1.20E-20 | 1.20E-20 | 1.20E-20 | 1.20E-20 | 1.20E-20 | 1.20E-20 |
| FE | 52 | 0.00E+00 | 2.23E-15 | 2.23E-15 | 2.23E-15 | 2.23E-15 | 2.23E-15 | 2.23E-15 | 2.23E-15 | 2.23E-15 | 2.23E-15 | 2.23E-15 |
| FE | 53 | 0.00E+00 | 2.80E-16 | 2.80E-16 | 2.80E-16 | 2.80E-16 | 2.80E-16 | 2.80E-16 | 2.80E-16 | 2.80E-16 | 2.80E-16 | 2.80E-16 |
| FE | 54 | 0.00E+00 | 3.27E-11 | 6.64E-11 | 9.96E-11 | 1.32E-10 | 2.65E-10 | 6.64E-10 | 1.32E-09 | 1.99E-09 | 2.65E-09 | 3.97E-09 |
| **FE** | **55** | **0.00E+00** | **8.61E-11** | **1.69E-10** | **2.46E-10** | **3.17E-10** | **5.63E-10** | **1.01E-09** | **1.29E-09** | **1.37E-09** | **1.39E-09** | **1.40E-09** |
| FE | 56 | 0.00E+00 | 3.89E-11 | 7.92E-11 | 1.19E-10 | 1.58E-10 | 3.18E-10 | 7.96E-10 | 1.59E-09 | 2.38E-09 | 3.18E-09 | 4.77E-09 |
| FE | 57 | 0.00E+00 | 1.38E-11 | 2.81E-11 | 4.21E-11 | 5.60E-11 | 1.12E-10 | 2.81E-10 | 5.60E-10 | 8.41E-10 | 1.12E-09 | 1.68E-09 |
| FE | 58 | 0.00E+00 | 3.14E-13 | 6.37E-13 | 9.56E-13 | 1.27E-12 | 2.55E-12 | 6.37E-12 | 1.27E-11 | 1.91E-11 | 2.55E-11 | 3.82E-11 |
| FE | 59 | 0.00E+00 | 2.96E-14 | 3.70E-14 | 3.87E-14 | 3.91E-14 | 3.93E-14 | 3.93E-14 | 3.93E-14 | 3.93E-14 | 3.93E-14 | 3.93E-14 |
| CO | 55 | 0.00E+00 | 4.73E-15 | 4.73E-15 | 4.73E-15 | 4.73E-15 | 4.73E-15 | 4.73E-15 | 4.73E-15 | 4.73E-15 | 4.73E-15 | 4.73E-15 |
| CO | 56 | 0.00E+00 | 2.79E-13 | 4.07E-13 | 4.64E-13 | 4.89E-13 | 5.09E-13 | 5.09E-13 | 5.09E-13 | 5.09E-13 | 5.09E-13 | 5.09E-13 |
| CO | 59 | 0.00E+00 | 2.54E-14 | 7.47E-14 | 1.29E-13 | 1.84E-13 | 4.07E-13 | 1.12E-12 | 2.27E-12 | 3.42E-12 | 4.58E-12 | 6.85E-12 |
| NI | 59 | 0.00E+00 | 4.04E-13 | 8.20E-13 | 1.23E-12 | 1.63E-12 | 3.27E-12 | 8.20E-12 | 1.63E-11 | 2.45E-11 | 3.27E-11 | 4.91E-11 |

**Table A.6. (continued)**

| Proton beam energy: 1 GeV | | | | | | | Operational line loss assumption: 1 nA/m (continuous) | | | | | |
|---|---|---|---|---|---|---|---|---|---|---|---|---|
| Nuclide masses integrated over the material zone volume in the HETC & MCNP calculational model | | | | | | | | | | | | |
| Nuclide concentration | | Time (s) | 7.88E+06 | 1.58E+07 | 2.37E+07 | 3.15E+07 | 6.31E+07 | 1.58E+08 | 3.15E+08 | 4.73E+08 | 6.31E+08 | 9.46E+08 |
| (gram-atoms) | | Initial | 3 months | 6 months | 9 months | 1 year | 2 years | 5 years | 10 years | 15 years | 20 years | 30 years |
| NI | 60 | 0.00E+00 | 6.00E-15 | 1.22E-14 | 1.83E-14 | 2.43E-14 | 4.87E-14 | 1.22E-13 | 2.43E-13 | 3.65E-13 | 4.87E-13 | 7.30E-13 |
| NI | 61 | 0.00E+00 | 3.67E-15 | 7.45E-15 | 1.12E-14 | 1.49E-14 | 2.98E-14 | 7.45E-14 | 1.49E-13 | 2.23E-13 | 2.98E-13 | 4.46E-13 |
| NI | 62 | 0.00E+00 | 4.04E-13 | 8.21E-13 | 1.23E-12 | 1.64E-12 | 3.28E-12 | 8.21E-12 | 1.64E-11 | 2.46E-11 | 3.28E-11 | 4.92E-11 |
| NI | 63 | 0.00E+00 | 2.33E-15 | 4.72E-15 | 7.08E-15 | 9.40E-15 | 1.88E-14 | 4.65E-14 | 9.11E-14 | 1.34E-13 | 1.76E-13 | 2.56E-13 |
| NI | 64 | 0.00E+00 | 5.14E-14 | 1.05E-13 | 1.57E-13 | 2.09E-13 | 4.18E-13 | 1.05E-12 | 2.08E-12 | 3.13E-12 | 4.17E-12 | 6.25E-12 |
| NI | 65 | 0.00E+00 | 8.53E-19 | 8.53E-19 | 8.53E-19 | 8.53E-19 | 8.53E-19 | 8.53E-19 | 8.53E-19 | 8.53E-19 | 8.53E-19 | 8.53E-19 |
| NI | 66 | 0.00E+00 | 4.94E-19 | 4.94E-19 | 4.94E-19 | 4.94E-19 | 4.94E-19 | 4.94E-19 | 4.94E-19 | 4.94E-19 | 4.94E-19 | 4.94E-19 |
| CU | 61 | 0.00E+00 | 4.25E-20 | 4.25E-20 | 4.25E-20 | 4.25E-20 | 4.25E-20 | 4.25E-20 | 4.25E-20 | 4.25E-20 | 4.25E-20 | 4.25E-20 |
| CU | 62 | 0.00E+00 | 4.37E-17 | 4.37E-17 | 4.37E-17 | 4.37E-17 | 4.37E-17 | 4.37E-17 | 4.37E-17 | 4.37E-17 | 4.37E-17 | 4.37E-17 |
| CU | 63 | 0.00E+00 | 1.31E-12 | 2.66E-12 | 3.99E-12 | 5.31E-12 | 1.06E-11 | 2.66E-11 | 5.31E-11 | 7.97E-11 | 1.06E-10 | 1.59E-10 |
| CU | 64 | 0.00E+00 | 7.14E-16 | 7.14E-16 | 7.14E-16 | 7.14E-16 | 7.14E-16 | 7.14E-16 | 7.14E-16 | 7.14E-16 | 7.14E-16 | 7.14E-16 |
| CU | 65 | 0.00E+00 | 5.27E-13 | 1.28E-12 | 2.17E-12 | 3.17E-12 | 7.97E-12 | 2.46E-11 | 5.28E-11 | 8.12E-11 | 1.10E-10 | 1.70E-10 |
| CU | 66 | 0.00E+00 | 4.05E-19 | 4.05E-19 | 4.05E-19 | 4.05E-19 | 4.05E-19 | 4.05E-19 | 4.05E-19 | 4.05E-19 | 4.05E-19 | 4.05E-19 |
| CU | 67 | 0.00E+00 | 4.37E-17 | 4.37E-17 | 4.37E-17 | 4.37E-17 | 4.37E-17 | 4.37E-17 | 4.37E-17 | 4.37E-17 | 4.37E-17 | 4.37E-17 |
| ZN | 63 | 0.00E+00 | 1.88E-16 | 1.88E-16 | 1.88E-16 | 1.88E-16 | 1.88E-16 | 1.88E-16 | 1.88E-16 | 1.88E-16 | 1.88E-16 | 1.88E-16 |
| ZN | 64 | 0.00E+00 | 4.37E-13 | 8.88E-13 | 1.33E-12 | 1.77E-12 | 3.55E-12 | 8.88E-12 | 1.77E-11 | 2.66E-11 | 3.54E-11 | 5.31E-11 |
| ZN | 65 | 0.00E+00 | 8.72E-13 | 1.57E-12 | 2.09E-12 | 2.49E-12 | 3.38E-12 | 3.84E-12 | 3.86E-12 | 3.86E-12 | 3.86E-12 | 3.86E-12 |
| ZN | 66 | 0.00E+00 | 2.13E-14 | 4.32E-14 | 6.49E-14 | 8.62E-14 | 1.73E-13 | 4.32E-13 | 8.62E-13 | 1.29E-12 | 1.73E-12 | 2.59E-12 |
| ZN | 67 | 0.00E+00 | 7.75E-14 | 1.57E-13 | 2.36E-13 | 3.14E-13 | 6.29E-13 | 1.57E-12 | 3.14E-12 | 4.71E-12 | 6.29E-12 | 9.43E-12 |
| ZN | 68 | 0.00E+00 | 2.51E-14 | 5.10E-14 | 7.65E-14 | 1.02E-13 | 2.04E-13 | 5.10E-13 | 1.02E-12 | 1.53E-12 | 2.04E-12 | 3.06E-12 |
| ZN | 69 | 0.00E+00 | 6.96E-18 | 6.96E-18 | 6.96E-18 | 6.96E-18 | 6.96E-18 | 6.96E-18 | 6.96E-18 | 6.96E-18 | 6.96E-18 | 6.96E-18 |
| ZN | 70 | 0.00E+00 | 5.00E-18 | 1.02E-17 | 1.52E-17 | 2.03E-17 | 4.06E-17 | 1.02E-16 | 2.03E-16 | 3.04E-16 | 4.06E-16 | 6.08E-16 |
| GA | 69 | 0.00E+00 | 1.13E-14 | 2.29E-14 | 3.43E-14 | 4.56E-14 | 9.13E-14 | 2.29E-13 | 4.56E-13 | 6.84E-13 | 9.13E-13 | 1.37E-12 |
| GA | 71 | 0.00E+00 | 3.06E-16 | 6.21E-16 | 9.32E-16 | 1.24E-15 | 2.48E-15 | 6.21E-15 | 1.24E-14 | 1.86E-14 | 2.48E-14 | 3.72E-14 |
| AS | 75 | 0.00E+00 | 8.99E-14 | 3.17E-13 | 6.18E-13 | 9.59E-13 | 2.52E-12 | 7.43E-12 | 1.63E-11 | 2.53E-11 | 3.43E-11 | 5.14E-11 |
| SE | 75 | 0.00E+00 | 3.14E-13 | 5.03E-13 | 6.12E-13 | 6.75E-13 | 7.55E-13 | 7.66E-13 | 7.66E-13 | 7.66E-13 | 7.66E-13 | 7.66E-13 |
| BR | 81 | 0.00E+00 | 4.04E-13 | 8.21E-13 | 1.23E-12 | 1.64E-12 | 3.28E-12 | 8.21E-12 | 1.64E-11 | 2.46E-11 | 3.28E-11 | 4.91E-11 |
| BR | 82 | 0.00E+00 | 3.19E-17 | 3.19E-17 | 3.19E-17 | 3.19E-17 | 3.19E-17 | 3.19E-17 | 3.19E-17 | 3.19E-17 | 3.19E-17 | 3.19E-17 |
| BR | 83 | 0.00E+00 | 2.73E-19 | 2.73E-19 | 2.73E-19 | 2.73E-19 | 2.73E-19 | 2.73E-19 | 2.73E-19 | 2.73E-19 | 2.73E-19 | 2.73E-19 |
| BR | 84 | 0.00E+00 | 1.35E-19 | 1.35E-19 | 1.35E-19 | 1.35E-19 | 1.35E-19 | 1.35E-19 | 1.35E-19 | 1.35E-19 | 1.35E-19 | 1.35E-19 |
| KR | 80 | 0.00E+00 | 4.04E-13 | 8.20E-13 | 1.23E-12 | 1.63E-12 | 3.27E-12 | 8.20E-12 | 1.63E-11 | 2.45E-11 | 3.27E-11 | 4.91E-11 |

**Table A.6. (continued)**

| Proton beam energy: 1 GeV | | | | | | | Operational line loss assumption: 1 nA/m (continuous) | | | | | |
|---|---|---|---|---|---|---|---|---|---|---|---|---|
| Nuclide masses integrated over the material zone volume in the HETC & MCNP calculational model | | | | | | | | | | | | |
| Nuclide concentration | | Time (s) | 7.88E+06 | 1.58E+07 | 2.37E+07 | 3.15E+07 | 6.31E+07 | 1.58E+08 | 3.15E+08 | 4.73E+08 | 6.31E+08 | 9.46E+08 |
| (gram-atoms) | | Initial | 3 months | 6 months | 9 months | 1 year | 2 years | 5 years | 10 years | 15 years | 20 years | 30 years |
| KR | 81 | 0.00E+00 | 1.21E-12 | 2.46E-12 | 3.69E-12 | 4.91E-12 | 9.83E-12 | 2.46E-11 | 4.90E-11 | 7.36E-11 | 9.82E-11 | 1.47E-10 |
| KR | 82 | 0.00E+00 | 8.09E-13 | 1.64E-12 | 2.46E-12 | 3.27E-12 | 6.56E-12 | 1.64E-11 | 3.27E-11 | 4.92E-11 | 6.56E-11 | 9.83E-11 |
| KR | 83 | 0.00E+00 | 9.26E-13 | 2.03E-12 | 3.20E-12 | 4.38E-12 | 9.28E-12 | 2.46E-11 | 4.97E-11 | 7.49E-11 | 1.00E-10 | 1.50E-10 |
| KR | 83M | 0.00E+00 | 2.12E-19 | 2.12E-19 | 2.12E-19 | 2.12E-19 | 2.12E-19 | 2.12E-19 | 2.12E-19 | 2.12E-19 | 2.12E-19 | 2.12E-19 |
| KR | 84 | 0.00E+00 | 1.24E-13 | 3.36E-13 | 5.56E-13 | 7.76E-13 | 1.78E-12 | 4.57E-12 | 9.11E-12 | 1.37E-11 | 1.83E-11 | 2.73E-11 |
| KR | 85 | 0.00E+00 | 4.14E-13 | 8.33E-13 | 1.24E-12 | 1.63E-12 | 3.17E-12 | 7.23E-12 | 1.24E-11 | 1.62E-11 | 1.90E-11 | 2.24E-11 |
| KR | 85M | 0.00E+00 | 1.26E-20 | 1.26E-20 | 1.26E-20 | 1.26E-20 | 1.26E-20 | 1.26E-20 | 1.26E-20 | 1.26E-20 | 1.26E-20 | 1.26E-20 |
| KR | 86 | 0.00E+00 | 6.91E-16 | 1.40E-15 | 2.11E-15 | 2.80E-15 | 5.61E-15 | 1.40E-14 | 2.80E-14 | 4.20E-14 | 5.61E-14 | 8.41E-14 |
| KR | 87 | 0.00E+00 | 1.26E-18 | 1.26E-18 | 1.26E-18 | 1.26E-18 | 1.26E-18 | 1.26E-18 | 1.26E-18 | 1.26E-18 | 1.26E-18 | 1.26E-18 |
| RB | 81 | 0.00E+00 | 2.47E-15 | 2.47E-15 | 2.47E-15 | 2.47E-15 | 2.47E-15 | 2.47E-15 | 2.47E-15 | 2.47E-15 | 2.47E-15 | 2.47E-15 |
| RB | 82 | 0.00E+00 | 5.61E-18 | 5.61E-18 | 5.61E-18 | 5.61E-18 | 5.61E-18 | 5.61E-18 | 5.61E-18 | 5.61E-18 | 5.61E-18 | 5.61E-18 |
| RB | 83 | 0.00E+00 | 2.87E-13 | 4.29E-13 | 4.96E-13 | 5.28E-13 | 5.56E-13 | 5.58E-13 | 5.57E-13 | 5.57E-13 | 5.57E-13 | 5.57E-13 |
| RB | 84 | 0.00E+00 | 9.88E-14 | 1.14E-13 | 1.16E-13 | 1.16E-13 | 1.16E-13 | 1.16E-13 | 1.16E-13 | 1.16E-13 | 1.16E-13 | 1.16E-13 |
| RB | 85 | 0.00E+00 | 3.59E-15 | 1.41E-14 | 3.12E-14 | 5.44E-14 | 2.12E-13 | 1.24E-12 | 4.45E-12 | 9.13E-12 | 1.49E-11 | 2.83E-11 |
| RB | 86 | 0.00E+00 | 3.16E-13 | 3.28E-13 | 3.28E-13 | 3.28E-13 | 3.28E-13 | 3.28E-13 | 3.28E-13 | 3.28E-13 | 3.28E-13 | 3.28E-13 |
| RB | 87 | 0.00E+00 | 4.05E-13 | 8.23E-13 | 1.23E-12 | 1.64E-12 | 3.29E-12 | 8.23E-12 | 1.64E-11 | 2.46E-11 | 3.29E-11 | 4.93E-11 |
| RB | 88 | 0.00E+00 | 9.80E-18 | 9.80E-18 | 9.80E-18 | 9.80E-18 | 9.80E-18 | 9.80E-18 | 9.80E-18 | 9.80E-18 | 9.80E-18 | 9.80E-18 |
| SR | 84 | 0.00E+00 | 3.67E-15 | 1.01E-14 | 1.67E-14 | 2.34E-14 | 5.38E-14 | 1.38E-13 | 2.76E-13 | 4.14E-13 | 5.52E-13 | 8.24E-13 |
| SR | 86 | 0.00E+00 | 7.81E-13 | 1.90E-12 | 3.02E-12 | 4.12E-12 | 8.90E-12 | 2.26E-11 | 4.51E-11 | 6.77E-11 | 9.03E-11 | 1.35E-10 |
| SR | 88 | 0.00E+00 | 4.98E-14 | 1.01E-13 | 1.52E-13 | 2.02E-13 | 4.04E-13 | 1.01E-12 | 2.02E-12 | 3.03E-12 | 4.04E-12 | 6.05E-12 |
| I | 127 | 0.00E+00 | 1.89E-19 | 5.30E-19 | 8.92E-19 | 1.25E-18 | 2.93E-18 | 7.55E-18 | 1.51E-17 | 2.26E-17 | 3.02E-17 | 4.50E-17 |
| XE | 126 | 0.00E+00 | 1.51E-19 | 3.06E-19 | 4.59E-19 | 6.10E-19 | 1.22E-18 | 3.06E-18 | 6.10E-18 | 9.16E-18 | 1.22E-17 | 1.83E-17 |
| XE | 127 | 0.00E+00 | 1.73E-19 | 2.04E-19 | 2.10E-19 | 2.11E-19 | 2.11E-19 | 2.11E-19 | 2.11E-19 | 2.11E-19 | 2.11E-19 | 2.11E-19 |
| XE | 128 | 0.00E+00 | 3.54E-18 | 7.31E-18 | 1.10E-17 | 1.47E-17 | 2.95E-17 | 7.41E-17 | 1.48E-16 | 2.22E-16 | 2.96E-16 | 4.44E-16 |
| XE | 129 | 0.00E+00 | 5.30E-17 | 1.09E-16 | 1.64E-16 | 2.18E-16 | 4.35E-16 | 1.08E-15 | 2.15E-15 | 3.23E-15 | 4.31E-15 | 6.46E-15 |
| XE | 130 | 0.00E+00 | 3.76E-18 | 7.65E-18 | 1.15E-17 | 1.52E-17 | 3.05E-17 | 7.65E-17 | 1.52E-16 | 2.29E-16 | 3.05E-16 | 4.58E-16 |
| XE | 131 | 0.00E+00 | 3.05E-16 | 7.78E-16 | 1.25E-15 | 1.71E-15 | 3.65E-15 | 9.34E-15 | 1.87E-14 | 2.81E-14 | 3.76E-14 | 5.63E-14 |
| XE | 132 | 0.00E+00 | 2.39E-17 | 4.93E-17 | 7.44E-17 | 9.91E-17 | 1.97E-16 | 4.90E-16 | 9.73E-16 | 1.46E-15 | 1.95E-15 | 2.92E-15 |
| XE | 133 | 0.00E+00 | 9.38E-19 | 9.38E-19 | 9.38E-19 | 9.38E-19 | 9.38E-19 | 9.38E-19 | 9.38E-19 | 9.38E-19 | 9.38E-19 | 9.38E-19 |
| XE | 134 | 0.00E+00 | 2.70E-17 | 5.49E-17 | 8.23E-17 | 1.09E-16 | 2.19E-16 | 5.49E-16 | 1.09E-15 | 1.64E-15 | 2.19E-15 | 3.28E-15 |
| XE | 135 | 0.00E+00 | 7.68E-19 | 7.68E-19 | 7.68E-19 | 7.68E-19 | 7.68E-19 | 7.68E-19 | 7.68E-19 | 7.68E-19 | 7.68E-19 | 7.68E-19 |

**Table A.6. (continued)**

| Proton beam energy: 1 GeV | | | | | | | Operational line loss assumption: 1 nA/m (continuous) | | | | | |
|---|---|---|---|---|---|---|---|---|---|---|---|---|
| Nuclide masses integrated over the material zone volume in the HETC & MCNP calculational model | | | | | | | | | | | | |
| Nuclide concentration | | Time (s) | 7.88E+06 | 1.58E+07 | 2.37E+07 | 3.15E+07 | 6.31E+07 | 1.58E+08 | 3.15E+08 | 4.73E+08 | 6.31E+08 | 9.46E+08 |
| (gram-atoms) | | Initial | 3 months | 6 months | 9 months | 1 year | 2 years | 5 years | 10 years | 15 years | 20 years | 30 years |
| XE | 136 | 0.00E+00 | 2.59E-18 | 5.26E-18 | 7.89E-18 | 1.05E-17 | 2.10E-17 | 5.26E-17 | 1.05E-16 | 1.57E-16 | 2.10E-16 | 3.15E-16 |
| CS | 129 | 0.00E+00 | 1.14E-18 | 1.14E-18 | 1.14E-18 | 1.14E-18 | 1.14E-18 | 1.14E-18 | 1.14E-18 | 1.14E-18 | 1.14E-18 | 1.14E-18 |
| CS | 131 | 0.00E+00 | 6.91E-17 | 7.06E-17 | 7.06E-17 | 7.06E-17 | 7.06E-17 | 7.06E-17 | 7.06E-17 | 7.06E-17 | 7.06E-17 | 7.06E-17 |
| CS | 132 | 0.00E+00 | 7.67E-19 | 7.67E-19 | 7.67E-19 | 7.67E-19 | 7.67E-19 | 7.67E-19 | 7.67E-19 | 7.67E-19 | 7.67E-19 | 7.67E-19 |
| CS | 133 | 0.00E+00 | 5.35E-17 | 1.51E-16 | 2.87E-16 | 4.60E-16 | 1.54E-15 | 8.12E-15 | 2.81E-14 | 5.69E-14 | 9.20E-14 | 1.74E-13 |
| CS | 134 | 0.00E+00 | 5.12E-17 | 9.97E-17 | 1.44E-16 | 1.83E-16 | 3.15E-16 | 5.24E-16 | 6.21E-16 | 6.39E-16 | 6.42E-16 | 6.43E-16 |
| CS | 135 | 0.00E+00 | 1.64E-16 | 3.33E-16 | 5.00E-16 | 6.65E-16 | 1.33E-15 | 3.33E-15 | 6.63E-15 | 9.95E-15 | 1.33E-14 | 1.99E-14 |
| CS | 136 | 0.00E+00 | 1.91E-17 | 1.92E-17 | 1.92E-17 | 1.92E-17 | 1.92E-17 | 1.92E-17 | 1.92E-17 | 1.92E-17 | 1.92E-17 | 1.92E-17 |
| CS | 137 | 0.00E+00 | 3.47E-16 | 7.02E-16 | 1.05E-15 | 1.39E-15 | 2.76E-15 | 6.67E-15 | 1.26E-14 | 1.79E-14 | 2.26E-14 | 3.05E-14 |
| CS | 138 | 0.00E+00 | 1.39E-19 | 1.39E-19 | 1.39E-19 | 1.39E-19 | 1.39E-19 | 1.39E-19 | 1.39E-19 | 1.39E-19 | 1.39E-19 | 1.39E-19 |
| BA | 128 | 0.00E+00 | 1.17E-19 | 1.17E-19 | 1.17E-19 | 1.17E-19 | 1.17E-19 | 1.17E-19 | 1.17E-19 | 1.17E-19 | 1.17E-19 | 1.17E-19 |
| BA | 129 | 0.00E+00 | 7.45E-20 | 7.45E-20 | 7.45E-20 | 7.45E-20 | 7.45E-20 | 7.45E-20 | 7.45E-20 | 7.45E-20 | 7.45E-20 | 7.45E-20 |
| BA | 130 | 0.00E+00 | 9.02E-18 | 1.83E-17 | 2.75E-17 | 3.65E-17 | 7.32E-17 | 1.83E-16 | 3.65E-16 | 5.49E-16 | 7.32E-16 | 1.10E-15 |
| BA | 131 | 0.00E+00 | 8.68E-17 | 8.73E-17 | 8.73E-17 | 8.73E-17 | 8.73E-17 | 8.73E-17 | 8.73E-17 | 8.73E-17 | 8.73E-17 | 8.73E-17 |
| BA | 132 | 0.00E+00 | 4.04E-13 | 8.21E-13 | 1.23E-12 | 1.64E-12 | 3.28E-12 | 8.21E-12 | 1.64E-11 | 2.46E-11 | 3.28E-11 | 4.91E-11 |
| BA | 133 | 0.00E+00 | 2.48E-15 | 5.00E-15 | 7.43E-15 | 9.80E-15 | 1.90E-14 | 4.33E-14 | 7.45E-14 | 9.71E-14 | 1.13E-13 | 1.34E-13 |
| BA | 134 | 0.00E+00 | 1.20E-14 | 2.43E-14 | 3.65E-14 | 4.85E-14 | 9.72E-14 | 2.44E-13 | 4.86E-13 | 7.30E-13 | 9.75E-13 | 1.46E-12 |
| BA | 135 | 0.00E+00 | 6.28E-15 | 1.27E-14 | 1.91E-14 | 2.54E-14 | 5.09E-14 | 1.27E-13 | 2.54E-13 | 3.82E-13 | 5.09E-13 | 7.63E-13 |
| BA | 136 | 0.00E+00 | 4.55E-14 | 9.24E-14 | 1.39E-13 | 1.84E-13 | 3.69E-13 | 9.24E-13 | 1.84E-12 | 2.77E-12 | 3.69E-12 | 5.53E-12 |
| BA | 137 | 0.00E+00 | 4.11E-14 | 8.35E-14 | 1.25E-13 | 1.66E-13 | 3.33E-13 | 8.35E-13 | 1.67E-12 | 2.50E-12 | 3.34E-12 | 5.01E-12 |
| BA | 138 | 0.00E+00 | 7.52E-15 | 1.53E-14 | 2.29E-14 | 3.05E-14 | 6.10E-14 | 1.53E-13 | 3.05E-13 | 4.57E-13 | 6.10E-13 | 9.15E-13 |
| BA | 139 | 0.00E+00 | 7.36E-18 | 7.36E-18 | 7.36E-18 | 7.36E-18 | 7.36E-18 | 7.36E-18 | 7.36E-18 | 7.36E-18 | 7.36E-18 | 7.36E-18 |
| LA | 139 | 0.00E+00 | 7.94E-15 | 1.61E-14 | 2.42E-14 | 3.22E-14 | 6.44E-14 | 1.61E-13 | 3.22E-13 | 4.83E-13 | 6.44E-13 | 9.66E-13 |
| EU | 155 | 0.00E+00 | 9.10E-20 | 1.81E-19 | 2.67E-19 | 3.49E-19 | 6.52E-19 | 1.34E-18 | 1.99E-18 | 2.30E-18 | 2.46E-18 | 2.57E-18 |
| EU | 156 | 0.00E+00 | 1.65E-19 | 1.68E-19 | 1.68E-19 | 1.68E-19 | 1.68E-19 | 1.68E-19 | 1.68E-19 | 1.68E-19 | 1.68E-19 | 1.68E-19 |
| GD | 156 | 0.00E+00 | 5.31E-19 | 1.24E-18 | 1.95E-18 | 2.65E-18 | 5.64E-18 | 1.43E-17 | 2.85E-17 | 4.28E-17 | 5.71E-17 | 8.54E-17 |
| GD | 157 | 0.00E+00 | 1.93E-19 | 5.11E-19 | 9.42E-19 | 1.48E-18 | 4.83E-18 | 2.60E-17 | 9.72E-17 | 2.14E-16 | 3.74E-16 | 8.19E-16 |
| GD | 158 | 0.00E+00 | 1.12E-18 | 2.44E-18 | 3.89E-18 | 5.49E-18 | 1.35E-17 | 5.30E-17 | 1.68E-16 | 3.44E-16 | 5.80E-16 | 1.22E-15 |
| GD | 159 | 0.00E+00 | 1.24E-20 | 1.24E-20 | 1.24E-20 | 1.24E-20 | 1.24E-20 | 1.24E-20 | 1.24E-20 | 1.24E-20 | 1.24E-20 | 1.24E-20 |
| TB | 157 | 0.00E+00 | 9.97E-17 | 2.02E-16 | 3.03E-16 | 4.03E-16 | 8.05E-16 | 2.00E-15 | 3.95E-15 | 5.86E-15 | 7.73E-15 | 1.13E-14 |
| TB | 158 | 0.00E+00 | 1.66E-16 | 3.37E-16 | 5.06E-16 | 6.72E-16 | 1.34E-15 | 3.34E-15 | 6.58E-15 | 9.77E-15 | 1.29E-14 | 1.89E-14 |

| Table A.6. (continued) | | | | | | | | | | | | |
|---|---|---|---|---|---|---|---|---|---|---|---|---|
| Proton beam energy: 1 GeV | | | | | | | Operational line loss assumption: 1 nA/m (continuous) | | | | | |
| Nuclide masses integrated over the material zone volume in the HETC & MCNP calculational model | | | | | | | | | | | | |
| Nuclide concentration | | Time (s) | 7.88E+06 | 1.58E+07 | 2.37E+07 | 3.15E+07 | 6.31E+07 | 1.58E+08 | 3.15E+08 | 4.73E+08 | 6.31E+08 | 9.46E+08 |
| (gram-atoms) | | Initial | 3 months | 6 months | 9 months | 1 year | 2 years | 5 years | 10 years | 15 years | 20 years | 30 years |
| TB | 159 | 0.00E+00 | 9.96E-19 | 2.04E-18 | 3.06E-18 | 4.07E-18 | 8.13E-18 | 2.03E-17 | 4.04E-17 | 6.07E-17 | 8.09E-17 | 1.21E-16 |
| TB | 160 | 0.00E+00 | 2.85E-15 | 4.08E-15 | 4.58E-15 | 4.78E-15 | 4.93E-15 | 4.93E-15 | 4.93E-15 | 4.93E-15 | 4.93E-15 | 4.93E-15 |
| DY | 158 | 0.00E+00 | 1.70E-20 | 7.03E-20 | 1.58E-19 | 2.79E-19 | 1.12E-18 | 6.98E-18 | 2.75E-17 | 6.16E-17 | 1.09E-16 | 2.41E-16 |
| DY | 160 | 0.00E+00 | 1.41E-15 | 4.57E-15 | 8.39E-15 | 1.25E-14 | 2.96E-14 | 8.65E-14 | 1.77E-13 | 2.69E-13 | 3.60E-13 | 5.37E-13 |
| Total | | 0.00E+00 | 4.32E-08 | 8.77E-08 | 1.32E-07 | 1.75E-07 | 3.50E-07 | 8.77E-07 | 1.75E-06 | 2.62E-06 | 3.50E-06 | 5.25E-06 |

| Table A.7. SNS nuclide production during normal proton beam operation: earth berm Zone 3 | | | | | | | | | | | | |
|---|---|---|---|---|---|---|---|---|---|---|---|---|
| Proton beam energy: 1 GeV | | | | | | | Operational line loss assumption: 1 nA/m (continuous) | | | | | |
| Nuclide masses integrated over the material zone volume in the HETC & MCNP calculational model | | | | | | | | | | | | |
| Nuclide concentration | | Time (s) | 7.88E+06 | 1.58E+07 | 2.37E+07 | 3.15E+07 | 6.31E+07 | 1.58E+08 | 3.15E+08 | 4.73E+08 | 6.31E+08 | 9.46E+08 |
| (gram-atoms) | | Initial | 3 months | 6 months | 9 months | 1 year | 2 years | 5 years | 10 years | 15 years | 20 years | 30 years |
| H | 1 | 0.00E+00 | 1.24E-08 | 2.51E-08 | 3.77E-08 | 5.01E-08 | 1.00E-07 | 2.51E-07 | 5.01E-07 | 7.52E-07 | 1.00E-06 | 1.50E-06 |
| H | 2 | 0.00E+00 | 3.67E-10 | 7.46E-10 | 1.12E-09 | 1.49E-09 | 2.98E-09 | 7.46E-09 | 1.49E-08 | 2.23E-08 | 2.98E-08 | 4.47E-08 |
| **H** | **3** | **0.00E+00** | **2.62E-10** | **5.28E-10** | **7.86E-10** | **1.04E-09** | **2.02E-09** | **4.66E-09** | **8.16E-09** | **1.08E-08** | **1.28E-08** | **1.55E-08** |
| HE | 3 | 0.00E+00 | 4.98E-11 | 1.05E-10 | 1.63E-10 | 2.24E-10 | 5.05E-10 | 1.66E-09 | 4.45E-09 | 8.12E-09 | 1.24E-08 | 2.24E-08 |
| HE | 4 | 0.00E+00 | 2.62E-09 | 5.32E-09 | 7.98E-09 | 1.06E-08 | 2.12E-08 | 5.32E-08 | 1.06E-07 | 1.59E-07 | 2.12E-07 | 3.18E-07 |
| LI | 6 | 0.00E+00 | 4.16E-11 | 8.44E-11 | 1.27E-10 | 1.68E-10 | 3.37E-10 | 8.44E-10 | 1.68E-09 | 2.53E-09 | 3.37E-09 | 5.06E-09 |
| LI | 7 | 0.00E+00 | 3.42E-12 | 7.96E-12 | 1.27E-11 | 1.76E-11 | 3.72E-11 | 9.84E-11 | 1.98E-10 | 2.99E-10 | 3.99E-10 | 5.97E-10 |
| LI | 8 | 0.00E+00 | 1.89E-19 | 1.89E-19 | 1.89E-19 | 1.89E-19 | 1.89E-19 | 1.89E-19 | 1.89E-19 | 1.89E-19 | 1.89E-19 | 1.89E-19 |
| BE | 7 | 0.00E+00 | 1.43E-12 | 1.88E-12 | 2.01E-12 | 2.05E-12 | 2.07E-12 | 2.07E-12 | 2.07E-12 | 2.07E-12 | 2.07E-12 | 2.07E-12 |
| BE | 9 | 0.00E+00 | 9.26E-12 | 1.88E-11 | 2.82E-11 | 3.75E-11 | 7.51E-11 | 1.88E-10 | 3.75E-10 | 5.63E-10 | 7.51E-10 | 1.13E-09 |
| **BE** | **10** | **0.00E+00** | **2.03E-12** | **4.12E-12** | **6.18E-12** | **8.21E-12** | **1.64E-11** | **4.12E-11** | **8.21E-11** | **1.23E-10** | **1.64E-10** | **2.47E-10** |
| BE | 11 | 0.00E+00 | 1.02E-18 | 1.02E-18 | 1.02E-18 | 1.02E-18 | 1.02E-18 | 1.02E-18 | 1.02E-18 | 1.02E-18 | 1.02E-18 | 1.02E-18 |
| B | 10 | 0.00E+00 | 9.36E-11 | 1.90E-10 | 2.85E-10 | 3.79E-10 | 7.60E-10 | 1.90E-09 | 3.79E-09 | 5.69E-09 | 7.60E-09 | 1.14E-08 |
| B | 11 | 0.00E+00 | 1.10E-10 | 2.23E-10 | 3.35E-10 | 4.45E-10 | 8.92E-10 | 2.23E-09 | 4.45E-09 | 6.68E-09 | 8.92E-09 | 1.34E-08 |
| B | 12 | 0.00E+00 | 7.49E-20 | 7.49E-20 | 7.49E-20 | 7.49E-20 | 7.49E-20 | 7.49E-20 | 7.49E-20 | 7.49E-20 | 7.49E-20 | 7.49E-20 |
| B | 13 | 0.00E+00 | 1.17E-20 | 1.17E-20 | 1.17E-20 | 1.17E-20 | 1.17E-20 | 1.17E-20 | 1.17E-20 | 1.17E-20 | 1.17E-20 | 1.17E-20 |
| C | 11 | 0.00E+00 | 6.59E-15 | 6.59E-15 | 6.59E-15 | 6.59E-15 | 6.59E-15 | 6.59E-15 | 6.59E-15 | 6.59E-15 | 6.59E-15 | 6.59E-15 |
| C | 12 | 0.00E+00 | 1.50E-09 | 3.04E-09 | 4.55E-09 | 6.05E-09 | 1.21E-08 | 3.04E-08 | 6.05E-08 | 9.09E-08 | 1.21E-07 | 1.82E-07 |
| C | 13 | 0.00E+00 | 1.13E-09 | 2.30E-09 | 3.46E-09 | 4.59E-09 | 9.20E-09 | 2.30E-08 | 4.59E-08 | 6.90E-08 | 9.20E-08 | 1.38E-07 |
| **C** | **14** | **0.00E+00** | **1.57E-10** | **3.19E-10** | **4.78E-10** | **6.35E-10** | **1.27E-09** | **3.18E-09** | **6.35E-09** | **9.53E-09** | **1.27E-08** | **1.90E-08** |
| N | 13 | 0.00E+00 | 1.47E-14 | 1.47E-14 | 1.47E-14 | 1.47E-14 | 1.47E-14 | 1.47E-14 | 1.47E-14 | 1.47E-14 | 1.47E-14 | 1.47E-14 |
| N | 14 | 0.00E+00 | 1.51E-09 | 3.07E-09 | 4.61E-09 | 6.12E-09 | 1.23E-08 | 3.07E-08 | 6.12E-08 | 9.19E-08 | 1.23E-07 | 1.84E-07 |
| N | 15 | 0.00E+00 | 2.31E-09 | 4.69E-09 | 7.04E-09 | 9.35E-09 | 1.87E-08 | 4.69E-08 | 9.35E-08 | 1.40E-07 | 1.87E-07 | 2.81E-07 |
| N | 16 | 0.00E+00 | 1.53E-16 | 1.53E-16 | 1.53E-16 | 1.53E-16 | 1.53E-16 | 1.53E-16 | 1.53E-16 | 1.53E-16 | 1.53E-16 | 1.53E-16 |
| N | 17 | 0.00E+00 | 1.74E-18 | 1.74E-18 | 1.74E-18 | 1.74E-18 | 1.74E-18 | 1.74E-18 | 1.74E-18 | 1.74E-18 | 1.74E-18 | 1.74E-18 |
| O | 14 | 0.00E+00 | 2.38E-16 | 2.38E-16 | 2.38E-16 | 2.38E-16 | 2.38E-16 | 2.38E-16 | 2.38E-16 | 2.38E-16 | 2.38E-16 | 2.38E-16 |
| O | 15 | 0.00E+00 | 1.18E-14 | 1.18E-14 | 1.18E-14 | 1.18E-14 | 1.18E-14 | 1.18E-14 | 1.18E-14 | 1.18E-14 | 1.18E-14 | 1.18E-14 |
| O | 16 | 0.00E+00 | 6.97E-10 | 1.42E-09 | 2.12E-09 | 2.82E-09 | 5.65E-09 | 1.42E-08 | 2.82E-08 | 4.24E-08 | 5.65E-08 | 8.47E-08 |
| O | 17 | 0.00E+00 | 5.20E-11 | 1.06E-10 | 1.58E-10 | 2.11E-10 | 4.22E-10 | 1.06E-09 | 2.11E-09 | 3.16E-09 | 4.22E-09 | 6.32E-09 |
| O | 18 | 0.00E+00 | 2.17E-11 | 4.40E-11 | 6.61E-11 | 8.78E-11 | 1.76E-10 | 4.40E-10 | 8.78E-10 | 1.32E-09 | 1.76E-09 | 2.64E-09 |
| O | 19 | 0.00E+00 | 4.59E-19 | 4.59E-19 | 4.59E-19 | 4.59E-19 | 4.59E-19 | 4.59E-19 | 4.59E-19 | 4.59E-19 | 4.59E-19 | 4.59E-19 |
| F | 17 | 0.00E+00 | 9.66E-18 | 9.66E-18 | 9.66E-18 | 9.66E-18 | 9.66E-18 | 9.66E-18 | 9.66E-18 | 9.66E-18 | 9.66E-18 | 9.66E-18 |
| F | 18 | 0.00E+00 | 2.25E-14 | 2.25E-14 | 2.25E-14 | 2.25E-14 | 2.25E-14 | 2.25E-14 | 2.25E-14 | 2.25E-14 | 2.25E-14 | 2.25E-14 |

**Table A.7. (continued)**

| Proton beam energy: 1 GeV | | | | | | | Operational line loss assumption: 1 nA/m (continuous) | | | | | |
|---|---|---|---|---|---|---|---|---|---|---|---|---|
| Nuclide masses integrated over the material zone volume in the HETC & MCNP calculational model | | | | | | | | | | | | |
| Nuclide concentration | | Time (s) | 7.88E+06 | 1.58E+07 | 2.37E+07 | 3.15E+07 | 6.31E+07 | 1.58E+08 | 3.15E+08 | 4.73E+08 | 6.31E+08 | 9.46E+08 |
| (gram-atoms) | | Initial | 3 months | 6 months | 9 months | 1 year | 2 years | 5 years | 10 years | 15 years | 20 years | 30 years |
| F | 19 | 0.00E+00 | 2.55E-11 | 5.18E-11 | 7.78E-11 | 1.03E-10 | 2.07E-10 | 5.18E-10 | 1.03E-09 | 1.55E-09 | 2.07E-09 | 3.10E-09 |
| F | 20 | 0.00E+00 | 5.02E-18 | 5.02E-18 | 5.02E-18 | 5.02E-18 | 5.02E-18 | 5.02E-18 | 5.02E-18 | 5.02E-18 | 5.02E-18 | 5.02E-18 |
| F | 21 | 0.00E+00 | 3.26E-19 | 3.26E-19 | 3.26E-19 | 3.26E-19 | 3.26E-19 | 3.26E-19 | 3.26E-19 | 3.26E-19 | 3.26E-19 | 3.26E-19 |
| F | 22 | 0.00E+00 | 3.17E-19 | 3.17E-19 | 3.17E-19 | 3.17E-19 | 3.17E-19 | 3.17E-19 | 3.17E-19 | 3.17E-19 | 3.17E-19 | 3.17E-19 |
| NE | 19 | 0.00E+00 | 1.03E-17 | 1.03E-17 | 1.03E-17 | 1.03E-17 | 1.03E-17 | 1.03E-17 | 1.03E-17 | 1.03E-17 | 1.03E-17 | 1.03E-17 |
| NE | 20 | 0.00E+00 | 5.41E-11 | 1.10E-10 | 1.65E-10 | 2.19E-10 | 4.38E-10 | 1.10E-09 | 2.19E-09 | 3.29E-09 | 4.38E-09 | 6.57E-09 |
| NE | 21 | 0.00E+00 | 2.23E-11 | 4.52E-11 | 6.78E-11 | 9.02E-11 | 1.81E-10 | 4.52E-10 | 9.02E-10 | 1.35E-09 | 1.81E-09 | 2.71E-09 |
| NE | 22 | 0.00E+00 | 1.23E-11 | 2.79E-11 | 4.60E-11 | 6.64E-11 | 1.71E-10 | 6.35E-10 | 1.64E-09 | 2.75E-09 | 3.89E-09 | 6.18E-09 |
| NE | 23 | 0.00E+00 | 1.27E-17 | 1.27E-17 | 1.27E-17 | 1.27E-17 | 1.27E-17 | 1.27E-17 | 1.27E-17 | 1.27E-17 | 1.27E-17 | 1.27E-17 |
| NE | 24 | 0.00E+00 | 6.10E-17 | 6.10E-17 | 6.10E-17 | 6.10E-17 | 6.10E-17 | 6.10E-17 | 6.10E-17 | 6.10E-17 | 6.10E-17 | 6.10E-17 |
| NA | 21 | 0.00E+00 | 6.73E-18 | 6.73E-18 | 6.73E-18 | 6.73E-18 | 6.73E-18 | 6.73E-18 | 6.73E-18 | 6.73E-18 | 6.73E-18 | 6.73E-18 |
| **NA** | **22** | **0.00E+00** | **4.43E-11** | **8.71E-11** | **1.26E-10** | **1.63E-10** | **2.88E-10** | **5.15E-10** | **6.52E-10** | **6.89E-10** | **6.98E-10** | **7.02E-10** |
| NA | 23 | 0.00E+00 | 2.20E-10 | 4.46E-10 | 6.69E-10 | 8.89E-10 | 1.78E-09 | 4.46E-09 | 8.89E-09 | 1.34E-08 | 1.78E-08 | 2.67E-08 |
| NA | 24 | 0.00E+00 | 5.47E-13 | 5.47E-13 | 5.47E-13 | 5.47E-13 | 5.47E-13 | 5.47E-13 | 5.47E-13 | 5.47E-13 | 5.47E-13 | 5.47E-13 |
| NA | 25 | 0.00E+00 | 1.45E-16 | 1.45E-16 | 1.45E-16 | 1.45E-16 | 1.45E-16 | 1.45E-16 | 1.45E-16 | 1.45E-16 | 1.45E-16 | 1.45E-16 |
| NA | 26 | 0.00E+00 | 5.14E-19 | 5.14E-19 | 5.14E-19 | 5.14E-19 | 5.14E-19 | 5.14E-19 | 5.14E-19 | 5.14E-19 | 5.14E-19 | 5.14E-19 |
| MG | 23 | 0.00E+00 | 1.72E-17 | 1.72E-17 | 1.72E-17 | 1.72E-17 | 1.72E-17 | 1.72E-17 | 1.72E-17 | 1.72E-17 | 1.72E-17 | 1.72E-17 |
| MG | 24 | 0.00E+00 | 6.65E-10 | 1.35E-09 | 2.03E-09 | 2.69E-09 | 5.39E-09 | 1.35E-08 | 2.69E-08 | 4.04E-08 | 5.39E-08 | 8.08E-08 |
| MG | 25 | 0.00E+00 | 3.95E-10 | 8.01E-10 | 1.20E-09 | 1.60E-09 | 3.20E-09 | 8.01E-09 | 1.60E-08 | 2.40E-08 | 3.20E-08 | 4.80E-08 |
| MG | 26 | 0.00E+00 | 3.59E-10 | 7.29E-10 | 1.09E-09 | 1.45E-09 | 2.91E-09 | 7.29E-09 | 1.45E-08 | 2.18E-08 | 2.91E-08 | 4.37E-08 |
| MG | 27 | 0.00E+00 | 6.55E-15 | 6.55E-15 | 6.55E-15 | 6.55E-15 | 6.55E-15 | 6.55E-15 | 6.55E-15 | 6.55E-15 | 6.55E-15 | 6.55E-15 |
| AL | 24 | 0.00E+00 | 1.54E-19 | 1.54E-19 | 1.54E-19 | 1.54E-19 | 1.54E-19 | 1.54E-19 | 1.54E-19 | 1.54E-19 | 1.54E-19 | 1.54E-19 |
| AL | 25 | 0.00E+00 | 1.77E-17 | 1.77E-17 | 1.77E-17 | 1.77E-17 | 1.77E-17 | 1.77E-17 | 1.77E-17 | 1.77E-17 | 1.77E-17 | 1.77E-17 |
| **AL** | **26** | **0.00E+00** | **4.08E-10** | **8.28E-10** | **1.24E-09** | **1.65E-09** | **3.31E-09** | **8.28E-09** | **1.65E-08** | **2.48E-08** | **3.31E-08** | **4.96E-08** |
| AL | 27 | 0.00E+00 | 1.14E-09 | 2.32E-09 | 3.48E-09 | 4.62E-09 | 9.26E-09 | 2.32E-08 | 4.62E-08 | 6.94E-08 | 9.26E-08 | 1.39E-07 |
| AL | 28 | 0.00E+00 | 6.47E-15 | 6.47E-15 | 6.47E-15 | 6.47E-15 | 6.47E-15 | 6.47E-15 | 6.47E-15 | 6.47E-15 | 6.47E-15 | 6.47E-15 |
| AL | 29 | 0.00E+00 | 1.35E-15 | 1.35E-15 | 1.35E-15 | 1.35E-15 | 1.35E-15 | 1.35E-15 | 1.35E-15 | 1.35E-15 | 1.35E-15 | 1.35E-15 |
| AL | 30 | 0.00E+00 | 1.59E-18 | 1.59E-18 | 1.59E-18 | 1.59E-18 | 1.59E-18 | 1.59E-18 | 1.59E-18 | 1.59E-18 | 1.59E-18 | 1.59E-18 |
| SI | 26 | 0.00E+00 | 1.65E-18 | 1.65E-18 | 1.65E-18 | 1.65E-18 | 1.65E-18 | 1.65E-18 | 1.65E-18 | 1.65E-18 | 1.65E-18 | 1.65E-18 |
| SI | 27 | 0.00E+00 | 9.45E-17 | 9.45E-17 | 9.45E-17 | 9.45E-17 | 9.45E-17 | 9.45E-17 | 9.45E-17 | 9.45E-17 | 9.45E-17 | 9.45E-17 |
| SI | 28 | 0.00E+00 | 5.00E-10 | 1.02E-09 | 1.52E-09 | 2.03E-09 | 4.06E-09 | 1.02E-08 | 2.03E-08 | 3.04E-08 | 4.06E-08 | 6.08E-08 |
| SI | 29 | 0.00E+00 | 6.16E-11 | 1.25E-10 | 1.88E-10 | 2.49E-10 | 5.00E-10 | 1.25E-09 | 2.49E-09 | 3.75E-09 | 5.00E-09 | 7.49E-09 |
| SI | 30 | 0.00E+00 | 1.12E-11 | 2.27E-11 | 3.41E-11 | 4.53E-11 | 9.07E-11 | 2.27E-10 | 4.53E-10 | 6.80E-10 | 9.07E-10 | 1.36E-09 |
| SI | 31 | 0.00E+00 | 1.96E-15 | 1.96E-15 | 1.96E-15 | 1.96E-15 | 1.96E-15 | 1.96E-15 | 1.96E-15 | 1.96E-15 | 1.96E-15 | 1.96E-15 |

| Table A.7. (continued) | | | | | | | | | | | | |
|---|---|---|---|---|---|---|---|---|---|---|---|---|
| Proton beam energy: 1 GeV | | | | | | | Operational line loss assumption: 1 nA/m (continuous) | | | | | |
| Nuclide masses integrated over the material zone volume in the HETC & MCNP calculational model | | | | | | | | | | | | |
| Nuclide concentration | | Time (s) | 7.88E+06 | 1.58E+07 | 2.37E+07 | 3.15E+07 | 6.31E+07 | 1.58E+08 | 3.15E+08 | 4.73E+08 | 6.31E+08 | 9.46E+08 |
| (gram-atoms) | | Initial | 3 months | 6 months | 9 months | 1 year | 2 years | 5 years | 10 years | 15 years | 20 years | 30 years |
| P | 31 | 0.00E+00 | 3.14E-12 | 6.37E-12 | 9.56E-12 | 1.27E-11 | 2.54E-11 | 6.37E-11 | 1.27E-10 | 1.91E-10 | 2.54E-10 | 3.81E-10 |
| P | 32 | 0.00E+00 | 1.00E-15 | 1.01E-15 | 1.01E-15 | 1.01E-15 | 1.01E-15 | 1.01E-15 | 1.01E-15 | 1.01E-15 | 1.01E-15 | 1.01E-15 |
| P | 33 | 0.00E+00 | 1.48E-13 | 1.61E-13 | 1.62E-13 | 1.62E-13 | 1.62E-13 | 1.62E-13 | 1.62E-13 | 1.62E-13 | 1.62E-13 | 1.62E-13 |
| S | 32 | 0.00E+00 | 3.43E-15 | 7.98E-15 | 1.25E-14 | 1.69E-14 | 3.59E-14 | 9.10E-14 | 1.81E-13 | 2.72E-13 | 3.63E-13 | 5.44E-13 |
| S | 33 | 0.00E+00 | 1.06E-12 | 2.30E-12 | 3.53E-12 | 4.74E-12 | 9.82E-12 | 2.48E-11 | 4.94E-11 | 7.41E-11 | 9.89E-11 | 1.48E-10 |
| S | 34 | 0.00E+00 | 8.07E-13 | 1.64E-12 | 2.46E-12 | 3.27E-12 | 6.55E-12 | 1.64E-11 | 3.27E-11 | 4.91E-11 | 6.55E-11 | 9.82E-11 |
| S | 35 | 0.00E+00 | 2.89E-13 | 4.34E-13 | 5.04E-13 | 5.37E-13 | 5.67E-13 | 5.69E-13 | 5.69E-13 | 5.69E-13 | 5.69E-13 | 5.69E-13 |
| S | 36 | 0.00E+00 | 3.51E-20 | 1.45E-19 | 3.26E-19 | 5.76E-19 | 2.31E-18 | 1.45E-17 | 5.76E-17 | 1.30E-16 | 2.31E-16 | 5.19E-16 |
| CL | 35 | 0.00E+00 | 4.44E-12 | 9.18E-12 | 1.39E-11 | 1.86E-11 | 3.78E-11 | 9.61E-11 | 1.92E-10 | 2.89E-10 | 3.86E-10 | 5.78E-10 |
| **CL** | **36** | **0.00E+00** | **6.71E-12** | **1.36E-11** | **2.04E-11** | **2.72E-11** | **5.44E-11** | **1.36E-10** | **2.72E-10** | **4.08E-10** | **5.44E-10** | **8.16E-10** |
| CL | 37 | 0.00E+00 | 8.73E-12 | 2.22E-11 | 3.61E-11 | 5.00E-11 | 1.13E-10 | 2.88E-10 | 5.74E-10 | 8.63E-10 | 1.15E-09 | 1.72E-09 |
| CL | 38 | 0.00E+00 | 2.56E-17 | 2.56E-17 | 2.56E-17 | 2.56E-17 | 2.56E-17 | 2.56E-17 | 2.56E-17 | 2.56E-17 | 2.56E-17 | 2.56E-17 |
| CL | 39 | 0.00E+00 | 2.35E-18 | 2.35E-18 | 2.35E-18 | 2.35E-18 | 2.35E-18 | 2.35E-18 | 2.35E-18 | 2.35E-18 | 2.35E-18 | 2.35E-18 |
| CL | 40 | 0.00E+00 | 1.75E-20 | 1.75E-20 | 1.75E-20 | 1.75E-20 | 1.75E-20 | 1.75E-20 | 1.75E-20 | 1.75E-20 | 1.75E-20 | 1.75E-20 |
| AR | 36 | 0.00E+00 | 2.44E-12 | 4.95E-12 | 7.43E-12 | 9.87E-12 | 1.98E-11 | 4.95E-11 | 9.87E-11 | 1.48E-10 | 1.98E-10 | 2.97E-10 |
| AR | 37 | 0.00E+00 | 5.15E-12 | 6.03E-12 | 6.17E-12 | 6.19E-12 | 6.20E-12 | 6.19E-12 | 6.19E-12 | 6.19E-12 | 6.19E-12 | 6.19E-12 |
| AR | 38 | 0.00E+00 | 2.27E-11 | 4.60E-11 | 6.90E-11 | 9.17E-11 | 1.84E-10 | 4.60E-10 | 9.17E-10 | 1.38E-09 | 1.84E-09 | 2.75E-09 |
| **AR** | **39** | **0.00E+00** | **1.25E-11** | **2.53E-11** | **3.80E-11** | **5.05E-11** | **1.01E-10** | **2.52E-10** | **4.99E-10** | **7.44E-10** | **9.87E-10** | **1.46E-09** |
| AR | 40 | 0.00E+00 | 4.23E-13 | 8.59E-13 | 1.29E-12 | 1.71E-12 | 3.43E-12 | 8.59E-12 | 1.71E-11 | 2.57E-11 | 3.43E-11 | 5.14E-11 |
| AR | 41 | 0.00E+00 | 6.28E-17 | 6.28E-17 | 6.28E-17 | 6.28E-17 | 6.28E-17 | 6.28E-17 | 6.28E-17 | 6.28E-17 | 6.28E-17 | 6.28E-17 |
| AR | 42 | 0.00E+00 | 1.77E-18 | 3.58E-18 | 5.36E-18 | 7.11E-18 | 1.41E-17 | 3.42E-17 | 6.48E-17 | 9.25E-17 | 1.17E-16 | 1.60E-16 |
| K | 38 | 0.00E+00 | 4.53E-16 | 4.53E-16 | 4.53E-16 | 4.53E-16 | 4.53E-16 | 4.53E-16 | 4.53E-16 | 4.53E-16 | 4.53E-16 | 4.53E-16 |
| K | 39 | 0.00E+00 | 3.80E-12 | 7.72E-12 | 1.16E-11 | 1.54E-11 | 3.10E-11 | 7.87E-11 | 1.60E-10 | 2.45E-10 | 3.33E-10 | 5.19E-10 |
| **K** | **40** | **0.00E+00** | **4.13E-12** | **8.40E-12** | **1.26E-11** | **1.67E-11** | **3.35E-11** | **8.40E-11** | **1.67E-10** | **2.51E-10** | **3.35E-10** | **5.03E-10** |
| K | 41 | 0.00E+00 | 4.56E-13 | 9.25E-13 | 1.39E-12 | 1.84E-12 | 3.70E-12 | 9.25E-12 | 1.84E-11 | 2.77E-11 | 3.70E-11 | 5.54E-11 |
| K | 42 | 0.00E+00 | 1.16E-15 | 1.16E-15 | 1.16E-15 | 1.16E-15 | 1.16E-15 | 1.16E-15 | 1.16E-15 | 1.16E-15 | 1.16E-15 | 1.16E-15 |
| K | 43 | 0.00E+00 | 1.74E-18 | 1.74E-18 | 1.74E-18 | 1.74E-18 | 1.74E-18 | 1.74E-18 | 1.74E-18 | 1.74E-18 | 1.74E-18 | 1.74E-18 |
| K | 44 | 0.00E+00 | 5.96E-20 | 5.96E-20 | 5.96E-20 | 5.96E-20 | 5.96E-20 | 5.96E-20 | 5.96E-20 | 5.96E-20 | 5.96E-20 | 5.96E-20 |
| CA | 40 | 0.00E+00 | 4.04E-13 | 8.20E-13 | 1.23E-12 | 1.63E-12 | 3.27E-12 | 8.20E-12 | 1.63E-11 | 2.45E-11 | 3.27E-11 | 4.91E-11 |
| **CA** | **41** | **0.00E+00** | **4.16E-13** | **8.45E-13** | **1.27E-12** | **1.68E-12** | **3.37E-12** | **8.45E-12** | **1.68E-11** | **2.53E-11** | **3.37E-11** | **5.06E-11** |
| CA | 42 | 0.00E+00 | 1.36E-12 | 2.75E-12 | 4.13E-12 | 5.49E-12 | 1.10E-11 | 2.75E-11 | 5.49E-11 | 8.24E-11 | 1.10E-10 | 1.65E-10 |
| CA | 43 | 0.00E+00 | 4.07E-12 | 8.26E-12 | 1.24E-11 | 1.65E-11 | 3.30E-11 | 8.26E-11 | 1.65E-10 | 2.47E-10 | 3.30E-10 | 4.94E-10 |
| CA | 44 | 0.00E+00 | 7.15E-12 | 1.45E-11 | 2.18E-11 | 2.90E-11 | 5.80E-11 | 1.45E-10 | 2.90E-10 | 4.35E-10 | 5.80E-10 | 8.69E-10 |
| CA | 45 | 0.00E+00 | 4.02E-13 | 6.84E-13 | 8.73E-13 | 1.00E-12 | 1.22E-12 | 1.28E-12 | 1.28E-12 | 1.28E-12 | 1.28E-12 | 1.28E-12 |

**Table A.7. (continued)**

| Proton beam energy: 1 GeV | | | | | | | Operational line loss assumption: 1 nA/m (continuous) | | | | | |
|---|---|---|---|---|---|---|---|---|---|---|---|---|
| Nuclide masses integrated over the material zone volume in the HETC & MCNP calculational model | | | | | | | | | | | | |
| Nuclide concentration | | Time (s) | 7.88E+06 | 1.58E+07 | 2.37E+07 | 3.15E+07 | 6.31E+07 | 1.58E+08 | 3.15E+08 | 4.73E+08 | 6.31E+08 | 9.46E+08 |
| (gram-atoms) | | Initial | 3 months | 6 months | 9 months | 1 year | 2 years | 5 years | 10 years | 15 years | 20 years | 30 years |
| CA | 46 | 0.00E+00 | 4.09E-13 | 8.30E-13 | 1.25E-12 | 1.66E-12 | 3.32E-12 | 8.30E-12 | 1.66E-11 | 2.49E-11 | 3.32E-11 | 4.97E-11 |
| CA | 47 | 0.00E+00 | 6.36E-16 | 6.36E-16 | 6.36E-16 | 6.36E-16 | 6.36E-16 | 6.36E-16 | 6.36E-16 | 6.36E-16 | 6.36E-16 | 6.36E-16 |
| CA | 48 | 0.00E+00 | 3.70E-16 | 7.51E-16 | 1.13E-15 | 1.50E-15 | 3.00E-15 | 7.51E-15 | 1.50E-14 | 2.25E-14 | 3.00E-14 | 4.49E-14 |
| SC | 43 | 0.00E+00 | 3.14E-15 | 3.14E-15 | 3.14E-15 | 3.14E-15 | 3.14E-15 | 3.14E-15 | 3.14E-15 | 3.14E-15 | 3.14E-15 | 3.14E-15 |
| SC | 44 | 0.00E+00 | 1.34E-14 | 1.34E-14 | 1.34E-14 | 1.34E-14 | 1.34E-14 | 1.34E-14 | 1.34E-14 | 1.34E-14 | 1.34E-14 | 1.34E-14 |
| SC | 45 | 0.00E+00 | 3.64E-12 | 7.52E-12 | 1.14E-11 | 1.54E-11 | 3.16E-11 | 8.08E-11 | 1.64E-10 | 2.47E-10 | 3.30E-10 | 4.95E-10 |
| SC | 46 | 0.00E+00 | 3.63E-13 | 5.40E-13 | 6.20E-13 | 6.58E-13 | 6.90E-13 | 6.92E-13 | 6.92E-13 | 6.92E-13 | 6.92E-13 | 6.92E-13 |
| SC | 47 | 0.00E+00 | 7.91E-14 | 7.91E-14 | 7.91E-14 | 7.91E-14 | 7.91E-14 | 7.91E-14 | 7.91E-14 | 7.91E-14 | 7.91E-14 | 7.91E-14 |
| SC | 48 | 0.00E+00 | 5.16E-15 | 5.16E-15 | 5.16E-15 | 5.16E-15 | 5.16E-15 | 5.16E-15 | 5.16E-15 | 5.16E-15 | 5.16E-15 | 5.16E-15 |
| SC | 49 | 0.00E+00 | 2.61E-16 | 2.61E-16 | 2.61E-16 | 2.61E-16 | 2.61E-16 | 2.61E-16 | 2.61E-16 | 2.61E-16 | 2.61E-16 | 2.61E-16 |
| SC | 50 | 0.00E+00 | 2.20E-20 | 2.20E-20 | 2.20E-20 | 2.20E-20 | 2.20E-20 | 2.20E-20 | 2.20E-20 | 2.20E-20 | 2.20E-20 | 2.20E-20 |
| TI | 45 | 0.00E+00 | 9.01E-16 | 9.01E-16 | 9.01E-16 | 9.01E-16 | 9.01E-16 | 9.01E-16 | 9.01E-16 | 9.01E-16 | 9.01E-16 | 9.01E-16 |
| TI | 46 | 0.00E+00 | 3.38E-12 | 7.06E-12 | 1.08E-11 | 1.45E-11 | 2.97E-11 | 7.60E-11 | 1.52E-10 | 2.29E-10 | 3.06E-10 | 4.58E-10 |
| TI | 47 | 0.00E+00 | 6.82E-12 | 1.39E-11 | 2.09E-11 | 2.78E-11 | 5.56E-11 | 1.39E-10 | 2.76E-10 | 4.15E-10 | 5.53E-10 | 8.30E-10 |
| TI | 48 | 0.00E+00 | 5.63E-12 | 1.23E-11 | 1.88E-11 | 2.53E-11 | 5.23E-11 | 1.32E-10 | 2.63E-10 | 3.94E-10 | 5.26E-10 | 7.88E-10 |
| TI | 49 | 0.00E+00 | 3.24E-12 | 7.39E-12 | 1.21E-11 | 1.73E-11 | 4.21E-11 | 1.31E-10 | 2.85E-10 | 4.40E-10 | 5.95E-10 | 9.31E-10 |
| TI | 50 | 0.00E+00 | 8.58E-13 | 1.74E-12 | 2.61E-12 | 3.47E-12 | 6.96E-12 | 1.74E-11 | 3.47E-11 | 5.22E-11 | 6.96E-11 | 1.04E-10 |
| TI | 51 | 0.00E+00 | 5.77E-19 | 5.77E-19 | 5.77E-19 | 5.77E-19 | 5.77E-19 | 5.77E-19 | 5.77E-19 | 5.77E-19 | 5.77E-19 | 5.77E-19 |
| V | 47 | 0.00E+00 | 1.46E-16 | 1.46E-16 | 1.46E-16 | 1.46E-16 | 1.46E-16 | 1.46E-16 | 1.46E-16 | 1.46E-16 | 1.46E-16 | 1.46E-16 |
| V | 48 | 0.00E+00 | 8.10E-13 | 8.26E-13 | 8.27E-13 | 8.27E-13 | 8.27E-13 | 8.27E-13 | 8.27E-13 | 8.27E-13 | 8.27E-13 | 8.27E-13 |
| V | 49 | 0.00E+00 | 4.41E-12 | 8.16E-12 | 1.12E-11 | 1.37E-11 | 2.00E-11 | 2.49E-11 | 2.54E-11 | 2.54E-11 | 2.54E-11 | 2.54E-11 |
| V | 50 | 0.00E+00 | 3.69E-12 | 7.50E-12 | 1.12E-11 | 1.49E-11 | 2.99E-11 | 7.50E-11 | 1.49E-10 | 2.24E-10 | 2.99E-10 | 4.49E-10 |
| V | 51 | 0.00E+00 | 1.06E-11 | 2.65E-11 | 4.27E-11 | 5.88E-11 | 1.30E-10 | 3.31E-10 | 6.60E-10 | 9.91E-10 | 1.32E-09 | 1.98E-09 |
| V | 52 | 0.00E+00 | 1.88E-17 | 1.88E-17 | 1.88E-17 | 1.88E-17 | 1.88E-17 | 1.88E-17 | 1.88E-17 | 1.88E-17 | 1.88E-17 | 1.88E-17 |
| CR | 49 | 0.00E+00 | 7.53E-16 | 7.53E-16 | 7.53E-16 | 7.53E-16 | 7.53E-16 | 7.53E-16 | 7.53E-16 | 7.53E-16 | 7.53E-16 | 7.53E-16 |
| CR | 50 | 0.00E+00 | 7.73E-12 | 1.57E-11 | 2.35E-11 | 3.13E-11 | 6.27E-11 | 1.57E-10 | 3.13E-10 | 4.70E-10 | 6.27E-10 | 9.39E-10 |
| CR | 51 | 0.00E+00 | 5.39E-12 | 5.96E-12 | 6.02E-12 | 6.02E-12 | 6.02E-12 | 6.02E-12 | 6.02E-12 | 6.02E-12 | 6.02E-12 | 6.02E-12 |
| CR | 52 | 0.00E+00 | 3.22E-11 | 6.72E-11 | 1.02E-10 | 1.36E-10 | 2.68E-10 | 6.63E-10 | 1.32E-09 | 1.97E-09 | 2.63E-09 | 3.94E-09 |
| CR | 53 | 0.00E+00 | 4.63E-12 | 9.41E-12 | 1.41E-11 | 1.88E-11 | 3.76E-11 | 9.41E-11 | 1.88E-10 | 2.82E-10 | 3.76E-10 | 5.63E-10 |
| CR | 54 | 0.00E+00 | 4.87E-12 | 1.43E-11 | 2.72E-11 | 4.27E-11 | 1.25E-10 | 4.46E-10 | 1.01E-09 | 1.59E-09 | 2.16E-09 | 3.43E-09 |
| CR | 55 | 0.00E+00 | 3.74E-19 | 3.74E-19 | 3.74E-19 | 3.74E-19 | 3.74E-19 | 3.74E-19 | 3.74E-19 | 3.74E-19 | 3.74E-19 | 3.74E-19 |
| CR | 56 | 0.00E+00 | 1.21E-19 | 1.21E-19 | 1.21E-19 | 1.21E-19 | 1.21E-19 | 1.21E-19 | 1.21E-19 | 1.21E-19 | 1.21E-19 | 1.21E-19 |
| MN | 51 | 0.00E+00 | 1.45E-15 | 1.45E-15 | 1.45E-15 | 1.45E-15 | 1.45E-15 | 1.45E-15 | 1.45E-15 | 1.45E-15 | 1.45E-15 | 1.45E-15 |
| MN | 52 | 0.00E+00 | 1.71E-12 | 1.71E-12 | 1.71E-12 | 1.71E-12 | 1.71E-12 | 1.71E-12 | 1.71E-12 | 1.71E-12 | 1.71E-12 | 1.71E-12 |

**Table A.7. (continued)**

| Proton beam energy: 1 GeV | | | | | | | Operational line loss assumption: 1 nA/m (continuous) | | | | | |
|---|---|---|---|---|---|---|---|---|---|---|---|---|
| Nuclide masses integrated over the material zone volume in the HETC & MCNP calculational model | | | | | | | | | | | | |
| Nuclide concentration | | Time (s) | 7.88E+06 | 1.58E+07 | 2.37E+07 | 3.15E+07 | 6.31E+07 | 1.58E+08 | 3.15E+08 | 4.73E+08 | 6.31E+08 | 9.46E+08 |
| (gram-atoms) | | Initial | 3 months | 6 months | 9 months | 1 year | 2 years | 5 years | 10 years | 15 years | 20 years | 30 years |
| **MN** | **53** | **0.00E+00** | **3.27E-11** | **6.64E-11** | **9.96E-11** | **1.32E-10** | **2.65E-10** | **6.64E-10** | **1.32E-09** | **1.99E-09** | **2.65E-09** | **3.98E-09** |
| MN | 54 | 0.00E+00 | 2.33E-11 | 4.29E-11 | 5.87E-11 | 7.14E-11 | 1.03E-10 | 1.26E-10 | 1.29E-10 | 1.29E-10 | 1.29E-10 | 1.29E-10 |
| MN | 55 | 0.00E+00 | 3.73E-11 | 7.97E-11 | 1.25E-10 | 1.73E-10 | 3.99E-10 | 1.28E-09 | 3.08E-09 | 5.04E-09 | 7.04E-09 | 1.10E-08 |
| MN | 56 | 0.00E+00 | 1.97E-14 | 1.97E-14 | 1.97E-14 | 1.97E-14 | 1.97E-14 | 1.97E-14 | 1.97E-14 | 1.97E-14 | 1.97E-14 | 1.97E-14 |
| MN | 57 | 0.00E+00 | 1.48E-17 | 1.48E-17 | 1.48E-17 | 1.48E-17 | 1.48E-17 | 1.48E-17 | 1.48E-17 | 1.48E-17 | 1.48E-17 | 1.48E-17 |
| FE | 52 | 0.00E+00 | 2.23E-15 | 2.23E-15 | 2.23E-15 | 2.23E-15 | 2.23E-15 | 2.23E-15 | 2.23E-15 | 2.23E-15 | 2.23E-15 | 2.23E-15 |
| FE | 53 | 0.00E+00 | 1.61E-16 | 1.61E-16 | 1.61E-16 | 1.61E-16 | 1.61E-16 | 1.61E-16 | 1.61E-16 | 1.61E-16 | 1.61E-16 | 1.61E-16 |
| FE | 54 | 0.00E+00 | 2.18E-11 | 4.43E-11 | 6.64E-11 | 8.83E-11 | 1.77E-10 | 4.43E-10 | 8.83E-10 | 1.33E-09 | 1.77E-09 | 2.65E-09 |
| **FE** | **55** | **0.00E+00** | **6.18E-11** | **1.21E-10** | **1.77E-10** | **2.28E-10** | **4.04E-10** | **7.27E-10** | **9.25E-10** | **9.81E-10** | **9.96E-10** | **1.00E-09** |
| FE | 56 | 0.00E+00 | 2.79E-11 | 5.74E-11 | 8.67E-11 | 1.16E-10 | 2.34E-10 | 5.90E-10 | 1.18E-09 | 1.77E-09 | 2.36E-09 | 3.54E-09 |
| FE | 57 | 0.00E+00 | 9.91E-12 | 2.01E-11 | 3.02E-11 | 4.01E-11 | 8.04E-11 | 2.01E-10 | 4.01E-10 | 6.03E-10 | 8.04E-10 | 1.21E-09 |
| FE | 58 | 0.00E+00 | 1.97E-13 | 4.01E-13 | 6.01E-13 | 7.99E-13 | 1.60E-12 | 4.01E-12 | 7.99E-12 | 1.20E-11 | 1.60E-11 | 2.40E-11 |
| FE | 59 | 0.00E+00 | 1.86E-14 | 2.33E-14 | 2.44E-14 | 2.46E-14 | 2.47E-14 | 2.47E-14 | 2.47E-14 | 2.47E-14 | 2.47E-14 | 2.47E-14 |
| CO | 56 | 0.00E+00 | 1.12E-12 | 1.63E-12 | 1.86E-12 | 1.96E-12 | 2.03E-12 | 2.04E-12 | 2.04E-12 | 2.04E-12 | 2.04E-12 | 2.04E-12 |
| CO | 59 | 0.00E+00 | 1.60E-14 | 4.70E-14 | 8.10E-14 | 1.15E-13 | 2.56E-13 | 7.03E-13 | 1.43E-12 | 2.15E-12 | 2.88E-12 | 4.31E-12 |
| NI | 60 | 0.00E+00 | 3.78E-15 | 7.68E-15 | 1.15E-14 | 1.53E-14 | 3.07E-14 | 7.68E-14 | 1.53E-13 | 2.30E-13 | 3.07E-13 | 4.60E-13 |
| NI | 61 | 0.00E+00 | 2.35E-15 | 4.77E-15 | 7.16E-15 | 9.52E-15 | 1.91E-14 | 4.77E-14 | 9.52E-14 | 1.43E-13 | 1.91E-13 | 2.86E-13 |
| NI | 62 | 0.00E+00 | 4.04E-13 | 8.21E-13 | 1.23E-12 | 1.64E-12 | 3.28E-12 | 8.21E-12 | 1.64E-11 | 2.46E-11 | 3.28E-11 | 4.91E-11 |
| NI | 63 | 0.00E+00 | 1.49E-15 | 3.03E-15 | 4.54E-15 | 6.03E-15 | 1.20E-14 | 2.98E-14 | 5.84E-14 | 8.63E-14 | 1.13E-13 | 1.64E-13 |
| NI | 64 | 0.00E+00 | 2.77E-13 | 5.64E-13 | 8.47E-13 | 1.13E-12 | 2.25E-12 | 5.63E-12 | 1.12E-11 | 1.68E-11 | 2.25E-11 | 3.37E-11 |
| NI | 65 | 0.00E+00 | 5.46E-19 | 5.46E-19 | 5.46E-19 | 5.46E-19 | 5.46E-19 | 5.46E-19 | 5.46E-19 | 5.46E-19 | 5.46E-19 | 5.46E-19 |
| NI | 66 | 0.00E+00 | 3.07E-19 | 3.07E-19 | 3.07E-19 | 3.07E-19 | 3.07E-19 | 3.07E-19 | 3.07E-19 | 3.07E-19 | 3.07E-19 | 3.07E-19 |
| CU | 61 | 0.00E+00 | 2.60E-20 | 2.60E-20 | 2.60E-20 | 2.60E-20 | 2.60E-20 | 2.60E-20 | 2.60E-20 | 2.60E-20 | 2.60E-20 | 2.60E-20 |
| CU | 62 | 0.00E+00 | 4.37E-17 | 4.37E-17 | 4.37E-17 | 4.37E-17 | 4.37E-17 | 4.37E-17 | 4.37E-17 | 4.37E-17 | 4.37E-17 | 4.37E-17 |
| CU | 63 | 0.00E+00 | 4.66E-13 | 9.46E-13 | 1.42E-12 | 1.89E-12 | 3.78E-12 | 9.46E-12 | 1.89E-11 | 2.83E-11 | 3.78E-11 | 5.67E-11 |
| CU | 64 | 0.00E+00 | 3.88E-15 | 3.88E-15 | 3.88E-15 | 3.88E-15 | 3.88E-15 | 3.88E-15 | 3.88E-15 | 3.88E-15 | 3.88E-15 | 3.88E-15 |
| CU | 65 | 0.00E+00 | 1.78E-14 | 5.98E-14 | 1.19E-13 | 1.92E-13 | 5.70E-13 | 1.96E-12 | 4.34E-12 | 6.74E-12 | 9.14E-12 | 1.44E-11 |
| CU | 66 | 0.00E+00 | 2.60E-19 | 2.60E-19 | 2.60E-19 | 2.60E-19 | 2.60E-19 | 2.60E-19 | 2.60E-19 | 2.60E-19 | 2.60E-19 | 2.60E-19 |
| CU | 67 | 0.00E+00 | 2.79E-17 | 2.79E-17 | 2.79E-17 | 2.79E-17 | 2.79E-17 | 2.79E-17 | 2.79E-17 | 2.79E-17 | 2.79E-17 | 2.79E-17 |
| ZN | 63 | 0.00E+00 | 1.10E-17 | 1.10E-17 | 1.10E-17 | 1.10E-17 | 1.10E-17 | 1.10E-17 | 1.10E-17 | 1.10E-17 | 1.10E-17 | 1.10E-17 |
| ZN | 64 | 0.00E+00 | 1.81E-13 | 3.69E-13 | 5.55E-13 | 7.38E-13 | 1.48E-12 | 3.69E-12 | 7.34E-12 | 1.10E-11 | 1.47E-11 | 2.20E-11 |
| ZN | 65 | 0.00E+00 | 1.00E-13 | 1.80E-13 | 2.41E-13 | 2.87E-13 | 3.89E-13 | 4.42E-13 | 4.45E-13 | 4.45E-13 | 4.45E-13 | 4.45E-13 |
| ZN | 66 | 0.00E+00 | 1.36E-14 | 2.76E-14 | 4.14E-14 | 5.50E-14 | 1.10E-13 | 2.76E-13 | 5.50E-13 | 8.25E-13 | 1.10E-12 | 1.65E-12 |
| ZN | 67 | 0.00E+00 | 4.49E-13 | 9.12E-13 | 1.37E-12 | 1.82E-12 | 3.64E-12 | 9.12E-12 | 1.82E-11 | 2.73E-11 | 3.64E-11 | 5.46E-11 |

**Table A.7. (continued)**

| Proton beam energy: 1 GeV | | | | | | | Operational line loss assumption: 1 nA/m (continuous) | | | | | |
|---|---|---|---|---|---|---|---|---|---|---|---|---|
| Nuclide masses integrated over the material zone volume in the HETC & MCNP calculational model | | | | | | | | | | | | |
| Nuclide concentration | | Time (s) | 7.88E+06 | 1.58E+07 | 2.37E+07 | 3.15E+07 | 6.31E+07 | 1.58E+08 | 3.15E+08 | 4.73E+08 | 6.31E+08 | 9.46E+08 |
| (gram-atoms) | | Initial | 3 months | 6 months | 9 months | 1 year | 2 years | 5 years | 10 years | 15 years | 20 years | 30 years |
| ZN | 68 | 0.00E+00 | 1.58E-14 | 3.21E-14 | 4.81E-14 | 6.40E-14 | 1.28E-13 | 3.21E-13 | 6.40E-13 | 9.61E-13 | 1.28E-12 | 1.92E-12 |
| ZN | 69 | 0.00E+00 | 4.38E-18 | 4.38E-18 | 4.38E-18 | 4.38E-18 | 4.38E-18 | 4.38E-18 | 4.38E-18 | 4.38E-18 | 4.38E-18 | 4.38E-18 |
| ZN | 70 | 0.00E+00 | 3.17E-18 | 6.45E-18 | 9.67E-18 | 1.29E-17 | 2.57E-17 | 6.45E-17 | 1.29E-16 | 1.93E-16 | 2.57E-16 | 3.86E-16 |
| GA | 69 | 0.00E+00 | 7.08E-15 | 1.44E-14 | 2.16E-14 | 2.87E-14 | 5.75E-14 | 1.44E-13 | 2.87E-13 | 4.31E-13 | 5.74E-13 | 8.61E-13 |
| GA | 71 | 0.00E+00 | 1.92E-16 | 3.91E-16 | 5.86E-16 | 7.79E-16 | 1.56E-15 | 3.91E-15 | 7.79E-15 | 1.17E-14 | 1.56E-14 | 2.34E-14 |
| BR | 81 | 0.00E+00 | 2.83E-16 | 5.75E-16 | 8.63E-16 | 1.15E-15 | 2.30E-15 | 5.75E-15 | 1.15E-14 | 1.72E-14 | 2.30E-14 | 3.44E-14 |
| BR | 82 | 0.00E+00 | 2.03E-17 | 2.03E-17 | 2.03E-17 | 2.03E-17 | 2.03E-17 | 2.03E-17 | 2.03E-17 | 2.03E-17 | 2.03E-17 | 2.03E-17 |
| BR | 83 | 0.00E+00 | 1.69E-19 | 1.69E-19 | 1.69E-19 | 1.69E-19 | 1.69E-19 | 1.69E-19 | 1.69E-19 | 1.69E-19 | 1.69E-19 | 1.69E-19 |
| BR | 84 | 0.00E+00 | 8.48E-20 | 8.48E-20 | 8.48E-20 | 8.48E-20 | 8.48E-20 | 8.48E-20 | 8.48E-20 | 8.48E-20 | 8.48E-20 | 8.48E-20 |
| KR | 82 | 0.00E+00 | 9.08E-16 | 1.87E-15 | 2.81E-15 | 3.74E-15 | 7.45E-15 | 1.85E-14 | 3.69E-14 | 5.54E-14 | 7.38E-14 | 1.11E-13 |
| KR | 83 | 0.00E+00 | 2.34E-13 | 7.83E-13 | 1.47E-12 | 2.22E-12 | 5.45E-12 | 1.64E-11 | 3.39E-11 | 5.14E-11 | 6.89E-11 | 1.03E-10 |
| KR | 83M | 0.00E+00 | 1.31E-19 | 1.31E-19 | 1.31E-19 | 1.31E-19 | 1.31E-19 | 1.31E-19 | 1.31E-19 | 1.31E-19 | 1.31E-19 | 1.31E-19 |
| KR | 84 | 0.00E+00 | 9.15E-13 | 2.22E-12 | 3.56E-12 | 4.88E-12 | 1.07E-11 | 2.74E-11 | 5.46E-11 | 8.20E-11 | 1.09E-10 | 1.64E-10 |
| KR | 85 | 0.00E+00 | 8.43E-15 | 1.70E-14 | 2.53E-14 | 3.33E-14 | 6.46E-14 | 1.47E-13 | 2.53E-13 | 3.31E-13 | 3.87E-13 | 4.56E-13 |
| KR | 86 | 0.00E+00 | 4.32E-16 | 8.77E-16 | 1.32E-15 | 1.75E-15 | 3.50E-15 | 8.77E-15 | 1.75E-14 | 2.63E-14 | 3.50E-14 | 5.25E-14 |
| KR | 87 | 0.00E+00 | 8.09E-19 | 8.09E-19 | 8.09E-19 | 8.09E-19 | 8.09E-19 | 8.09E-19 | 8.09E-19 | 8.09E-19 | 8.09E-19 | 8.09E-19 |
| RB | 83 | 0.00E+00 | 5.74E-13 | 8.59E-13 | 9.92E-13 | 1.06E-12 | 1.11E-12 | 1.12E-12 | 1.11E-12 | 1.11E-12 | 1.11E-12 | 1.11E-12 |
| RB | 84 | 0.00E+00 | 4.23E-13 | 4.87E-13 | 4.96E-13 | 4.97E-13 | 4.97E-13 | 4.97E-13 | 4.97E-13 | 4.97E-13 | 4.97E-13 | 4.97E-13 |
| RB | 85 | 0.00E+00 | 2.44E-16 | 6.35E-16 | 1.16E-15 | 1.80E-15 | 5.70E-15 | 2.87E-14 | 9.76E-14 | 1.96E-13 | 3.17E-13 | 5.98E-13 |
| RB | 86 | 0.00E+00 | 3.15E-13 | 3.27E-13 | 3.27E-13 | 3.27E-13 | 3.27E-13 | 3.27E-13 | 3.27E-13 | 3.27E-13 | 3.27E-13 | 3.27E-13 |
| RB | 87 | 0.00E+00 | 9.57E-16 | 1.94E-15 | 2.92E-15 | 3.88E-15 | 7.76E-15 | 1.94E-14 | 3.87E-14 | 5.82E-14 | 7.76E-14 | 1.16E-13 |
| RB | 88 | 0.00E+00 | 6.17E-18 | 6.17E-18 | 6.17E-18 | 6.17E-18 | 6.17E-18 | 6.17E-18 | 6.17E-18 | 6.17E-18 | 6.17E-18 | 6.17E-18 |
| SR | 84 | 0.00E+00 | 1.57E-14 | 4.31E-14 | 7.17E-14 | 1.00E-13 | 2.30E-13 | 5.92E-13 | 1.18E-12 | 1.77E-12 | 2.36E-12 | 3.53E-12 |
| SR | 86 | 0.00E+00 | 7.79E-13 | 1.90E-12 | 3.01E-12 | 4.10E-12 | 8.88E-12 | 2.26E-11 | 4.50E-11 | 6.75E-11 | 9.01E-11 | 1.35E-10 |
| SR | 88 | 0.00E+00 | 3.13E-14 | 6.36E-14 | 9.54E-14 | 1.27E-13 | 2.54E-13 | 6.36E-13 | 1.27E-12 | 1.90E-12 | 2.54E-12 | 3.81E-12 |
| I | 127 | 0.00E+00 | 1.19E-19 | 3.35E-19 | 5.64E-19 | 7.93E-19 | 1.86E-18 | 4.78E-18 | 9.53E-18 | 1.43E-17 | 1.91E-17 | 2.85E-17 |
| XE | 126 | 0.00E+00 | 9.45E-20 | 1.92E-19 | 2.88E-19 | 3.82E-19 | 7.66E-19 | 1.92E-18 | 3.82E-18 | 5.74E-18 | 7.66E-18 | 1.15E-17 |
| XE | 127 | 0.00E+00 | 1.09E-19 | 1.29E-19 | 1.33E-19 | 1.33E-19 | 1.34E-19 | 1.33E-19 | 1.33E-19 | 1.33E-19 | 1.33E-19 | 1.33E-19 |
| XE | 128 | 0.00E+00 | 2.17E-18 | 4.48E-18 | 6.76E-18 | 9.00E-18 | 1.81E-17 | 4.54E-17 | 9.07E-17 | 1.36E-16 | 1.82E-16 | 2.72E-16 |
| XE | 129 | 0.00E+00 | 3.35E-17 | 6.88E-17 | 1.04E-16 | 1.38E-16 | 2.75E-16 | 6.85E-16 | 1.36E-15 | 2.05E-15 | 2.73E-15 | 4.09E-15 |
| XE | 130 | 0.00E+00 | 2.37E-18 | 4.82E-18 | 7.23E-18 | 9.60E-18 | 1.92E-17 | 4.82E-17 | 9.60E-17 | 1.44E-16 | 1.92E-16 | 2.88E-16 |
| XE | 131 | 0.00E+00 | 1.92E-16 | 4.90E-16 | 7.85E-16 | 1.08E-15 | 2.30E-15 | 5.89E-15 | 1.18E-14 | 1.77E-14 | 2.37E-14 | 3.55E-14 |
| XE | 132 | 0.00E+00 | 1.51E-17 | 3.10E-17 | 4.68E-17 | 6.24E-17 | 1.24E-16 | 3.08E-16 | 6.12E-16 | 9.19E-16 | 1.22E-15 | 1.83E-15 |
| XE | 133 | 0.00E+00 | 5.89E-19 | 5.89E-19 | 5.89E-19 | 5.89E-19 | 5.89E-19 | 5.89E-19 | 5.89E-19 | 5.89E-19 | 5.89E-19 | 5.89E-19 |

**Table A.7. (continued)**

| Proton beam energy: 1 GeV | | | | | | | Operational line loss assumption: 1 nA/m (continuous) | | | | | |
|---|---|---|---|---|---|---|---|---|---|---|---|---|
| Nuclide masses integrated over the material zone volume in the HETC & MCNP calculational model | | | | | | | | | | | | |
| Nuclide concentration | | Time (s) | 7.88E+06 | 1.58E+07 | 2.37E+07 | 3.15E+07 | 6.31E+07 | 1.58E+08 | 3.15E+08 | 4.73E+08 | 6.31E+08 | 9.46E+08 |
| (gram-atoms) | | Initial | 3 months | 6 months | 9 months | 1 year | 2 years | 5 years | 10 years | 15 years | 20 years | 30 years |
| XE | 134 | 0.00E+00 | 1.69E-17 | 3.44E-17 | 5.16E-17 | 6.85E-17 | 1.37E-16 | 3.44E-16 | 6.85E-16 | 1.03E-15 | 1.37E-15 | 2.06E-15 |
| XE | 135 | 0.00E+00 | 4.82E-19 | 4.82E-19 | 4.82E-19 | 4.82E-19 | 4.82E-19 | 4.82E-19 | 4.82E-19 | 4.82E-19 | 4.82E-19 | 4.82E-19 |
| XE | 136 | 0.00E+00 | 1.60E-18 | 3.24E-18 | 4.86E-18 | 6.46E-18 | 1.29E-17 | 3.24E-17 | 6.46E-17 | 9.70E-17 | 1.29E-16 | 1.94E-16 |
| CS | 129 | 0.00E+00 | 7.21E-19 | 7.21E-19 | 7.21E-19 | 7.21E-19 | 7.21E-19 | 7.21E-19 | 7.21E-19 | 7.21E-19 | 7.21E-19 | 7.21E-19 |
| CS | 131 | 0.00E+00 | 4.36E-17 | 4.45E-17 | 4.45E-17 | 4.45E-17 | 4.45E-17 | 4.45E-17 | 4.45E-17 | 4.45E-17 | 4.45E-17 | 4.45E-17 |
| CS | 132 | 0.00E+00 | 4.75E-19 | 4.75E-19 | 4.75E-19 | 4.75E-19 | 4.75E-19 | 4.75E-19 | 4.75E-19 | 4.75E-19 | 4.75E-19 | 4.75E-19 |
| CS | 133 | 0.00E+00 | 3.35E-17 | 9.49E-17 | 1.81E-16 | 2.90E-16 | 9.72E-16 | 5.14E-15 | 1.78E-14 | 3.61E-14 | 5.83E-14 | 1.10E-13 |
| CS | 134 | 0.00E+00 | 3.18E-17 | 6.20E-17 | 8.93E-17 | 1.14E-16 | 1.96E-16 | 3.26E-16 | 3.86E-16 | 3.97E-16 | 3.99E-16 | 4.00E-16 |
| CS | 135 | 0.00E+00 | 1.03E-16 | 2.09E-16 | 3.14E-16 | 4.17E-16 | 8.34E-16 | 2.09E-15 | 4.16E-15 | 6.24E-15 | 8.33E-15 | 1.25E-14 |
| CS | 136 | 0.00E+00 | 1.18E-17 | 1.19E-17 | 1.19E-17 | 1.19E-17 | 1.19E-17 | 1.19E-17 | 1.19E-17 | 1.19E-17 | 1.19E-17 | 1.19E-17 |
| CS | 137 | 0.00E+00 | 2.15E-16 | 4.36E-16 | 6.52E-16 | 8.64E-16 | 1.71E-15 | 4.14E-15 | 7.81E-15 | 1.11E-14 | 1.40E-14 | 1.90E-14 |
| CS | 138 | 0.00E+00 | 8.66E-20 | 8.66E-20 | 8.66E-20 | 8.66E-20 | 8.66E-20 | 8.66E-20 | 8.66E-20 | 8.66E-20 | 8.66E-20 | 8.66E-20 |
| BA | 128 | 0.00E+00 | 7.15E-20 | 7.15E-20 | 7.15E-20 | 7.15E-20 | 7.15E-20 | 7.15E-20 | 7.15E-20 | 7.15E-20 | 7.15E-20 | 7.15E-20 |
| BA | 129 | 0.00E+00 | 4.72E-20 | 4.72E-20 | 4.72E-20 | 4.72E-20 | 4.72E-20 | 4.72E-20 | 4.72E-20 | 4.72E-20 | 4.72E-20 | 4.72E-20 |
| BA | 130 | 0.00E+00 | 5.53E-18 | 1.12E-17 | 1.68E-17 | 2.24E-17 | 4.48E-17 | 1.12E-16 | 2.24E-16 | 3.36E-16 | 4.48E-16 | 6.72E-16 |
| BA | 131 | 0.00E+00 | 5.47E-17 | 5.50E-17 | 5.50E-17 | 5.50E-17 | 5.50E-17 | 5.50E-17 | 5.50E-17 | 5.50E-17 | 5.50E-17 | 5.50E-17 |
| BA | 132 | 0.00E+00 | 2.54E-16 | 5.16E-16 | 7.75E-16 | 1.03E-15 | 2.06E-15 | 5.16E-15 | 1.03E-14 | 1.55E-14 | 2.06E-14 | 3.09E-14 |
| BA | 133 | 0.00E+00 | 1.57E-15 | 3.16E-15 | 4.71E-15 | 6.21E-15 | 1.20E-14 | 2.75E-14 | 4.72E-14 | 6.15E-14 | 7.19E-14 | 8.47E-14 |
| BA | 134 | 0.00E+00 | 7.63E-15 | 1.55E-14 | 2.32E-14 | 3.09E-14 | 6.19E-14 | 1.55E-13 | 3.10E-13 | 4.65E-13 | 6.21E-13 | 9.31E-13 |
| BA | 135 | 0.00E+00 | 3.98E-15 | 8.08E-15 | 1.21E-14 | 1.61E-14 | 3.23E-14 | 8.08E-14 | 1.61E-13 | 2.42E-13 | 3.23E-13 | 4.84E-13 |
| BA | 136 | 0.00E+00 | 2.86E-14 | 5.80E-14 | 8.70E-14 | 1.16E-13 | 2.32E-13 | 5.80E-13 | 1.16E-12 | 1.74E-12 | 2.32E-12 | 3.47E-12 |
| BA | 137 | 0.00E+00 | 2.65E-14 | 5.38E-14 | 8.07E-14 | 1.07E-13 | 2.15E-13 | 5.38E-13 | 1.07E-12 | 1.61E-12 | 2.15E-12 | 3.23E-12 |
| BA | 138 | 0.00E+00 | 4.73E-15 | 9.61E-15 | 1.44E-14 | 1.92E-14 | 3.84E-14 | 9.61E-14 | 1.92E-13 | 2.88E-13 | 3.84E-13 | 5.75E-13 |
| BA | 139 | 0.00E+00 | 4.63E-18 | 4.63E-18 | 4.63E-18 | 4.63E-18 | 4.63E-18 | 4.63E-18 | 4.63E-18 | 4.63E-18 | 4.63E-18 | 4.63E-18 |
| LA | 139 | 0.00E+00 | 5.00E-15 | 1.02E-14 | 1.52E-14 | 2.02E-14 | 4.05E-14 | 1.02E-13 | 2.02E-13 | 3.04E-13 | 4.05E-13 | 6.08E-13 |
| EU | 155 | 0.00E+00 | 5.66E-20 | 1.13E-19 | 1.66E-19 | 2.17E-19 | 4.06E-19 | 8.33E-19 | 1.23E-18 | 1.43E-18 | 1.53E-18 | 1.60E-18 |
| EU | 156 | 0.00E+00 | 1.03E-19 | 1.05E-19 | 1.05E-19 | 1.05E-19 | 1.05E-19 | 1.05E-19 | 1.05E-19 | 1.05E-19 | 1.05E-19 | 1.05E-19 |
| GD | 156 | 0.00E+00 | 3.32E-19 | 7.79E-19 | 1.22E-18 | 1.66E-18 | 3.53E-18 | 8.94E-18 | 1.78E-17 | 2.68E-17 | 3.57E-17 | 5.34E-17 |
| GD | 157 | 0.00E+00 | 1.19E-19 | 3.15E-19 | 5.81E-19 | 9.15E-19 | 2.98E-18 | 1.61E-17 | 6.00E-17 | 1.32E-16 | 2.31E-16 | 5.06E-16 |
| GD | 158 | 0.00E+00 | 6.96E-19 | 1.52E-18 | 2.44E-18 | 3.44E-18 | 8.55E-18 | 3.38E-17 | 1.08E-16 | 2.22E-16 | 3.75E-16 | 7.92E-16 |
| TB | 157 | 0.00E+00 | 6.15E-17 | 1.25E-16 | 1.87E-16 | 2.49E-16 | 4.97E-16 | 1.24E-15 | 2.44E-15 | 3.62E-15 | 4.77E-15 | 6.99E-15 |
| TB | 158 | 0.00E+00 | 1.08E-16 | 2.19E-16 | 3.29E-16 | 4.37E-16 | 8.73E-16 | 2.17E-15 | 4.28E-15 | 6.35E-15 | 8.38E-15 | 1.23E-14 |
| TB | 159 | 0.00E+00 | 6.26E-19 | 1.28E-18 | 1.92E-18 | 2.56E-18 | 5.10E-18 | 1.27E-17 | 2.54E-17 | 3.81E-17 | 5.08E-17 | 7.61E-17 |
| TB | 160 | 0.00E+00 | 1.79E-15 | 2.56E-15 | 2.88E-15 | 3.01E-15 | 3.10E-15 | 3.10E-15 | 3.10E-15 | 3.10E-15 | 3.10E-15 | 3.10E-15 |

| Table A.7. (continued) | | | | | | | | | | | | |
|---|---|---|---|---|---|---|---|---|---|---|---|---|
| Proton beam energy: 1 GeV | | | | | | | Operational line loss assumption: 1 nA/m (continuous) | | | | | |
| Nuclide masses integrated over the material zone volume in the HETC & MCNP calculational model | | | | | | | | | | | | |
| Nuclide concentration | | Time (s) | 7.88E+06 | 1.58E+07 | 2.37E+07 | 3.15E+07 | 6.31E+07 | 1.58E+08 | 3.15E+08 | 4.73E+08 | 6.31E+08 | 9.46E+08 |
| (gram-atoms) | | Initial | 3 months | 6 months | 9 months | 1 year | 2 years | 5 years | 10 years | 15 years | 20 years | 30 years |
| DY | 158 | 0.00E+00 | 1.11E-20 | 4.57E-20 | 1.03E-19 | 1.82E-19 | 7.27E-19 | 4.54E-18 | 1.79E-17 | 4.01E-17 | 7.08E-17 | 1.57E-16 |
| DY | 160 | 0.00E+00 | 8.84E-16 | 2.87E-15 | 5.28E-15 | 7.83E-15 | 1.86E-14 | 5.44E-14 | 1.11E-13 | 1.69E-13 | 2.26E-13 | 3.38E-13 |
| Total | | 0.00E+00 | 2.76E-08 | 5.61E-08 | 8.42E-08 | 1.12E-07 | 2.24E-07 | 5.61E-07 | 1.12E-06 | 1.68E-06 | 2.24E-06 | 3.36E-06 |

| Table A.8. SNS nuclide production during normal proton beam operation: earth berm Zone 4 | | | | | | | | | | | | |
|---|---|---|---|---|---|---|---|---|---|---|---|---|
| Proton beam energy: 1 GeV | | | | | | | Operational line loss assumption: 1 nA/m (continuous) | | | | | |
| Nuclide masses integrated over the material zone volume in the HETC & MCNP calculational model | | | | | | | | | | | | |
| Nuclide concentration | | Time (s) | 7.88E+06 | 1.58E+07 | 2.37E+07 | 3.15E+07 | 6.31E+07 | 1.58E+08 | 3.15E+08 | 4.73E+08 | 6.31E+08 | 9.46E+08 |
| (gram-atoms) | | Initial | 3 months | 6 months | 9 months | 1 year | 2 years | 5 years | 10 years | 15 years | 20 years | 30 years |
| H | 1 | 0.00E+00 | 2.62E-09 | 5.33E-09 | 7.99E-09 | 1.06E-08 | 2.13E-08 | 5.33E-08 | 1.06E-07 | 1.59E-07 | 2.13E-07 | 3.19E-07 |
| H | 2 | 0.00E+00 | 7.70E-11 | 1.56E-10 | 2.35E-10 | 3.12E-10 | 6.25E-10 | 1.56E-09 | 3.12E-09 | 4.68E-09 | 6.25E-09 | 9.36E-09 |
| **H** | **3** | **0.00E+00** | **4.86E-11** | **9.79E-11** | **1.46E-10** | **1.92E-10** | **3.75E-10** | **8.65E-10** | **1.51E-09** | **2.01E-09** | **2.38E-09** | **2.87E-09** |
| HE | 3 | 0.00E+00 | 1.20E-11 | 2.51E-11 | 3.86E-11 | 5.27E-11 | 1.16E-10 | 3.65E-10 | 9.38E-10 | 1.67E-09 | 2.53E-09 | 4.49E-09 |
| HE | 4 | 0.00E+00 | 5.28E-10 | 1.07E-09 | 1.61E-09 | 2.14E-09 | 4.28E-09 | 1.07E-08 | 2.14E-08 | 3.21E-08 | 4.28E-08 | 6.42E-08 |
| LI | 6 | 0.00E+00 | 9.69E-12 | 1.97E-11 | 2.95E-11 | 3.92E-11 | 7.86E-11 | 1.97E-10 | 3.92E-10 | 5.89E-10 | 7.86E-10 | 1.18E-09 |
| LI | 7 | 0.00E+00 | 4.04E-13 | 8.20E-13 | 1.23E-12 | 1.63E-12 | 3.27E-12 | 8.20E-12 | 1.63E-11 | 2.45E-11 | 3.27E-11 | 4.91E-11 |
| BE | 9 | 0.00E+00 | 3.39E-12 | 6.88E-12 | 1.03E-11 | 1.37E-11 | 2.75E-11 | 6.88E-11 | 1.37E-10 | 2.06E-10 | 2.75E-10 | 4.12E-10 |
| **BE** | **10** | **0.00E+00** | **4.06E-13** | **8.24E-13** | **1.24E-12** | **1.64E-12** | **3.29E-12** | **8.24E-12** | **1.64E-11** | **2.47E-11** | **3.29E-11** | **4.93E-11** |
| B | 10 | 0.00E+00 | 1.90E-11 | 3.85E-11 | 5.78E-11 | 7.68E-11 | 1.54E-10 | 3.85E-10 | 7.68E-10 | 1.15E-09 | 1.54E-09 | 2.31E-09 |
| B | 11 | 0.00E+00 | 2.57E-11 | 5.22E-11 | 7.84E-11 | 1.04E-10 | 2.09E-10 | 5.22E-10 | 1.04E-09 | 1.56E-09 | 2.09E-09 | 3.13E-09 |
| C | 11 | 0.00E+00 | 1.37E-15 | 1.37E-15 | 1.37E-15 | 1.37E-15 | 1.37E-15 | 1.37E-15 | 1.37E-15 | 1.37E-15 | 1.37E-15 | 1.37E-15 |
| C | 12 | 0.00E+00 | 2.99E-10 | 6.07E-10 | 9.10E-10 | 1.21E-09 | 2.42E-09 | 6.07E-09 | 1.21E-08 | 1.82E-08 | 2.42E-08 | 3.63E-08 |
| C | 13 | 0.00E+00 | 2.43E-10 | 4.94E-10 | 7.41E-10 | 9.85E-10 | 1.97E-09 | 4.94E-09 | 9.85E-09 | 1.48E-08 | 1.97E-08 | 2.96E-08 |
| **C** | **14** | **0.00E+00** | **3.01E-11** | **6.12E-11** | **9.18E-11** | **1.22E-10** | **2.44E-10** | **6.12E-10** | **1.22E-09** | **1.83E-09** | **2.44E-09** | **3.66E-09** |
| N | 13 | 0.00E+00 | 2.64E-15 | 2.64E-15 | 2.64E-15 | 2.64E-15 | 2.64E-15 | 2.64E-15 | 2.64E-15 | 2.64E-15 | 2.64E-15 | 2.64E-15 |
| N | 14 | 0.00E+00 | 3.15E-10 | 6.39E-10 | 9.58E-10 | 1.27E-09 | 2.55E-09 | 6.39E-09 | 1.27E-08 | 1.91E-08 | 2.55E-08 | 3.83E-08 |
| N | 15 | 0.00E+00 | 4.93E-10 | 1.00E-09 | 1.50E-09 | 1.99E-09 | 4.00E-09 | 1.00E-08 | 1.99E-08 | 3.00E-08 | 4.00E-08 | 5.99E-08 |
| N | 16 | 0.00E+00 | 2.80E-17 | 2.80E-17 | 2.80E-17 | 2.80E-17 | 2.80E-17 | 2.80E-17 | 2.80E-17 | 2.80E-17 | 2.80E-17 | 2.80E-17 |
| N | 17 | 0.00E+00 | 3.47E-19 | 3.47E-19 | 3.47E-19 | 3.47E-19 | 3.47E-19 | 3.47E-19 | 3.47E-19 | 3.47E-19 | 3.47E-19 | 3.47E-19 |
| O | 14 | 0.00E+00 | 2.64E-17 | 2.64E-17 | 2.64E-17 | 2.64E-17 | 2.64E-17 | 2.64E-17 | 2.64E-17 | 2.64E-17 | 2.64E-17 | 2.64E-17 |
| O | 15 | 0.00E+00 | 2.40E-15 | 2.40E-15 | 2.40E-15 | 2.40E-15 | 2.40E-15 | 2.40E-15 | 2.40E-15 | 2.40E-15 | 2.40E-15 | 2.40E-15 |
| O | 16 | 0.00E+00 | 1.57E-10 | 3.18E-10 | 4.77E-10 | 6.34E-10 | 1.27E-09 | 3.18E-09 | 6.34E-09 | 9.52E-09 | 1.27E-08 | 1.90E-08 |
| O | 17 | 0.00E+00 | 1.08E-11 | 2.19E-11 | 3.29E-11 | 4.38E-11 | 8.76E-11 | 2.19E-10 | 4.38E-10 | 6.57E-10 | 8.76E-10 | 1.31E-09 |
| O | 18 | 0.00E+00 | 4.44E-12 | 9.03E-12 | 1.35E-11 | 1.80E-11 | 3.61E-11 | 9.03E-11 | 1.80E-10 | 2.70E-10 | 3.60E-10 | 5.40E-10 |
| O | 19 | 0.00E+00 | 9.57E-20 | 9.57E-20 | 9.57E-20 | 9.57E-20 | 9.57E-20 | 9.57E-20 | 9.57E-20 | 9.57E-20 | 9.57E-20 | 9.57E-20 |
| F | 18 | 0.00E+00 | 4.93E-15 | 4.93E-15 | 4.93E-15 | 4.93E-15 | 4.93E-15 | 4.93E-15 | 4.93E-15 | 4.93E-15 | 4.93E-15 | 4.93E-15 |
| F | 19 | 0.00E+00 | 4.46E-12 | 9.06E-12 | 1.36E-11 | 1.81E-11 | 3.62E-11 | 9.06E-11 | 1.81E-10 | 2.71E-10 | 3.62E-10 | 5.42E-10 |
| F | 20 | 0.00E+00 | 1.70E-20 | 1.70E-20 | 1.70E-20 | 1.70E-20 | 1.70E-20 | 1.70E-20 | 1.70E-20 | 1.70E-20 | 1.70E-20 | 1.70E-20 |
| NE | 20 | 0.00E+00 | 1.04E-11 | 2.11E-11 | 3.17E-11 | 4.21E-11 | 8.43E-11 | 2.11E-10 | 4.21E-10 | 6.32E-10 | 8.43E-10 | 1.26E-09 |
| NE | 21 | 0.00E+00 | 6.23E-12 | 1.27E-11 | 1.90E-11 | 2.52E-11 | 5.05E-11 | 1.27E-10 | 2.52E-10 | 3.79E-10 | 5.05E-10 | 7.58E-10 |
| NE | 22 | 0.00E+00 | 2.44E-12 | 5.66E-12 | 9.49E-12 | 1.39E-11 | 3.69E-11 | 1.42E-10 | 3.74E-10 | 6.31E-10 | 8.95E-10 | 1.42E-09 |
| NE | 23 | 0.00E+00 | 5.91E-18 | 5.91E-18 | 5.91E-18 | 5.91E-18 | 5.91E-18 | 5.91E-18 | 5.91E-18 | 5.91E-18 | 5.91E-18 | 5.91E-18 |

**Table A.8. (continued)**

| Proton beam energy: 1 GeV | | | | | | | Operational line loss assumption: 1 nA/m (continuous) | | | | | |
|---|---|---|---|---|---|---|---|---|---|---|---|---|
| Nuclide masses integrated over the material zone volume in the HETC & MCNP calculational model | | | | | | | | | | | | |
| Nuclide concentration | | Time (s) | 7.88E+06 | 1.58E+07 | 2.37E+07 | 3.15E+07 | 6.31E+07 | 1.58E+08 | 3.15E+08 | 4.73E+08 | 6.31E+08 | 9.46E+08 |
| (gram-atoms) | | Initial | 3 months | 6 months | 9 months | 1 year | 2 years | 5 years | 10 years | 15 years | 20 years | 30 years |
| NE | 24 | 0.00E+00 | 4.76E-20 | 4.76E-20 | 4.76E-20 | 4.76E-20 | 4.76E-20 | 4.76E-20 | 4.76E-20 | 4.76E-20 | 4.76E-20 | 4.76E-20 |
| NA | 21 | 0.00E+00 | 3.36E-18 | 3.36E-18 | 3.36E-18 | 3.36E-18 | 3.36E-18 | 3.36E-18 | 3.36E-18 | 3.36E-18 | 3.36E-18 | 3.36E-18 |
| **NA** | **22** | **0.00E+00** | **1.07E-11** | **2.09E-11** | **3.04E-11** | **3.92E-11** | **6.93E-11** | **1.24E-10** | **1.57E-10** | **1.66E-10** | **1.68E-10** | **1.69E-10** |
| NA | 23 | 0.00E+00 | 4.89E-11 | 9.94E-11 | 1.49E-10 | 1.98E-10 | 3.97E-10 | 9.94E-10 | 1.98E-09 | 2.97E-09 | 3.97E-09 | 5.95E-09 |
| NA | 24 | 0.00E+00 | 7.98E-14 | 7.98E-14 | 7.98E-14 | 7.98E-14 | 7.98E-14 | 7.98E-14 | 7.98E-14 | 7.98E-14 | 7.98E-14 | 7.98E-14 |
| NA | 25 | 0.00E+00 | 2.00E-17 | 2.00E-17 | 2.00E-17 | 2.00E-17 | 2.00E-17 | 2.00E-17 | 2.00E-17 | 2.00E-17 | 2.00E-17 | 2.00E-17 |
| NA | 26 | 0.00E+00 | 2.22E-20 | 2.22E-20 | 2.22E-20 | 2.22E-20 | 2.22E-20 | 2.22E-20 | 2.22E-20 | 2.22E-20 | 2.22E-20 | 2.22E-20 |
| MG | 23 | 0.00E+00 | 3.44E-18 | 3.44E-18 | 3.44E-18 | 3.44E-18 | 3.44E-18 | 3.44E-18 | 3.44E-18 | 3.44E-18 | 3.44E-18 | 3.44E-18 |
| MG | 24 | 0.00E+00 | 1.29E-10 | 2.63E-10 | 3.94E-10 | 5.24E-10 | 1.05E-09 | 2.63E-09 | 5.24E-09 | 7.87E-09 | 1.05E-08 | 1.57E-08 |
| MG | 25 | 0.00E+00 | 8.44E-11 | 1.71E-10 | 2.57E-10 | 3.42E-10 | 6.85E-10 | 1.71E-09 | 3.42E-09 | 5.13E-09 | 6.85E-09 | 1.03E-08 |
| MG | 26 | 0.00E+00 | 7.73E-11 | 1.57E-10 | 2.35E-10 | 3.13E-10 | 6.27E-10 | 1.57E-09 | 3.13E-09 | 4.70E-09 | 6.27E-09 | 9.39E-09 |
| MG | 27 | 0.00E+00 | 1.68E-15 | 1.68E-15 | 1.68E-15 | 1.68E-15 | 1.68E-15 | 1.68E-15 | 1.68E-15 | 1.68E-15 | 1.68E-15 | 1.68E-15 |
| AL | 25 | 0.00E+00 | 3.22E-18 | 3.22E-18 | 3.22E-18 | 3.22E-18 | 3.22E-18 | 3.22E-18 | 3.22E-18 | 3.22E-18 | 3.22E-18 | 3.22E-18 |
| **AL** | **26** | **0.00E+00** | **8.57E-11** | **1.74E-10** | **2.61E-10** | **3.47E-10** | **6.95E-10** | **1.74E-09** | **3.47E-09** | **5.21E-09** | **6.95E-09** | **1.04E-08** |
| AL | 27 | 0.00E+00 | 2.53E-10 | 5.13E-10 | 7.70E-10 | 1.02E-09 | 2.05E-09 | 5.13E-09 | 1.02E-08 | 1.54E-08 | 2.05E-08 | 3.07E-08 |
| AL | 28 | 0.00E+00 | 1.39E-15 | 1.39E-15 | 1.39E-15 | 1.39E-15 | 1.39E-15 | 1.39E-15 | 1.39E-15 | 1.39E-15 | 1.39E-15 | 1.39E-15 |
| AL | 29 | 0.00E+00 | 2.82E-16 | 2.82E-16 | 2.82E-16 | 2.82E-16 | 2.82E-16 | 2.82E-16 | 2.82E-16 | 2.82E-16 | 2.82E-16 | 2.82E-16 |
| AL | 30 | 0.00E+00 | 4.28E-19 | 4.28E-19 | 4.28E-19 | 4.28E-19 | 4.28E-19 | 4.28E-19 | 4.28E-19 | 4.28E-19 | 4.28E-19 | 4.28E-19 |
| SI | 26 | 0.00E+00 | 4.96E-19 | 4.96E-19 | 4.96E-19 | 4.96E-19 | 4.96E-19 | 4.96E-19 | 4.96E-19 | 4.96E-19 | 4.96E-19 | 4.96E-19 |
| SI | 27 | 0.00E+00 | 2.28E-17 | 2.28E-17 | 2.28E-17 | 2.28E-17 | 2.28E-17 | 2.28E-17 | 2.28E-17 | 2.28E-17 | 2.28E-17 | 2.28E-17 |
| SI | 28 | 0.00E+00 | 1.05E-10 | 2.13E-10 | 3.20E-10 | 4.25E-10 | 8.52E-10 | 2.13E-09 | 4.25E-09 | 6.38E-09 | 8.52E-09 | 1.28E-08 |
| SI | 29 | 0.00E+00 | 1.08E-11 | 2.20E-11 | 3.30E-11 | 4.39E-11 | 8.79E-11 | 2.20E-10 | 4.39E-10 | 6.59E-10 | 8.79E-10 | 1.32E-09 |
| SI | 30 | 0.00E+00 | 1.62E-12 | 3.29E-12 | 4.93E-12 | 6.55E-12 | 1.31E-11 | 3.29E-11 | 6.55E-11 | 9.83E-11 | 1.31E-10 | 1.97E-10 |
| SI | 31 | 0.00E+00 | 4.09E-16 | 4.09E-16 | 4.09E-16 | 4.09E-16 | 4.09E-16 | 4.09E-16 | 4.09E-16 | 4.09E-16 | 4.09E-16 | 4.09E-16 |
| P | 31 | 0.00E+00 | 2.34E-13 | 4.76E-13 | 7.14E-13 | 9.49E-13 | 1.90E-12 | 4.75E-12 | 9.48E-12 | 1.42E-11 | 1.90E-11 | 2.85E-11 |
| P | 32 | 0.00E+00 | 2.11E-16 | 2.14E-16 | 2.14E-16 | 2.14E-16 | 2.14E-16 | 2.14E-16 | 2.14E-16 | 2.14E-16 | 2.14E-16 | 2.14E-16 |
| S | 32 | 0.00E+00 | 7.21E-16 | 1.68E-15 | 2.63E-15 | 3.56E-15 | 7.56E-15 | 1.91E-14 | 3.82E-14 | 5.73E-14 | 7.65E-14 | 1.14E-13 |
| CL | 35 | 0.00E+00 | 1.35E-12 | 2.74E-12 | 4.10E-12 | 5.46E-12 | 1.09E-11 | 2.74E-11 | 5.46E-11 | 8.19E-11 | 1.09E-10 | 1.64E-10 |
| **CL** | **36** | **0.00E+00** | **1.19E-12** | **2.41E-12** | **3.62E-12** | **4.81E-12** | **9.64E-12** | **2.41E-11** | **4.81E-11** | **7.23E-11** | **9.64E-11** | **1.45E-10** |
| CL | 37 | 0.00E+00 | 2.55E-12 | 6.48E-12 | 1.06E-11 | 1.46E-11 | 3.30E-11 | 8.45E-11 | 1.68E-10 | 2.53E-10 | 3.37E-10 | 5.04E-10 |
| CL | 38 | 0.00E+00 | 5.10E-18 | 5.10E-18 | 5.10E-18 | 5.10E-18 | 5.10E-18 | 5.10E-18 | 5.10E-18 | 5.10E-18 | 5.10E-18 | 5.10E-18 |
| CL | 39 | 0.00E+00 | 4.59E-19 | 4.59E-19 | 4.59E-19 | 4.59E-19 | 4.59E-19 | 4.59E-19 | 4.59E-19 | 4.59E-19 | 4.59E-19 | 4.59E-19 |
| AR | 36 | 0.00E+00 | 3.41E-15 | 6.92E-15 | 1.04E-14 | 1.38E-14 | 2.76E-14 | 6.93E-14 | 1.38E-13 | 2.08E-13 | 2.78E-13 | 4.19E-13 |
| AR | 37 | 0.00E+00 | 1.52E-12 | 1.78E-12 | 1.82E-12 | 1.83E-12 | 1.83E-12 | 1.83E-12 | 1.83E-12 | 1.83E-12 | 1.83E-12 | 1.83E-12 |

**Table A.8. (continued)**

| Proton beam energy: 1 GeV | | | | | | | Operational line loss assumption: 1 nA/m (continuous) | | | | | |
|---|---|---|---|---|---|---|---|---|---|---|---|---|
| Nuclide masses integrated over the material zone volume in the HETC & MCNP calculational model | | | | | | | | | | | | |
| Nuclide concentration | | Time (s) | 7.88E+06 | 1.58E+07 | 2.37E+07 | 3.15E+07 | 6.31E+07 | 1.58E+08 | 3.15E+08 | 4.73E+08 | 6.31E+08 | 9.46E+08 |
| (gram-atoms) | | Initial | 3 months | 6 months | 9 months | 1 year | 2 years | 5 years | 10 years | 15 years | 20 years | 30 years |
| AR | 38 | 0.00E+00 | 4.85E-12 | 9.85E-12 | 1.48E-11 | 1.96E-11 | 3.94E-11 | 9.85E-11 | 1.96E-10 | 2.95E-10 | 3.94E-10 | 5.90E-10 |
| **AR** | **39** | **0.00E+00** | **1.91E-12** | **3.87E-12** | **5.80E-12** | **7.71E-12** | **1.54E-11** | **3.85E-11** | **7.62E-11** | **1.14E-10** | **1.51E-10** | **2.23E-10** |
| AR | 40 | 0.00E+00 | 3.84E-15 | 7.80E-15 | 1.17E-14 | 1.56E-14 | 3.12E-14 | 7.80E-14 | 1.56E-13 | 2.34E-13 | 3.12E-13 | 4.67E-13 |
| AR | 41 | 0.00E+00 | 1.28E-17 | 1.28E-17 | 1.28E-17 | 1.28E-17 | 1.28E-17 | 1.28E-17 | 1.28E-17 | 1.28E-17 | 1.28E-17 | 1.28E-17 |
| AR | 42 | 0.00E+00 | 3.49E-19 | 7.07E-19 | 1.06E-18 | 1.40E-18 | 2.78E-18 | 6.75E-18 | 1.28E-17 | 1.83E-17 | 2.32E-17 | 3.16E-17 |
| K | 38 | 0.00E+00 | 3.58E-17 | 3.58E-17 | 3.58E-17 | 3.58E-17 | 3.58E-17 | 3.58E-17 | 3.58E-17 | 3.58E-17 | 3.58E-17 | 3.58E-17 |
| K | 39 | 0.00E+00 | 8.40E-13 | 1.71E-12 | 2.56E-12 | 3.41E-12 | 6.85E-12 | 1.73E-11 | 3.50E-11 | 5.33E-11 | 7.20E-11 | 1.11E-10 |
| **K** | **40** | **0.00E+00** | **1.33E-12** | **2.71E-12** | **4.06E-12** | **5.39E-12** | **1.08E-11** | **2.71E-11** | **5.39E-11** | **8.10E-11** | **1.08E-10** | **1.62E-10** |
| K | 41 | 0.00E+00 | 1.06E-14 | 2.15E-14 | 3.23E-14 | 4.30E-14 | 8.60E-14 | 2.15E-13 | 4.29E-13 | 6.45E-13 | 8.60E-13 | 1.29E-12 |
| K | 42 | 0.00E+00 | 2.44E-16 | 2.44E-16 | 2.44E-16 | 2.44E-16 | 2.44E-16 | 2.44E-16 | 2.44E-16 | 2.44E-16 | 2.44E-16 | 2.44E-16 |
| K | 43 | 0.00E+00 | 3.52E-19 | 3.52E-19 | 3.52E-19 | 3.52E-19 | 3.52E-19 | 3.52E-19 | 3.52E-19 | 3.52E-19 | 3.52E-19 | 3.52E-19 |
| K | 44 | 0.00E+00 | 1.20E-20 | 1.20E-20 | 1.20E-20 | 1.20E-20 | 1.20E-20 | 1.20E-20 | 1.20E-20 | 1.20E-20 | 1.20E-20 | 1.20E-20 |
| **CA** | **41** | **0.00E+00** | **2.57E-15** | **5.21E-15** | **7.82E-15** | **1.04E-14** | **2.08E-14** | **5.21E-14** | **1.04E-13** | **1.56E-13** | **2.08E-13** | **3.12E-13** |
| CA | 42 | 0.00E+00 | 4.34E-13 | 8.81E-13 | 1.32E-12 | 1.76E-12 | 3.52E-12 | 8.81E-12 | 1.76E-11 | 2.64E-11 | 3.52E-11 | 5.28E-11 |
| CA | 43 | 0.00E+00 | 5.74E-15 | 1.17E-14 | 1.75E-14 | 2.32E-14 | 4.65E-14 | 1.17E-13 | 2.32E-13 | 3.49E-13 | 4.65E-13 | 6.98E-13 |
| CA | 44 | 0.00E+00 | 3.70E-13 | 7.52E-13 | 1.13E-12 | 1.50E-12 | 3.00E-12 | 7.51E-12 | 1.50E-11 | 2.25E-11 | 3.00E-11 | 4.50E-11 |
| CA | 45 | 0.00E+00 | 1.32E-14 | 2.25E-14 | 2.87E-14 | 3.29E-14 | 4.00E-14 | 4.19E-14 | 4.20E-14 | 4.20E-14 | 4.20E-14 | 4.19E-14 |
| CA | 46 | 0.00E+00 | 1.03E-15 | 2.09E-15 | 3.13E-15 | 4.16E-15 | 8.33E-15 | 2.09E-14 | 4.16E-14 | 6.24E-14 | 8.33E-14 | 1.25E-13 |
| CA | 47 | 0.00E+00 | 1.25E-16 | 1.25E-16 | 1.25E-16 | 1.25E-16 | 1.25E-16 | 1.25E-16 | 1.25E-16 | 1.25E-16 | 1.25E-16 | 1.25E-16 |
| CA | 48 | 0.00E+00 | 7.29E-17 | 1.48E-16 | 2.22E-16 | 2.95E-16 | 5.92E-16 | 1.48E-15 | 2.95E-15 | 4.43E-15 | 5.92E-15 | 8.87E-15 |
| SC | 44 | 0.00E+00 | 9.58E-16 | 9.58E-16 | 9.58E-16 | 9.58E-16 | 9.58E-16 | 9.58E-16 | 9.58E-16 | 9.58E-16 | 9.58E-16 | 9.58E-16 |
| SC | 45 | 0.00E+00 | 8.76E-13 | 1.78E-12 | 2.68E-12 | 3.57E-12 | 7.17E-12 | 1.80E-11 | 3.60E-11 | 5.41E-11 | 7.22E-11 | 1.08E-10 |
| SC | 46 | 0.00E+00 | 5.85E-13 | 8.69E-13 | 9.99E-13 | 1.06E-12 | 1.11E-12 | 1.11E-12 | 1.11E-12 | 1.11E-12 | 1.11E-12 | 1.11E-12 |
| SC | 47 | 0.00E+00 | 2.47E-14 | 2.47E-14 | 2.47E-14 | 2.47E-14 | 2.47E-14 | 2.47E-14 | 2.47E-14 | 2.47E-14 | 2.47E-14 | 2.47E-14 |
| SC | 48 | 0.00E+00 | 1.28E-14 | 1.28E-14 | 1.28E-14 | 1.28E-14 | 1.28E-14 | 1.28E-14 | 1.28E-14 | 1.28E-14 | 1.28E-14 | 1.28E-14 |
| SC | 49 | 0.00E+00 | 9.42E-19 | 9.42E-19 | 9.42E-19 | 9.42E-19 | 9.42E-19 | 9.42E-19 | 9.42E-19 | 9.42E-19 | 9.42E-19 | 9.42E-19 |
| TI | 45 | 0.00E+00 | 1.41E-17 | 1.41E-17 | 1.41E-17 | 1.41E-17 | 1.41E-17 | 1.41E-17 | 1.41E-17 | 1.41E-17 | 1.41E-17 | 1.41E-17 |
| TI | 46 | 0.00E+00 | 6.64E-13 | 1.67E-12 | 2.81E-12 | 4.00E-12 | 9.02E-12 | 2.54E-11 | 5.17E-11 | 7.82E-11 | 1.05E-10 | 1.56E-10 |
| TI | 47 | 0.00E+00 | 2.66E-12 | 5.42E-12 | 8.14E-12 | 1.08E-11 | 2.16E-11 | 5.41E-11 | 1.08E-10 | 1.62E-10 | 2.16E-10 | 3.23E-10 |
| TI | 48 | 0.00E+00 | 1.19E-12 | 2.53E-12 | 3.85E-12 | 5.16E-12 | 1.05E-11 | 2.64E-11 | 5.25E-11 | 7.88E-11 | 1.05E-10 | 1.57E-10 |
| TI | 49 | 0.00E+00 | 2.37E-13 | 6.16E-13 | 1.10E-12 | 1.66E-12 | 4.56E-12 | 1.56E-11 | 3.51E-11 | 5.49E-11 | 7.46E-11 | 1.18E-10 |
| TI | 50 | 0.00E+00 | 1.05E-14 | 2.13E-14 | 3.20E-14 | 4.25E-14 | 8.51E-14 | 2.13E-13 | 4.25E-13 | 6.38E-13 | 8.51E-13 | 1.28E-12 |
| TI | 51 | 0.00E+00 | 1.18E-19 | 1.18E-19 | 1.18E-19 | 1.18E-19 | 1.18E-19 | 1.18E-19 | 1.18E-19 | 1.18E-19 | 1.18E-19 | 1.18E-19 |
| V | 47 | 0.00E+00 | 2.93E-16 | 2.93E-16 | 2.93E-16 | 2.93E-16 | 2.93E-16 | 2.93E-16 | 2.93E-16 | 2.93E-16 | 2.93E-16 | 2.93E-16 |

**Table A.8. (continued)**

| Proton beam energy: 1 GeV | | | | | | | Operational line loss assumption: 1 nA/m (continuous) | | | | | |
|---|---|---|---|---|---|---|---|---|---|---|---|---|
| Nuclide masses integrated over the material zone volume in the HETC & MCNP calculational model | | | | | | | | | | | | |
| Nuclide concentration | | Time (s) | 7.88E+06 | 1.58E+07 | 2.37E+07 | 3.15E+07 | 6.31E+07 | 1.58E+08 | 3.15E+08 | 4.73E+08 | 6.31E+08 | 9.46E+08 |
| (gram-atoms) | | Initial | 3 months | 6 months | 9 months | 1 year | 2 years | 5 years | 10 years | 15 years | 20 years | 30 years |
| V | 48 | 0.00E+00 | 1.01E-13 | 1.03E-13 | 1.03E-13 | 1.03E-13 | 1.03E-13 | 1.03E-13 | 1.03E-13 | 1.03E-13 | 1.03E-13 | 1.03E-13 |
| V | 49 | 0.00E+00 | 7.35E-13 | 1.36E-12 | 1.87E-12 | 2.28E-12 | 3.33E-12 | 4.14E-12 | 4.23E-12 | 4.23E-12 | 4.23E-12 | 4.23E-12 |
| V | 50 | 0.00E+00 | 8.19E-13 | 1.66E-12 | 2.49E-12 | 3.32E-12 | 6.64E-12 | 1.66E-11 | 3.32E-11 | 4.98E-11 | 6.64E-11 | 9.96E-11 |
| V | 51 | 0.00E+00 | 2.47E-12 | 6.51E-12 | 1.06E-11 | 1.47E-11 | 3.32E-11 | 8.49E-11 | 1.69E-10 | 2.54E-10 | 3.39E-10 | 5.06E-10 |
| V | 52 | 0.00E+00 | 4.05E-19 | 4.05E-19 | 4.05E-19 | 4.05E-19 | 4.05E-19 | 4.05E-19 | 4.05E-19 | 4.05E-19 | 4.05E-19 | 4.05E-19 |
| CR | 49 | 0.00E+00 | 1.88E-16 | 1.88E-16 | 1.88E-16 | 1.88E-16 | 1.88E-16 | 1.88E-16 | 1.88E-16 | 1.88E-16 | 1.88E-16 | 1.88E-16 |
| CR | 50 | 0.00E+00 | 3.24E-12 | 6.58E-12 | 9.87E-12 | 1.31E-11 | 2.63E-11 | 6.58E-11 | 1.31E-10 | 1.97E-10 | 2.63E-10 | 3.94E-10 |
| CR | 51 | 0.00E+00 | 1.62E-12 | 1.80E-12 | 1.81E-12 | 1.81E-12 | 1.81E-12 | 1.81E-12 | 1.81E-12 | 1.81E-12 | 1.81E-12 | 1.81E-12 |
| CR | 52 | 0.00E+00 | 5.80E-12 | 1.21E-11 | 1.83E-11 | 2.44E-11 | 4.82E-11 | 1.19E-10 | 2.37E-10 | 3.55E-10 | 4.73E-10 | 7.08E-10 |
| CR | 53 | 0.00E+00 | 1.90E-12 | 3.85E-12 | 5.78E-12 | 7.68E-12 | 1.54E-11 | 3.85E-11 | 7.68E-11 | 1.15E-10 | 1.54E-10 | 2.31E-10 |
| CR | 54 | 0.00E+00 | 7.86E-13 | 3.02E-12 | 6.38E-12 | 1.06E-11 | 3.41E-11 | 1.28E-10 | 2.95E-10 | 4.64E-10 | 6.33E-10 | 1.01E-09 |
| CR | 55 | 0.00E+00 | 7.53E-20 | 7.53E-20 | 7.53E-20 | 7.53E-20 | 7.53E-20 | 7.53E-20 | 7.53E-20 | 7.53E-20 | 7.53E-20 | 7.53E-20 |
| CR | 56 | 0.00E+00 | 2.37E-20 | 2.37E-20 | 2.37E-20 | 2.37E-20 | 2.37E-20 | 2.37E-20 | 2.37E-20 | 2.37E-20 | 2.37E-20 | 2.37E-20 |
| MN | 52 | 0.00E+00 | 2.91E-13 | 2.91E-13 | 2.91E-13 | 2.91E-13 | 2.91E-13 | 2.91E-13 | 2.91E-13 | 2.91E-13 | 2.91E-13 | 2.91E-13 |
| **MN** | **53** | **0.00E+00** | **7.58E-12** | **1.54E-11** | **2.31E-11** | **3.07E-11** | **6.15E-11** | **1.54E-10** | **3.07E-10** | **4.61E-10** | **6.15E-10** | **9.22E-10** |
| MN | 54 | 0.00E+00 | 7.53E-12 | 1.39E-11 | 1.90E-11 | 2.31E-11 | 3.34E-11 | 4.09E-11 | 4.16E-11 | 4.16E-11 | 4.16E-11 | 4.16E-11 |
| MN | 55 | 0.00E+00 | 5.27E-12 | 1.14E-11 | 1.80E-11 | 2.51E-11 | 5.89E-11 | 1.95E-10 | 4.74E-10 | 7.80E-10 | 1.09E-09 | 1.72E-09 |
| MN | 56 | 0.00E+00 | 2.89E-15 | 2.89E-15 | 2.89E-15 | 2.89E-15 | 2.89E-15 | 2.89E-15 | 2.89E-15 | 2.89E-15 | 2.89E-15 | 2.89E-15 |
| MN | 57 | 0.00E+00 | 2.05E-19 | 2.05E-19 | 2.05E-19 | 2.05E-19 | 2.05E-19 | 2.05E-19 | 2.05E-19 | 2.05E-19 | 2.05E-19 | 2.05E-19 |
| FE | 53 | 0.00E+00 | 3.98E-17 | 3.98E-17 | 3.98E-17 | 3.98E-17 | 3.98E-17 | 3.98E-17 | 3.98E-17 | 3.98E-17 | 3.98E-17 | 3.98E-17 |
| FE | 54 | 0.00E+00 | 4.04E-12 | 8.20E-12 | 1.23E-11 | 1.63E-11 | 3.27E-11 | 8.20E-11 | 1.63E-10 | 2.45E-10 | 3.27E-10 | 4.91E-10 |
| **FE** | **55** | **0.00E+00** | **1.02E-11** | **2.01E-11** | **2.92E-11** | **3.77E-11** | **6.69E-11** | **1.20E-10** | **1.53E-10** | **1.62E-10** | **1.65E-10** | **1.66E-10** |
| FE | 56 | 0.00E+00 | 3.83E-12 | 7.78E-12 | 1.17E-11 | 1.55E-11 | 3.11E-11 | 7.78E-11 | 1.55E-10 | 2.33E-10 | 3.11E-10 | 4.65E-10 |
| FE | 57 | 0.00E+00 | 2.23E-12 | 4.53E-12 | 6.79E-12 | 9.02E-12 | 1.81E-11 | 4.53E-11 | 9.02E-11 | 1.35E-10 | 1.81E-10 | 2.71E-10 |
| FE | 58 | 0.00E+00 | 4.45E-13 | 9.04E-13 | 1.36E-12 | 1.80E-12 | 3.61E-12 | 9.04E-12 | 1.80E-11 | 2.71E-11 | 3.61E-11 | 5.41E-11 |
| FE | 59 | 0.00E+00 | 3.91E-15 | 4.88E-15 | 5.11E-15 | 5.17E-15 | 5.18E-15 | 5.18E-15 | 5.18E-15 | 5.18E-15 | 5.18E-15 | 5.18E-15 |
| CO | 59 | 0.00E+00 | 3.36E-15 | 9.86E-15 | 1.70E-14 | 2.42E-14 | 5.37E-14 | 1.47E-13 | 2.99E-13 | 4.52E-13 | 6.05E-13 | 9.04E-13 |
| NI | 60 | 0.00E+00 | 7.50E-16 | 1.52E-15 | 2.28E-15 | 3.03E-15 | 6.08E-15 | 1.52E-14 | 3.03E-14 | 4.56E-14 | 6.08E-14 | 9.11E-14 |
| NI | 61 | 0.00E+00 | 4.75E-16 | 9.66E-16 | 1.45E-15 | 1.93E-15 | 3.86E-15 | 9.66E-15 | 1.93E-14 | 2.89E-14 | 3.86E-14 | 5.78E-14 |
| NI | 62 | 0.00E+00 | 6.99E-17 | 1.42E-16 | 2.13E-16 | 2.83E-16 | 5.67E-16 | 1.42E-15 | 2.83E-15 | 4.25E-15 | 5.67E-15 | 8.50E-15 |
| NI | 63 | 0.00E+00 | 3.01E-16 | 6.10E-16 | 9.14E-16 | 1.21E-15 | 2.42E-15 | 6.01E-15 | 1.18E-14 | 1.74E-14 | 2.28E-14 | 3.30E-14 |
| NI | 64 | 0.00E+00 | 6.74E-15 | 1.37E-14 | 2.06E-14 | 2.74E-14 | 5.49E-14 | 1.37E-13 | 2.73E-13 | 4.10E-13 | 5.47E-13 | 8.20E-13 |
| NI | 65 | 0.00E+00 | 1.10E-19 | 1.10E-19 | 1.10E-19 | 1.10E-19 | 1.10E-19 | 1.10E-19 | 1.10E-19 | 1.10E-19 | 1.10E-19 | 1.10E-19 |
| NI | 66 | 0.00E+00 | 6.05E-20 | 6.05E-20 | 6.05E-20 | 6.05E-20 | 6.05E-20 | 6.05E-20 | 6.05E-20 | 6.05E-20 | 6.05E-20 | 6.05E-20 |

**Table A.8. (continued)**

| Proton beam energy: 1 GeV | | | | | | | Operational line loss assumption: 1 nA/m (continuous) | | | | | |
|---|---|---|---|---|---|---|---|---|---|---|---|---|
| Nuclide masses integrated over the material zone volume in the HETC & MCNP calculational model | | | | | | | | | | | | |
| Nuclide concentration | | Time (s) | 7.88E+06 | 1.58E+07 | 2.37E+07 | 3.15E+07 | 6.31E+07 | 1.58E+08 | 3.15E+08 | 4.73E+08 | 6.31E+08 | 9.46E+08 |
| (gram-atoms) | | Initial | 3 months | 6 months | 9 months | 1 year | 2 years | 5 years | 10 years | 15 years | 20 years | 30 years |
| CU | 63 | 0.00E+00 | 1.23E-14 | 2.50E-14 | 3.76E-14 | 4.99E-14 | 1.00E-13 | 2.50E-13 | 4.99E-13 | 7.50E-13 | 1.00E-12 | 1.50E-12 |
| CU | 64 | 0.00E+00 | 9.36E-17 | 9.36E-17 | 9.36E-17 | 9.36E-17 | 9.36E-17 | 9.36E-17 | 9.36E-17 | 9.36E-17 | 9.36E-17 | 9.36E-17 |
| CU | 65 | 0.00E+00 | 3.64E-15 | 1.23E-14 | 2.45E-14 | 3.94E-14 | 1.17E-13 | 4.03E-13 | 8.94E-13 | 1.39E-12 | 1.88E-12 | 2.96E-12 |
| CU | 66 | 0.00E+00 | 5.28E-20 | 5.28E-20 | 5.28E-20 | 5.28E-20 | 5.28E-20 | 5.28E-20 | 5.28E-20 | 5.28E-20 | 5.28E-20 | 5.28E-20 |
| CU | 67 | 0.00E+00 | 5.66E-18 | 5.66E-18 | 5.66E-18 | 5.66E-18 | 5.66E-18 | 5.66E-18 | 5.66E-18 | 5.66E-18 | 5.66E-18 | 5.66E-18 |
| ZN | 63 | 0.00E+00 | 2.18E-18 | 2.18E-18 | 2.18E-18 | 2.18E-18 | 2.18E-18 | 2.18E-18 | 2.18E-18 | 2.18E-18 | 2.18E-18 | 2.18E-18 |
| ZN | 64 | 0.00E+00 | 4.37E-15 | 8.92E-15 | 1.34E-14 | 1.78E-14 | 3.56E-14 | 8.90E-14 | 1.77E-13 | 2.66E-13 | 3.55E-13 | 5.32E-13 |
| ZN | 65 | 0.00E+00 | 2.07E-14 | 3.72E-14 | 4.97E-14 | 5.92E-14 | 8.02E-14 | 9.13E-14 | 9.18E-14 | 9.18E-14 | 9.18E-14 | 9.18E-14 |
| ZN | 66 | 0.00E+00 | 2.72E-15 | 5.52E-15 | 8.28E-15 | 1.10E-14 | 2.20E-14 | 5.52E-14 | 1.10E-13 | 1.65E-13 | 2.20E-13 | 3.31E-13 |
| ZN | 67 | 0.00E+00 | 9.97E-15 | 2.02E-14 | 3.04E-14 | 4.04E-14 | 8.09E-14 | 2.02E-13 | 4.04E-13 | 6.06E-13 | 8.08E-13 | 1.21E-12 |
| ZN | 68 | 0.00E+00 | 3.31E-15 | 6.73E-15 | 1.01E-14 | 1.34E-14 | 2.69E-14 | 6.73E-14 | 1.34E-13 | 2.01E-13 | 2.69E-13 | 4.03E-13 |
| ZN | 69 | 0.00E+00 | 9.18E-19 | 9.18E-19 | 9.18E-19 | 9.18E-19 | 9.18E-19 | 9.18E-19 | 9.18E-19 | 9.18E-19 | 9.18E-19 | 9.18E-19 |
| ZN | 70 | 0.00E+00 | 6.34E-19 | 1.29E-18 | 1.93E-18 | 2.57E-18 | 5.14E-18 | 1.29E-17 | 2.57E-17 | 3.85E-17 | 5.14E-17 | 7.71E-17 |
| GA | 69 | 0.00E+00 | 1.48E-15 | 3.01E-15 | 4.52E-15 | 6.01E-15 | 1.20E-14 | 3.01E-14 | 6.01E-14 | 9.02E-14 | 1.20E-13 | 1.80E-13 |
| GA | 71 | 0.00E+00 | 4.04E-17 | 8.21E-17 | 1.23E-16 | 1.64E-16 | 3.28E-16 | 8.21E-16 | 1.64E-15 | 2.46E-15 | 3.28E-15 | 4.91E-15 |
| BR | 81 | 0.00E+00 | 5.60E-17 | 1.14E-16 | 1.71E-16 | 2.27E-16 | 4.55E-16 | 1.14E-15 | 2.27E-15 | 3.41E-15 | 4.55E-15 | 6.82E-15 |
| BR | 82 | 0.00E+00 | 4.07E-18 | 4.07E-18 | 4.07E-18 | 4.07E-18 | 4.07E-18 | 4.07E-18 | 4.07E-18 | 4.07E-18 | 4.07E-18 | 4.07E-18 |
| BR | 83 | 0.00E+00 | 3.33E-20 | 3.33E-20 | 3.33E-20 | 3.33E-20 | 3.33E-20 | 3.33E-20 | 3.33E-20 | 3.33E-20 | 3.33E-20 | 3.33E-20 |
| BR | 84 | 0.00E+00 | 1.68E-20 | 1.68E-20 | 1.68E-20 | 1.68E-20 | 1.68E-20 | 1.68E-20 | 1.68E-20 | 1.68E-20 | 1.68E-20 | 1.68E-20 |
| KR | 82 | 0.00E+00 | 8.08E-13 | 1.64E-12 | 2.46E-12 | 3.27E-12 | 6.55E-12 | 1.64E-11 | 3.27E-11 | 4.91E-11 | 6.55E-11 | 9.82E-11 |
| KR | 83 | 0.00E+00 | 2.48E-16 | 5.04E-16 | 7.56E-16 | 1.00E-15 | 2.01E-15 | 5.04E-15 | 1.00E-14 | 1.51E-14 | 2.01E-14 | 3.02E-14 |
| KR | 83M | 0.00E+00 | 2.58E-20 | 2.58E-20 | 2.58E-20 | 2.58E-20 | 2.58E-20 | 2.58E-20 | 2.58E-20 | 2.58E-20 | 2.58E-20 | 2.58E-20 |
| KR | 84 | 0.00E+00 | 1.55E-14 | 4.22E-14 | 7.00E-14 | 9.76E-14 | 2.24E-13 | 5.75E-13 | 1.15E-12 | 1.72E-12 | 2.30E-12 | 3.43E-12 |
| KR | 85 | 0.00E+00 | 1.72E-15 | 3.46E-15 | 5.15E-15 | 6.79E-15 | 1.32E-14 | 3.00E-14 | 5.17E-14 | 6.74E-14 | 7.88E-14 | 9.30E-14 |
| KR | 86 | 0.00E+00 | 8.54E-17 | 1.73E-16 | 2.60E-16 | 3.46E-16 | 6.93E-16 | 1.73E-15 | 3.46E-15 | 5.19E-15 | 6.93E-15 | 1.04E-14 |
| KR | 87 | 0.00E+00 | 1.63E-19 | 1.63E-19 | 1.63E-19 | 1.63E-19 | 1.63E-19 | 1.63E-19 | 1.63E-19 | 1.63E-19 | 1.63E-19 | 1.63E-19 |
| RB | 82 | 0.00E+00 | 1.12E-17 | 1.12E-17 | 1.12E-17 | 1.12E-17 | 1.12E-17 | 1.12E-17 | 1.12E-17 | 1.12E-17 | 1.12E-17 | 1.12E-17 |
| RB | 84 | 0.00E+00 | 1.24E-14 | 1.43E-14 | 1.46E-14 | 1.46E-14 | 1.46E-14 | 1.46E-14 | 1.46E-14 | 1.46E-14 | 1.46E-14 | 1.46E-14 |
| RB | 85 | 0.00E+00 | 4.79E-17 | 1.26E-16 | 2.30E-16 | 3.60E-16 | 1.15E-15 | 5.81E-15 | 1.98E-14 | 3.99E-14 | 6.44E-14 | 1.22E-13 |
| RB | 86 | 0.00E+00 | 4.15E-14 | 4.30E-14 | 4.30E-14 | 4.30E-14 | 4.30E-14 | 4.30E-14 | 4.30E-14 | 4.30E-14 | 4.30E-14 | 4.30E-14 |
| RB | 87 | 0.00E+00 | 1.92E-16 | 3.91E-16 | 5.86E-16 | 7.79E-16 | 1.56E-15 | 3.91E-15 | 7.79E-15 | 1.17E-14 | 1.56E-14 | 2.34E-14 |
| RB | 88 | 0.00E+00 | 1.29E-18 | 1.29E-18 | 1.29E-18 | 1.29E-18 | 1.29E-18 | 1.29E-18 | 1.29E-18 | 1.29E-18 | 1.29E-18 | 1.29E-18 |
| SR | 84 | 0.00E+00 | 4.62E-16 | 1.27E-15 | 2.11E-15 | 2.94E-15 | 6.77E-15 | 1.74E-14 | 3.47E-14 | 5.21E-14 | 6.94E-14 | 1.04E-13 |
| SR | 86 | 0.00E+00 | 1.03E-13 | 2.50E-13 | 3.96E-13 | 5.40E-13 | 1.17E-12 | 2.97E-12 | 5.92E-12 | 8.89E-12 | 1.19E-11 | 1.77E-11 |

**Table A.8. (continued)**

| Proton beam energy: 1 GeV | | | | | | | Operational line loss assumption: 1 nA/m (continuous) | | | | | |
|---|---|---|---|---|---|---|---|---|---|---|---|---|
| Nuclide masses integrated over the material zone volume in the HETC & MCNP calculational model | | | | | | | | | | | | |
| Nuclide concentration | | Time (s) | 7.88E+06 | 1.58E+07 | 2.37E+07 | 3.15E+07 | 6.31E+07 | 1.58E+08 | 3.15E+08 | 4.73E+08 | 6.31E+08 | 9.46E+08 |
| (gram-atoms) | | Initial | 3 months | 6 months | 9 months | 1 year | 2 years | 5 years | 10 years | 15 years | 20 years | 30 years |
| SR | 88 | 0.00E+00 | 6.57E-15 | 1.34E-14 | 2.00E-14 | 2.66E-14 | 5.33E-14 | 1.34E-13 | 2.66E-13 | 4.00E-13 | 5.33E-13 | 7.99E-13 |
| I | 127 | 0.00E+00 | 2.38E-20 | 6.70E-20 | 1.13E-19 | 1.58E-19 | 3.71E-19 | 9.55E-19 | 1.90E-18 | 2.86E-18 | 3.81E-18 | 5.69E-18 |
| XE | 126 | 0.00E+00 | 1.87E-20 | 3.80E-20 | 5.70E-20 | 7.58E-20 | 1.52E-19 | 3.80E-19 | 7.58E-19 | 1.14E-18 | 1.52E-18 | 2.28E-18 |
| XE | 127 | 0.00E+00 | 2.19E-20 | 2.58E-20 | 2.65E-20 | 2.66E-20 | 2.67E-20 | 2.67E-20 | 2.67E-20 | 2.67E-20 | 2.67E-20 | 2.67E-20 |
| XE | 128 | 0.00E+00 | 4.20E-19 | 8.68E-19 | 1.31E-18 | 1.74E-18 | 3.51E-18 | 8.80E-18 | 1.76E-17 | 2.64E-17 | 3.52E-17 | 5.28E-17 |
| XE | 129 | 0.00E+00 | 6.68E-18 | 1.37E-17 | 2.07E-17 | 2.75E-17 | 5.48E-17 | 1.37E-16 | 2.72E-16 | 4.08E-16 | 5.44E-16 | 8.15E-16 |
| XE | 130 | 0.00E+00 | 4.71E-19 | 9.57E-19 | 1.44E-18 | 1.91E-18 | 3.82E-18 | 9.57E-18 | 1.91E-17 | 2.86E-17 | 3.82E-17 | 5.73E-17 |
| XE | 131 | 0.00E+00 | 3.99E-17 | 1.02E-16 | 1.63E-16 | 2.24E-16 | 4.78E-16 | 1.22E-15 | 2.45E-15 | 3.69E-15 | 4.92E-15 | 7.38E-15 |
| XE | 132 | 0.00E+00 | 2.99E-18 | 6.16E-18 | 9.29E-18 | 1.24E-17 | 2.46E-17 | 6.12E-17 | 1.22E-16 | 1.82E-16 | 2.43E-16 | 3.64E-16 |
| XE | 133 | 0.00E+00 | 1.17E-19 | 1.17E-19 | 1.17E-19 | 1.17E-19 | 1.17E-19 | 1.17E-19 | 1.17E-19 | 1.17E-19 | 1.17E-19 | 1.17E-19 |
| XE | 134 | 0.00E+00 | 3.35E-18 | 6.81E-18 | 1.02E-17 | 1.36E-17 | 2.72E-17 | 6.81E-17 | 1.36E-16 | 2.04E-16 | 2.72E-16 | 4.08E-16 |
| XE | 135 | 0.00E+00 | 9.57E-20 | 9.57E-20 | 9.57E-20 | 9.57E-20 | 9.57E-20 | 9.57E-20 | 9.57E-20 | 9.57E-20 | 9.57E-20 | 9.57E-20 |
| XE | 136 | 0.00E+00 | 3.11E-19 | 6.31E-19 | 9.47E-19 | 1.26E-18 | 2.52E-18 | 6.31E-18 | 1.26E-17 | 1.89E-17 | 2.52E-17 | 3.78E-17 |
| CS | 129 | 0.00E+00 | 1.44E-19 | 1.44E-19 | 1.44E-19 | 1.44E-19 | 1.44E-19 | 1.44E-19 | 1.44E-19 | 1.44E-19 | 1.44E-19 | 1.44E-19 |
| CS | 131 | 0.00E+00 | 9.06E-18 | 9.26E-18 | 9.27E-18 | 9.27E-18 | 9.27E-18 | 9.27E-18 | 9.27E-18 | 9.27E-18 | 9.27E-18 | 9.27E-18 |
| CS | 132 | 0.00E+00 | 9.30E-20 | 9.30E-20 | 9.30E-20 | 9.30E-20 | 9.30E-20 | 9.30E-20 | 9.30E-20 | 9.30E-20 | 9.30E-20 | 9.30E-20 |
| CS | 133 | 0.00E+00 | 6.64E-18 | 1.88E-17 | 3.60E-17 | 5.78E-17 | 1.94E-16 | 1.03E-15 | 3.56E-15 | 7.21E-15 | 1.17E-14 | 2.21E-14 |
| CS | 134 | 0.00E+00 | 6.27E-18 | 1.22E-17 | 1.76E-17 | 2.25E-17 | 3.85E-17 | 6.41E-17 | 7.60E-17 | 7.82E-17 | 7.86E-17 | 7.87E-17 |
| CS | 135 | 0.00E+00 | 2.03E-17 | 4.14E-17 | 6.22E-17 | 8.27E-17 | 1.65E-16 | 4.14E-16 | 8.24E-16 | 1.24E-15 | 1.65E-15 | 2.47E-15 |
| CS | 136 | 0.00E+00 | 2.33E-18 | 2.35E-18 | 2.35E-18 | 2.35E-18 | 2.35E-18 | 2.35E-18 | 2.35E-18 | 2.35E-18 | 2.35E-18 | 2.35E-18 |
| CS | 137 | 0.00E+00 | 4.23E-17 | 8.56E-17 | 1.28E-16 | 1.70E-16 | 3.36E-16 | 8.13E-16 | 1.53E-15 | 2.18E-15 | 2.75E-15 | 3.72E-15 |
| CS | 138 | 0.00E+00 | 1.71E-20 | 1.71E-20 | 1.71E-20 | 1.71E-20 | 1.71E-20 | 1.71E-20 | 1.71E-20 | 1.71E-20 | 1.71E-20 | 1.71E-20 |
| BA | 128 | 0.00E+00 | 1.38E-20 | 1.38E-20 | 1.38E-20 | 1.38E-20 | 1.38E-20 | 1.38E-20 | 1.38E-20 | 1.38E-20 | 1.38E-20 | 1.38E-20 |
| BA | 130 | 0.00E+00 | 1.07E-18 | 2.17E-18 | 3.26E-18 | 4.33E-18 | 8.67E-18 | 2.17E-17 | 4.33E-17 | 6.50E-17 | 8.67E-17 | 1.30E-16 |
| BA | 131 | 0.00E+00 | 1.14E-17 | 1.14E-17 | 1.14E-17 | 1.14E-17 | 1.14E-17 | 1.14E-17 | 1.14E-17 | 1.14E-17 | 1.14E-17 | 1.14E-17 |
| BA | 132 | 0.00E+00 | 4.93E-17 | 1.00E-16 | 1.50E-16 | 2.00E-16 | 4.00E-16 | 1.00E-15 | 1.99E-15 | 3.00E-15 | 4.00E-15 | 5.99E-15 |
| BA | 133 | 0.00E+00 | 3.14E-16 | 6.33E-16 | 9.42E-16 | 1.24E-15 | 2.41E-15 | 5.49E-15 | 9.44E-15 | 1.23E-14 | 1.44E-14 | 1.70E-14 |
| BA | 134 | 0.00E+00 | 1.52E-15 | 3.10E-15 | 4.65E-15 | 6.18E-15 | 1.24E-14 | 3.10E-14 | 6.19E-14 | 9.30E-14 | 1.24E-13 | 1.86E-13 |
| BA | 135 | 0.00E+00 | 8.04E-16 | 1.63E-15 | 2.45E-15 | 3.25E-15 | 6.52E-15 | 1.63E-14 | 3.25E-14 | 4.89E-14 | 6.52E-14 | 9.77E-14 |
| BA | 136 | 0.00E+00 | 5.81E-15 | 1.18E-14 | 1.77E-14 | 2.35E-14 | 4.71E-14 | 1.18E-13 | 2.35E-13 | 3.53E-13 | 4.71E-13 | 7.07E-13 |
| BA | 137 | 0.00E+00 | 5.32E-15 | 1.08E-14 | 1.62E-14 | 2.15E-14 | 4.31E-14 | 1.08E-13 | 2.15E-13 | 3.24E-13 | 4.32E-13 | 6.48E-13 |
| BA | 138 | 0.00E+00 | 9.90E-16 | 2.01E-15 | 3.01E-15 | 4.01E-15 | 8.03E-15 | 2.01E-14 | 4.01E-14 | 6.02E-14 | 8.03E-14 | 1.20E-13 |
| BA | 139 | 0.00E+00 | 9.71E-19 | 9.71E-19 | 9.71E-19 | 9.71E-19 | 9.71E-19 | 9.71E-19 | 9.71E-19 | 9.71E-19 | 9.71E-19 | 9.71E-19 |
| LA | 139 | 0.00E+00 | 1.05E-15 | 2.13E-15 | 3.19E-15 | 4.25E-15 | 8.50E-15 | 2.13E-14 | 4.24E-14 | 6.37E-14 | 8.50E-14 | 1.27E-13 |

| Table A.8. (continued) | | | | | | | | | | | | |
|---|---|---|---|---|---|---|---|---|---|---|---|---|
| Proton beam energy: 1 GeV | | | | | | | Operational line loss assumption: 1 nA/m (continuous) | | | | | |
| Nuclide masses integrated over the material zone volume in the HETC & MCNP calculational model | | | | | | | | | | | | |
| Nuclide concentration | | Time (s) | 7.88E+06 | 1.58E+07 | 2.37E+07 | 3.15E+07 | 6.31E+07 | 1.58E+08 | 3.15E+08 | 4.73E+08 | 6.31E+08 | 9.46E+08 |
| (gram-atoms) | | Initial | 3 months | 6 months | 9 months | 1 year | 2 years | 5 years | 10 years | 15 years | 20 years | 30 years |
| EU | 155 | 0.00E+00 | 1.11E-20 | 2.22E-20 | 3.27E-20 | 4.28E-20 | 7.99E-20 | 1.64E-19 | 2.43E-19 | 2.82E-19 | 3.01E-19 | 3.14E-19 |
| EU | 156 | 0.00E+00 | 2.04E-20 | 2.08E-20 | 2.08E-20 | 2.08E-20 | 2.08E-20 | 2.08E-20 | 2.08E-20 | 2.08E-20 | 2.08E-20 | 2.08E-20 |
| GD | 156 | 0.00E+00 | 6.57E-20 | 1.54E-19 | 2.42E-19 | 3.28E-19 | 6.99E-19 | 1.77E-18 | 3.53E-18 | 5.30E-18 | 7.07E-18 | 1.06E-17 |
| GD | 157 | 0.00E+00 | 2.33E-20 | 6.16E-20 | 1.14E-19 | 1.79E-19 | 5.83E-19 | 3.14E-18 | 1.17E-17 | 2.58E-17 | 4.51E-17 | 9.88E-17 |
| GD | 158 | 0.00E+00 | 1.37E-19 | 2.99E-19 | 4.80E-19 | 6.79E-19 | 1.69E-18 | 6.72E-18 | 2.15E-17 | 4.43E-17 | 7.49E-17 | 1.58E-16 |
| TB | 157 | 0.00E+00 | 1.20E-17 | 2.44E-17 | 3.66E-17 | 4.86E-17 | 9.72E-17 | 2.42E-16 | 4.76E-16 | 7.07E-16 | 9.32E-16 | 1.37E-15 |
| TB | 158 | 0.00E+00 | 2.17E-17 | 4.40E-17 | 6.59E-17 | 8.76E-17 | 1.75E-16 | 4.35E-16 | 8.58E-16 | 1.27E-15 | 1.68E-15 | 2.46E-15 |
| TB | 159 | 0.00E+00 | 1.24E-19 | 2.54E-19 | 3.82E-19 | 5.08E-19 | 1.01E-18 | 2.53E-18 | 5.04E-18 | 7.56E-18 | 1.01E-17 | 1.51E-17 |
| TB | 160 | 0.00E+00 | 3.77E-16 | 5.39E-16 | 6.04E-16 | 6.32E-16 | 6.51E-16 | 6.51E-16 | 6.51E-16 | 6.51E-16 | 6.51E-16 | 6.51E-16 |
| DY | 160 | 0.00E+00 | 1.86E-16 | 6.03E-16 | 1.11E-15 | 1.64E-15 | 3.91E-15 | 1.14E-14 | 2.34E-14 | 3.55E-14 | 4.76E-14 | 7.10E-14 |
| Total | | 0.00E+00 | 5.81E-09 | 1.18E-08 | 1.77E-08 | 2.35E-08 | 4.71E-08 | 1.18E-07 | 2.35E-07 | 3.53E-07 | 4.71E-07 | 7.07E-07 |

| Table A.9. SNS nuclide production during normal proton beam operation: earth berm Zone 5 | | | | | | | | | | | | |
|---|---|---|---|---|---|---|---|---|---|---|---|---|
| Proton beam energy: 1 GeV | | | | | | | Operational line loss assumption: 1 nA/m (continuous) | | | | | |
| Nuclide masses integrated over the material zone volume in the HETC & MCNP calculational model | | | | | | | | | | | | |
| Nuclide concentration | | Time (s) | 7.88E+06 | 1.58E+07 | 2.37E+07 | 3.15E+07 | 6.31E+07 | 1.58E+08 | 3.15E+08 | 4.73E+08 | 6.31E+08 | 9.46E+08 |
| (gram-atoms) | | Initial | 3 months | 6 months | 9 months | 1 year | 2 years | 5 years | 10 years | 15 years | 20 years | 30 years |
| H | 1 | 0.00E+00 | 5.64E-10 | 1.15E-09 | 1.72E-09 | 2.28E-09 | 4.58E-09 | 1.15E-08 | 2.28E-08 | 3.43E-08 | 4.58E-08 | 6.86E-08 |
| H | 2 | 0.00E+00 | 1.18E-11 | 2.39E-11 | 3.58E-11 | 4.76E-11 | 9.54E-11 | 2.39E-10 | 4.76E-10 | 7.15E-10 | 9.54E-10 | 1.43E-09 |
| **H** | **3** | **0.00E+00** | **9.23E-12** | **1.86E-11** | **2.77E-11** | **3.66E-11** | **7.13E-11** | **1.64E-10** | **2.88E-10** | **3.81E-10** | **4.52E-10** | **5.45E-10** |
| HE | 3 | 0.00E+00 | 3.73E-12 | 7.71E-12 | 1.18E-11 | 1.59E-11 | 3.38E-11 | 9.87E-11 | 2.37E-10 | 4.06E-10 | 5.99E-10 | 1.03E-09 |
| HE | 4 | 0.00E+00 | 1.19E-10 | 2.41E-10 | 3.61E-10 | 4.80E-10 | 9.61E-10 | 2.41E-09 | 4.80E-09 | 7.21E-09 | 9.61E-09 | 1.44E-08 |
| LI | 6 | 0.00E+00 | 2.02E-12 | 4.10E-12 | 6.15E-12 | 8.17E-12 | 1.64E-11 | 4.10E-11 | 8.17E-11 | 1.23E-10 | 1.64E-10 | 2.45E-10 |
| BE | 9 | 0.00E+00 | 8.45E-13 | 1.72E-12 | 2.57E-12 | 3.42E-12 | 6.85E-12 | 1.72E-11 | 3.42E-11 | 5.14E-11 | 6.85E-11 | 1.03E-10 |
| **BE** | **10** | **0.00E+00** | **4.04E-13** | **8.21E-13** | **1.23E-12** | **1.64E-12** | **3.28E-12** | **8.21E-12** | **1.64E-11** | **2.46E-11** | **3.28E-11** | **4.91E-11** |
| B | 10 | 0.00E+00 | 3.23E-12 | 6.56E-12 | 9.84E-12 | 1.31E-11 | 2.62E-11 | 6.56E-11 | 1.31E-10 | 1.96E-10 | 2.62E-10 | 3.93E-10 |
| B | 11 | 0.00E+00 | 6.12E-12 | 1.24E-11 | 1.86E-11 | 2.48E-11 | 4.96E-11 | 1.24E-10 | 2.48E-10 | 3.72E-10 | 4.96E-10 | 7.44E-10 |
| C | 11 | 0.00E+00 | 4.58E-16 | 4.58E-16 | 4.58E-16 | 4.58E-16 | 4.58E-16 | 4.58E-16 | 4.58E-16 | 4.58E-16 | 4.58E-16 | 4.58E-16 |
| C | 12 | 0.00E+00 | 6.97E-11 | 1.42E-10 | 2.12E-10 | 2.82E-10 | 5.65E-10 | 1.42E-09 | 2.82E-09 | 4.24E-09 | 5.65E-09 | 8.47E-09 |
| C | 13 | 0.00E+00 | 5.14E-11 | 1.04E-10 | 1.57E-10 | 2.08E-10 | 4.17E-10 | 1.04E-09 | 2.08E-09 | 3.13E-09 | 4.17E-09 | 6.25E-09 |
| **C** | **14** | **0.00E+00** | **7.32E-12** | **1.49E-11** | **2.23E-11** | **2.97E-11** | **5.94E-11** | **1.49E-10** | **2.96E-10** | **4.45E-10** | **5.93E-10** | **8.89E-10** |
| N | 13 | 0.00E+00 | 5.82E-16 | 5.82E-16 | 5.82E-16 | 5.82E-16 | 5.82E-16 | 5.82E-16 | 5.82E-16 | 5.82E-16 | 5.82E-16 | 5.82E-16 |
| N | 14 | 0.00E+00 | 5.97E-11 | 1.21E-10 | 1.82E-10 | 2.42E-10 | 4.84E-10 | 1.21E-09 | 2.42E-09 | 3.63E-09 | 4.84E-09 | 7.26E-09 |
| N | 15 | 0.00E+00 | 1.11E-10 | 2.26E-10 | 3.39E-10 | 4.51E-10 | 9.03E-10 | 2.26E-09 | 4.51E-09 | 6.77E-09 | 9.03E-09 | 1.35E-08 |
| N | 16 | 0.00E+00 | 4.21E-18 | 4.21E-18 | 4.21E-18 | 4.21E-18 | 4.21E-18 | 4.21E-18 | 4.21E-18 | 4.21E-18 | 4.21E-18 | 4.21E-18 |
| O | 14 | 0.00E+00 | 1.06E-17 | 1.06E-17 | 1.06E-17 | 1.06E-17 | 1.06E-17 | 1.06E-17 | 1.06E-17 | 1.06E-17 | 1.06E-17 | 1.06E-17 |
| O | 15 | 0.00E+00 | 5.50E-16 | 5.50E-16 | 5.50E-16 | 5.50E-16 | 5.50E-16 | 5.50E-16 | 5.50E-16 | 5.50E-16 | 5.50E-16 | 5.50E-16 |
| O | 16 | 0.00E+00 | 2.99E-11 | 6.06E-11 | 9.09E-11 | 1.21E-10 | 2.42E-10 | 6.06E-10 | 1.21E-09 | 1.82E-09 | 2.42E-09 | 3.63E-09 |
| O | 17 | 0.00E+00 | 1.96E-12 | 3.99E-12 | 5.98E-12 | 7.95E-12 | 1.59E-11 | 3.99E-11 | 7.95E-11 | 1.19E-10 | 1.59E-10 | 2.39E-10 |
| O | 18 | 0.00E+00 | 6.49E-16 | 1.32E-15 | 1.98E-15 | 2.63E-15 | 5.26E-15 | 1.32E-14 | 2.63E-14 | 3.95E-14 | 5.26E-14 | 7.89E-14 |
| O | 19 | 0.00E+00 | 2.25E-20 | 2.25E-20 | 2.25E-20 | 2.25E-20 | 2.25E-20 | 2.25E-20 | 2.25E-20 | 2.25E-20 | 2.25E-20 | 2.25E-20 |
| F | 19 | 0.00E+00 | 2.02E-12 | 4.11E-12 | 6.16E-12 | 8.19E-12 | 1.64E-11 | 4.11E-11 | 8.19E-11 | 1.23E-10 | 1.64E-10 | 2.46E-10 |
| NE | 20 | 0.00E+00 | 1.34E-12 | 2.73E-12 | 4.09E-12 | 5.44E-12 | 1.09E-11 | 2.73E-11 | 5.44E-11 | 8.16E-11 | 1.09E-10 | 1.63E-10 |
| NE | 21 | 0.00E+00 | 1.65E-12 | 3.36E-12 | 5.04E-12 | 6.70E-12 | 1.34E-11 | 3.36E-11 | 6.70E-11 | 1.01E-10 | 1.34E-10 | 2.01E-10 |
| NE | 22 | 0.00E+00 | 1.32E-12 | 2.86E-12 | 4.54E-12 | 6.36E-12 | 1.51E-11 | 5.07E-11 | 1.24E-10 | 2.05E-10 | 2.87E-10 | 4.51E-10 |
| NE | 23 | 0.00E+00 | 2.87E-18 | 2.87E-18 | 2.87E-18 | 2.87E-18 | 2.87E-18 | 2.87E-18 | 2.87E-18 | 2.87E-18 | 2.87E-18 | 2.87E-18 |
| **NA** | **22** | **0.00E+00** | **2.75E-12** | **5.41E-12** | **7.86E-12** | **1.01E-11** | **1.79E-11** | **3.20E-11** | **4.05E-11** | **4.28E-11** | **4.34E-11** | **4.36E-11** |
| NA | 23 | 0.00E+00 | 8.43E-12 | 1.71E-11 | 2.57E-11 | 3.41E-11 | 6.84E-11 | 1.71E-10 | 3.41E-10 | 5.13E-10 | 6.84E-10 | 1.03E-09 |
| NA | 24 | 0.00E+00 | 6.20E-15 | 6.20E-15 | 6.20E-15 | 6.20E-15 | 6.20E-15 | 6.20E-15 | 6.20E-15 | 6.20E-15 | 6.20E-15 | 6.20E-15 |
| NA | 25 | 0.00E+00 | 1.38E-17 | 1.38E-17 | 1.38E-17 | 1.38E-17 | 1.38E-17 | 1.38E-17 | 1.38E-17 | 1.38E-17 | 1.38E-17 | 1.38E-17 |

**Table A.9. (continued)**

| Proton beam energy: 1 GeV | | | | | | | Operational line loss assumption: 1 nA/m (continuous) | | | | | |
|---|---|---|---|---|---|---|---|---|---|---|---|---|
| Nuclide masses integrated over the material zone volume in the HETC & MCNP calculational model | | | | | | | | | | | | |
| Nuclide concentration | | Time (s) | 7.88E+06 | 1.58E+07 | 2.37E+07 | 3.15E+07 | 6.31E+07 | 1.58E+08 | 3.15E+08 | 4.73E+08 | 6.31E+08 | 9.46E+08 |
| (gram-atoms) | | Initial | 3 months | 6 months | 9 months | 1 year | 2 years | 5 years | 10 years | 15 years | 20 years | 30 years |
| MG | 23 | 0.00E+00 | 8.57E-19 | 8.57E-19 | 8.57E-19 | 8.57E-19 | 8.57E-19 | 8.57E-19 | 8.57E-19 | 8.57E-19 | 8.57E-19 | 8.57E-19 |
| MG | 24 | 0.00E+00 | 2.53E-11 | 5.13E-11 | 7.70E-11 | 1.02E-10 | 2.05E-10 | 5.13E-10 | 1.02E-09 | 1.54E-09 | 2.05E-09 | 3.07E-09 |
| MG | 25 | 0.00E+00 | 2.15E-11 | 4.36E-11 | 6.55E-11 | 8.70E-11 | 1.74E-10 | 4.36E-10 | 8.70E-10 | 1.31E-09 | 1.74E-09 | 2.61E-09 |
| MG | 26 | 0.00E+00 | 1.79E-11 | 3.64E-11 | 5.46E-11 | 7.26E-11 | 1.45E-10 | 3.64E-10 | 7.26E-10 | 1.09E-09 | 1.45E-09 | 2.18E-09 |
| MG | 27 | 0.00E+00 | 2.81E-16 | 2.81E-16 | 2.81E-16 | 2.81E-16 | 2.81E-16 | 2.81E-16 | 2.81E-16 | 2.81E-16 | 2.81E-16 | 2.81E-16 |
| AL | 25 | 0.00E+00 | 1.61E-18 | 1.61E-18 | 1.61E-18 | 1.61E-18 | 1.61E-18 | 1.61E-18 | 1.61E-18 | 1.61E-18 | 1.61E-18 | 1.61E-18 |
| **AL** | **26** | **0.00E+00** | **2.31E-11** | **4.68E-11** | **7.02E-11** | **9.33E-11** | **1.87E-10** | **4.68E-10** | **9.33E-10** | **1.40E-09** | **1.87E-09** | **2.80E-09** |
| AL | 27 | 0.00E+00 | 4.52E-11 | 9.18E-11 | 1.38E-10 | 1.83E-10 | 3.67E-10 | 9.18E-10 | 1.83E-09 | 2.75E-09 | 3.67E-09 | 5.50E-09 |
| AL | 28 | 0.00E+00 | 2.71E-16 | 2.71E-16 | 2.71E-16 | 2.71E-16 | 2.71E-16 | 2.71E-16 | 2.71E-16 | 2.71E-16 | 2.71E-16 | 2.71E-16 |
| AL | 29 | 0.00E+00 | 7.57E-17 | 7.57E-17 | 7.57E-17 | 7.57E-17 | 7.57E-17 | 7.57E-17 | 7.57E-17 | 7.57E-17 | 7.57E-17 | 7.57E-17 |
| AL | 30 | 0.00E+00 | 3.30E-20 | 3.30E-20 | 3.30E-20 | 3.30E-20 | 3.30E-20 | 3.30E-20 | 3.30E-20 | 3.30E-20 | 3.30E-20 | 3.30E-20 |
| SI | 27 | 0.00E+00 | 2.48E-18 | 2.48E-18 | 2.48E-18 | 2.48E-18 | 2.48E-18 | 2.48E-18 | 2.48E-18 | 2.48E-18 | 2.48E-18 | 2.48E-18 |
| SI | 28 | 0.00E+00 | 2.15E-11 | 4.38E-11 | 6.56E-11 | 8.73E-11 | 1.75E-10 | 4.38E-10 | 8.73E-10 | 1.31E-09 | 1.75E-09 | 2.62E-09 |
| SI | 29 | 0.00E+00 | 3.72E-12 | 7.55E-12 | 1.13E-11 | 1.51E-11 | 3.02E-11 | 7.55E-11 | 1.51E-10 | 2.26E-10 | 3.02E-10 | 4.52E-10 |
| SI | 30 | 0.00E+00 | 1.89E-13 | 3.83E-13 | 5.74E-13 | 7.64E-13 | 1.53E-12 | 3.83E-12 | 7.64E-12 | 1.15E-11 | 1.53E-11 | 2.29E-11 |
| SI | 31 | 0.00E+00 | 9.69E-17 | 9.69E-17 | 9.69E-17 | 9.69E-17 | 9.69E-17 | 9.69E-17 | 9.69E-17 | 9.69E-17 | 9.69E-17 | 9.69E-17 |
| P | 31 | 0.00E+00 | 5.54E-14 | 1.13E-13 | 1.69E-13 | 2.25E-13 | 4.50E-13 | 1.13E-12 | 2.24E-12 | 3.37E-12 | 4.50E-12 | 6.74E-12 |
| P | 32 | 0.00E+00 | 9.14E-14 | 9.25E-14 | 9.25E-14 | 9.25E-14 | 9.25E-14 | 9.25E-14 | 9.25E-14 | 9.25E-14 | 9.25E-14 | 9.25E-14 |
| S | 32 | 0.00E+00 | 3.13E-13 | 7.28E-13 | 1.14E-12 | 1.54E-12 | 3.28E-12 | 8.29E-12 | 1.65E-11 | 2.48E-11 | 3.31E-11 | 4.96E-11 |
| S | 33 | 0.00E+00 | 4.04E-13 | 8.20E-13 | 1.23E-12 | 1.63E-12 | 3.27E-12 | 8.20E-12 | 1.63E-11 | 2.45E-11 | 3.27E-11 | 4.91E-11 |
| S | 34 | 0.00E+00 | 4.04E-13 | 8.20E-13 | 1.23E-12 | 1.63E-12 | 3.27E-12 | 8.20E-12 | 1.63E-11 | 2.45E-11 | 3.27E-11 | 4.91E-11 |
| CL | 35 | 0.00E+00 | 2.47E-14 | 5.02E-14 | 7.53E-14 | 1.00E-13 | 2.00E-13 | 5.02E-13 | 1.00E-12 | 1.50E-12 | 2.00E-12 | 3.01E-12 |
| **CL** | **36** | **0.00E+00** | **4.91E-13** | **9.97E-13** | **1.49E-12** | **1.99E-12** | **3.98E-12** | **9.97E-12** | **1.99E-11** | **2.98E-11** | **3.98E-11** | **5.97E-11** |
| CL | 37 | 0.00E+00 | 4.08E-13 | 8.30E-13 | 1.25E-12 | 1.66E-12 | 3.33E-12 | 8.34E-12 | 1.66E-11 | 2.50E-11 | 3.33E-11 | 4.99E-11 |
| CL | 38 | 0.00E+00 | 1.04E-18 | 1.04E-18 | 1.04E-18 | 1.04E-18 | 1.04E-18 | 1.04E-18 | 1.04E-18 | 1.04E-18 | 1.04E-18 | 1.04E-18 |
| CL | 39 | 0.00E+00 | 8.00E-20 | 8.00E-20 | 8.00E-20 | 8.00E-20 | 8.00E-20 | 8.00E-20 | 8.00E-20 | 8.00E-20 | 8.00E-20 | 8.00E-20 |
| AR | 36 | 0.00E+00 | 6.19E-16 | 1.26E-15 | 1.89E-15 | 2.51E-15 | 5.03E-15 | 1.26E-14 | 2.53E-14 | 3.81E-14 | 5.11E-14 | 7.73E-14 |
| AR | 37 | 0.00E+00 | 3.07E-15 | 3.59E-15 | 3.67E-15 | 3.69E-15 | 3.69E-15 | 3.69E-15 | 3.69E-15 | 3.69E-15 | 3.69E-15 | 3.69E-15 |
| AR | 38 | 0.00E+00 | 8.94E-13 | 1.82E-12 | 2.72E-12 | 3.62E-12 | 7.25E-12 | 1.82E-11 | 3.62E-11 | 5.44E-11 | 7.25E-11 | 1.09E-10 |
| **AR** | **39** | **0.00E+00** | **4.31E-13** | **8.75E-13** | **1.31E-12** | **1.74E-12** | **3.49E-12** | **8.70E-12** | **1.72E-11** | **2.57E-11** | **3.41E-11** | **5.05E-11** |
| AR | 40 | 0.00E+00 | 8.00E-16 | 1.62E-15 | 2.44E-15 | 3.24E-15 | 6.49E-15 | 1.62E-14 | 3.24E-14 | 4.86E-14 | 6.49E-14 | 9.73E-14 |
| AR | 41 | 0.00E+00 | 2.94E-18 | 2.94E-18 | 2.94E-18 | 2.94E-18 | 2.94E-18 | 2.94E-18 | 2.94E-18 | 2.94E-18 | 2.94E-18 | 2.94E-18 |
| AR | 42 | 0.00E+00 | 6.73E-20 | 1.36E-19 | 2.04E-19 | 2.70E-19 | 5.36E-19 | 1.30E-18 | 2.46E-18 | 3.52E-18 | 4.46E-18 | 6.08E-18 |
| K | 38 | 0.00E+00 | 6.87E-17 | 6.87E-17 | 6.87E-17 | 6.87E-17 | 6.87E-17 | 6.87E-17 | 6.87E-17 | 6.87E-17 | 6.87E-17 | 6.87E-17 |

**Table A.9. (continued)**

| Proton beam energy: 1 GeV | | | | | | | Operational line loss assumption: 1 nA/m (continuous) | | | | | |
|---|---|---|---|---|---|---|---|---|---|---|---|---|
| Nuclide masses integrated over the material zone volume in the HETC & MCNP calculational model | | | | | | | | | | | | |
| Nuclide concentration | | Time (s) | 7.88E+06 | 1.58E+07 | 2.37E+07 | 3.15E+07 | 6.31E+07 | 1.58E+08 | 3.15E+08 | 4.73E+08 | 6.31E+08 | 9.46E+08 |
| (gram-atoms) | | Initial | 3 months | 6 months | 9 months | 1 year | 2 years | 5 years | 10 years | 15 years | 20 years | 30 years |
| K | 39 | 0.00E+00 | 6.89E-15 | 1.43E-14 | 2.18E-14 | 2.96E-14 | 6.37E-14 | 1.93E-13 | 4.96E-13 | 9.10E-13 | 1.43E-12 | 2.79E-12 |
| **K** | **40** | **0.00E+00** | **1.23E-13** | **2.50E-13** | **3.75E-13** | **4.98E-13** | **9.98E-13** | **2.50E-12** | **4.98E-12** | **7.48E-12** | **9.98E-12** | **1.50E-11** |
| K | 41 | 0.00E+00 | 2.43E-15 | 4.94E-15 | 7.42E-15 | 9.86E-15 | 1.97E-14 | 4.94E-14 | 9.85E-14 | 1.48E-13 | 1.97E-13 | 2.96E-13 |
| K | 42 | 0.00E+00 | 5.81E-17 | 5.81E-17 | 5.81E-17 | 5.81E-17 | 5.81E-17 | 5.81E-17 | 5.81E-17 | 5.81E-17 | 5.81E-17 | 5.81E-17 |
| K | 43 | 0.00E+00 | 7.61E-20 | 7.61E-20 | 7.61E-20 | 7.61E-20 | 7.61E-20 | 7.61E-20 | 7.61E-20 | 7.61E-20 | 7.61E-20 | 7.61E-20 |
| **CA** | **41** | **0.00E+00** | **6.08E-16** | **1.24E-15** | **1.85E-15** | **2.46E-15** | **4.93E-15** | **1.24E-14** | **2.46E-14** | **3.70E-14** | **4.93E-14** | **7.40E-14** |
| CA | 42 | 0.00E+00 | 7.17E-15 | 1.46E-14 | 2.20E-14 | 2.92E-14 | 5.84E-14 | 1.46E-13 | 2.91E-13 | 4.36E-13 | 5.82E-13 | 8.73E-13 |
| CA | 43 | 0.00E+00 | 4.05E-13 | 8.23E-13 | 1.24E-12 | 1.64E-12 | 3.29E-12 | 8.23E-12 | 1.64E-11 | 2.46E-11 | 3.29E-11 | 4.92E-11 |
| CA | 44 | 0.00E+00 | 6.27E-14 | 1.28E-13 | 1.91E-13 | 2.54E-13 | 5.09E-13 | 1.27E-12 | 2.54E-12 | 3.81E-12 | 5.09E-12 | 7.63E-12 |
| CA | 45 | 0.00E+00 | 2.90E-15 | 4.93E-15 | 6.29E-15 | 7.21E-15 | 8.78E-15 | 9.20E-15 | 9.21E-15 | 9.21E-15 | 9.21E-15 | 9.20E-15 |
| CA | 46 | 0.00E+00 | 2.17E-16 | 4.41E-16 | 6.62E-16 | 8.80E-16 | 1.76E-15 | 4.41E-15 | 8.80E-15 | 1.32E-14 | 1.76E-14 | 2.64E-14 |
| CA | 47 | 0.00E+00 | 2.34E-17 | 2.34E-17 | 2.34E-17 | 2.34E-17 | 2.34E-17 | 2.34E-17 | 2.34E-17 | 2.34E-17 | 2.34E-17 | 2.34E-17 |
| CA | 48 | 0.00E+00 | 1.40E-17 | 2.85E-17 | 4.27E-17 | 5.68E-17 | 1.14E-16 | 2.85E-16 | 5.68E-16 | 8.53E-16 | 1.14E-15 | 1.71E-15 |
| SC | 43 | 0.00E+00 | 1.05E-15 | 1.05E-15 | 1.05E-15 | 1.05E-15 | 1.05E-15 | 1.05E-15 | 1.05E-15 | 1.05E-15 | 1.05E-15 | 1.05E-15 |
| SC | 44 | 0.00E+00 | 1.62E-16 | 1.62E-16 | 1.62E-16 | 1.62E-16 | 1.62E-16 | 1.62E-16 | 1.62E-16 | 1.62E-16 | 1.62E-16 | 1.62E-16 |
| SC | 45 | 0.00E+00 | 4.17E-13 | 8.47E-13 | 1.27E-12 | 1.69E-12 | 3.39E-12 | 8.51E-12 | 1.70E-11 | 2.55E-11 | 3.40E-11 | 5.10E-11 |
| SC | 46 | 0.00E+00 | 3.44E-15 | 5.11E-15 | 5.87E-15 | 6.23E-15 | 6.53E-15 | 6.55E-15 | 6.55E-15 | 6.55E-15 | 6.55E-15 | 6.55E-15 |
| SC | 47 | 0.00E+00 | 5.40E-16 | 5.40E-16 | 5.40E-16 | 5.40E-16 | 5.40E-16 | 5.40E-16 | 5.40E-16 | 5.40E-16 | 5.40E-16 | 5.40E-16 |
| SC | 48 | 0.00E+00 | 2.28E-16 | 2.28E-16 | 2.28E-16 | 2.28E-16 | 2.28E-16 | 2.28E-16 | 2.28E-16 | 2.28E-16 | 2.28E-16 | 2.28E-16 |
| SC | 49 | 0.00E+00 | 2.07E-19 | 2.07E-19 | 2.07E-19 | 2.07E-19 | 2.07E-19 | 2.07E-19 | 2.07E-19 | 2.07E-19 | 2.07E-19 | 2.07E-19 |
| TI | 45 | 0.00E+00 | 2.67E-18 | 2.67E-18 | 2.67E-18 | 2.67E-18 | 2.67E-18 | 2.67E-18 | 2.67E-18 | 2.67E-18 | 2.67E-18 | 2.67E-18 |
| TI | 46 | 0.00E+00 | 4.70E-15 | 1.14E-14 | 1.89E-14 | 2.67E-14 | 5.95E-14 | 1.65E-13 | 3.36E-13 | 5.08E-13 | 6.80E-13 | 1.02E-12 |
| TI | 47 | 0.00E+00 | 4.84E-14 | 9.88E-14 | 1.49E-13 | 1.98E-13 | 3.95E-13 | 9.86E-13 | 1.96E-12 | 2.95E-12 | 3.93E-12 | 5.89E-12 |
| TI | 48 | 0.00E+00 | 1.75E-14 | 3.58E-14 | 5.39E-14 | 7.17E-14 | 1.43E-13 | 3.57E-13 | 7.11E-13 | 1.07E-12 | 1.42E-12 | 2.13E-12 |
| TI | 49 | 0.00E+00 | 3.87E-14 | 7.86E-14 | 1.18E-13 | 1.57E-13 | 3.14E-13 | 7.86E-13 | 1.57E-12 | 2.35E-12 | 3.14E-12 | 4.70E-12 |
| TI | 50 | 0.00E+00 | 2.40E-15 | 4.88E-15 | 7.32E-15 | 9.73E-15 | 1.95E-14 | 4.88E-14 | 9.73E-14 | 1.46E-13 | 1.95E-13 | 2.92E-13 |
| TI | 51 | 0.00E+00 | 2.70E-20 | 2.70E-20 | 2.70E-20 | 2.70E-20 | 2.70E-20 | 2.70E-20 | 2.70E-20 | 2.70E-20 | 2.70E-20 | 2.70E-20 |
| V | 49 | 0.00E+00 | 6.37E-18 | 1.18E-17 | 1.62E-17 | 1.97E-17 | 2.89E-17 | 3.59E-17 | 3.66E-17 | 3.67E-17 | 3.67E-17 | 3.67E-17 |
| V | 50 | 0.00E+00 | 2.36E-15 | 4.80E-15 | 7.20E-15 | 9.57E-15 | 1.92E-14 | 4.80E-14 | 9.57E-14 | 1.44E-13 | 1.92E-13 | 2.87E-13 |
| V | 51 | 0.00E+00 | 7.38E-15 | 1.92E-14 | 3.13E-14 | 4.32E-14 | 9.68E-14 | 2.47E-13 | 4.93E-13 | 7.41E-13 | 9.88E-13 | 1.48E-12 |
| V | 52 | 0.00E+00 | 9.64E-20 | 9.64E-20 | 9.64E-20 | 9.64E-20 | 9.64E-20 | 9.64E-20 | 9.64E-20 | 9.64E-20 | 9.64E-20 | 9.64E-20 |
| CR | 50 | 0.00E+00 | 1.91E-15 | 3.88E-15 | 5.81E-15 | 7.73E-15 | 1.55E-14 | 3.88E-14 | 7.73E-14 | 1.16E-13 | 1.55E-13 | 2.32E-13 |
| CR | 51 | 0.00E+00 | 4.56E-15 | 5.04E-15 | 5.09E-15 | 5.10E-15 | 5.10E-15 | 5.10E-15 | 5.10E-15 | 5.10E-15 | 5.10E-15 | 5.10E-15 |
| CR | 52 | 0.00E+00 | 2.05E-12 | 4.26E-12 | 6.45E-12 | 8.61E-12 | 1.70E-11 | 4.21E-11 | 8.35E-11 | 1.25E-10 | 1.67E-10 | 2.50E-10 |

**Table A.9. (continued)**

| Proton beam energy: 1 GeV | | | | | | | Operational line loss assumption: 1 nA/m (continuous) | | | | | |
|---|---|---|---|---|---|---|---|---|---|---|---|---|
| Nuclide masses integrated over the material zone volume in the HETC & MCNP calculational model | | | | | | | | | | | | |
| Nuclide concentration | | Time (s) | 7.88E+06 | 1.58E+07 | 2.37E+07 | 3.15E+07 | 6.31E+07 | 1.58E+08 | 3.15E+08 | 4.73E+08 | 6.31E+08 | 9.46E+08 |
| (gram-atoms) | | Initial | 3 months | 6 months | 9 months | 1 year | 2 years | 5 years | 10 years | 15 years | 20 years | 30 years |
| CR | 53 | 0.00E+00 | 6.14E-14 | 1.25E-13 | 1.87E-13 | 2.48E-13 | 4.98E-13 | 1.25E-12 | 2.48E-12 | 3.73E-12 | 4.98E-12 | 7.46E-12 |
| CR | 54 | 0.00E+00 | 6.08E-13 | 1.61E-12 | 2.89E-12 | 4.39E-12 | 1.21E-11 | 4.15E-11 | 9.32E-11 | 1.45E-10 | 1.97E-10 | 3.12E-10 |
| CR | 55 | 0.00E+00 | 1.65E-20 | 1.65E-20 | 1.65E-20 | 1.65E-20 | 1.65E-20 | 1.65E-20 | 1.65E-20 | 1.65E-20 | 1.65E-20 | 1.65E-20 |
| MN | 52 | 0.00E+00 | 1.09E-13 | 1.09E-13 | 1.09E-13 | 1.09E-13 | 1.09E-13 | 1.09E-13 | 1.09E-13 | 1.09E-13 | 1.09E-13 | 1.09E-13 |
| **MN** | **53** | **0.00E+00** | **2.08E-12** | **4.23E-12** | **6.35E-12** | **8.44E-12** | **1.69E-11** | **4.23E-11** | **8.44E-11** | **1.27E-10** | **1.69E-10** | **2.53E-10** |
| MN | 54 | 0.00E+00 | 1.96E-12 | 3.61E-12 | 4.93E-12 | 6.00E-12 | 8.68E-12 | 1.06E-11 | 1.08E-11 | 1.08E-11 | 1.08E-11 | 1.08E-11 |
| MN | 55 | 0.00E+00 | 1.86E-12 | 3.93E-12 | 6.09E-12 | 8.35E-12 | 1.86E-11 | 5.68E-11 | 1.32E-10 | 2.13E-10 | 2.95E-10 | 4.60E-10 |
| MN | 56 | 0.00E+00 | 3.39E-16 | 3.39E-16 | 3.39E-16 | 3.39E-16 | 3.39E-16 | 3.39E-16 | 3.39E-16 | 3.39E-16 | 3.39E-16 | 3.39E-16 |
| MN | 57 | 0.00E+00 | 4.63E-20 | 4.63E-20 | 4.63E-20 | 4.63E-20 | 4.63E-20 | 4.63E-20 | 4.63E-20 | 4.63E-20 | 4.63E-20 | 4.63E-20 |
| FE | 53 | 0.00E+00 | 3.85E-17 | 3.85E-17 | 3.85E-17 | 3.85E-17 | 3.85E-17 | 3.85E-17 | 3.85E-17 | 3.85E-17 | 3.85E-17 | 3.85E-17 |
| FE | 54 | 0.00E+00 | 4.04E-13 | 8.20E-13 | 1.23E-12 | 1.63E-12 | 3.27E-12 | 8.20E-12 | 1.63E-11 | 2.45E-11 | 3.27E-11 | 4.91E-11 |
| **FE** | **55** | **0.00E+00** | **2.22E-12** | **4.36E-12** | **6.34E-12** | **8.18E-12** | **1.45E-11** | **2.61E-11** | **3.33E-11** | **3.52E-11** | **3.58E-11** | **3.60E-11** |
| FE | 56 | 0.00E+00 | 1.44E-12 | 2.92E-12 | 4.38E-12 | 5.82E-12 | 1.16E-11 | 2.92E-11 | 5.82E-11 | 8.73E-11 | 1.16E-10 | 1.75E-10 |
| FE | 57 | 0.00E+00 | 4.34E-13 | 8.82E-13 | 1.32E-12 | 1.76E-12 | 3.52E-12 | 8.82E-12 | 1.76E-11 | 2.64E-11 | 3.52E-11 | 5.28E-11 |
| FE | 58 | 0.00E+00 | 9.88E-15 | 2.01E-14 | 3.01E-14 | 4.00E-14 | 8.01E-14 | 2.01E-13 | 4.00E-13 | 6.01E-13 | 8.01E-13 | 1.20E-12 |
| FE | 59 | 0.00E+00 | 9.32E-16 | 1.16E-15 | 1.22E-15 | 1.23E-15 | 1.24E-15 | 1.24E-15 | 1.24E-15 | 1.24E-15 | 1.24E-15 | 1.24E-15 |
| CO | 59 | 0.00E+00 | 8.00E-16 | 2.35E-15 | 4.06E-15 | 5.78E-15 | 1.28E-14 | 3.52E-14 | 7.14E-14 | 1.08E-13 | 1.44E-13 | 2.16E-13 |
| NI | 60 | 0.00E+00 | 1.52E-16 | 3.09E-16 | 4.63E-16 | 6.15E-16 | 1.23E-15 | 3.09E-15 | 6.15E-15 | 9.24E-15 | 1.23E-14 | 1.85E-14 |
| NI | 61 | 0.00E+00 | 1.06E-16 | 2.16E-16 | 3.23E-16 | 4.30E-16 | 8.61E-16 | 2.16E-15 | 4.30E-15 | 6.45E-15 | 8.61E-15 | 1.29E-14 |
| NI | 62 | 0.00E+00 | 1.32E-17 | 2.69E-17 | 4.03E-17 | 5.36E-17 | 1.07E-16 | 2.69E-16 | 5.36E-16 | 8.05E-16 | 1.07E-15 | 1.61E-15 |
| NI | 63 | 0.00E+00 | 6.70E-17 | 1.36E-16 | 2.04E-16 | 2.70E-16 | 5.40E-16 | 1.34E-15 | 2.62E-15 | 3.87E-15 | 5.08E-15 | 7.36E-15 |
| NI | 64 | 0.00E+00 | 1.53E-15 | 3.11E-15 | 4.68E-15 | 6.22E-15 | 1.24E-14 | 3.11E-14 | 6.19E-14 | 9.29E-14 | 1.24E-13 | 1.86E-13 |
| NI | 65 | 0.00E+00 | 2.42E-20 | 2.42E-20 | 2.42E-20 | 2.42E-20 | 2.42E-20 | 2.42E-20 | 2.42E-20 | 2.42E-20 | 2.42E-20 | 2.42E-20 |
| NI | 66 | 0.00E+00 | 1.15E-20 | 1.15E-20 | 1.15E-20 | 1.15E-20 | 1.15E-20 | 1.15E-20 | 1.15E-20 | 1.15E-20 | 1.15E-20 | 1.15E-20 |
| CU | 63 | 0.00E+00 | 2.40E-15 | 4.88E-15 | 7.32E-15 | 9.73E-15 | 1.95E-14 | 4.88E-14 | 9.73E-14 | 1.46E-13 | 1.95E-13 | 2.93E-13 |
| CU | 64 | 0.00E+00 | 2.12E-17 | 2.12E-17 | 2.12E-17 | 2.12E-17 | 2.12E-17 | 2.12E-17 | 2.12E-17 | 2.12E-17 | 2.12E-17 | 2.12E-17 |
| CU | 65 | 0.00E+00 | 8.00E-16 | 2.74E-15 | 5.50E-15 | 8.87E-15 | 2.65E-14 | 9.14E-14 | 2.03E-13 | 3.15E-13 | 4.27E-13 | 6.72E-13 |
| CU | 66 | 0.00E+00 | 1.19E-20 | 1.19E-20 | 1.19E-20 | 1.19E-20 | 1.19E-20 | 1.19E-20 | 1.19E-20 | 1.19E-20 | 1.19E-20 | 1.19E-20 |
| CU | 67 | 0.00E+00 | 1.26E-18 | 1.26E-18 | 1.26E-18 | 1.26E-18 | 1.26E-18 | 1.26E-18 | 1.26E-18 | 1.26E-18 | 1.26E-18 | 1.26E-18 |
| ZN | 63 | 0.00E+00 | 4.28E-19 | 4.28E-19 | 4.28E-19 | 4.28E-19 | 4.28E-19 | 4.28E-19 | 4.28E-19 | 4.28E-19 | 4.28E-19 | 4.28E-19 |
| ZN | 64 | 0.00E+00 | 9.91E-16 | 2.02E-15 | 3.04E-15 | 4.04E-15 | 8.07E-15 | 2.02E-14 | 4.02E-14 | 6.03E-14 | 8.05E-14 | 1.21E-13 |
| ZN | 65 | 0.00E+00 | 4.73E-15 | 8.49E-15 | 1.13E-14 | 1.35E-14 | 1.83E-14 | 2.08E-14 | 2.09E-14 | 2.09E-14 | 2.09E-14 | 2.09E-14 |
| ZN | 66 | 0.00E+00 | 5.89E-16 | 1.20E-15 | 1.79E-15 | 2.38E-15 | 4.77E-15 | 1.20E-14 | 2.38E-14 | 3.58E-14 | 4.77E-14 | 7.16E-14 |
| ZN | 67 | 0.00E+00 | 2.21E-15 | 4.49E-15 | 6.74E-15 | 8.96E-15 | 1.79E-14 | 4.49E-14 | 8.96E-14 | 1.34E-13 | 1.79E-13 | 2.69E-13 |

**Table A.9. (continued)**

| Proton beam energy: 1 GeV | | | | | | | Operational line loss assumption: 1 nA/m (continuous) | | | | | |
|---|---|---|---|---|---|---|---|---|---|---|---|---|
| Nuclide masses integrated over the material zone volume in the HETC & MCNP calculational model | | | | | | | | | | | | |
| Nuclide concentration | | Time (s) | 7.88E+06 | 1.58E+07 | 2.37E+07 | 3.15E+07 | 6.31E+07 | 1.58E+08 | 3.15E+08 | 4.73E+08 | 6.31E+08 | 9.46E+08 |
| (gram-atoms) | | Initial | 3 months | 6 months | 9 months | 1 year | 2 years | 5 years | 10 years | 15 years | 20 years | 30 years |
| ZN | 68 | 0.00E+00 | 7.88E-16 | 1.60E-15 | 2.40E-15 | 3.19E-15 | 6.39E-15 | 1.60E-14 | 3.19E-14 | 4.79E-14 | 6.39E-14 | 9.58E-14 |
| ZN | 69 | 0.00E+00 | 2.18E-19 | 2.18E-19 | 2.18E-19 | 2.18E-19 | 2.18E-19 | 2.18E-19 | 2.18E-19 | 2.18E-19 | 2.18E-19 | 2.18E-19 |
| ZN | 70 | 0.00E+00 | 1.35E-19 | 2.73E-19 | 4.10E-19 | 5.45E-19 | 1.09E-18 | 2.73E-18 | 5.45E-18 | 8.19E-18 | 1.09E-17 | 1.64E-17 |
| GA | 69 | 0.00E+00 | 3.53E-16 | 7.16E-16 | 1.07E-15 | 1.43E-15 | 2.86E-15 | 7.16E-15 | 1.43E-14 | 2.14E-14 | 2.86E-14 | 4.29E-14 |
| GA | 71 | 0.00E+00 | 9.64E-18 | 1.96E-17 | 2.94E-17 | 3.90E-17 | 7.82E-17 | 1.96E-16 | 3.90E-16 | 5.86E-16 | 7.82E-16 | 1.17E-15 |
| BR | 81 | 0.00E+00 | 1.11E-17 | 2.24E-17 | 3.37E-17 | 4.48E-17 | 8.97E-17 | 2.24E-16 | 4.48E-16 | 6.72E-16 | 8.97E-16 | 1.34E-15 |
| BR | 82 | 0.00E+00 | 8.75E-19 | 8.75E-19 | 8.75E-19 | 8.75E-19 | 8.75E-19 | 8.75E-19 | 8.75E-19 | 8.75E-19 | 8.75E-19 | 8.75E-19 |
| KR | 82 | 0.00E+00 | 3.86E-17 | 7.93E-17 | 1.19E-16 | 1.59E-16 | 3.17E-16 | 7.89E-16 | 1.57E-15 | 2.36E-15 | 3.14E-15 | 4.71E-15 |
| KR | 83 | 0.00E+00 | 4.36E-17 | 8.85E-17 | 1.33E-16 | 1.76E-16 | 3.54E-16 | 8.85E-16 | 1.76E-15 | 2.65E-15 | 3.54E-15 | 5.30E-15 |
| KR | 84 | 0.00E+00 | 3.22E-15 | 8.75E-15 | 1.45E-14 | 2.03E-14 | 4.65E-14 | 1.19E-13 | 2.38E-13 | 3.57E-13 | 4.76E-13 | 7.11E-13 |
| KR | 85 | 0.00E+00 | 3.93E-16 | 7.91E-16 | 1.18E-15 | 1.55E-15 | 3.01E-15 | 6.87E-15 | 1.18E-14 | 1.54E-14 | 1.80E-14 | 2.13E-14 |
| KR | 86 | 0.00E+00 | 1.67E-17 | 3.40E-17 | 5.09E-17 | 6.77E-17 | 1.36E-16 | 3.40E-16 | 6.77E-16 | 1.02E-15 | 1.36E-15 | 2.03E-15 |
| KR | 87 | 0.00E+00 | 3.64E-20 | 3.64E-20 | 3.64E-20 | 3.64E-20 | 3.64E-20 | 3.64E-20 | 3.64E-20 | 3.64E-20 | 3.64E-20 | 3.64E-20 |
| RB | 84 | 0.00E+00 | 2.58E-15 | 2.97E-15 | 3.02E-15 | 3.03E-15 | 3.03E-15 | 3.03E-15 | 3.03E-15 | 3.03E-15 | 3.03E-15 | 3.03E-15 |
| RB | 85 | 0.00E+00 | 8.62E-18 | 2.40E-17 | 4.55E-17 | 7.28E-17 | 2.43E-16 | 1.28E-15 | 4.44E-15 | 8.98E-15 | 1.45E-14 | 2.75E-14 |
| RB | 86 | 0.00E+00 | 9.75E-15 | 1.01E-14 | 1.01E-14 | 1.01E-14 | 1.01E-14 | 1.01E-14 | 1.01E-14 | 1.01E-14 | 1.01E-14 | 1.01E-14 |
| RB | 87 | 0.00E+00 | 4.31E-17 | 8.76E-17 | 1.31E-16 | 1.75E-16 | 3.50E-16 | 8.75E-16 | 1.75E-15 | 2.62E-15 | 3.50E-15 | 5.24E-15 |
| RB | 88 | 0.00E+00 | 3.09E-19 | 3.09E-19 | 3.09E-19 | 3.09E-19 | 3.09E-19 | 3.09E-19 | 3.09E-19 | 3.09E-19 | 3.09E-19 | 3.09E-19 |
| SR | 84 | 0.00E+00 | 9.58E-17 | 2.63E-16 | 4.37E-16 | 6.11E-16 | 1.41E-15 | 3.61E-15 | 7.20E-15 | 1.08E-14 | 1.44E-14 | 2.15E-14 |
| SR | 86 | 0.00E+00 | 2.41E-14 | 5.86E-14 | 9.30E-14 | 1.27E-13 | 2.74E-13 | 6.97E-13 | 1.39E-12 | 2.09E-12 | 2.78E-12 | 4.16E-12 |
| SR | 88 | 0.00E+00 | 1.57E-15 | 3.18E-15 | 4.78E-15 | 6.35E-15 | 1.27E-14 | 3.18E-14 | 6.35E-14 | 9.53E-14 | 1.27E-13 | 1.91E-13 |
| XE | 128 | 0.00E+00 | 6.89E-20 | 1.42E-19 | 2.14E-19 | 2.86E-19 | 5.74E-19 | 1.44E-18 | 2.88E-18 | 4.32E-18 | 5.76E-18 | 8.64E-18 |
| XE | 129 | 0.00E+00 | 1.40E-18 | 2.88E-18 | 4.33E-18 | 5.77E-18 | 1.15E-17 | 2.86E-17 | 5.70E-17 | 8.55E-17 | 1.14E-16 | 1.71E-16 |
| XE | 130 | 0.00E+00 | 9.61E-20 | 1.95E-19 | 2.93E-19 | 3.89E-19 | 7.80E-19 | 1.95E-18 | 3.89E-18 | 5.85E-18 | 7.80E-18 | 1.17E-17 |
| XE | 131 | 0.00E+00 | 9.33E-18 | 2.38E-17 | 3.82E-17 | 5.23E-17 | 1.12E-16 | 2.86E-16 | 5.73E-16 | 8.62E-16 | 1.15E-15 | 1.73E-15 |
| XE | 132 | 0.00E+00 | 6.05E-19 | 1.24E-18 | 1.88E-18 | 2.50E-18 | 4.97E-18 | 1.24E-17 | 2.46E-17 | 3.69E-17 | 4.92E-17 | 7.37E-17 |
| XE | 133 | 0.00E+00 | 2.37E-20 | 2.37E-20 | 2.37E-20 | 2.37E-20 | 2.37E-20 | 2.37E-20 | 2.37E-20 | 2.37E-20 | 2.37E-20 | 2.37E-20 |
| XE | 134 | 0.00E+00 | 6.64E-19 | 1.35E-18 | 2.02E-18 | 2.69E-18 | 5.39E-18 | 1.35E-17 | 2.69E-17 | 4.04E-17 | 5.39E-17 | 8.08E-17 |
| XE | 135 | 0.00E+00 | 1.93E-20 | 1.93E-20 | 1.93E-20 | 1.93E-20 | 1.93E-20 | 1.93E-20 | 1.93E-20 | 1.93E-20 | 1.93E-20 | 1.93E-20 |
| XE | 136 | 0.00E+00 | 5.37E-20 | 1.09E-19 | 1.64E-19 | 2.18E-19 | 4.36E-19 | 1.09E-18 | 2.18E-18 | 3.27E-18 | 4.36E-18 | 6.53E-18 |
| CS | 129 | 0.00E+00 | 3.01E-20 | 3.01E-20 | 3.01E-20 | 3.01E-20 | 3.01E-20 | 3.01E-20 | 3.01E-20 | 3.01E-20 | 3.01E-20 | 3.01E-20 |
| CS | 131 | 0.00E+00 | 2.12E-18 | 2.17E-18 | 2.17E-18 | 2.17E-18 | 2.17E-18 | 2.17E-18 | 2.17E-18 | 2.17E-18 | 2.17E-18 | 2.17E-18 |
| CS | 132 | 0.00E+00 | 1.68E-20 | 1.68E-20 | 1.68E-20 | 1.68E-20 | 1.68E-20 | 1.68E-20 | 1.68E-20 | 1.68E-20 | 1.68E-20 | 1.68E-20 |
| CS | 133 | 0.00E+00 | 1.31E-18 | 3.80E-18 | 7.33E-18 | 1.19E-17 | 4.03E-17 | 2.15E-16 | 7.50E-16 | 1.52E-15 | 2.46E-15 | 4.66E-15 |

**Table A.9. (continued)**

| Proton beam energy: 1 GeV | | | | | | | Operational line loss assumption: 1 nA/m (continuous) | | | | | |
|---|---|---|---|---|---|---|---|---|---|---|---|---|
| Nuclide masses integrated over the material zone volume in the HETC & MCNP calculational model | | | | | | | | | | | | |
| Nuclide concentration | | Time (s) | 7.88E+06 | 1.58E+07 | 2.37E+07 | 3.15E+07 | 6.31E+07 | 1.58E+08 | 3.15E+08 | 4.73E+08 | 6.31E+08 | 9.46E+08 |
| (gram-atoms) | | Initial | 3 months | 6 months | 9 months | 1 year | 2 years | 5 years | 10 years | 15 years | 20 years | 30 years |
| CS | 134 | 0.00E+00 | 1.18E-18 | 2.29E-18 | 3.31E-18 | 4.22E-18 | 7.25E-18 | 1.21E-17 | 1.43E-17 | 1.47E-17 | 1.48E-17 | 1.48E-17 |
| CS | 135 | 0.00E+00 | 4.07E-18 | 8.28E-18 | 1.24E-17 | 1.65E-17 | 3.31E-17 | 8.27E-17 | 1.65E-16 | 2.47E-16 | 3.30E-16 | 4.95E-16 |
| CS | 136 | 0.00E+00 | 4.34E-19 | 4.38E-19 | 4.38E-19 | 4.38E-19 | 4.38E-19 | 4.38E-19 | 4.38E-19 | 4.38E-19 | 4.38E-19 | 4.38E-19 |
| CS | 137 | 0.00E+00 | 7.79E-18 | 1.58E-17 | 2.36E-17 | 3.13E-17 | 6.19E-17 | 1.50E-16 | 2.83E-16 | 4.02E-16 | 5.08E-16 | 6.86E-16 |
| BA | 130 | 0.00E+00 | 1.73E-19 | 3.50E-19 | 5.26E-19 | 6.98E-19 | 1.40E-18 | 3.50E-18 | 6.98E-18 | 1.05E-17 | 1.40E-17 | 2.10E-17 |
| BA | 131 | 0.00E+00 | 2.67E-18 | 2.68E-18 | 2.68E-18 | 2.68E-18 | 2.68E-18 | 2.68E-18 | 2.68E-18 | 2.68E-18 | 2.68E-18 | 2.68E-18 |
| BA | 132 | 0.00E+00 | 8.06E-18 | 1.64E-17 | 2.46E-17 | 3.26E-17 | 6.54E-17 | 1.64E-16 | 3.26E-16 | 4.90E-16 | 6.54E-16 | 9.80E-16 |
| BA | 133 | 0.00E+00 | 6.65E-17 | 1.34E-16 | 1.99E-16 | 2.63E-16 | 5.10E-16 | 1.16E-15 | 2.00E-15 | 2.61E-15 | 3.04E-15 | 3.59E-15 |
| BA | 134 | 0.00E+00 | 3.31E-16 | 6.72E-16 | 1.01E-15 | 1.34E-15 | 2.68E-15 | 6.73E-15 | 1.34E-14 | 2.02E-14 | 2.69E-14 | 4.03E-14 |
| BA | 135 | 0.00E+00 | 1.76E-16 | 3.57E-16 | 5.35E-16 | 7.11E-16 | 1.42E-15 | 3.57E-15 | 7.11E-15 | 1.07E-14 | 1.42E-14 | 2.14E-14 |
| BA | 136 | 0.00E+00 | 1.26E-15 | 2.56E-15 | 3.84E-15 | 5.10E-15 | 1.02E-14 | 2.56E-14 | 5.10E-14 | 7.66E-14 | 1.02E-13 | 1.53E-13 |
| BA | 137 | 0.00E+00 | 1.21E-15 | 2.45E-15 | 3.68E-15 | 4.89E-15 | 9.80E-15 | 2.45E-14 | 4.89E-14 | 7.35E-14 | 9.81E-14 | 1.47E-13 |
| BA | 138 | 0.00E+00 | 2.34E-16 | 4.74E-16 | 7.12E-16 | 9.46E-16 | 1.89E-15 | 4.74E-15 | 9.46E-15 | 1.42E-14 | 1.89E-14 | 2.84E-14 |
| BA | 139 | 0.00E+00 | 2.32E-19 | 2.32E-19 | 2.32E-19 | 2.32E-19 | 2.32E-19 | 2.32E-19 | 2.32E-19 | 2.32E-19 | 2.32E-19 | 2.32E-19 |
| LA | 139 | 0.00E+00 | 2.50E-16 | 5.08E-16 | 7.62E-16 | 1.01E-15 | 2.03E-15 | 5.08E-15 | 1.01E-14 | 1.52E-14 | 2.03E-14 | 3.04E-14 |
| GD | 156 | 0.00E+00 | 1.30E-20 | 3.05E-20 | 4.78E-20 | 6.49E-20 | 1.38E-19 | 3.50E-19 | 6.98E-19 | 1.05E-18 | 1.40E-18 | 2.09E-18 |
| GD | 158 | 0.00E+00 | 2.57E-20 | 5.70E-20 | 9.29E-20 | 1.33E-19 | 3.44E-19 | 1.44E-18 | 4.77E-18 | 9.97E-18 | 1.70E-17 | 3.63E-17 |
| TB | 157 | 0.00E+00 | 2.14E-18 | 4.34E-18 | 6.50E-18 | 8.64E-18 | 1.73E-17 | 4.29E-17 | 8.46E-17 | 1.26E-16 | 1.66E-16 | 2.43E-16 |
| TB | 158 | 0.00E+00 | 5.07E-18 | 1.03E-17 | 1.54E-17 | 2.05E-17 | 4.09E-17 | 1.02E-16 | 2.01E-16 | 2.98E-16 | 3.93E-16 | 5.76E-16 |
| TB | 159 | 0.00E+00 | 2.52E-20 | 5.14E-20 | 7.73E-20 | 1.03E-19 | 2.05E-19 | 5.13E-19 | 1.02E-18 | 1.53E-18 | 2.04E-18 | 3.06E-18 |
| TB | 160 | 0.00E+00 | 8.99E-17 | 1.29E-16 | 1.44E-16 | 1.51E-16 | 1.55E-16 | 1.55E-16 | 1.55E-16 | 1.55E-16 | 1.55E-16 | 1.55E-16 |
| DY | 160 | 0.00E+00 | 4.43E-17 | 1.44E-16 | 2.65E-16 | 3.93E-16 | 9.33E-16 | 2.73E-15 | 5.59E-15 | 8.47E-15 | 1.14E-14 | 1.69E-14 |
| Total | | 0.00E+00 | 1.25E-09 | 2.53E-09 | 3.79E-09 | 5.04E-09 | 1.01E-08 | 2.53E-08 | 5.04E-08 | 7.57E-08 | 1.01E-07 | 1.51E-07 |

| Table A.10. SNS nuclide production during normal proton beam operation: Limestone Rock Zone | | | | | | | | | | | | |
|---|---|---|---|---|---|---|---|---|---|---|---|---|
| Proton beam energy: 1 GeV | | | | | | | Operational line loss assumption: 1 nA/m (continuous) | | | | | |
| Nuclide masses integrated over the material zone volume in the HETC & MCNP calculational model | | | | | | | | | | | | |
| Nuclide concentration | | Time (s) | 7.88E+06 | 1.58E+07 | 2.37E+07 | 3.15E+07 | 6.31E+07 | 1.58E+08 | 3.15E+08 | 4.73E+08 | 6.31E+08 | 9.46E+08 |
| (gram-atoms) | | Initial | 3 months | 6 months | 9 months | 1 year | 2 years | 5 years | 10 years | 15 years | 20 years | 30 years |
| H | 1 | 0.00E+00 | 1.44E-10 | 2.92E-10 | 4.38E-10 | 5.83E-10 | 1.17E-09 | 2.92E-09 | 5.83E-09 | 8.75E-09 | 1.17E-08 | 1.75E-08 |
| H | 2 | 0.00E+00 | 3.36E-12 | 6.82E-12 | 1.02E-11 | 1.36E-11 | 2.72E-11 | 6.82E-11 | 1.36E-10 | 2.04E-10 | 2.72E-10 | 4.08E-10 |
| **H** | **3** | **0.00E+00** | **1.18E-12** | **2.39E-12** | **3.56E-12** | **4.70E-12** | **9.15E-12** | **2.11E-11** | **3.69E-11** | **4.90E-11** | **5.80E-11** | **7.00E-11** |
| HE | 3 | 0.00E+00 | 3.02E-13 | 6.30E-13 | 9.70E-13 | 1.32E-12 | 2.91E-12 | 9.08E-12 | 2.32E-11 | 4.14E-11 | 6.25E-11 | 1.11E-10 |
| HE | 4 | 0.00E+00 | 2.95E-11 | 6.00E-11 | 9.00E-11 | 1.20E-10 | 2.40E-10 | 6.00E-10 | 1.20E-09 | 1.80E-09 | 2.40E-09 | 3.59E-09 |
| LI | 6 | 0.00E+00 | 1.61E-12 | 3.28E-12 | 4.92E-12 | 6.54E-12 | 1.31E-11 | 3.28E-11 | 6.54E-11 | 9.82E-11 | 1.31E-10 | 1.96E-10 |
| LI | 7 | 0.00E+00 | 4.04E-13 | 8.20E-13 | 1.23E-12 | 1.63E-12 | 3.27E-12 | 8.20E-12 | 1.63E-11 | 2.45E-11 | 3.27E-11 | 4.91E-11 |
| BE | 9 | 0.00E+00 | 7.70E-13 | 1.56E-12 | 2.35E-12 | 3.12E-12 | 6.25E-12 | 1.56E-11 | 3.12E-11 | 4.68E-11 | 6.25E-11 | 9.36E-11 |
| **BE** | **10** | **0.00E+00** | **9.09E-15** | **1.85E-14** | **2.77E-14** | **3.68E-14** | **7.37E-14** | **1.85E-13** | **3.68E-13** | **5.52E-13** | **7.37E-13** | **1.10E-12** |
| B | 10 | 0.00E+00 | 4.44E-12 | 9.02E-12 | 1.35E-11 | 1.80E-11 | 3.60E-11 | 9.02E-11 | 1.80E-10 | 2.70E-10 | 3.60E-10 | 5.40E-10 |
| B | 11 | 0.00E+00 | 5.54E-12 | 1.12E-11 | 1.69E-11 | 2.24E-11 | 4.49E-11 | 1.12E-10 | 2.24E-10 | 3.37E-10 | 4.49E-10 | 6.73E-10 |
| C | 11 | 0.00E+00 | 3.65E-16 | 3.65E-16 | 3.65E-16 | 3.65E-16 | 3.65E-16 | 3.65E-16 | 3.65E-16 | 3.65E-16 | 3.65E-16 | 3.65E-16 |
| C | 12 | 0.00E+00 | 1.67E-11 | 3.40E-11 | 5.10E-11 | 6.77E-11 | 1.36E-10 | 3.40E-10 | 6.77E-10 | 1.02E-09 | 1.36E-09 | 2.03E-09 |
| C | 13 | 0.00E+00 | 1.42E-11 | 2.88E-11 | 4.32E-11 | 5.75E-11 | 1.15E-10 | 2.88E-10 | 5.75E-10 | 8.63E-10 | 1.15E-09 | 1.73E-09 |
| **C** | **14** | **0.00E+00** | **2.20E-12** | **4.46E-12** | **6.69E-12** | **8.89E-12** | **1.78E-11** | **4.46E-11** | **8.88E-11** | **1.33E-10** | **1.78E-10** | **2.66E-10** |
| N | 13 | 0.00E+00 | 1.34E-16 | 1.34E-16 | 1.34E-16 | 1.34E-16 | 1.34E-16 | 1.34E-16 | 1.34E-16 | 1.34E-16 | 1.34E-16 | 1.34E-16 |
| N | 14 | 0.00E+00 | 1.32E-11 | 2.68E-11 | 4.03E-11 | 5.35E-11 | 1.07E-10 | 2.68E-10 | 5.35E-10 | 8.04E-10 | 1.07E-09 | 1.61E-09 |
| N | 15 | 0.00E+00 | 2.17E-11 | 4.42E-11 | 6.62E-11 | 8.80E-11 | 1.76E-10 | 4.42E-10 | 8.80E-10 | 1.32E-09 | 1.76E-09 | 2.64E-09 |
| N | 16 | 0.00E+00 | 1.80E-18 | 1.80E-18 | 1.80E-18 | 1.80E-18 | 1.80E-18 | 1.80E-18 | 1.80E-18 | 1.80E-18 | 1.80E-18 | 1.80E-18 |
| O | 14 | 0.00E+00 | 5.28E-18 | 5.28E-18 | 5.28E-18 | 5.28E-18 | 5.28E-18 | 5.28E-18 | 5.28E-18 | 5.28E-18 | 5.28E-18 | 5.28E-18 |
| O | 15 | 0.00E+00 | 1.10E-16 | 1.10E-16 | 1.10E-16 | 1.10E-16 | 1.10E-16 | 1.10E-16 | 1.10E-16 | 1.10E-16 | 1.10E-16 | 1.10E-16 |
| O | 16 | 0.00E+00 | 6.62E-12 | 1.34E-11 | 2.02E-11 | 2.68E-11 | 5.37E-11 | 1.34E-10 | 2.68E-10 | 4.02E-10 | 5.37E-10 | 8.05E-10 |
| O | 17 | 0.00E+00 | 1.01E-12 | 2.05E-12 | 3.08E-12 | 4.09E-12 | 8.19E-12 | 2.05E-11 | 4.09E-11 | 6.14E-11 | 8.19E-11 | 1.23E-10 |
| O | 18 | 0.00E+00 | 4.04E-13 | 8.20E-13 | 1.23E-12 | 1.63E-12 | 3.27E-12 | 8.20E-12 | 1.63E-11 | 2.45E-11 | 3.27E-11 | 4.91E-11 |
| O | 19 | 0.00E+00 | 1.18E-20 | 1.18E-20 | 1.18E-20 | 1.18E-20 | 1.18E-20 | 1.18E-20 | 1.18E-20 | 1.18E-20 | 1.18E-20 | 1.18E-20 |
| F | 19 | 0.00E+00 | 2.28E-15 | 4.62E-15 | 6.93E-15 | 9.21E-15 | 1.85E-14 | 4.62E-14 | 9.21E-14 | 1.38E-13 | 1.85E-13 | 2.77E-13 |
| NE | 20 | 0.00E+00 | 8.73E-13 | 1.77E-12 | 2.66E-12 | 3.54E-12 | 7.08E-12 | 1.77E-11 | 3.54E-11 | 5.31E-11 | 7.08E-11 | 1.06E-10 |
| NE | 21 | 0.00E+00 | 1.65E-13 | 3.35E-13 | 5.02E-13 | 6.67E-13 | 1.34E-12 | 3.35E-12 | 6.67E-12 | 1.00E-11 | 1.34E-11 | 2.00E-11 |
| NE | 22 | 0.00E+00 | 8.54E-13 | 1.74E-12 | 2.62E-12 | 3.48E-12 | 7.04E-12 | 1.79E-11 | 3.63E-11 | 5.50E-11 | 7.37E-11 | 1.11E-10 |
| NE | 23 | 0.00E+00 | 1.87E-19 | 1.87E-19 | 1.87E-19 | 1.87E-19 | 1.87E-19 | 1.87E-19 | 1.87E-19 | 1.87E-19 | 1.87E-19 | 1.87E-19 |
| NE | 24 | 0.00E+00 | 3.08E-20 | 3.08E-20 | 3.08E-20 | 3.08E-20 | 3.08E-20 | 3.08E-20 | 3.08E-20 | 3.08E-20 | 3.08E-20 | 3.08E-20 |
| **NA** | **22** | **0.00E+00** | **6.72E-14** | **1.32E-13** | **1.92E-13** | **2.47E-13** | **4.37E-13** | **7.81E-13** | **9.88E-13** | **1.04E-12** | **1.06E-12** | **1.06E-12** |
| NA | 23 | 0.00E+00 | 4.22E-12 | 8.57E-12 | 1.29E-11 | 1.71E-11 | 3.42E-11 | 8.57E-11 | 1.71E-10 | 2.57E-10 | 3.42E-10 | 5.13E-10 |

| Table A.11. SNS nuclide production during normal proton beam operation: earth berm Zone 6 | | | | | | | | | | | | |
|---|---|---|---|---|---|---|---|---|---|---|---|---|
| Proton beam energy: 1 GeV | | | | | | | Operational line loss assumption: 1 nA/m (continuous) | | | | | |
| Nuclide masses integrated over the material zone volume in the HETC & MCNP calculational model | | | | | | | | | | | | |
| Nuclide concentration | | Time (s) | 7.88E+06 | 1.58E+07 | 2.37E+07 | 3.15E+07 | 6.31E+07 | 1.58E+08 | 3.15E+08 | 4.73E+08 | 6.31E+08 | 9.46E+08 |
| (gram-atoms) | | Initial | 3 months | 6 months | 9 months | 1 year | 2 years | 5 years | 10 years | 15 years | 20 years | 30 years |
| H | 1 | 0.00E+00 | 2.34E-11 | 4.74E-11 | 7.11E-11 | 9.45E-11 | 1.89E-10 | 4.74E-10 | 9.45E-10 | 1.42E-09 | 1.89E-09 | 2.84E-09 |
| H | 2 | 0.00E+00 | 4.04E-13 | 8.21E-13 | 1.23E-12 | 1.64E-12 | 3.28E-12 | 8.21E-12 | 1.64E-11 | 2.46E-11 | 3.28E-11 | 4.92E-11 |
| **H** | **3** | **0.00E+00** | **1.14E-12** | **2.29E-12** | **3.41E-12** | **4.50E-12** | **8.77E-12** | **2.02E-11** | **3.54E-11** | **4.69E-11** | **5.56E-11** | **6.71E-11** |
| HE | 3 | 0.00E+00 | 1.45E-13 | 3.11E-13 | 4.90E-13 | 6.83E-13 | 1.61E-12 | 5.77E-12 | 1.64E-11 | 3.09E-11 | 4.82E-11 | 8.86E-11 |
| HE | 4 | 0.00E+00 | 8.73E-12 | 1.77E-11 | 2.66E-11 | 3.54E-11 | 7.08E-11 | 1.77E-10 | 3.54E-10 | 5.31E-10 | 7.08E-10 | 1.06E-09 |
| BE | 9 | 0.00E+00 | 2.69E-15 | 5.47E-15 | 8.20E-15 | 1.09E-14 | 2.18E-14 | 5.47E-14 | 1.09E-13 | 1.64E-13 | 2.18E-13 | 3.27E-13 |
| **BE** | **10** | **0.00E+00** | **3.73E-17** | **7.57E-17** | **1.14E-16** | **1.51E-16** | **3.02E-16** | **7.57E-16** | **1.51E-15** | **2.27E-15** | **3.02E-15** | **4.53E-15** |
| B | 10 | 0.00E+00 | 8.07E-13 | 1.64E-12 | 2.46E-12 | 3.27E-12 | 6.55E-12 | 1.64E-11 | 3.27E-11 | 4.91E-11 | 6.55E-11 | 9.82E-11 |
| B | 11 | 0.00E+00 | 7.43E-15 | 1.51E-14 | 2.26E-14 | 3.01E-14 | 6.03E-14 | 1.51E-13 | 3.01E-13 | 4.52E-13 | 6.03E-13 | 9.04E-13 |
| C | 12 | 0.00E+00 | 3.93E-12 | 7.98E-12 | 1.20E-11 | 1.59E-11 | 3.19E-11 | 7.98E-11 | 1.59E-10 | 2.39E-10 | 3.19E-10 | 4.78E-10 |
| C | 13 | 0.00E+00 | 2.38E-12 | 4.83E-12 | 7.24E-12 | 9.63E-12 | 1.93E-11 | 4.83E-11 | 9.63E-11 | 1.45E-10 | 1.93E-10 | 2.89E-10 |
| **C** | **14** | **0.00E+00** | **5.41E-13** | **1.10E-12** | **1.65E-12** | **2.19E-12** | **4.39E-12** | **1.10E-11** | **2.19E-11** | **3.29E-11** | **4.38E-11** | **6.57E-11** |
| N | 14 | 0.00E+00 | 3.30E-12 | 6.70E-12 | 1.00E-11 | 1.34E-11 | 2.68E-11 | 6.70E-11 | 1.34E-10 | 2.01E-10 | 2.68E-10 | 4.01E-10 |
| N | 15 | 0.00E+00 | 2.22E-12 | 4.51E-12 | 6.77E-12 | 9.00E-12 | 1.80E-11 | 4.51E-11 | 9.00E-11 | 1.35E-10 | 1.80E-10 | 2.70E-10 |
| N | 16 | 0.00E+00 | 3.15E-19 | 3.15E-19 | 3.15E-19 | 3.15E-19 | 3.15E-19 | 3.15E-19 | 3.15E-19 | 3.15E-19 | 3.15E-19 | 3.15E-19 |
| O | 15 | 0.00E+00 | 2.77E-17 | 2.77E-17 | 2.77E-17 | 2.77E-17 | 2.77E-17 | 2.77E-17 | 2.77E-17 | 2.77E-17 | 2.77E-17 | 2.77E-17 |
| O | 16 | 0.00E+00 | 2.26E-12 | 4.59E-12 | 6.88E-12 | 9.15E-12 | 1.83E-11 | 4.59E-11 | 9.15E-11 | 1.37E-10 | 1.83E-10 | 2.75E-10 |
| O | 17 | 0.00E+00 | 2.08E-13 | 4.23E-13 | 6.35E-13 | 8.43E-13 | 1.69E-12 | 4.23E-12 | 8.43E-12 | 1.27E-11 | 1.69E-11 | 2.53E-11 |
| O | 18 | 0.00E+00 | 7.84E-17 | 1.59E-16 | 2.39E-16 | 3.17E-16 | 6.36E-16 | 1.59E-15 | 3.17E-15 | 4.77E-15 | 6.36E-15 | 9.53E-15 |
| F | 19 | 0.00E+00 | 4.84E-16 | 9.83E-16 | 1.47E-15 | 1.96E-15 | 3.93E-15 | 9.83E-15 | 1.96E-14 | 2.94E-14 | 3.93E-14 | 5.89E-14 |
| NE | 20 | 0.00E+00 | 1.89E-14 | 3.83E-14 | 5.75E-14 | 7.64E-14 | 1.53E-13 | 3.83E-13 | 7.64E-13 | 1.15E-12 | 1.53E-12 | 2.29E-12 |
| NE | 21 | 0.00E+00 | 3.14E-15 | 6.37E-15 | 9.56E-15 | 1.27E-14 | 2.54E-14 | 6.37E-14 | 1.27E-13 | 1.91E-13 | 2.54E-13 | 3.82E-13 |
| NE | 22 | 0.00E+00 | 1.70E-15 | 3.65E-15 | 5.76E-15 | 8.01E-15 | 1.86E-14 | 6.07E-14 | 1.46E-13 | 2.40E-13 | 3.35E-13 | 5.25E-13 |
| **NA** | **22** | **0.00E+00** | **3.01E-15** | **5.91E-15** | **8.59E-15** | **1.11E-14** | **1.96E-14** | **3.50E-14** | **4.43E-14** | **4.68E-14** | **4.74E-14** | **4.77E-14** |
| NA | 23 | 0.00E+00 | 6.35E-13 | 1.29E-12 | 1.93E-12 | 2.57E-12 | 5.15E-12 | 1.29E-11 | 2.57E-11 | 3.86E-11 | 5.15E-11 | 7.72E-11 |
| NA | 24 | 0.00E+00 | 4.56E-16 | 4.56E-16 | 4.56E-16 | 4.56E-16 | 4.56E-16 | 4.56E-16 | 4.56E-16 | 4.56E-16 | 4.56E-16 | 4.56E-16 |
| NA | 25 | 0.00E+00 | 5.50E-20 | 5.50E-20 | 5.50E-20 | 5.50E-20 | 5.50E-20 | 5.50E-20 | 5.50E-20 | 5.50E-20 | 5.50E-20 | 5.50E-20 |
| MG | 24 | 0.00E+00 | 2.88E-12 | 5.85E-12 | 8.77E-12 | 1.17E-11 | 2.34E-11 | 5.85E-11 | 1.17E-10 | 1.75E-10 | 2.34E-10 | 3.50E-10 |
| MG | 25 | 0.00E+00 | 6.81E-13 | 1.38E-12 | 2.07E-12 | 2.76E-12 | 5.52E-12 | 1.38E-11 | 2.76E-11 | 4.14E-11 | 5.52E-11 | 8.28E-11 |
| MG | 26 | 0.00E+00 | 3.74E-13 | 7.60E-13 | 1.14E-12 | 1.52E-12 | 3.04E-12 | 7.60E-12 | 1.52E-11 | 2.28E-11 | 3.04E-11 | 4.55E-11 |
| MG | 27 | 0.00E+00 | 1.42E-17 | 1.42E-17 | 1.42E-17 | 1.42E-17 | 1.42E-17 | 1.42E-17 | 1.42E-17 | 1.42E-17 | 1.42E-17 | 1.42E-17 |
| **AL** | **26** | **0.00E+00** | **1.41E-12** | **2.85E-12** | **4.28E-12** | **5.69E-12** | **1.14E-11** | **2.85E-11** | **5.69E-11** | **8.54E-11** | **1.14E-10** | **1.71E-10** |
| AL | 27 | 0.00E+00 | 4.38E-12 | 8.90E-12 | 1.33E-11 | 1.77E-11 | 3.55E-11 | 8.90E-11 | 1.77E-10 | 2.66E-10 | 3.55E-10 | 5.33E-10 |

**Table A.11. (continued)**

| Proton beam energy: 1 GeV | | | | | | | Operational line loss assumption: 1 nA/m (continuous) | | | | | |
|---|---|---|---|---|---|---|---|---|---|---|---|---|
| Nuclide masses integrated over the material zone volume in the HETC & MCNP calculational model | | | | | | | | | | | | |
| Nuclide concentration | | Time (s) | 7.88E+06 | 1.58E+07 | 2.37E+07 | 3.15E+07 | 6.31E+07 | 1.58E+08 | 3.15E+08 | 4.73E+08 | 6.31E+08 | 9.46E+08 |
| (gram-atoms) | | Initial | 3 months | 6 months | 9 months | 1 year | 2 years | 5 years | 10 years | 15 years | 20 years | 30 years |
| AL | 28 | 0.00E+00 | 1.54E-17 | 1.54E-17 | 1.54E-17 | 1.54E-17 | 1.54E-17 | 1.54E-17 | 1.54E-17 | 1.54E-17 | 1.54E-17 | 1.54E-17 |
| AL | 29 | 0.00E+00 | 1.48E-18 | 1.48E-18 | 1.48E-18 | 1.48E-18 | 1.48E-18 | 1.48E-18 | 1.48E-18 | 1.48E-18 | 1.48E-18 | 1.48E-18 |
| SI | 28 | 0.00E+00 | 1.42E-12 | 2.88E-12 | 4.32E-12 | 5.74E-12 | 1.15E-11 | 2.88E-11 | 5.74E-11 | 8.62E-11 | 1.15E-10 | 1.72E-10 |
| SI | 29 | 0.00E+00 | 1.37E-13 | 2.78E-13 | 4.17E-13 | 5.54E-13 | 1.11E-12 | 2.78E-12 | 5.54E-12 | 8.32E-12 | 1.11E-11 | 1.66E-11 |
| SI | 30 | 0.00E+00 | 1.96E-14 | 3.97E-14 | 5.96E-14 | 7.92E-14 | 1.59E-13 | 3.97E-13 | 7.92E-13 | 1.19E-12 | 1.59E-12 | 2.38E-12 |
| SI | 31 | 0.00E+00 | 1.04E-17 | 1.04E-17 | 1.04E-17 | 1.04E-17 | 1.04E-17 | 1.04E-17 | 1.04E-17 | 1.04E-17 | 1.04E-17 | 1.04E-17 |
| P | 31 | 0.00E+00 | 5.96E-15 | 1.21E-14 | 1.82E-14 | 2.42E-14 | 4.84E-14 | 1.21E-13 | 2.41E-13 | 3.63E-13 | 4.84E-13 | 7.25E-13 |
| P | 32 | 0.00E+00 | 5.44E-18 | 5.51E-18 | 5.51E-18 | 5.51E-18 | 5.51E-18 | 5.51E-18 | 5.51E-18 | 5.51E-18 | 5.51E-18 | 5.51E-18 |
| S | 32 | 0.00E+00 | 1.86E-17 | 4.33E-17 | 6.78E-17 | 9.19E-17 | 1.95E-16 | 4.94E-16 | 9.85E-16 | 1.48E-15 | 1.97E-15 | 2.95E-15 |
| CL | 35 | 0.00E+00 | 3.74E-15 | 7.60E-15 | 1.14E-14 | 1.51E-14 | 3.03E-14 | 7.60E-14 | 1.51E-13 | 2.27E-13 | 3.03E-13 | 4.55E-13 |
| **CL** | **36** | **0.00E+00** | **7.09E-15** | **1.44E-14** | **2.16E-14** | **2.87E-14** | **5.75E-14** | **1.44E-13** | **2.87E-13** | **4.31E-13** | **5.75E-13** | **8.63E-13** |
| CL | 37 | 0.00E+00 | 4.24E-16 | 1.14E-15 | 1.90E-15 | 2.65E-15 | 6.10E-15 | 1.57E-14 | 3.12E-14 | 4.69E-14 | 6.25E-14 | 9.34E-14 |
| CL | 38 | 0.00E+00 | 1.16E-19 | 1.16E-19 | 1.16E-19 | 1.16E-19 | 1.16E-19 | 1.16E-19 | 1.16E-19 | 1.16E-19 | 1.16E-19 | 1.16E-19 |
| CL | 39 | 0.00E+00 | 1.32E-20 | 1.32E-20 | 1.32E-20 | 1.32E-20 | 1.32E-20 | 1.32E-20 | 1.32E-20 | 1.32E-20 | 1.32E-20 | 1.32E-20 |
| AR | 36 | 0.00E+00 | 9.16E-17 | 1.86E-16 | 2.79E-16 | 3.71E-16 | 7.43E-16 | 1.86E-15 | 3.71E-15 | 5.58E-15 | 7.44E-15 | 1.12E-14 |
| AR | 37 | 0.00E+00 | 3.28E-16 | 3.84E-16 | 3.93E-16 | 3.94E-16 | 3.95E-16 | 3.94E-16 | 3.94E-16 | 3.94E-16 | 3.94E-16 | 3.94E-16 |
| AR | 38 | 0.00E+00 | 8.32E-15 | 1.69E-14 | 2.53E-14 | 3.37E-14 | 6.75E-14 | 1.69E-13 | 3.37E-13 | 5.06E-13 | 6.75E-13 | 1.01E-12 |
| **AR** | **39** | **0.00E+00** | **4.18E-14** | **8.49E-14** | **1.27E-13** | **1.69E-13** | **3.38E-13** | **8.44E-13** | **1.67E-12** | **2.49E-12** | **3.31E-12** | **4.90E-12** |
| AR | 40 | 0.00E+00 | 8.46E-17 | 1.72E-16 | 2.58E-16 | 3.43E-16 | 6.86E-16 | 1.72E-15 | 3.43E-15 | 5.14E-15 | 6.86E-15 | 1.03E-14 |
| AR | 41 | 0.00E+00 | 2.35E-19 | 2.35E-19 | 2.35E-19 | 2.35E-19 | 2.35E-19 | 2.35E-19 | 2.35E-19 | 2.35E-19 | 2.35E-19 | 2.35E-19 |
| K | 38 | 0.00E+00 | 4.18E-20 | 4.18E-20 | 4.18E-20 | 4.18E-20 | 4.18E-20 | 4.18E-20 | 4.18E-20 | 4.18E-20 | 4.18E-20 | 4.18E-20 |
| K | 39 | 0.00E+00 | 7.02E-16 | 1.45E-15 | 2.22E-15 | 3.01E-15 | 6.46E-15 | 1.94E-14 | 4.95E-14 | 9.04E-14 | 1.42E-13 | 2.75E-13 |
| **K** | **40** | **0.00E+00** | **1.32E-14** | **2.68E-14** | **4.01E-14** | **5.34E-14** | **1.07E-13** | **2.68E-13** | **5.34E-13** | **8.01E-13** | **1.07E-12** | **1.60E-12** |
| K | 41 | 0.00E+00 | 1.95E-16 | 3.96E-16 | 5.94E-16 | 7.89E-16 | 1.58E-15 | 3.96E-15 | 7.89E-15 | 1.18E-14 | 1.58E-14 | 2.37E-14 |
| K | 42 | 0.00E+00 | 6.29E-18 | 6.29E-18 | 6.29E-18 | 6.29E-18 | 6.29E-18 | 6.29E-18 | 6.29E-18 | 6.29E-18 | 6.29E-18 | 6.29E-18 |
| **CA** | **41** | **0.00E+00** | **6.62E-17** | **1.34E-16** | **2.02E-16** | **2.68E-16** | **5.37E-16** | **1.34E-15** | **2.68E-15** | **4.02E-15** | **5.37E-15** | **8.04E-15** |
| CA | 42 | 0.00E+00 | 7.83E-16 | 1.60E-15 | 2.40E-15 | 3.19E-15 | 6.37E-15 | 1.59E-14 | 3.17E-14 | 4.76E-14 | 6.35E-14 | 9.52E-14 |
| CA | 43 | 0.00E+00 | 1.08E-16 | 2.19E-16 | 3.29E-16 | 4.37E-16 | 8.75E-16 | 2.19E-15 | 4.37E-15 | 6.56E-15 | 8.75E-15 | 1.31E-14 |
| CA | 44 | 0.00E+00 | 1.09E-14 | 2.23E-14 | 3.34E-14 | 4.44E-14 | 8.89E-14 | 2.22E-13 | 4.43E-13 | 6.66E-13 | 8.88E-13 | 1.33E-12 |
| CA | 45 | 0.00E+00 | 2.49E-16 | 4.24E-16 | 5.42E-16 | 6.20E-16 | 7.55E-16 | 7.91E-16 | 7.92E-16 | 7.92E-16 | 7.92E-16 | 7.92E-16 |
| CA | 46 | 0.00E+00 | 2.11E-17 | 4.29E-17 | 6.43E-17 | 8.54E-17 | 1.71E-16 | 4.29E-16 | 8.54E-16 | 1.28E-15 | 1.71E-15 | 2.57E-15 |
| CA | 47 | 0.00E+00 | 3.29E-18 | 3.29E-18 | 3.29E-18 | 3.29E-18 | 3.29E-18 | 3.29E-18 | 3.29E-18 | 3.29E-18 | 3.29E-18 | 3.29E-18 |
| CA | 48 | 0.00E+00 | 1.83E-18 | 3.72E-18 | 5.58E-18 | 7.42E-18 | 1.49E-17 | 3.72E-17 | 7.42E-17 | 1.11E-16 | 1.49E-16 | 2.23E-16 |
| SC | 44 | 0.00E+00 | 2.85E-17 | 2.85E-17 | 2.85E-17 | 2.85E-17 | 2.85E-17 | 2.85E-17 | 2.85E-17 | 2.85E-17 | 2.85E-17 | 2.85E-17 |

**Table A.11. (continued)**

| Proton beam energy: 1 GeV | | | | | | | Operational line loss assumption: 1 nA/m (continuous) | | | | | |
|---|---|---|---|---|---|---|---|---|---|---|---|---|
| Nuclide masses integrated over the material zone volume in the HETC & MCNP calculational model | | | | | | | | | | | | |
| Nuclide concentration | | Time (s) | 7.88E+06 | 1.58E+07 | 2.37E+07 | 3.15E+07 | 6.31E+07 | 1.58E+08 | 3.15E+08 | 4.73E+08 | 6.31E+08 | 9.46E+08 |
| (gram-atoms) | | Initial | 3 months | 6 months | 9 months | 1 year | 2 years | 5 years | 10 years | 15 years | 20 years | 30 years |
| SC | 45 | 0.00E+00 | 1.75E-15 | 3.64E-15 | 5.56E-15 | 7.48E-15 | 1.55E-14 | 3.99E-14 | 8.10E-14 | 1.22E-13 | 1.64E-13 | 2.46E-13 |
| SC | 46 | 0.00E+00 | 3.30E-16 | 4.90E-16 | 5.64E-16 | 5.98E-16 | 6.27E-16 | 6.29E-16 | 6.29E-16 | 6.29E-16 | 6.29E-16 | 6.29E-16 |
| SC | 47 | 0.00E+00 | 5.84E-17 | 5.84E-17 | 5.84E-17 | 5.84E-17 | 5.84E-17 | 5.84E-17 | 5.84E-17 | 5.84E-17 | 5.84E-17 | 5.84E-17 |
| SC | 48 | 0.00E+00 | 1.93E-17 | 1.93E-17 | 1.93E-17 | 1.93E-17 | 1.93E-17 | 1.93E-17 | 1.93E-17 | 1.93E-17 | 1.93E-17 | 1.93E-17 |
| SC | 49 | 0.00E+00 | 1.86E-20 | 1.86E-20 | 1.86E-20 | 1.86E-20 | 1.86E-20 | 1.86E-20 | 1.86E-20 | 1.86E-20 | 1.86E-20 | 1.86E-20 |
| TI | 45 | 0.00E+00 | 3.64E-19 | 3.64E-19 | 3.64E-19 | 3.64E-19 | 3.64E-19 | 3.64E-19 | 3.64E-19 | 3.64E-19 | 3.64E-19 | 3.64E-19 |
| TI | 46 | 0.00E+00 | 4.56E-16 | 1.11E-15 | 1.83E-15 | 2.58E-15 | 5.75E-15 | 1.60E-14 | 3.25E-14 | 4.90E-14 | 6.56E-14 | 9.81E-14 |
| TI | 47 | 0.00E+00 | 5.51E-15 | 1.13E-14 | 1.69E-14 | 2.25E-14 | 4.50E-14 | 1.12E-13 | 2.24E-13 | 3.36E-13 | 4.48E-13 | 6.71E-13 |
| TI | 48 | 0.00E+00 | 1.64E-15 | 3.35E-15 | 5.03E-15 | 6.70E-15 | 1.34E-14 | 3.34E-14 | 6.65E-14 | 9.99E-14 | 1.33E-13 | 2.00E-13 |
| TI | 49 | 0.00E+00 | 4.04E-14 | 1.49E-13 | 3.10E-13 | 5.13E-13 | 1.64E-12 | 6.21E-12 | 1.44E-11 | 2.27E-11 | 3.10E-11 | 4.96E-11 |
| TI | 50 | 0.00E+00 | 2.61E-16 | 5.30E-16 | 7.95E-16 | 1.06E-15 | 2.12E-15 | 5.30E-15 | 1.06E-14 | 1.59E-14 | 2.12E-14 | 3.17E-14 |
| V | 49 | 0.00E+00 | 3.67E-13 | 6.80E-13 | 9.32E-13 | 1.14E-12 | 1.67E-12 | 2.07E-12 | 2.11E-12 | 2.11E-12 | 2.11E-12 | 2.12E-12 |
| V | 50 | 0.00E+00 | 2.63E-16 | 5.35E-16 | 8.03E-16 | 1.07E-15 | 2.14E-15 | 5.35E-15 | 1.07E-14 | 1.60E-14 | 2.14E-14 | 3.20E-14 |
| V | 51 | 0.00E+00 | 6.14E-16 | 1.59E-15 | 2.59E-15 | 3.59E-15 | 8.02E-15 | 2.05E-14 | 4.09E-14 | 6.14E-14 | 8.19E-14 | 1.22E-13 |
| V | 52 | 0.00E+00 | 1.04E-20 | 1.04E-20 | 1.04E-20 | 1.04E-20 | 1.04E-20 | 1.04E-20 | 1.04E-20 | 1.04E-20 | 1.04E-20 | 1.04E-20 |
| CR | 50 | 0.00E+00 | 3.11E-16 | 6.31E-16 | 9.46E-16 | 1.26E-15 | 2.52E-15 | 6.31E-15 | 1.26E-14 | 1.89E-14 | 2.52E-14 | 3.78E-14 |
| CR | 51 | 0.00E+00 | 3.75E-16 | 4.14E-16 | 4.18E-16 | 4.18E-16 | 4.19E-16 | 4.19E-16 | 4.19E-16 | 4.19E-16 | 4.19E-16 | 4.19E-16 |
| CR | 52 | 0.00E+00 | 4.27E-15 | 8.71E-15 | 1.31E-14 | 1.74E-14 | 3.48E-14 | 8.69E-14 | 1.73E-13 | 2.60E-13 | 3.47E-13 | 5.20E-13 |
| CR | 53 | 0.00E+00 | 5.52E-15 | 1.12E-14 | 1.68E-14 | 2.23E-14 | 4.47E-14 | 1.12E-13 | 2.23E-13 | 3.35E-13 | 4.47E-13 | 6.71E-13 |
| CR | 54 | 0.00E+00 | 1.44E-15 | 5.29E-15 | 1.10E-14 | 1.81E-14 | 5.76E-14 | 2.15E-13 | 4.94E-13 | 7.77E-13 | 1.06E-12 | 1.69E-12 |
| MN | 52 | 0.00E+00 | 3.90E-17 | 3.90E-17 | 3.90E-17 | 3.90E-17 | 3.90E-17 | 3.90E-17 | 3.90E-17 | 3.90E-17 | 3.90E-17 | 3.90E-17 |
| **MN** | **53** | **0.00E+00** | **7.30E-15** | **1.48E-14** | **2.22E-14** | **2.96E-14** | **5.92E-14** | **1.48E-13** | **2.96E-13** | **4.44E-13** | **5.92E-13** | **8.88E-13** |
| MN | 54 | 0.00E+00 | 1.25E-14 | 2.30E-14 | 3.14E-14 | 3.82E-14 | 5.52E-14 | 6.76E-14 | 6.88E-14 | 6.88E-14 | 6.88E-14 | 6.88E-14 |
| MN | 55 | 0.00E+00 | 2.52E-14 | 5.60E-14 | 9.07E-14 | 1.29E-13 | 3.20E-13 | 1.14E-12 | 2.90E-12 | 4.84E-12 | 6.83E-12 | 1.08E-11 |
| MN | 56 | 0.00E+00 | 2.65E-17 | 2.65E-17 | 2.65E-17 | 2.65E-17 | 2.65E-17 | 2.65E-17 | 2.65E-17 | 2.65E-17 | 2.65E-17 | 2.65E-17 |
| FE | 53 | 0.00E+00 | 4.10E-20 | 4.10E-20 | 4.10E-20 | 4.10E-20 | 4.10E-20 | 4.10E-20 | 4.10E-20 | 4.10E-20 | 4.10E-20 | 4.10E-20 |
| FE | 54 | 0.00E+00 | 4.04E-13 | 8.20E-13 | 1.23E-12 | 1.63E-12 | 3.27E-12 | 8.20E-12 | 1.63E-11 | 2.45E-11 | 3.27E-11 | 4.91E-11 |
| **FE** | **55** | **0.00E+00** | **7.36E-14** | **1.45E-13** | **2.10E-13** | **2.71E-13** | **4.81E-13** | **8.65E-13** | **1.10E-12** | **1.17E-12** | **1.19E-12** | **1.19E-12** |
| FE | 56 | 0.00E+00 | 1.79E-14 | 3.63E-14 | 5.45E-14 | 7.25E-14 | 1.45E-13 | 3.63E-13 | 7.24E-13 | 1.09E-12 | 1.45E-12 | 2.17E-12 |
| FE | 57 | 0.00E+00 | 4.72E-14 | 9.59E-14 | 1.44E-13 | 1.91E-13 | 3.83E-13 | 9.59E-13 | 1.91E-12 | 2.87E-12 | 3.83E-12 | 5.74E-12 |
| FE | 58 | 0.00E+00 | 1.07E-15 | 2.18E-15 | 3.27E-15 | 4.35E-15 | 8.72E-15 | 2.18E-14 | 4.35E-14 | 6.54E-14 | 8.72E-14 | 1.31E-13 |
| FE | 59 | 0.00E+00 | 1.02E-16 | 1.27E-16 | 1.33E-16 | 1.34E-16 | 1.35E-16 | 1.35E-16 | 1.35E-16 | 1.35E-16 | 1.35E-16 | 1.35E-16 |
| CO | 59 | 0.00E+00 | 8.72E-17 | 2.56E-16 | 4.42E-16 | 6.30E-16 | 1.40E-15 | 3.83E-15 | 7.78E-15 | 1.17E-14 | 1.57E-14 | 2.35E-14 |
| NI | 60 | 0.00E+00 | 1.68E-17 | 3.42E-17 | 5.13E-17 | 6.82E-17 | 1.37E-16 | 3.42E-16 | 6.82E-16 | 1.02E-15 | 1.37E-15 | 2.05E-15 |

**Table A.11. (continued)**

| Proton beam energy: 1 GeV | | | | | | | Operational line loss assumption: 1 nA/m (continuous) | | | | | |
|---|---|---|---|---|---|---|---|---|---|---|---|---|
| Nuclide masses integrated over the material zone volume in the HETC & MCNP calculational model | | | | | | | | | | | | |
| Nuclide concentration | | Time (s) | 7.88E+06 | 1.58E+07 | 2.37E+07 | 3.15E+07 | 6.31E+07 | 1.58E+08 | 3.15E+08 | 4.73E+08 | 6.31E+08 | 9.46E+08 |
| (gram-atoms) | | Initial | 3 months | 6 months | 9 months | 1 year | 2 years | 5 years | 10 years | 15 years | 20 years | 30 years |
| NI | 61 | 0.00E+00 | 8.92E-18 | 1.81E-17 | 2.72E-17 | 3.61E-17 | 7.24E-17 | 1.81E-16 | 3.61E-16 | 5.42E-16 | 7.24E-16 | 1.08E-15 |
| NI | 62 | 0.00E+00 | 1.78E-18 | 3.62E-18 | 5.43E-18 | 7.22E-18 | 1.45E-17 | 3.62E-17 | 7.22E-17 | 1.08E-16 | 1.45E-16 | 2.17E-16 |
| NI | 63 | 0.00E+00 | 5.50E-18 | 1.12E-17 | 1.67E-17 | 2.22E-17 | 4.43E-17 | 1.10E-16 | 2.15E-16 | 3.18E-16 | 4.17E-16 | 6.04E-16 |
| NI | 64 | 0.00E+00 | 1.38E-16 | 2.82E-16 | 4.23E-16 | 5.63E-16 | 1.12E-15 | 2.81E-15 | 5.60E-15 | 8.41E-15 | 1.12E-14 | 1.68E-14 |
| CU | 63 | 0.00E+00 | 3.05E-16 | 6.19E-16 | 9.29E-16 | 1.23E-15 | 2.47E-15 | 6.19E-15 | 1.23E-14 | 1.85E-14 | 2.48E-14 | 3.71E-14 |
| CU | 64 | 0.00E+00 | 1.92E-18 | 1.92E-18 | 1.92E-18 | 1.92E-18 | 1.92E-18 | 1.92E-18 | 1.92E-18 | 1.92E-18 | 1.92E-18 | 1.92E-18 |
| CU | 65 | 0.00E+00 | 9.09E-17 | 3.07E-16 | 6.12E-16 | 9.84E-16 | 2.93E-15 | 1.01E-14 | 2.23E-14 | 3.47E-14 | 4.71E-14 | 7.40E-14 |
| CU | 67 | 0.00E+00 | 1.15E-19 | 1.15E-19 | 1.15E-19 | 1.15E-19 | 1.15E-19 | 1.15E-19 | 1.15E-19 | 1.15E-19 | 1.15E-19 | 1.15E-19 |
| ZN | 63 | 0.00E+00 | 5.35E-20 | 5.35E-20 | 5.35E-20 | 5.35E-20 | 5.35E-20 | 5.35E-20 | 5.35E-20 | 5.35E-20 | 5.35E-20 | 5.35E-20 |
| ZN | 64 | 0.00E+00 | 8.97E-17 | 1.83E-16 | 2.75E-16 | 3.66E-16 | 7.31E-16 | 1.83E-15 | 3.64E-15 | 5.46E-15 | 7.29E-15 | 1.09E-14 |
| ZN | 65 | 0.00E+00 | 5.18E-16 | 9.29E-16 | 1.24E-15 | 1.48E-15 | 2.01E-15 | 2.28E-15 | 2.29E-15 | 2.29E-15 | 2.29E-15 | 2.29E-15 |
| ZN | 66 | 0.00E+00 | 5.26E-17 | 1.07E-16 | 1.60E-16 | 2.13E-16 | 4.27E-16 | 1.07E-15 | 2.13E-15 | 3.20E-15 | 4.27E-15 | 6.40E-15 |
| ZN | 67 | 0.00E+00 | 2.33E-16 | 4.73E-16 | 7.10E-16 | 9.44E-16 | 1.89E-15 | 4.73E-15 | 9.43E-15 | 1.42E-14 | 1.89E-14 | 2.83E-14 |
| ZN | 68 | 0.00E+00 | 8.58E-17 | 1.74E-16 | 2.61E-16 | 3.47E-16 | 6.96E-16 | 1.74E-15 | 3.47E-15 | 5.22E-15 | 6.96E-15 | 1.04E-14 |
| ZN | 69 | 0.00E+00 | 2.36E-20 | 2.36E-20 | 2.36E-20 | 2.36E-20 | 2.36E-20 | 2.36E-20 | 2.36E-20 | 2.36E-20 | 2.36E-20 | 2.36E-20 |
| ZN | 70 | 0.00E+00 | 1.30E-20 | 2.64E-20 | 3.95E-20 | 5.25E-20 | 1.05E-19 | 2.64E-19 | 5.25E-19 | 7.89E-19 | 1.05E-18 | 1.58E-18 |
| GA | 69 | 0.00E+00 | 3.82E-17 | 7.75E-17 | 1.16E-16 | 1.55E-16 | 3.10E-16 | 7.75E-16 | 1.55E-15 | 2.32E-15 | 3.10E-15 | 4.64E-15 |
| GA | 71 | 0.00E+00 | 1.05E-18 | 2.14E-18 | 3.20E-18 | 4.26E-18 | 8.53E-18 | 2.14E-17 | 4.26E-17 | 6.39E-17 | 8.53E-17 | 1.28E-16 |
| BR | 81 | 0.00E+00 | 1.36E-18 | 2.76E-18 | 4.13E-18 | 5.49E-18 | 1.10E-17 | 2.76E-17 | 5.49E-17 | 8.25E-17 | 1.10E-16 | 1.65E-16 |
| BR | 82 | 0.00E+00 | 8.08E-20 | 8.08E-20 | 8.08E-20 | 8.08E-20 | 8.08E-20 | 8.08E-20 | 8.08E-20 | 8.08E-20 | 8.08E-20 | 8.08E-20 |
| KR | 82 | 0.00E+00 | 3.69E-18 | 7.58E-18 | 1.14E-17 | 1.52E-17 | 3.03E-17 | 7.54E-17 | 1.50E-16 | 2.25E-16 | 3.00E-16 | 4.50E-16 |
| KR | 83 | 0.00E+00 | 7.06E-18 | 1.43E-17 | 2.15E-17 | 2.86E-17 | 5.72E-17 | 1.43E-16 | 2.86E-16 | 4.29E-16 | 5.72E-16 | 8.58E-16 |
| KR | 84 | 0.00E+00 | 3.39E-16 | 9.18E-16 | 1.52E-15 | 2.12E-15 | 4.87E-15 | 1.25E-14 | 2.49E-14 | 3.74E-14 | 4.99E-14 | 7.46E-14 |
| KR | 85 | 0.00E+00 | 3.12E-17 | 6.28E-17 | 9.35E-17 | 1.23E-16 | 2.39E-16 | 5.45E-16 | 9.38E-16 | 1.22E-15 | 1.43E-15 | 1.69E-15 |
| KR | 86 | 0.00E+00 | 2.09E-18 | 4.24E-18 | 6.36E-18 | 8.45E-18 | 1.69E-17 | 4.24E-17 | 8.45E-17 | 1.27E-16 | 1.69E-16 | 2.54E-16 |
| RB | 84 | 0.00E+00 | 2.70E-16 | 3.11E-16 | 3.16E-16 | 3.17E-16 | 3.18E-16 | 3.17E-16 | 3.17E-16 | 3.17E-16 | 3.17E-16 | 3.17E-16 |
| RB | 85 | 0.00E+00 | 1.32E-18 | 3.20E-18 | 5.55E-18 | 8.35E-18 | 2.45E-17 | 1.15E-16 | 3.78E-16 | 7.52E-16 | 1.21E-15 | 2.26E-15 |
| RB | 86 | 0.00E+00 | 1.06E-15 | 1.09E-15 | 1.09E-15 | 1.09E-15 | 1.09E-15 | 1.09E-15 | 1.09E-15 | 1.09E-15 | 1.09E-15 | 1.09E-15 |
| RB | 87 | 0.00E+00 | 3.40E-18 | 6.91E-18 | 1.04E-17 | 1.38E-17 | 2.76E-17 | 6.91E-17 | 1.38E-16 | 2.07E-16 | 2.76E-16 | 4.14E-16 |
| RB | 88 | 0.00E+00 | 3.36E-20 | 3.36E-20 | 3.36E-20 | 3.36E-20 | 3.36E-20 | 3.36E-20 | 3.36E-20 | 3.36E-20 | 3.36E-20 | 3.36E-20 |
| SR | 84 | 0.00E+00 | 1.00E-17 | 2.75E-17 | 4.57E-17 | 6.39E-17 | 1.47E-16 | 3.78E-16 | 7.53E-16 | 1.13E-15 | 1.51E-15 | 2.25E-15 |
| SR | 86 | 0.00E+00 | 2.61E-15 | 6.34E-15 | 1.01E-14 | 1.37E-14 | 2.97E-14 | 7.54E-14 | 1.50E-13 | 2.26E-13 | 3.01E-13 | 4.51E-13 |
| SR | 88 | 0.00E+00 | 1.71E-16 | 3.47E-16 | 5.20E-16 | 6.92E-16 | 1.39E-15 | 3.47E-15 | 6.92E-15 | 1.04E-14 | 1.39E-14 | 2.08E-14 |
| XE | 128 | 0.00E+00 | 1.29E-20 | 2.66E-20 | 4.02E-20 | 5.35E-20 | 1.08E-19 | 2.70E-19 | 5.39E-19 | 8.10E-19 | 1.08E-18 | 1.62E-18 |

**Table A.11. (continued)**

| Proton beam energy: 1 GeV | | | | | | | Operational line loss assumption: 1 nA/m (continuous) | | | | | |
|---|---|---|---|---|---|---|---|---|---|---|---|---|
| Nuclide masses integrated over the material zone volume in the HETC & MCNP calculational model | | | | | | | | | | | | |
| Nuclide concentration | | Time (s) | 7.88E+06 | 1.58E+07 | 2.37E+07 | 3.15E+07 | 6.31E+07 | 1.58E+08 | 3.15E+08 | 4.73E+08 | 6.31E+08 | 9.46E+08 |
| (gram-atoms) | | Initial | 3 months | 6 months | 9 months | 1 year | 2 years | 5 years | 10 years | 15 years | 20 years | 30 years |
| XE | 129 | 0.00E+00 | 1.41E-19 | 2.91E-19 | 4.37E-19 | 5.83E-19 | 1.16E-18 | 2.89E-18 | 5.75E-18 | 8.63E-18 | 1.15E-17 | 1.73E-17 |
| XE | 130 | 0.00E+00 | 1.06E-20 | 2.15E-20 | 3.22E-20 | 4.29E-20 | 8.58E-20 | 2.15E-19 | 4.29E-19 | 6.43E-19 | 8.58E-19 | 1.29E-18 |
| XE | 131 | 0.00E+00 | 9.94E-19 | 2.54E-18 | 4.06E-18 | 5.57E-18 | 1.19E-17 | 3.05E-17 | 6.10E-17 | 9.18E-17 | 1.23E-16 | 1.84E-16 |
| XE | 132 | 0.00E+00 | 6.82E-20 | 1.41E-19 | 2.13E-19 | 2.84E-19 | 5.63E-19 | 1.40E-18 | 2.78E-18 | 4.16E-18 | 5.55E-18 | 8.32E-18 |
| XE | 134 | 0.00E+00 | 7.99E-20 | 1.62E-19 | 2.44E-19 | 3.24E-19 | 6.48E-19 | 1.62E-18 | 3.24E-18 | 4.86E-18 | 6.48E-18 | 9.72E-18 |
| CS | 131 | 0.00E+00 | 2.26E-19 | 2.31E-19 | 2.31E-19 | 2.31E-19 | 2.31E-19 | 2.31E-19 | 2.31E-19 | 2.31E-19 | 2.31E-19 | 2.31E-19 |
| CS | 133 | 0.00E+00 | 1.61E-19 | 4.45E-19 | 8.36E-19 | 1.33E-18 | 4.38E-18 | 2.28E-17 | 7.86E-17 | 1.59E-16 | 2.57E-16 | 4.86E-16 |
| CS | 134 | 0.00E+00 | 1.62E-19 | 3.16E-19 | 4.56E-19 | 5.82E-19 | 9.99E-19 | 1.66E-18 | 1.97E-18 | 2.03E-18 | 2.04E-18 | 2.04E-18 |
| CS | 135 | 0.00E+00 | 4.79E-19 | 9.74E-19 | 1.46E-18 | 1.94E-18 | 3.89E-18 | 9.73E-18 | 1.94E-17 | 2.91E-17 | 3.88E-17 | 5.82E-17 |
| CS | 136 | 0.00E+00 | 6.12E-20 | 6.17E-20 | 6.17E-20 | 6.17E-20 | 6.17E-20 | 6.17E-20 | 6.17E-20 | 6.17E-20 | 6.17E-20 | 6.17E-20 |
| CS | 137 | 0.00E+00 | 1.13E-18 | 2.28E-18 | 3.41E-18 | 4.52E-18 | 8.95E-18 | 2.17E-17 | 4.09E-17 | 5.81E-17 | 7.34E-17 | 9.92E-17 |
| BA | 130 | 0.00E+00 | 3.33E-20 | 6.76E-20 | 1.01E-19 | 1.35E-19 | 2.70E-19 | 6.76E-19 | 1.35E-18 | 2.02E-18 | 2.70E-18 | 4.05E-18 |
| BA | 131 | 0.00E+00 | 2.84E-19 | 2.85E-19 | 2.85E-19 | 2.85E-19 | 2.85E-19 | 2.85E-19 | 2.85E-19 | 2.85E-19 | 2.85E-19 | 2.85E-19 |
| BA | 132 | 0.00E+00 | 1.51E-18 | 3.07E-18 | 4.61E-18 | 6.13E-18 | 1.23E-17 | 3.07E-17 | 6.13E-17 | 9.20E-17 | 1.23E-16 | 1.84E-16 |
| BA | 133 | 0.00E+00 | 6.89E-18 | 1.39E-17 | 2.06E-17 | 2.72E-17 | 5.28E-17 | 1.20E-16 | 2.07E-16 | 2.70E-16 | 3.15E-16 | 3.71E-16 |
| BA | 134 | 0.00E+00 | 2.91E-17 | 5.91E-17 | 8.87E-17 | 1.18E-16 | 2.36E-16 | 5.93E-16 | 1.18E-15 | 1.78E-15 | 2.37E-15 | 3.56E-15 |
| BA | 135 | 0.00E+00 | 1.80E-17 | 3.66E-17 | 5.48E-17 | 7.29E-17 | 1.46E-16 | 3.66E-16 | 7.29E-16 | 1.09E-15 | 1.46E-15 | 2.19E-15 |
| BA | 136 | 0.00E+00 | 1.44E-16 | 2.91E-16 | 4.37E-16 | 5.81E-16 | 1.16E-15 | 2.92E-15 | 5.81E-15 | 8.73E-15 | 1.16E-14 | 1.75E-14 |
| BA | 137 | 0.00E+00 | 8.98E-17 | 1.82E-16 | 2.74E-16 | 3.64E-16 | 7.29E-16 | 1.82E-15 | 3.64E-15 | 5.47E-15 | 7.30E-15 | 1.10E-14 |
| BA | 138 | 0.00E+00 | 2.57E-17 | 5.21E-17 | 7.82E-17 | 1.04E-16 | 2.08E-16 | 5.21E-16 | 1.04E-15 | 1.56E-15 | 2.08E-15 | 3.12E-15 |
| BA | 139 | 0.00E+00 | 2.52E-20 | 2.52E-20 | 2.52E-20 | 2.52E-20 | 2.52E-20 | 2.52E-20 | 2.52E-20 | 2.52E-20 | 2.52E-20 | 2.52E-20 |
| LA | 139 | 0.00E+00 | 2.72E-17 | 5.53E-17 | 8.29E-17 | 1.10E-16 | 2.21E-16 | 5.53E-16 | 1.10E-15 | 1.65E-15 | 2.21E-15 | 3.31E-15 |
| TB | 157 | 0.00E+00 | 3.39E-19 | 6.87E-19 | 1.03E-18 | 1.37E-18 | 2.74E-18 | 6.80E-18 | 1.34E-17 | 1.99E-17 | 2.62E-17 | 3.85E-17 |
| TB | 158 | 0.00E+00 | 3.03E-19 | 6.15E-19 | 9.22E-19 | 1.22E-18 | 2.45E-18 | 6.08E-18 | 1.20E-17 | 1.78E-17 | 2.35E-17 | 3.44E-17 |
| TB | 160 | 0.00E+00 | 9.81E-18 | 1.40E-17 | 1.57E-17 | 1.64E-17 | 1.69E-17 | 1.70E-17 | 1.70E-17 | 1.70E-17 | 1.70E-17 | 1.70E-17 |
| DY | 160 | 0.00E+00 | 4.83E-18 | 1.57E-17 | 2.89E-17 | 4.28E-17 | 1.02E-16 | 2.97E-16 | 6.10E-16 | 9.24E-16 | 1.24E-15 | 1.85E-15 |
| Total | | 0.00E+00 | 6.25E-11 | 1.27E-10 | 1.90E-10 | 2.53E-10 | 5.07E-10 | 1.27E-09 | 2.53E-09 | 3.80E-09 | 5.07E-09 | 7.60E-09 |

# Appendix B

# SAMPLED CALCULATIONS OF $^{12}C$ AND $^{22}Na$ RELEASES FROM THE SNS SHIELD BERM

## Release Model for 14C from the SNS Shield Berm

### Berm Parameters:

### SNS Tunnel Lengths:

$Linac := 492 \cdot m$

$High_energy_transfer := 165 \cdot m$

$Ring := 221 \cdot m$

$Ring_transfer := 167 \cdot m$

$Tunnel_rad := 2.7572 \cdot m$

$Inner_soil_rad := 6.7572 \cdot m$

$Outer_zone_rad := 10.81 \cdot m$

$Tunnel_crossection := \pi \cdot Tunnel_rad^2$

$Inner_soil_crossection := \pi \cdot Inner_soil_rad^2 - Tunnel_crossection$

$Outer_soil_crossection := \pi \cdot Outer_zone_rad^2 - \pi \cdot Inner_soil_rad^2$

$Total_length := Linac + High_energy_transfer + Ring + Ring_transfer$

$Total_length = 1.045 \cdot 10^3 \cdot m$

$Tunnel_crossection = 23.883 \cdot m^2$

$Tunnel_volume := Tunnel_crossection \cdot Total_length$ $\quad Tunnel_volume = 2.496 \cdot 10^4 \cdot m^3$

$Inner_soil_crossection = 119.561 \cdot m^2$

$Inner_soil_volume := Inner_soil_crossection \cdot Total_length$ $\quad Inner_soil_volume = 1.249 \cdot 10^5 \cdot m^3$

$Outer_soil_crossection = 223.67 \cdot m^2$

$Outer_soil_volume := Outer_soil_crossection \cdot Total_length$ $\quad Outer_soil_volume = 2.337 \cdot 10^5 \cdot m^3$

### Berm Crossectional Dimenstions, Volume, and Surface Area:

$Berm_thickness := Inner_soil_rad - Tunnel_rad$ $\quad Berm_thickness = 4 \cdot m$

$Berm_radius := Berm_thickness + Tunnel_rad$ $\quad Berm_crossection := \pi \cdot Berm_radius^2 - \pi \cdot Tunnel_rad^2$

$Berm_crossection = 119.561 \cdot m^2$ $\quad Berm_volume := Berm_crossection \cdot Total_length$

$Berm_volume = 1.249 \cdot 10^5 \cdot m^3$ $\quad Berm_radius = 6.7572 \cdot m$

$Berm_surface_area := 2 \cdot \pi \cdot Berm_radius \cdot Total_length + 2 \cdot \pi \cdot Berm_radius^2$

$Berm_surface_area = 4.465 \cdot 10^4 \cdot m^2$

$Berm_Surface_Volume_Ratio := \frac{Berm_surface_area}{Berm_volume}$ $\quad Berm_Surface_Volume_Ratio = 0.357 \cdot m^{-1}$

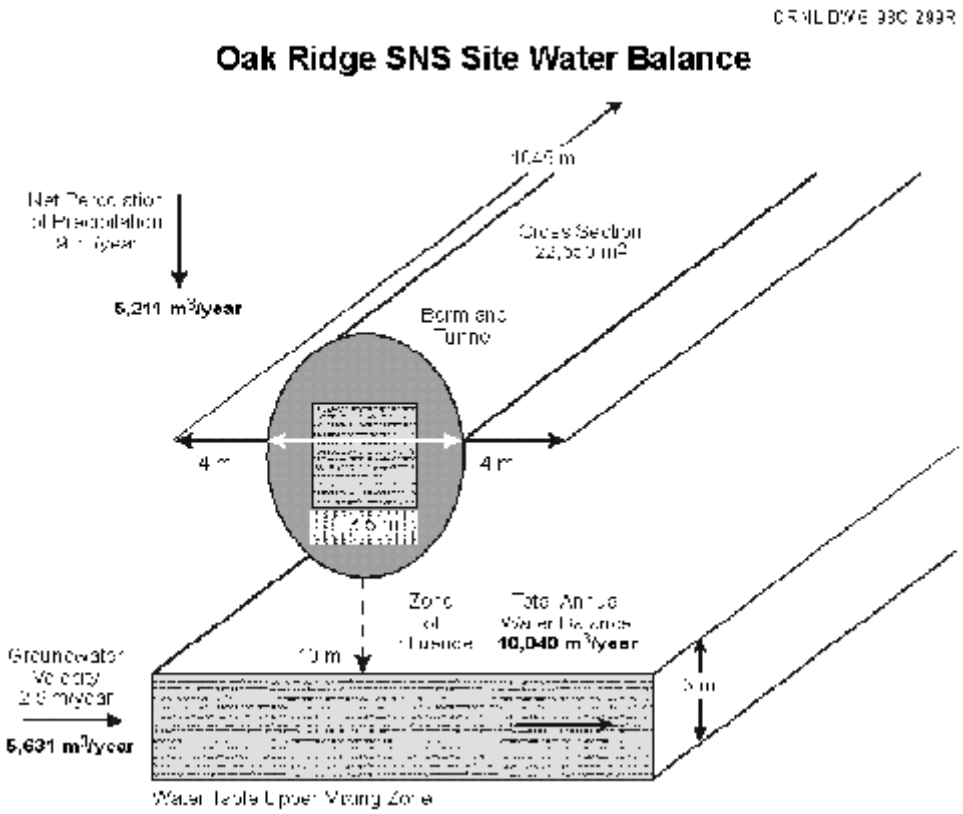


**Fig. B.1. Oak Ridge SNS site water balance.**

## Berm Hydrologic Crossection and Vadose Zone Hydrology:

$Hydro_width := 2 \cdot Berm_radius + 2 \cdot 4 \cdot m$

$Hydro_length := Total_length + 2 \cdot 4 \cdot m$

$Hydro_crossection := Hydro_length \cdot Hydro_width$

$Hydro_crossection = 2.265 \cdot 10^{4}\ m^{2}$

$Recharge_volume = 5.211 \cdot 10^{3}\ m^{3} \cdot y^{-1}$

$Recharge_mass := Recharge_volume \cdot mass_volume$

$Down_particle_velocity := \frac{Recharge_rate}{Vadose_zone_porosity}$

$Down_travel_time := \frac{Depth_to_water_table}{Down_particle_velocity}$

$Recharge_rate := 9.055 \cdot \frac{in}{y}$

$Recharge_rate = 0.23\ m \cdot y^{-1}$

$Vadose_zone_porosity := 0.37$

$Recharge_volume := Hydro_crossection \cdot Recharge_rate$

$mass_volume := 1000 \cdot \frac{kg}{m^{3}}$

$Recharge_mass = 5.211 \cdot 10^{6}\ kg \cdot y^{-1}$

$Down_particle_velocity = 0.622\ m \cdot y^{-1}$

$Depth_to_water_table := 10 \cdot m$

$Down_travel_time = 16.087\ y$

$Down_travel_time = 195.861\ month$

## Saturated Zone Hydrology

$Hydraulic_conductivity := 0.244 \cdot \frac{m}{d}$

$Hydraulic_gradient := 0.02$

$Hydraulic_conductivity = 89.121\ m \cdot y^{-1}$

$Saturated_zone_porosity := 0.37$

$Groundwater_speed := Hydraulic_conductivity \cdot Hydraulic_gradient$

$Groundwater_speed = 1.782\ m \cdot y^{-1}$

$Groundwater_velocity := \frac{Groundwater_speed}{Saturated_zone_porosity}$

$Groundwater_mix_depth := 3 \cdot m$

$Groundwater_velocity = 4.817\ m \cdot y^{-1}$

$Groundwater_volume := Groundwater_speed \cdot Groundwater_mix_depth \cdot Hydro_length$

$Groundwater_mass := Groundwater_volume \cdot mass_volume$

$Groundwater_volume = 5.631 \cdot 10^{3}\ m^{3} \cdot y^{-1}$

$Groundwater_mass = 5.631 \cdot 10^{6}\ kg \cdot y^{-1}$

$Recharge_volume = 5.211 \cdot 10^{3}\ m^{3} \cdot y^{-1}$

$Recharge_mass = 5.211 \cdot 10^{6}\ kg \cdot y^{-1}$

### Combined Recharge and Saturated Flow

$Site_flow := Groundwater_volume + Recharge_volume$ $Site_flow_Mass := Site_flow \cdot mass_volume$

$Site_flow = 1.084 \cdot 10^{4} \cdot m^{3} \cdot y^{-1}$

$Site_flow_Mass = 1.084 \cdot 10^{7} \cdot kg \cdot y^{-1}$ $Recharge_ratio := \frac{Recharge_volume}{Groundwater_volume}$

$Recharge_ratio = 0.925$

$Percent_Recharge := 100 \cdot \frac{Recharge_volume}{Site_flow}$

$Percent_Recharge = 48.062$

### Berm Mass and concentrations:

$\rho_{Berm} := 1.61 \cdot \frac{g}{cc}$ $Berm_volume = 1.249 \cdot 10^{5} \cdot m^{3}$

$Berm_mass := Berm_volume \cdot \rho_{Berm}$

$Berm_mass = 2.012 \cdot 10^{11} \cdot kg$

$C14_curies := 2.68 \cdot 10^{-4} \cdot Ci$ $C14_concentration := \frac{C14_curies}{Berm_mass}$

$C14_concentration = 1.332 \cdot 10^{-15} \cdot \frac{Ci}{g}$ $C14_concentration = 1.332 \cdot 10^{-6} \cdot \frac{nanoCi}{g}$

$C14_concentration = 1.332 \cdot 10^{-9} \cdot \frac{microCi}{g}$ $C14_concentration \cdot \rho_{Berm} = 2.145 \cdot 10^{-9} \cdot \frac{microCi}{cc}$

### 14C Radioactivity and mass:

$C14_curies := 2.68 \cdot 10^{-4} \cdot Ci$ $C14_SpecAct := 62.44179387 \cdot \frac{Ci}{g_atom}$ $C14_Atomic_wgt := 14.003242 \cdot g$

$C14_g_atom := \frac{C14_curies}{C14_SpecAct}$ $C14_g_atom = 4.292 \cdot 10^{-6} \cdot g_atom$

$C14_mass := C14_Atomic_wgt \cdot C14_g_atom$

$C14_mass = 6.01 \cdot 10^{-5} \cdot g$ $C14_mass_concentration := \frac{C14_mass}{Berm_mass}$

$C14_mass_concentration\text{-}ppm = 2.988 \cdot 10^{-10}$

$C14_mass_concentration\text{-}ppt = 2.988 \cdot 10^{-4}$

**Diffusion Calculations:**

**Effective diffusion Coefficient:**

$$De := \left(1.58 \cdot 10^{-6}\right) \cdot \frac{cm^2}{s}$$

**Surface to Volume:**

$$Berm_surface_area = 4.465 \cdot 10^{4} \cdot m^2 \qquad Berm_volume = 1.249 \cdot 10^{5} \cdot m^3$$

$$Berm_surface_volume_ratio := \frac{Berm_surface_area}{Berm_volume}$$

$$S := Berm_surface_area \qquad V := Berm_volume$$

$$\frac{S}{V} = 0.357 \cdot cm^{-1} \qquad a := Berm_radius \qquad L := \frac{Total_length}{2}$$

$$a = 6.757 \cdot m \qquad L = 522.5 \cdot m$$

**Semi-infinite Slab:**

$$F(1) := 2 \cdot \frac{S}{V} \cdot \sqrt{De \cdot t \cdot \frac{s}{\pi}} \qquad T2 := \left(0.2 \cdot \frac{V}{S \cdot 2}\right)^2 \cdot \left(\frac{\pi}{De}\right) \qquad T2 = 0.005 \cdot y$$

$$t2 := \left(0.2 \cdot \frac{V}{S \cdot 2}\right)^2 \cdot \left(\frac{\pi}{De \cdot s}\right)$$

**Geometry Specific Analytical Solution:**

$m := 3, 6 .. 30$ $\quad n := 1 .. 60$

$i := 0, 1 .. 725$ $\quad t_i := i \cdot month$

$j := 0, 1 .. 725$ $\quad t_j := j \cdot month$

$$F(t) := 2 \cdot \frac{S}{V} \cdot \sqrt{\frac{De \cdot t}{\pi}} \qquad t2 := \left(0.2 \cdot \frac{V}{S \cdot 2}\right)^2 \cdot \left(\frac{\pi}{De}\right)$$

$t2 = 0.005 \cdot y$

$t2 = 0.06 \cdot month$

$$\alpha_m := \frac{root(J0(m), m)}{a}$$

| $\alpha_m$ |
|---|
| $0.356 \cdot m^{-1}$ |
| $0.817 \cdot m^{-1}$ |
| $1.281 \cdot m^{-1}$ |
| $1.745 \cdot m^{-1}$ |
| $2.21 \cdot m^{-1}$ |
| $2.674 \cdot m^{-1}$ |
| $3.139 \cdot m^{-1}$ |
| $3.604 \cdot m^{-1}$ |
| $4.069 \cdot m^{-1}$ |
| $4.534 \cdot m^{-1}$ |

$$FC(t) := 1 - \frac{32}{\pi^2 \cdot a^2} \cdot \sum_n \sum_m \frac{e^{-\left[De \cdot \left[(\alpha_m)^2 + (2 \cdot n - 1)^2 \cdot \frac{\pi^2}{4 \cdot L^2}\right] \cdot t\right]}}{(2 \cdot n - 1)^2 \cdot (\alpha_m)^2}$$

$FC(t2) = 0.163$

**Geometry specific release faction**

$FS(t) := if(t > t2, FC(t), F(t))$

**Decay half-life factor**

$C14_\lambda := 5.73 \cdot 10^3 \cdot y$ $\quad C14_DF_i := e^{-\left(\ln(2) \cdot \frac{t_i}{C14_\lambda}\right)}$

**Calculate arrays**

$FS_i := FS(t_i)$ $\quad F_i := F(t_i)$

**Diffusion and decay**

$C14_i := FS_i \cdot C14_curies \cdot C14_DF_i$

$C14_{300} = 9.886 \cdot 10^6 \cdot sec^{-1}$

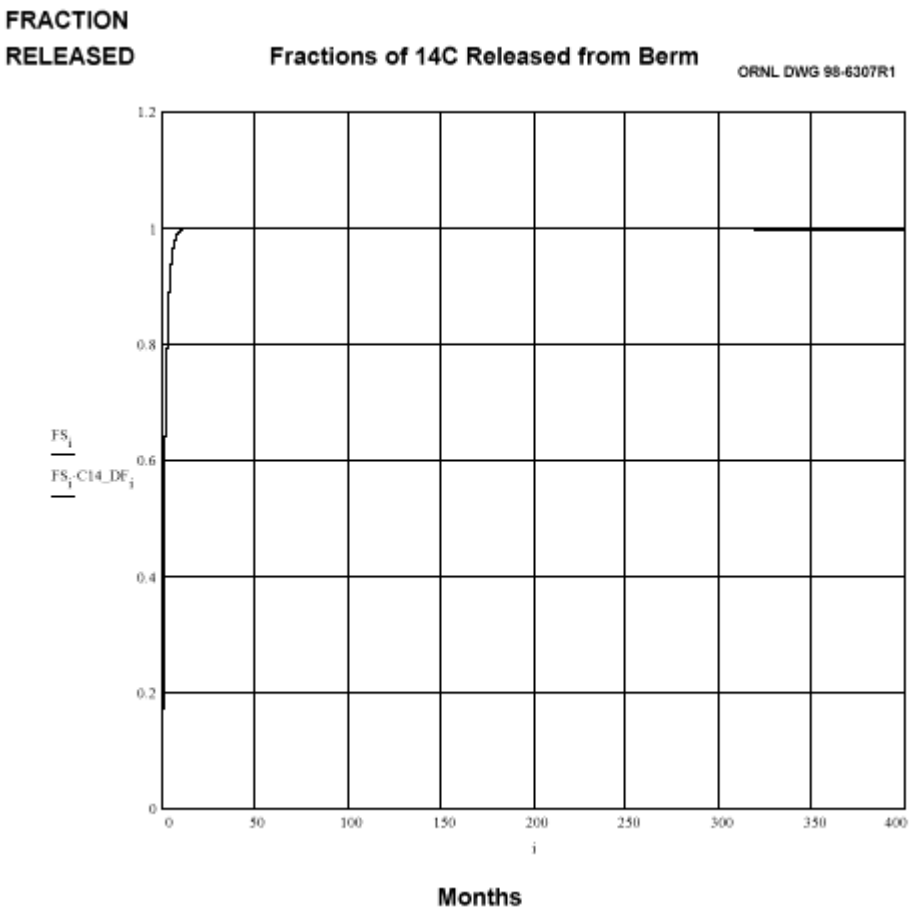


**Fig. B.2. Fractions of $^{14}C$ released from berm.**

$Total_Flow_i := Site_flow \cdot t_i$ $Pore_Flow_i := Recharge_volume \cdot t_i$

$C14_curies = 2.68 \cdot 10^{-4}\ \cdot Ci$ $Recharge_volume = 5.211 \cdot 10^{3}\ \cdot m^{3}\ \cdot y^{-1}$

$Site_flow = 1.084 \cdot 10^{4}\ \cdot m^{3}\ \cdot y^{-1}$ $Pore_C14_i := \frac{C14_i}{Pore_Flow_i} \cdot \frac{cc}{microCi}$

**Table of Results:**

| $t_i$ / month | $FS_i$ | $C14_i \cdot Ci^{-1}$ | $Pore_Flow_i$ | $(Pore_C14)_i$ |
|---|---|---|---|---|
| 0 | 0 | 0 | $0 \cdot m^3$ | 0 |
| 1 | $5.818 \cdot 10^{-1}$ | $1.559 \cdot 10^{-4}$ | $427.968 \cdot m^3$ | $3.643 \cdot 10^{-7}$ |
| 2 | $7.559 \cdot 10^{-1}$ | $2.026 \cdot 10^{-4}$ | $855.935 \cdot m^3$ | $2.367 \cdot 10^{-7}$ |
| 3 | $8.552 \cdot 10^{-1}$ | $2.292 \cdot 10^{-4}$ | $1.284 \cdot 10^{3} \cdot m^3$ | $1.785 \cdot 10^{-7}$ |
| 4 | $9.139 \cdot 10^{-1}$ | $2.449 \cdot 10^{-4}$ | $1.712 \cdot 10^{3} \cdot m^3$ | $1.431 \cdot 10^{-7}$ |
| 5 | $9.488 \cdot 10^{-1}$ | $2.543 \cdot 10^{-4}$ | $2.14 \cdot 10^{3} \cdot m^3$ | $1.188 \cdot 10^{-7}$ |
| 6 | $9.696 \cdot 10^{-1}$ | $2.598 \cdot 10^{-4}$ | $2.568 \cdot 10^{3} \cdot m^3$ | $1.012 \cdot 10^{-7}$ |
| 7 | $9.819 \cdot 10^{-1}$ | $2.631 \cdot 10^{-4}$ | $2.996 \cdot 10^{3} \cdot m^3$ | $8.783 \cdot 10^{-8}$ |
| 8 | $9.892 \cdot 10^{-1}$ | $2.651 \cdot 10^{-4}$ | $3.424 \cdot 10^{3} \cdot m^3$ | $7.743 \cdot 10^{-8}$ |
| 9 | $9.936 \cdot 10^{-1}$ | $2.663 \cdot 10^{-4}$ | $3.852 \cdot 10^{3} \cdot m^3$ | $6.913 \cdot 10^{-8}$ |
| 1·10 | $9.962 \cdot 10^{-1}$ | $2.67 \cdot 10^{-4}$ | $4.28 \cdot 10^{3} \cdot m^3$ | $6.238 \cdot 10^{-8}$ |
| 1.1·10 | $9.977 \cdot 10^{-1}$ | $2.674 \cdot 10^{-4}$ | $4.708 \cdot 10^{3} \cdot m^3$ | $5.679 \cdot 10^{-8}$ |
| 1.2·10 | $9.987 \cdot 10^{-1}$ | $2.676 \cdot 10^{-4}$ | $5.136 \cdot 10^{3} \cdot m^3$ | $5.211 \cdot 10^{-8}$ |
| 1.3·10 | $9.992 \cdot 10^{-1}$ | $2.678 \cdot 10^{-4}$ | $5.564 \cdot 10^{3} \cdot m^3$ | $4.813 \cdot 10^{-8}$ |
| 1.4·10 | $9.995 \cdot 10^{-1}$ | $2.678 \cdot 10^{-4}$ | $5.992 \cdot 10^{3} \cdot m^3$ | $4.47 \cdot 10^{-8}$ |
| 1.5·10 | $9.997 \cdot 10^{-1}$ | $2.679 \cdot 10^{-4}$ | $6.42 \cdot 10^{3} \cdot m^3$ | $4.173 \cdot 10^{-8}$ |
| 1.6·10 | $9.998 \cdot 10^{-1}$ | $2.679 \cdot 10^{-4}$ | $6.847 \cdot 10^{3} \cdot m^3$ | $3.913 \cdot 10^{-8}$ |
| 1.7·10 | $9.999 \cdot 10^{-1}$ | $2.679 \cdot 10^{-4}$ | $7.275 \cdot 10^{3} \cdot m^3$ | $3.683 \cdot 10^{-8}$ |
| 1.8·10 | $9.999 \cdot 10^{-1}$ | $2.679 \cdot 10^{-4}$ | $7.703 \cdot 10^{3} \cdot m^3$ | $3.478 \cdot 10^{-8}$ |
| 1.9·10 | 1 | $2.679 \cdot 10^{-4}$ | $8.131 \cdot 10^{3} \cdot m^3$ | $3.295 \cdot 10^{-8}$ |
| 2·10 | 1 | $2.679 \cdot 10^{-4}$ | $8.559 \cdot 10^{3} \cdot m^3$ | $3.13 \cdot 10^{-8}$ |
| 2.1·10 | 1 | $2.679 \cdot 10^{-4}$ | $8.987 \cdot 10^{3} \cdot m^3$ | $2.981 \cdot 10^{-8}$ |
| 2.2·10 | 1 | $2.679 \cdot 10^{-4}$ | $9.415 \cdot 10^{3} \cdot m^3$ | $2.846 \cdot 10^{-8}$ |
| 2.3·10 | 1 | $2.679 \cdot 10^{-4}$ | $9.843 \cdot 10^{3} \cdot m^3$ | $2.722 \cdot 10^{-8}$ |
| 2.4·10 | 1 | $2.679 \cdot 10^{-4}$ | $1.027 \cdot 10^{4} \cdot m^3$ | $2.609 \cdot 10^{-8}$ |
| 2.5·10 | 1 | $2.679 \cdot 10^{-4}$ | $1.07 \cdot 10^{4} \cdot m^3$ | $2.504 \cdot 10^{-8}$ |
| 2.6·10 | 1 | $2.679 \cdot 10^{-4}$ | $1.113 \cdot 10^{4} \cdot m^3$ | $2.408 \cdot 10^{-8}$ |
| 2.7·10 | 1 | $2.679 \cdot 10^{-4}$ | $1.156 \cdot 10^{4} \cdot m^3$ | $2.319 \cdot 10^{-8}$ |
| 2.8·10 | 1 | $2.679 \cdot 10^{-4}$ | | |
| 2.9·10 | 1 | $2.679 \cdot 10^{-4}$ | | |
| 3·10 | 1 | $2.679 \cdot 10^{-4}$ | | |
| 3.1·10 | 1 | $2.679 \cdot 10^{-4}$ | | |
| 3.2·10 | 1 | $2.679 \cdot 10^{-4}$ | | |
| 3.3·10 | 1 | $2.679 \cdot 10^{-4}$ | | |

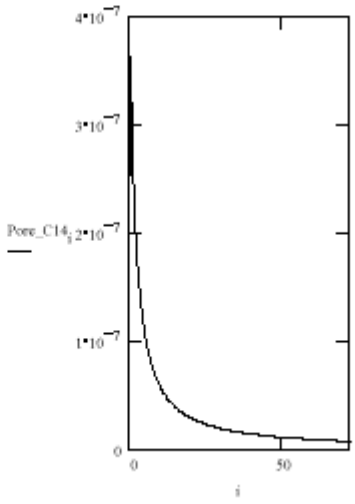


$Pore_C14_{196} = 3.189 \cdot 10^{-9}$

| | | | | |
|---|---|---|---|---|
| 3.4·10 | 1 | $2.679 \cdot 10^{-4}$ | $1.198 \cdot 10^{4} \cdot m^{3}$ | $2.236 \cdot 10^{-8}$ |
| 3.5·10 | 1 | $2.679 \cdot 10^{-4}$ | $1.241 \cdot 10^{4} \cdot m^{3}$ | $2.159 \cdot 10^{-8}$ |
| 3.6·10 | 1 | $2.679 \cdot 10^{-4}$ | $1.284 \cdot 10^{4} \cdot m^{3}$ | $2.087 \cdot 10^{-8}$ |
| 3.7·10 | 1 | $2.679 \cdot 10^{-4}$ | $1.327 \cdot 10^{4} \cdot m^{3}$ | $2.019 \cdot 10^{-8}$ |
| 3.8·10 | 1 | $2.679 \cdot 10^{-4}$ | $1.369 \cdot 10^{4} \cdot m^{3}$ | $1.956 \cdot 10^{-8}$ |
| 3.9·10 | 1 | $2.679 \cdot 10^{-4}$ | $1.412 \cdot 10^{4} \cdot m^{3}$ | $1.897 \cdot 10^{-8}$ |
| 4·10 | 1 | $2.679 \cdot 10^{-4}$ | $1.455 \cdot 10^{4} \cdot m^{3}$ | $1.841 \cdot 10^{-8}$ |
| 4.1·10 | 1 | $2.679 \cdot 10^{-4}$ | $1.498 \cdot 10^{4} \cdot m^{3}$ | $1.789 \cdot 10^{-8}$ |
| 4.2·10 | 1 | $2.679 \cdot 10^{-4}$ | $1.541 \cdot 10^{4} \cdot m^{3}$ | $1.739 \cdot 10^{-8}$ |
| 4.3·10 | 1 | $2.679 \cdot 10^{-4}$ | $1.583 \cdot 10^{4} \cdot m^{3}$ | $1.692 \cdot 10^{-8}$ |
| 4.4·10 | 1 | $2.679 \cdot 10^{-4}$ | $1.626 \cdot 10^{4} \cdot m^{3}$ | $1.647 \cdot 10^{-8}$ |
| 4.5·10 | 1 | $2.679 \cdot 10^{-4}$ | $1.669 \cdot 10^{4} \cdot m^{3}$ | $1.605 \cdot 10^{-8}$ |
| 4.6·10 | 1 | $2.679 \cdot 10^{-4}$ | $1.712 \cdot 10^{4} \cdot m^{3}$ | $1.565 \cdot 10^{-8}$ |
| 4.7·10 | 1 | $2.679 \cdot 10^{-4}$ | $1.755 \cdot 10^{4} \cdot m^{3}$ | $1.527 \cdot 10^{-8}$ |
| 4.8·10 | 1 | $2.679 \cdot 10^{-4}$ | $1.797 \cdot 10^{4} \cdot m^{3}$ | $1.49 \cdot 10^{-8}$ |
| 4.9·10 | 1 | $2.679 \cdot 10^{-4}$ | $1.84 \cdot 10^{4} \cdot m^{3}$ | $1.456 \cdot 10^{-8}$ |
| | 1 | $2.679 \cdot 10^{-4}$ | $1.883 \cdot 10^{4} \cdot m^{3}$ | $1.423 \cdot 10^{-8}$ |
| | 1 | $2.679 \cdot 10^{-4}$ | $1.926 \cdot 10^{4} \cdot m^{3}$ | $1.391 \cdot 10^{-8}$ |
| | 1 | $2.679 \cdot 10^{-4}$ | $1.969 \cdot 10^{4} \cdot m^{3}$ | $1.361 \cdot 10^{-8}$ |
| | 1 | $2.679 \cdot 10^{-4}$ | $2.011 \cdot 10^{4} \cdot m^{3}$ | $1.332 \cdot 10^{-8}$ |
| | 1 | $2.679 \cdot 10^{-4}$ | $2.054 \cdot 10^{4} \cdot m^{3}$ | $1.304 \cdot 10^{-8}$ |
| | 1 | $2.679 \cdot 10^{-4}$ | $2.097 \cdot 10^{4} \cdot m^{3}$ | $1.277 \cdot 10^{-8}$ |

**Fig. B.3. National Drinking Water Standards for $^{14}C$ = 3.00E-5 μCi/cm$^2$.**

**Incremental C14 Production and Diffusion**

**Fractional Linear C14 production over 30 years of operations**

$FG1(t) := \frac{1}{360}$ $FG2(t) := 0$

$Fg(t) := if(t \le 359 \cdot month, FG1(t), FG2(t))$

$Fg_j := Fg\left(t_j\right)$ $\sum_{i=0}^{360} Fg_i = 1$

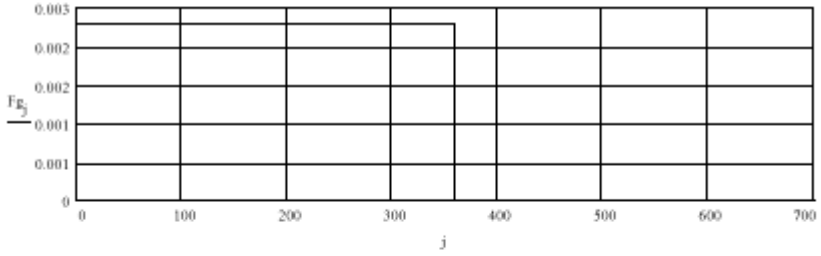


**Monthly Incremental Fractional Release**

$i := 0, 1 .. 724$

$delta_FS_i := \left|FS_{i+1} - FS_i\right|$ $\sum_{m=0}^{720} Fg_m = 1$ $\sum_{n=0}^{720} delta_FS_n = 1$

$Total_F := \sum_{j=0}^{360} \sum_{k=0}^{360} delta_FS_k \cdot Fg_j$

$Total_F = 1$

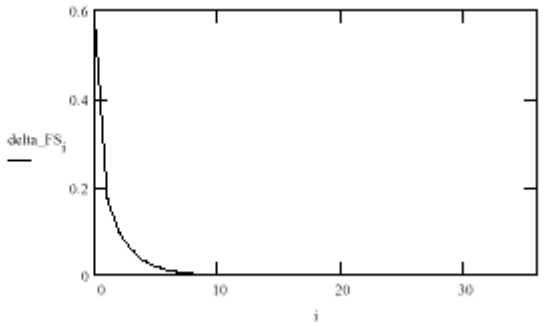

**Silmutaneous Production and Diffusion Calculations**

**month 1**

$FT_1 := Fg_1 \cdot delta_FS_1$

**month 2**

$FT_2 := Fg_1 \cdot delta_FS_2 + Fg_2 \cdot delta_FS_1$

**month 3**

$FT_3 := Fg_1 \cdot delta_FS_3 + Fg_2 \cdot delta_FS_2 + Fg_3 \cdot delta_FS_1$

**month 4**

$FT_4 := Fg_4 \cdot delta_FS_1 + Fg_3 \cdot delta_FS_2 + Fg_2 \cdot delta_FS_3 + Fg_1 \cdot delta_FS_4$

**Monthly Recursion Formula for Total Incremental Fractional Release**

$k := 1, 2 .. 724$

$$FT_{k+4} := \sum_{n=1}^{k} Fg_n \cdot delta_FS_{k-n}$$

$$\sum_{n=1}^{724} FT_n = 1$$

**Sample results:**

| | | | |
|---|---|---|---|
| $FT_1 = 4.837 \cdot 10^{-4}$ | $FT_2 = 7.594 \cdot 10^{-4}$ | $FT_{30} = 2.778 \cdot 10^{-3}$ | $FT_{100} = 2.778 \cdot 10^{-3}$ |
| $FT_3 = 9.226 \cdot 10^{-4}$ | $FT_4 = 0.001$ | $FT_{196} = 2.778 \cdot 10^{-3}$ | $FT_{300} = 2.778 \cdot 10^{-3}$ |
| $FT_5 = 0.002$ | $FT_{10} = 0.003$ | $FT_{360} = 2.778 \cdot 10^{-3}$ | $FT_{400} = 8.645 \cdot 10^{-12}$ |

**Incremental Fraction of Production in and Diffusion from Berm**

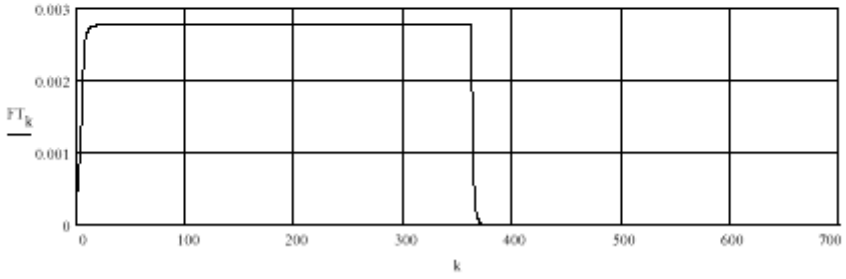

**Silmutaneous Production, Diffusion, and Decay Calculations**

**month 1**

$FT_DF_1 := Fg_1 \cdot delta_FS_1$

**month 2**

$FT_DF_2 := Fg_1 \cdot delta_FS_2 \cdot C14_DF_1 + Fg_2 \cdot delta_FS_1$

**month 3**

$FT_DF_3 := Fg_1 \cdot delta_FS_3 \cdot C14_DF_2 + Fg_2 \cdot delta_FS_2 \cdot C14_DF_1 + Fg_3 \cdot delta_FS_1$

**month 4**

$FT_DF_4 := Fg_4 \cdot delta_FS_1 \cdot C14_DF_3 + Fg_3 \cdot delta_FS_2 \cdot C14_DF_2 + Fg_2 \cdot delta_FS_3 \cdot C14_DF_1 + Fg_1 \cdot delta_FS_4$

**Monthly Recursion Formula for Total Incremental Fractional Release**

$$FT_DF_{k+4} := \sum_{n=1}^{k} Fg_n \cdot delta_FS_{k-n} \cdot C14_DF_{n-1} \qquad \sum_{n=1}^{724} FT_DF_n = 0.999$$

**Sample results:**

$FT_DF_1 = 4.837 \cdot 10^{-4}$ $FT_DF_2 = 7.594 \cdot 10^{-4}$ $FT_DF_{30} = 2.777 \cdot 10^{-3}$ $FT_DF_{100} = 2.775 \cdot 10^{-3}$

$FT_DF_3 = 9.226 \cdot 10^{-4}$ $FT_DF_4 = 0.001$ $FT_DF_{196} = 2.773 \cdot 10^{-3}$ $FT_DF_{300} = 2.77 \cdot 10^{-3}$

$FT_DF_5 = 0.002$ $FT_DF_{10} = 0.003$ $FT_DF_{360} = 2.768 \cdot 10^{-3}$ $FT_DF_{400} = 8.615 \cdot 10^{-12}$

**Incremental Fraction of Production in and Diffusion from Berm with Decay**

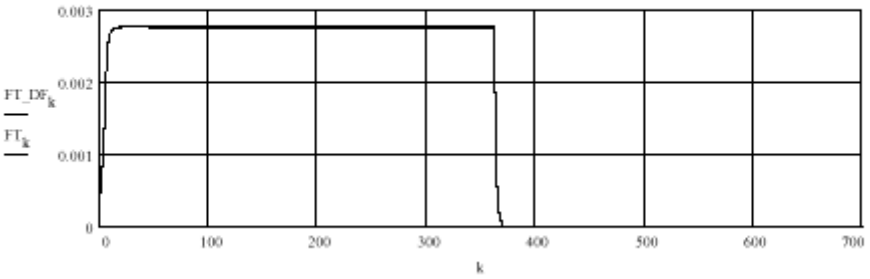

$TC14_k := FT_DF_k \cdot C14_curies$

$C14_curies = 2.68 \cdot 10^{-4} \cdot Ci$

$Recharge_volume = 427.968 \cdot m^3 \cdot month^{-1}$

$TPore_C14_k := \frac{TC14_k}{Pore_Flow_k} \cdot microCi^{-1} \cdot cc$

| k | $FT_k$ | $TPore_C14_k$ |
|---|---|---|
| 1 | 0.00048 | $3.029 \cdot 10^{-10}$ |
| 2 | 0.00076 | $2.378 \cdot 10^{-10}$ |
| 3 | 0.00092 | $1.926 \cdot 10^{-10}$ |
| 4 | 0.00102 | $1.596 \cdot 10^{-10}$ |
| 5 | 0.00162 | $2.024 \cdot 10^{-10}$ |
| 6 | 0.0021 | $2.192 \cdot 10^{-10}$ |
| 7 | 0.00238 | $2.125 \cdot 10^{-10}$ |
| 8 | 0.00254 | $1.987 \cdot 10^{-10}$ |
| 9 | 0.00264 | $1.834 \cdot 10^{-10}$ |
| 10 | 0.00269 | $1.686 \cdot 10^{-10}$ |
| 11 | 0.00273 | $1.553 \cdot 10^{-10}$ |
| 12 | 0.00275 | $1.434 \cdot 10^{-10}$ |
| 13 | 0.00276 | $1.329 \cdot 10^{-10}$ |
| 14 | 0.00277 | $1.238 \cdot 10^{-10}$ |
| 15 | 0.00277 | $1.157 \cdot 10^{-10}$ |
| 16 | 0.00277 | $1.086 \cdot 10^{-10}$ |
| 17 | 0.00278 | $1.022 \cdot 10^{-10}$ |
| 18 | 0.00278 | $9.658 \cdot 10^{-11}$ |
| 19 | 0.00278 | $9.151 \cdot 10^{-11}$ |
| 20 | 0.00278 | $8.695 \cdot 10^{-11}$ |
| 21 | 0.00278 | $8.281 \cdot 10^{-11}$ |
| 22 | 0.00278 | $7.905 \cdot 10^{-11}$ |
| 23 | 0.00278 | $7.561 \cdot 10^{-11}$ |
| 24 | 0.00278 | $7.246 \cdot 10^{-11}$ |
| 25 | 0.00278 | $6.957 \cdot 10^{-11}$ |
| 26 | 0.00278 | $6.689 \cdot 10^{-11}$ |
| 27 | 0.00278 | $6.441 \cdot 10^{-11}$ |
| 28 | 0.00278 | $6.211 \cdot 10^{-11}$ |
| 29 | 0.00278 | $5.997 \cdot 10^{-11}$ |
| 30 | 0.00278 | $5.797 \cdot 10^{-11}$ |
| 31 | 0.00278 | |
| 32 | 0.00278 | |
| 33 | 0.00278 | |
| 34 | 0.00278 | |
| 35 | 0.00278 | |
| 36 | 0.00278 | |
| 37 | 0.00278 | |

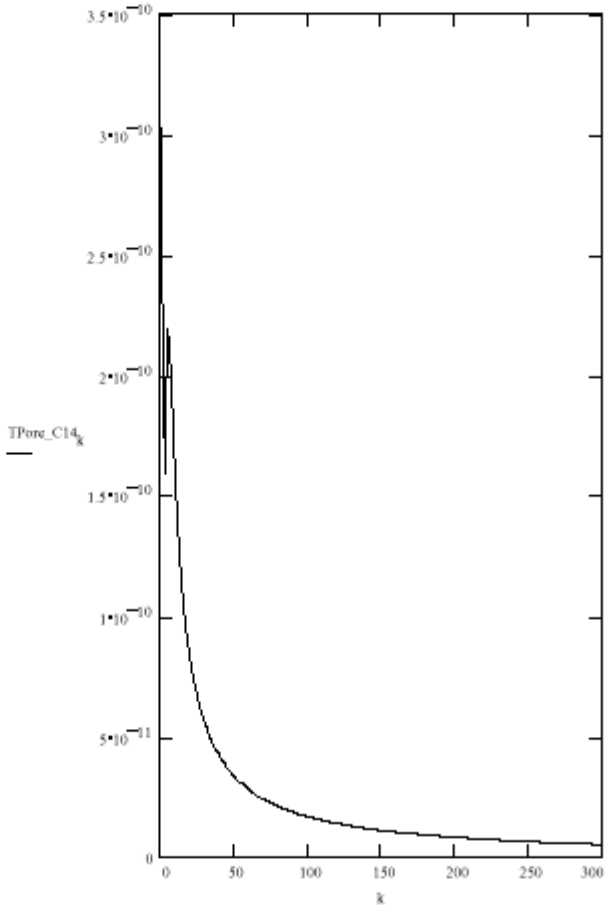


$TPore_C14_{196} = 8.858 \cdot 10^{-12}$

$Pore_C14_{196} = 3.189 \cdot 10^{-9}$

ORRC14R4.mcd

| | | |
|---|---|---|
| 38 | 0.00278 | $5.61 \cdot 10^{11}$ |
| 39 | 0.00278 | $5.434 \cdot 10^{11}$ |
| 40 | 0.00278 | $5.27 \cdot 10^{11}$ |
| 41 | 0.00278 | $5.115 \cdot 10^{11}$ |
| 42 | 0.00278 | $4.969 \cdot 10^{11}$ |
| 43 | 0.00278 | $4.83 \cdot 10^{11}$ |
| 44 | 0.00278 | $4.7 \cdot 10^{11}$ |
| 45 | 0.00278 | $4.576 \cdot 10^{11}$ |
| 46 | 0.00278 | $4.459 \cdot 10^{11}$ |
| 47 | 0.00278 | $4.347 \cdot 10^{11}$ |
| 48 | 0.00278 | $4.241 \cdot 10^{11}$ |
| 49 | 0.00278 | $4.14 \cdot 10^{11}$ |
| 50 | 0.00278 | $4.044 \cdot 10^{11}$ |
| | | $3.952 \cdot 10^{11}$ |
| | | $3.864 \cdot 10^{11}$ |
| | | $3.78 \cdot 10^{11}$ |
| | | $3.7 \cdot 10^{11}$ |
| | | $3.622 \cdot 10^{11}$ |
| | | $3.548 \cdot 10^{11}$ |
| | | $3.477 \cdot 10^{11}$ |

$$Case_Ratio := \frac{TPore_C14_{196}}{Pore_C14_{196}} \qquad Case_Ratio = 0.003$$

**Fig. B.4. National Drinking Water Standards for $^{14}C$ = 3.00E-5 μCi/cm$^3$.**

## Release Model for 22Na from the SNS Shield Berm

### Berm Parameters:

### SNS Tunnel Lengths:

Linac := 492·m

High_energy_transfer := 165·m

Ring := 221·m

Ring_transfer := 167·m

Tunnel_rad := 2.7572·m

Inner_soil_rad := 6.7572·m

Outer_zone_rad := 10.81·m

Tunnel_crossection := $\pi \cdot \text{Tunnel_rad}^2$

Inner_soil_crossection := $\pi \cdot \text{Inner_soil_rad}^2 - \text{Tunnel_crossection}$

Outer_soil_crossection := $\pi \cdot \text{Outer_zone_rad}^2 - \pi \cdot \text{Inner_soil_rad}^2$

Total_length := Linac + High_energy_transfer + Ring + Ring_transfer

Total_length = $1.045 \cdot 10^3 \cdot \text{m}$

Tunnel_crossection = $23.883 \cdot \text{m}^2$

Tunnel_volume := Tunnel_crossection·Total_length

Tunnel_volume = $2.496 \cdot 10^4 \cdot \text{m}^3$

Inner_soil_crossection = $119.561 \cdot \text{m}^2$

Inner_soil_volume := Inner_soil_crossection·Total_length

Inner_soil_volume = $1.249 \cdot 10^5 \cdot \text{m}^3$

Outer_soil_crossection = $223.67 \cdot \text{m}^2$

Outer_soil_volume := Outer_soil_crossection·Total_length

Outer_soil_volume = $2.337 \cdot 10^5 \cdot \text{m}^3$

### Berm Crossectional Dimenstions, Volume, and Surface Area:

Berm_thickness := Inner_soil_rad − Tunnel_rad

Berm_thickness = 4·m

Berm_radius := Berm_thickness + Tunnel_rad

Berm_crossection := $\pi \cdot \text{Berm_radius}^2 - \pi \cdot \text{Tunnel_rad}^2$

Berm_crossection = $119.561 \cdot \text{m}^2$

Berm_volume := Berm_crossection·Total_length

Berm_volume = $1.249 \cdot 10^5 \cdot \text{m}^3$

Berm_radius = 6.7572·m

Berm_surface_area := $2 \cdot \pi \cdot \text{Berm_radius} \cdot \text{Total_length} + 2 \cdot \pi \cdot \text{Berm_radius}^2$

Berm_surface_area = $4.465 \cdot 10^4 \cdot \text{m}^2$

$$\text{Berm_Surface_Volume_Ratio} := \frac{\text{Berm_surface_area}}{\text{Berm_volume}}$$

Berm_Surface_Volume_Ratio = $0.357 \cdot \text{m}^{-1}$

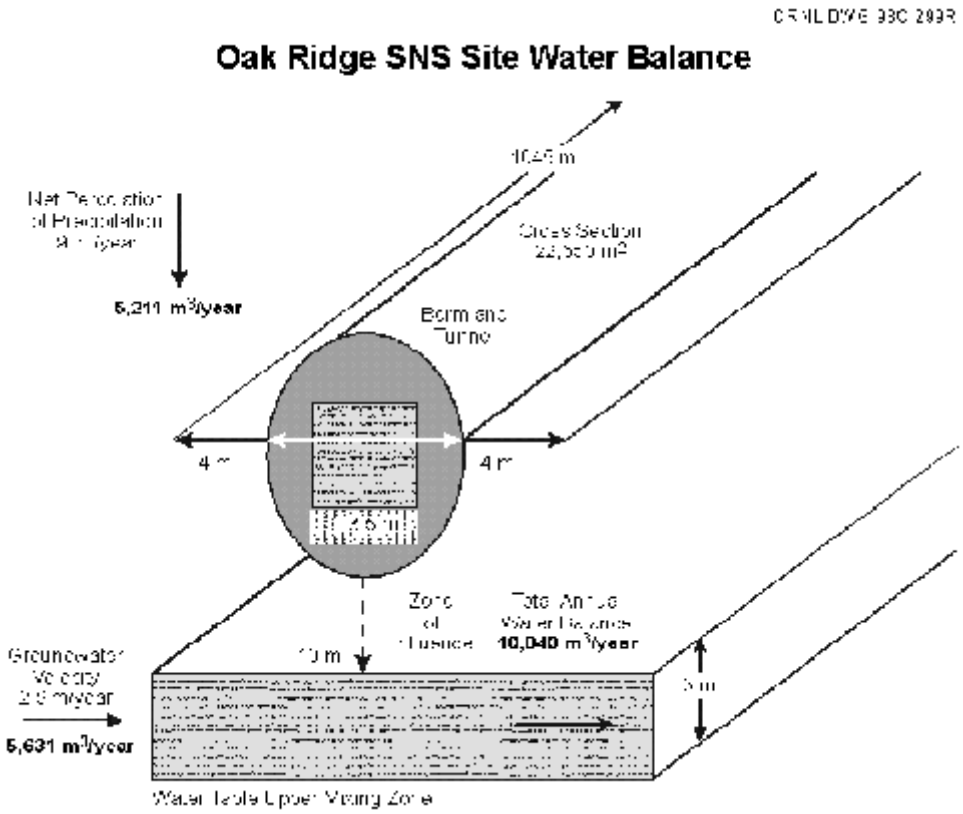


**Fig. B.5. Oak Ridge SNS site water balance.**

**Berm Hydrologic Cross section and Vadose Zone Hydrology:**

$Hydro_width := 2 \cdot Berm_radius + 2 \cdot 4 \cdot m$

$Hydro_length := Total_length + 2 \cdot 4 \cdot m$

$Hydro_crossection := Hydro_length \cdot Hydro_width$

$Hydro_crossection = 2.265 \cdot 10^{4}\ m^{2}$

$Recharge_volume = 5.211 \cdot 10^{3}\ m^{3} \cdot y^{-1}$

$Recharge_mass := Recharge_volume \cdot mass_volume$

$Down_particle_velocity := \frac{Recharge_rate}{Vadose_zone_porosity}$

$Down_travel_time := \frac{Depth_to_water_table}{Down_particle_velocity}$

$Recharge_rate := 9.055 \cdot \frac{in}{y}$

$Recharge_rate = 0.23 \cdot m \cdot y^{-1}$

$Vadose_zone_porosity := 0.37$

$Recharge_volume := Hydro_crossection \cdot Recharge_rate$

$mass_volume := 1000 \cdot \frac{kg}{m^{3}}$

$Recharge_mass = 5.211 \cdot 10^{6}\ kg \cdot y^{-1}$

$Down_particle_velocity = 0.622 \cdot m \cdot y^{-1}$

$Depth_to_water_table := 10 \cdot m$

$Down_travel_time = 16.087 \cdot y$

$Down_travel_time = 195.861 \cdot month$

## Saturated Zone Hydrology

$Hydraulic_conductivity := 0.244 \cdot \frac{m}{d}$

$Hydraulic_gradient := 0.02$

$Groundwater_speed := Hydraulic_conductivity \cdot Hydraulic_gradient$

$Groundwater_speed = 1.782 \cdot m \cdot y^{-1}$

$Groundwater_mix_depth := 3 \cdot m$

$Groundwater_volume := Groundwater_speed \cdot Groundwater_mix_depth \cdot Hydro_length$

$Groundwater_mass := Groundwater_volume \cdot mass_volume$

$Groundwater_volume = 5.631 \cdot 10^{3}\ m^{3} \cdot y^{-1}$

$Groundwater_mass = 5.631 \cdot 10^{6}\ kg \cdot y^{-1}$

$Hydraulic_conductivity = 89.121 \cdot m \cdot y^{-1}$

$Saturated_zone_porosity := 0.37$

$Groundwater_velocity := \frac{Groundwater_speed}{Saturated_zone_porosity}$

$Groundwater_velocity = 4.817 \cdot m \cdot y^{-1}$

$Recharge_volume = 5.211 \cdot 10^{3}\ m^{3} \cdot y^{-1}$

$Recharge_mass = 5.211 \cdot 10^{6}\ kg \cdot y^{-1}$

## Combined Recharge and Saturated Flow

$Site_flow := Groundwater_volume + Recharge_volume$

$Site_flow = 1.084 \cdot 10^{4} \cdot m^{3} \cdot y^{-1}$

$Site_flow_Mass := Site_flow \cdot mass_volume$

$Site_flow_Mass = 1.084 \cdot 10^{7} \cdot kg \cdot y^{-1}$

$Recharge_ratio := \frac{Recharge_volume}{Groundwater_volume}$

$Recharge_ratio = 0.925$

$Percent_Recharge := 100 \cdot \frac{Recharge_volume}{Site_flow}$

$Percent_Recharge = 48.062$

## Berm Mass and concentrations:

$\rho_{Berm} := 1.61 \cdot \frac{g}{cc}$

$Berm_volume = 1.249 \cdot 10^{5} \cdot m^{3}$

$Berm_mass := Berm_volume \cdot \rho_{Berm}$

$Berm_mass = 2.012 \cdot 10^{11} \cdot kg$

$Na22_curies := 2.30 \cdot 10^{-2} \cdot Ci$

$Na22_concentration := \frac{Na22_curies}{Berm_mass}$

$Na22_concentration = 1.143 \cdot 10^{-13} \cdot \frac{Ci}{g}$

$Na22_concentration \cdot \rho_{Berm} = 1.841 \cdot 10^{-7} \cdot \frac{microCi}{cc}$

$Na22_concentration = 1.143 \cdot 10^{-7} \cdot \frac{microCi}{g}$

$Na22_concentration = 1.143 \cdot 10^{-4} \cdot \frac{nanoCi}{g}$

## 22Na Radioactivity and mass:

$Na22_SpecAct := 136561 \cdot \frac{Ci}{g_atom}$

$Na22_Atomic_wgt := 21.994437 \cdot g$

$Na22_g_atom := \frac{Na22_curies}{Na22_SpecAct}$

$Na22_g_atom = 1.684 \cdot 10^{-7} \cdot g_atom$

$Na22_mass := Na22_Atomic_wgt \cdot Na22_g_atom$

$Na22_mass_concentration := \frac{Na22_mass}{Berm_mass}$

$Na22_mass = 3.704 \cdot 10^{-6} \cdot g$

$Na22_mass_concentration \cdot ppb = 1.842 \cdot 10^{-8}$

$Na22_mass_concentration \cdot ppt = 1.842 \cdot 10^{-5}$

**Diffusion Calculations**:

**Effective diffusion Coefficient:**

$$De := \left(1.58 \cdot 10^{-7}\right) \cdot \frac{cm^2}{s}$$

**Surface to Volume:**

$Berm_surface_area = 4.465 \cdot 10^{4} \cdot m^2$ $Berm_volume = 1.249 \cdot 10^{5} \cdot m^3$

$$Berm_surface_volume_ratio := \frac{Berm_surface_area}{Berm_volume}$$

$S := Berm_surface_area$ $V := Berm_volume$

$\frac{S}{V} = 0.357 \cdot cm^{-1}$ $a := Berm_radius$ $a = 6.757 \cdot m$ $L := \frac{Total_length}{2}$ $L = 522.5 \cdot m$

**Semi-infinite Slab:**

$$F(t) := 2 \cdot \frac{S}{V} \cdot \sqrt{De \cdot t \cdot \frac{s}{\pi}}$$ $$T2 := \left(0.2 \cdot \frac{V}{S \cdot 2}\right)^2 \cdot \left(\frac{\pi}{De}\right)$$ $T2 = 0.049 \cdot y$

$$t2 := \left(0.2 \cdot \frac{V}{S \cdot 2}\right)^2 \cdot \left(\frac{\pi}{De \cdot s}\right)$$

**Geometry Specific Analytical Solution:**

$m := 3, 6 .. 30$ $n := 1 .. 60$

$i := 0, 1 .. 725$ $t_i := i \cdot month$

$j := 0, 1 .. 725$ $t_j := j \cdot month$

$$F(t) := 2 \cdot \frac{S}{V} \cdot \sqrt{\frac{De \cdot t}{\pi}} \qquad t2 := \left(0.2 \cdot \frac{V}{S \cdot 2}\right)^2 \cdot \left(\frac{\pi}{De}\right) \qquad t2 = 0.049 \cdot y$$

$t2 = 0.601 \cdot month$

$$\alpha_m := \frac{root(J0(m), m)}{a}$$

| $\alpha_m$ |
|---|
| $0.356 \cdot m^{-1}$ |
| $0.817 \cdot m^{-1}$ |
| $1.281 \cdot m^{-1}$ |
| $1.745 \cdot m^{-1}$ |
| $2.21 \cdot m^{-1}$ |
| $2.674 \cdot m^{-1}$ |
| $3.139 \cdot m^{-1}$ |
| $3.604 \cdot m^{-1}$ |
| $4.069 \cdot m^{-1}$ |
| $4.534 \cdot m^{-1}$ |

$$FC(t) := 1 - \frac{32}{\pi^2 \cdot a^2} \cdot \sum_n \sum_m \frac{e^{-\left[De \cdot \left[\left(\alpha_m\right)^2 + (2 \cdot n - 1)^2 \cdot \frac{\pi^2}{4 \cdot L^2}\right] \cdot t\right]}}{(2 \cdot n - 1)^2 \cdot \left(\alpha_m\right)^2}$$

$FC(t2) = 0.163$

**Geometry specific release faction**

$FS(t) := if(t > t2, FC(t), F(t))$

**Decay half-life factor**

$Na22_\lambda := 2.62 \cdot y$ $Na22_DF_i := e^{-\left(\ln(2) \cdot \frac{t_i}{Na22_\lambda}\right)}$

**Calculate arrays**

$FS_i := FS\left(t_i\right)$ $F_i := F\left(t_i\right)$

**Diffusion and decay**

$Na22_i := FS_i \cdot Na22_curies \cdot Na22_DF_i$

$Na22_{196} = 325.118 \cdot microCi$

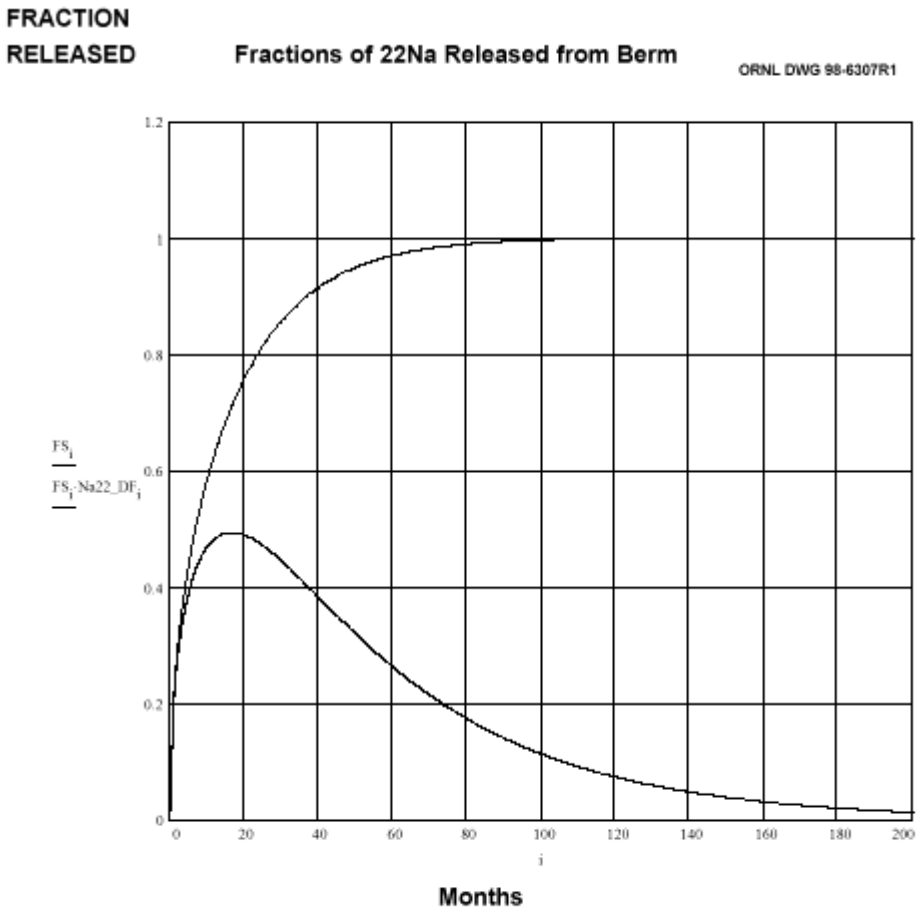


**Fig. B.6. Fractions of $^{22}$Na released from berm.**

$Total_Flow_i := Site_flow \cdot t_i$ $Pore_Flow_i := Recharge_volume \cdot t_i$

$Na22_curies = 0.023 \cdot Ci$ $Recharge_volume = 5.211 \cdot 10^3 \cdot m^3 \cdot y^{-1}$

$Site_flow = 1.084 \cdot 10^4 \cdot m^3 \cdot y^{-1}$ $Pore_Na22_i := \frac{Na22_i}{Pore_Flow_i} \cdot \frac{cc}{microCi}$

**Table of Results:**

| $t_i$ / month | $FS_i$ | $Pore_Na22_i$ |
|---|---|---|
| 0 | 0 | 0 |
| 1 | $2.074 \cdot 10^{-1}$ | $1.091 \cdot 10^{-5}$ |
| 2 | $2.865 \cdot 10^{-1}$ | $7.371 \cdot 10^{-6}$ |
| 3 | $3.449 \cdot 10^{-1}$ | $5.789 \cdot 10^{-6}$ |
| 4 | $3.926 \cdot 10^{-1}$ | $4.836 \cdot 10^{-6}$ |
| 5 | $4.334 \cdot 10^{-1}$ | $4.179 \cdot 10^{-6}$ |
| 6 | $4.692 \cdot 10^{-1}$ | $3.689 \cdot 10^{-6}$ |
| 7 | $5.014 \cdot 10^{-1}$ | $3.306 \cdot 10^{-6}$ |
| 8 | $5.305 \cdot 10^{-1}$ | $2.995 \cdot 10^{-6}$ |
| 9 | $5.572 \cdot 10^{-1}$ | $2.736 \cdot 10^{-6}$ |
| 1·10 | $5.818 \cdot 10^{-1}$ | $2.516 \cdot 10^{-6}$ |
| 1.1·10 | $6.046 \cdot 10^{-1}$ | $2.326 \cdot 10^{-6}$ |
| 1.2·10 | $6.259 \cdot 10^{-1}$ | $2.16 \cdot 10^{-6}$ |
| 1.3·10 | $6.458 \cdot 10^{-1}$ | $2.013 \cdot 10^{-6}$ |
| 1.4·10 | $6.644 \cdot 10^{-1}$ | $1.882 \cdot 10^{-6}$ |
| 1.5·10 | $6.82 \cdot 10^{-1}$ | $1.764 \cdot 10^{-6}$ |
| 1.6·10 | $6.985 \cdot 10^{-1}$ | $1.657 \cdot 10^{-6}$ |
| 1.7·10 | $7.141 \cdot 10^{-1}$ | $1.56 \cdot 10^{-6}$ |
| 1.8·10 | $7.288 \cdot 10^{-1}$ | $1.472 \cdot 10^{-6}$ |
| 1.9·10 | $7.428 \cdot 10^{-1}$ | $1.39 \cdot 10^{-6}$ |
| 2·10 | $7.559 \cdot 10^{-1}$ | $1.315 \cdot 10^{-6}$ |
| 2.1·10 | $7.684 \cdot 10^{-1}$ | $1.246 \cdot 10^{-6}$ |
| 2.2·10 | $7.802 \cdot 10^{-1}$ | $1.182 \cdot 10^{-6}$ |
| 2.3·10 | $7.914 \cdot 10^{-1}$ | $1.122 \cdot 10^{-6}$ |
| 2.4·10 | $8.02 \cdot 10^{-1}$ | $1.066 \cdot 10^{-6}$ |
| 2.5·10 | $8.121 \cdot 10^{-1}$ | $1.014 \cdot 10^{-6}$ |
| 2.6·10 | $8.216 \cdot 10^{-1}$ | $9.653 \cdot 10^{-7}$ |
| 2.7·10 | $8.307 \cdot 10^{-1}$ | $9.196 \cdot 10^{-7}$ |
| 2.8·10 | | |

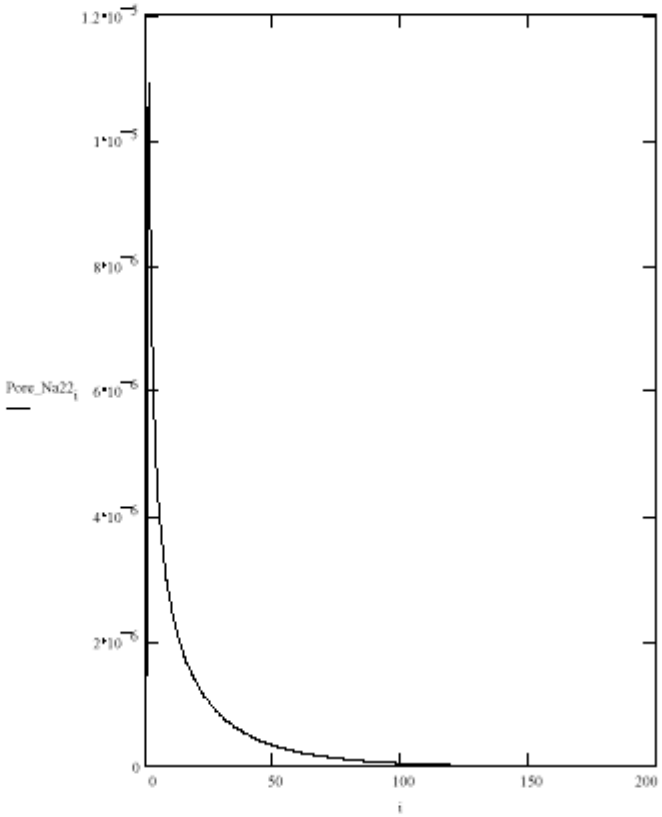


$Pore_Na22_{196} = 3.876 \cdot 10^{-9}$

ORRNa22R4.mcd

| | | |
|---|---|---|
| 3.4·10 | $8.393 \cdot 10^{-1}$ | $8.767 \cdot 10^{-7}$ |
| 3.5·10 | $8.474 \cdot 10^{-1}$ | $8.363 \cdot 10^{-7}$ |
| 3.6·10 | $8.552 \cdot 10^{-1}$ | $7.983 \cdot 10^{-7}$ |
| 3.7·10 | $8.625 \cdot 10^{-1}$ | $7.624 \cdot 10^{-7}$ |
| 3.8·10 | $8.695 \cdot 10^{-1}$ | $7.285 \cdot 10^{-7}$ |
| 3.9·10 | $8.761 \cdot 10^{-1}$ | $6.965 \cdot 10^{-7}$ |
| 4·10 | $8.824 \cdot 10^{-1}$ | $6.662 \cdot 10^{-7}$ |
| 4.1·10 | $8.883 \cdot 10^{-1}$ | $6.376 \cdot 10^{-7}$ |
| 4.2·10 | $8.94 \cdot 10^{-1}$ | $6.104 \cdot 10^{-7}$ |
| 4.3·10 | $8.994 \cdot 10^{-1}$ | $5.846 \cdot 10^{-7}$ |
| 4.4·10 | $9.045 \cdot 10^{-1}$ | $5.602 \cdot 10^{-7}$ |
| 4.5·10 | $9.093 \cdot 10^{-1}$ | $5.369 \cdot 10^{-7}$ |
| 4.6·10 | $9.139 \cdot 10^{-1}$ | $5.148 \cdot 10^{-7}$ |
| 4.7·10 | $9.183 \cdot 10^{-1}$ | $4.938 \cdot 10^{-7}$ |
| 4.8·10 | $9.224 \cdot 10^{-1}$ | $4.738 \cdot 10^{-7}$ |
| 4.9·10 | $9.263 \cdot 10^{-1}$ | $4.548 \cdot 10^{-7}$ |
| | $9.301 \cdot 10^{-1}$ | $4.367 \cdot 10^{-7}$ |
| | $9.336 \cdot 10^{-1}$ | $4.194 \cdot 10^{-7}$ |
| | $9.37 \cdot 10^{-1}$ | $4.029 \cdot 10^{-7}$ |
| | $9.402 \cdot 10^{-1}$ | $3.871 \cdot 10^{-7}$ |
| | $9.432 \cdot 10^{-1}$ | $3.721 \cdot 10^{-7}$ |
| | $9.461 \cdot 10^{-1}$ | $3.578 \cdot 10^{-7}$ |

**Incremental Na22 Production and Diffusion**

**Fractional Linear Na22 production over 30 years of operations**

$FG1(t) := \frac{1}{360}$ $\quad FG2(t) := 0$

$Fg(t) := if(t \le 359 \cdot month, FG1(t), FG2(t))$

$Fg_j := Fg\left(\frac{1}{j}\right)$ $\quad \sum_{l=0}^{360} Fg_l = 1$

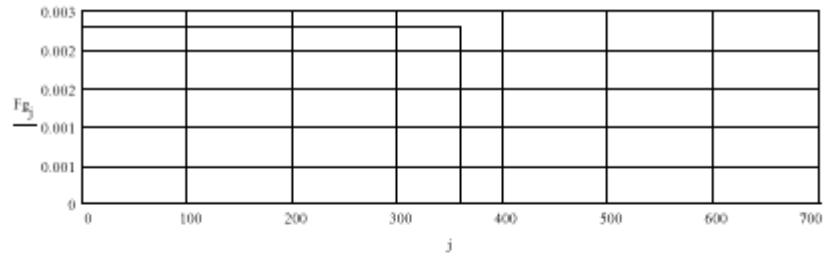


**Monthly Incremental Fractional Release**

$i := 0, 1 .. 724$

$delta_FS_i := \left| FS_{i+1} - FS_i \right|$

$\sum_{m=0}^{720} Fg_m = 1$ $\quad \sum_{n=0}^{720} delta_FS_n = 1$

$Total_F := \sum_{j=0}^{640} \sum_{k=0}^{640} delta_FS_k \cdot Fg_j$

$Total_F = 1$

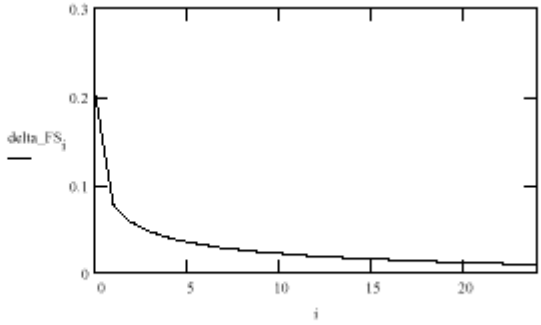

**Silmutaneous Production and Diffusion Calculations**

**month 1**

$FT_1 := Fg_1 \cdot delta_FS_1$

**month 2**

$FT_2 := Fg_1 \cdot delta_FS_2 + Fg_2 \cdot delta_FS_1$

**month 3**

$FT_3 := Fg_1 \cdot delta_FS_3 + Fg_2 \cdot delta_FS_2 + Fg_3 \cdot delta_FS_1$

**month 4**

$FT_4 := Fg_4 \cdot delta_FS_1 + Fg_3 \cdot delta_FS_2 + Fg_2 \cdot delta_FS_3 + Fg_1 \cdot delta_FS_4$

**Monthly Recursion Formula for Total Incremental Fractional Release**

$k := 1, 2 .. 724$

$$FT_{k+4} := \sum_{n=1}^{k} Fg_n \cdot delta_FS_{k-n}$$

$$\sum_{n=1}^{724} FT_n = 0.999$$

**Sample results:**

| | | | |
|---|---|---|---|
| $FT_1 = 2.197 \cdot 10^{-4}$ | $FT_2 = 3.819 \cdot 10^{-4}$ | $FT_{30} = 2.282 \cdot 10^{-3}$ | $FT_{100} = 2.765 \cdot 10^{-3}$ |
| $FT_3 = 5.144 \cdot 10^{-4}$ | $FT_4 = 6.277 \cdot 10^{-4}$ | $FT_{196} = 2.778 \cdot 10^{-3}$ | $FT_{300} = 2.778 \cdot 10^{-3}$ |
| $FT_5 = 5.762 \cdot 10^{-4}$ | $FT_{10} = 0.001$ | $FT_{360} = 2.778 \cdot 10^{-3}$ | $FT_{400} = 2.795 \cdot 10^{-4}$ |

**Incremental Fraction of Production in and Diffusion from Berm**

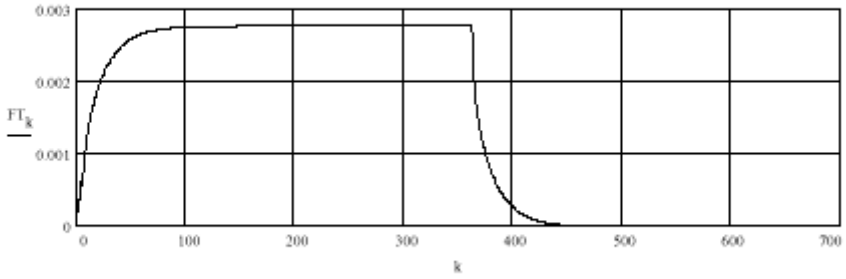

**Silmutaneous Production, Diffusion, and Decay Calculations**

**month 1**

$FT_DF_1 := Fg_1 \cdot delta_FS_1$

**month 2**

$FT_DF_2 := Fg_1 \cdot delta_FS_2 \cdot Na22_DF_1 + Fg_2 \cdot delta_FS_1$

**month 3**

$FT_DF_3 := Fg_1 \cdot delta_FS_3 \cdot Na22_DF_2 + Fg_2 \cdot delta_FS_2 \cdot Na22_DF_1 + Fg_3 \cdot delta_FS_1$

**month 4**

$FT_DF_4 := Fg_4 \cdot delta_FS_1 \cdot Na22_DF_3 + Fg_3 \cdot delta_FS_2 \cdot Na22_DF_2 + Fg_2 \cdot delta_FS_3 \cdot Na22_DF_1 + Fg_1 \cdot delta_FS_4$

**Monthly Recursion Formula for Total Incremental Fractional Release**

$$FT_DF_{k+4} := \sum_{n=1}^{k} Fg_n \cdot delta_FS_{k-n} \cdot Na22_DF_{n-1} \qquad \sum_{n=1}^{724} FT_DF_n = 0.131$$

**Sample results:**

| | | | |
|---|---|---|---|
| $FT_DF_1 = 2.197 \cdot 10^{-4}$ | $FT_DF_2 = 3.784 \cdot 10^{-4}$ | $FT_DF_{30} = 1.549 \cdot 10^{-3}$ | $FT_DF_{100} = 5.038 \cdot 10^{-4}$ |
| $FT_DF_3 = 5.052 \cdot 10^{-4}$ | $FT_DF_4 = 6.04 \cdot 10^{-4}$ | $FT_DF_{196} = 6.522 \cdot 10^{-5}$ | $FT_DF_{300} = 6.822 \cdot 10^{-6}$ |
| $FT_DF_5 = 5.762 \cdot 10^{-4}$ | $FT_DF_{10} = 0.001$ | $FT_DF_{360} = 1.852 \cdot 10^{-6}$ | $FT_DF_{400} = 1.988 \cdot 10^{-7}$ |

**Incremental Fraction of Production in and Diffusion from Berm with Decay**

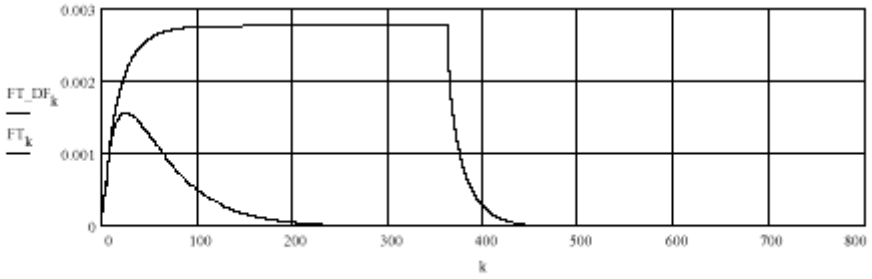

$TNa22_k := FT_DF_k \cdot Na22_curies$

$Na22_curies = 0.023 \cdot Ci$

$Recharge_volume = 427.968 \cdot m^3 \cdot month^{-1}$

$TPore_Na22_k := \frac{TNa22_k}{Pore_Flow_k} \cdot microCi^{-1} \cdot cc$

| k | $FT_k$ | $TPore_Na22_k$ |
|---|---|---|
| 1 | 0.00022 | $1.18 \cdot 10^{-8}$ |
| 2 | 0.00038 | $1.017 \cdot 10^{-8}$ |
| 3 | 0.00051 | $9.051 \cdot 10^{-9}$ |
| 4 | 0.00063 | $8.116 \cdot 10^{-9}$ |
| 5 | 0.00058 | $6.193 \cdot 10^{-9}$ |
| 6 | 0.0008 | $7.017 \cdot 10^{-9}$ |
| 7 | 0.00096 | $7.131 \cdot 10^{-9}$ |
| 8 | 0.00109 | $6.995 \cdot 10^{-9}$ |
| 9 | 0.0012 | $6.761 \cdot 10^{-9}$ |
| 10 | 0.0013 | $6.49 \cdot 10^{-9}$ |
| 11 | 0.00139 | $6.209 \cdot 10^{-9}$ |
| 12 | 0.00147 | $5.931 \cdot 10^{-9}$ |
| 13 | 0.00155 | $5.664 \cdot 10^{-9}$ |
| 14 | 0.00162 | $5.409 \cdot 10^{-9}$ |
| 15 | 0.00168 | $5.167 \cdot 10^{-9}$ |
| 16 | 0.00174 | $4.938 \cdot 10^{-9}$ |
| 17 | 0.00179 | $4.723 \cdot 10^{-9}$ |
| 18 | 0.00185 | $4.519 \cdot 10^{-9}$ |
| 19 | 0.00189 | $4.327 \cdot 10^{-9}$ |
| 20 | 0.00194 | $4.146 \cdot 10^{-9}$ |
| 21 | 0.00198 | $3.974 \cdot 10^{-9}$ |
| 22 | 0.00202 | $3.812 \cdot 10^{-9}$ |
| 23 | 0.00206 | $3.658 \cdot 10^{-9}$ |
| 24 | 0.0021 | $3.512 \cdot 10^{-9}$ |
| 25 | 0.00213 | $3.374 \cdot 10^{-9}$ |
| 26 | 0.00217 | $3.242 \cdot 10^{-9}$ |
| 27 | 0.0022 | $3.117 \cdot 10^{-9}$ |
| 28 | 0.00223 | $2.998 \cdot 10^{-9}$ |
| 29 | 0.00226 | $2.884 \cdot 10^{-9}$ |
| 30 | 0.00228 | $2.775 \cdot 10^{-9}$ |
| 31 | 0.00231 | |
| 32 | 0.00233 | |
| 33 | 0.00235 | |
| 34 | 0.00238 | |
| 35 | 0.0024 | |
| 36 | 0.00242 | |
| 37 | 0.00243 | |

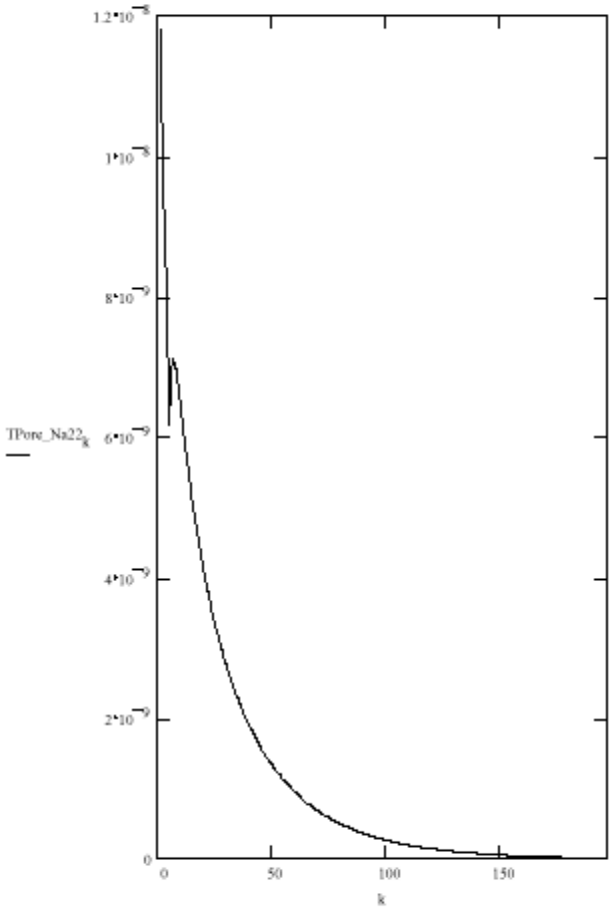


$TPore_Na22_{196} = 1.788 \cdot 10^{-11}$

$Pore_Na22_{196} = 3.876 \cdot 10^{-9}$

$TNa22_k := FT_DF_k \cdot Na22_curies$

$Na22_curies = 0.023 \cdot Ci$

$Recharge_volume = 427.968 \cdot m^3 \cdot month^{-1}$

$TPore_Na22_k := \frac{TNa22_k}{Pore_Flow_k} \cdot microCi^{-1} \cdot cc$

| k | $FT_k$ | $TPore_Na22_k$ |
|---|---|---|
| 1 | 0.00022 | $1.18 \cdot 10^{-8}$ |
| 2 | 0.00038 | $1.017 \cdot 10^{-8}$ |
| 3 | 0.00051 | $9.051 \cdot 10^{-9}$ |
| 4 | 0.00063 | $8.116 \cdot 10^{-9}$ |
| 5 | 0.00058 | $8.116 \cdot 10^{-9}$ |
| 6 | 0.0008 | $6.193 \cdot 10^{-9}$ |
| 7 | 0.00096 | $7.017 \cdot 10^{-9}$ |
| 8 | 0.00109 | $7.131 \cdot 10^{-9}$ |
| 9 | 0.0012 | $6.995 \cdot 10^{-9}$ |
| 10 | 0.0013 | $6.761 \cdot 10^{-9}$ |
| 11 | 0.00139 | $6.49 \cdot 10^{-9}$ |
| 12 | 0.00147 | $6.209 \cdot 10^{-9}$ |
| 13 | 0.00155 | $5.931 \cdot 10^{-9}$ |
| 14 | 0.00162 | $5.664 \cdot 10^{-9}$ |
| 15 | 0.00168 | $5.409 \cdot 10^{-9}$ |
| 16 | 0.00174 | $5.167 \cdot 10^{-9}$ |
| 17 | 0.00179 | $4.938 \cdot 10^{-9}$ |
| 18 | 0.00185 | $4.723 \cdot 10^{-9}$ |
| 19 | 0.00189 | $4.519 \cdot 10^{-9}$ |
| 20 | 0.00194 | $4.327 \cdot 10^{-9}$ |
| 21 | 0.00198 | $4.146 \cdot 10^{-9}$ |
| 22 | 0.00202 | $3.974 \cdot 10^{-9}$ |
| 23 | 0.00206 | $3.812 \cdot 10^{-9}$ |
| 24 | 0.0021 | $3.658 \cdot 10^{-9}$ |
| 25 | 0.00213 | $3.512 \cdot 10^{-9}$ |
| 26 | 0.00217 | $3.374 \cdot 10^{-9}$ |
| 27 | 0.0022 | $3.242 \cdot 10^{-9}$ |
| 28 | 0.00223 | $3.117 \cdot 10^{-9}$ |
| 29 | 0.00226 | $2.998 \cdot 10^{-9}$ |
| 30 | 0.00228 | $2.884 \cdot 10^{-9}$ |
| 31 | 0.00231 | $2.775 \cdot 10^{-9}$ |
| 32 | 0.00233 | |
| 33 | 0.00235 | |
| 34 | 0.00238 | |
| 35 | 0.0024 | |
| 36 | 0.00242 | |
| 37 | 0.00243 | |

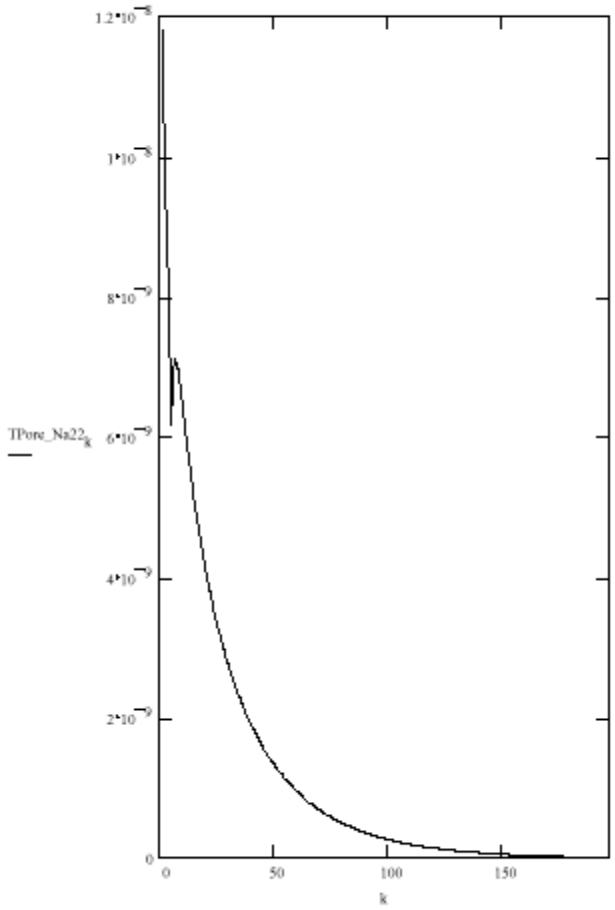


$TPore_Na22_{196} = 1.788 \cdot 10^{-11}$

$Pore_Na22_{196} = 3.876 \cdot 10^{-9}$

| | | |
|---|---|---|
| 38 | 0.00245 | $2.672 \cdot 10^{-9}$ |
| 39 | 0.00247 | $2.573 \cdot 10^{-9}$ |
| 40 | 0.00248 | $2.478 \cdot 10^{-9}$ |
| 41 | 0.0025 | $2.387 \cdot 10^{-9}$ |
| 42 | 0.00251 | $2.301 \cdot 10^{-9}$ |
| 43 | 0.00253 | $2.217 \cdot 10^{-9}$ |
| 44 | 0.00254 | $2.138 \cdot 10^{-9}$ |
| 45 | 0.00255 | $2.062 \cdot 10^{-9}$ |
| 46 | 0.00256 | $1.988 \cdot 10^{-9}$ |
| 47 | 0.00257 | $1.918 \cdot 10^{-9}$ |
| 48 | 0.00258 | $1.851 \cdot 10^{-9}$ |
| 49 | 0.00259 | $1.786 \cdot 10^{-9}$ |
| 50 | 0.0026 | $1.724 \cdot 10^{-9}$ |
| | | $1.664 \cdot 10^{-9}$ |
| | | $1.606 \cdot 10^{-9}$ |
| | | $1.551 \cdot 10^{-9}$ |
| | | $1.498 \cdot 10^{-9}$ |
| | | $1.447 \cdot 10^{-9}$ |
| | | $1.398 \cdot 10^{-9}$ |
| | | $1.35 \cdot 10^{-9}$ |

$$Case_Ratio := \frac{TPore_Na22_{196}}{Pore_Na22_{196}} \qquad Case_Ratio = 0.005$$